The petrology and geochemistry of the tertiary dyke swarm associated with the Mourne mountain granites, Northern Ireland

Orhan Akiman

THE PETROLOGY AND GEOCHEMISTRY OF THE TERTIARY DYKE SWARM ASSOCIATED WITH THE MOURNE MOUNTAIN GRANITES, NORTHERN IRELAND

by

ORHAN AKIMAN

B.Sc., M.Sc., Middle East Technical University (Ankara),

Graduate Society, Durham.

A THESIS SUBMITTED FOR THE DEGREE OF

DOCTOR OF PHILOSOPHY IN THE

UNIVERSITY OF DURHAM

JANUARY, 1971.

The petrology and geochemistry of the Tertiary dyke-swarm associated with the Mourne Mountain granites, Northern Ireland

by

Orhan Akiman

Abstract

The Tertiary dyke-swarm of the Mourne area consists principally of basic and intermediate dykes and an inclined, composite cone-sheet surrounding the Mourne Mountain granites.

The basic dykes are of two types: alkali basaltic dykes on the one hand, and the tholeiitic on the other. The alkali basaltic dykes make their appearances in the northern part of the swarm, while the tholeiitic types are mainly confined to the middle and southern parts.

The tholeiitic series of the Mourne dyke-swarm form a differentiated sequence from olivine-tholeiites to granophyres, containing augite and sparse Ca-poor pyroxene and olivine in the basic rocks. Plagioclase is the sole feldspar phase in these rocks. The differentiated rocks of this series are typified by iron-enrichment (to tholeiitic andesites - "icelandites"). There are many textural variations within the rocks of the Mourne tholeiitic series, from medium-grained ophitic dolerites to very fine-grained spherulitic variolites and tachylytes.

The origin of the basaltic parent magma and mechanism of differentiation are discussed. The ratios of various chemically determined oxides and trace element distributions indicate possible measures of parent-daughter relationships of rocks believed to represent magmas in the Mourne dyke-swarm.

The chemistry of the alkali basalts of the Mourne area is related to magma generation at greater depths than in the case of tholeiitic

basalts of the same swarm.

A correlation is made between the alkali basalts of the Mourne area and those of the Killough-Ardglass dyke-swarm.

The simultaneous intrusion of acid and basic magmas and the nature of the composite minor intrusions in the Mourne area are discussed; and a geochemical difference between the cone-sheet granophyres and the Eastern Mourne granites is demonstrated.

The presence of sparse gabbroic xenoliths in the basic dykes of the Mourne area is related to a deep-seated gabbro formation beneath the Mourne Mountain granites and supports the geophysical evidence (Cook and Murphy, 1952). The other acid xenoliths contained in the intermediate dykes of the Mourne swarm are also described in detail.

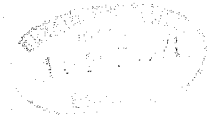

Acknowledgements

The author wishes to express his thanks to Professor G.M. Brown, Head of the Department of Geology, for the facilities provided for this research.

Dr. C.H. Emeleus has given constructive supervision and invaluable help throughout the study. The writer is greatly indebted to him.

The help of Mr. R. Phillips for his kindly reading a part of the manuscript is gratefully acknowledged.

The author is equally grateful to Dr. J.G. Holland for his kind supervision of the use of the X-ray fluorescence spectrograph.

Thanks are due to Mr. R.C.O. Gill who supplied the computer programme for the calculation of CIPW norms.

The author wishes to thank Mr. L. MacGregor and Mr. G. Randall who cut and polished the thin sections with great skill. He is also grateful to Mr. G. Dresser for photographic work executed with great care and patience.

A grant from CENTO Fellowship made this research possible, is also gratefully acknowledged.

TABLE OF CONTENTS

List of figures

List of plates

List of tables

CHAPTER I

INTRODUCTION

a) Geographic location and topography

The Tertiary dykes of Northern Ireland may be divided into two major sets:

1) The Antrim set, coinciding with the area of plateau lavas.

2) The Donegal-Down set, stretching diagonally across Northern Ireland and probably continuing across the floor of the Irish Sea to Anglesey, NW Wales, and the English Midlands (Figure 1). The dykes of this set are frequently exposed in elevated regions inland, but are best seen along the coast from Strangford Lough in the north to Dundalk Bay in the south (Figure 2). Three separate concentrations of dykes can be distinguished in this region:

1) the Killough-Ardglass dyke-swarm,

2) the Mourne dyke-swarm, and,

3) the Carlingford dyke-swarm.

The Mourne dyke-swarm lies between Newcastle and Kilkeel, some 50 km. south of Belfast, the capital of Northern Ireland.

The dykes of the Mourne swarm, associated with the Eastern Mournes only and well seen south of Newcastle, are concentrated into a narrow belt which measures 11 km. across the trend and extends to about 2 km. south of Annalong. They become very sparse near Newcastle.

The dyke-swarm over the 13 km. long coastal section, together

---

Fig. 1: Map of the Tertiary dyke-swarms and central intrusive complexes of the British Isles. (After Geological Survey, U.K.).

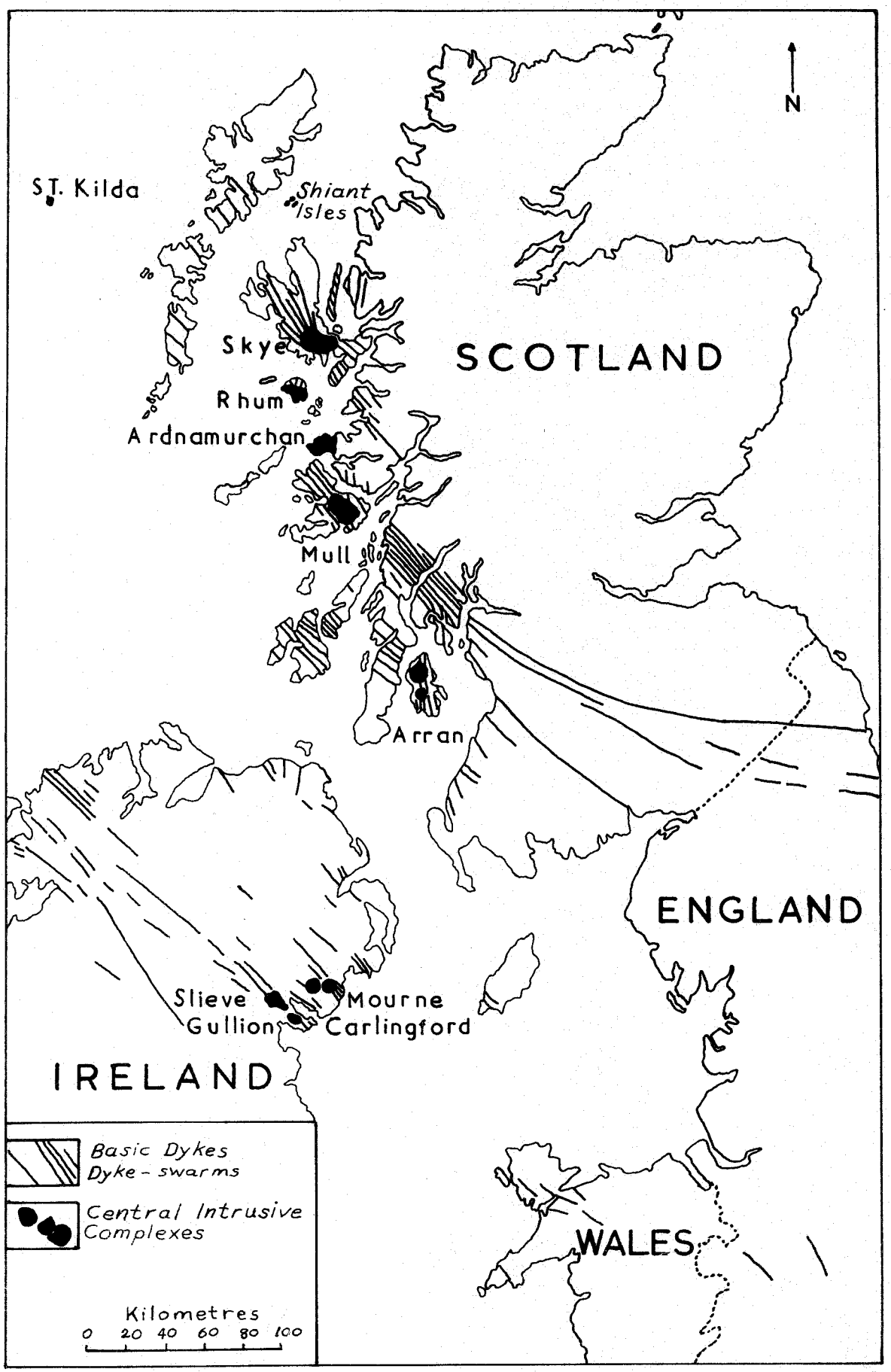
N
St. Kilda
Shiant Isles
Skye
SCOTLAND
Rhum
Ardnamurchan
Mull
Arran
ENGLAND
Slieve Gullion
Mourne Carlingford
IRELAND
WALES
Basic Dykes
Dyke-swarms
Central Intrusive Complexes
Kilometres
0 20 40 60 80 100

with its associated cone-sheet, surrounds the Eastern Mournes. The Eastern Mournes are one of the four Tertiary igneous centres of NE Ireland; the other three are the Western Mournes, the Carlingford and the Slieve Gullion intrusive complexes (Figure 2).

The Mourne range is 21 km. long by 8 km. broad, aligned from NE to SW, and formed of granites of Tertiary age. More than a dozen summits exceed 600 m. and the highest, Slieve Donard, 852 m. stands at the NE end of the range. On the east, between Newcastle and Kilkeel, the hills rise steeply from the surrounding lowland which consists of Silurian sediments.

The precipitious character of the rocky shore beyond and up to the mouth of Bloody Bridge River, about 3 km. south of Newcastle makes it extremely difficult of access in some places, but farther south, the dykes become easy to observe due to the emergence of a sea-cut platform and can be traced southwards as far as Ballymartin, about 2 km. south of Annalong (Figure 2). There, the sea-cut platform dies out and cliffs formed of fluvio-glacial and raised beach deposits obscure the solid geology.

The Eastern Mourne Mountains show a youthful type of topography which has been modified by the Pleistocene glaciation moving from north to south during the period of Scottish glaciation and NW to SE during the subsequent period of confluent ice (Charlesworth, 1963, p.453, fig. 122).

The Mourne dyke-swarm is approached by main road from Belfast and the coastal section is easily traversed along the road linking Newcastle

---

Fig. 2: Map of the Mourne area showing the location of the Tertiary igneous centres (After Tomkeieff and Marshall, 1935).

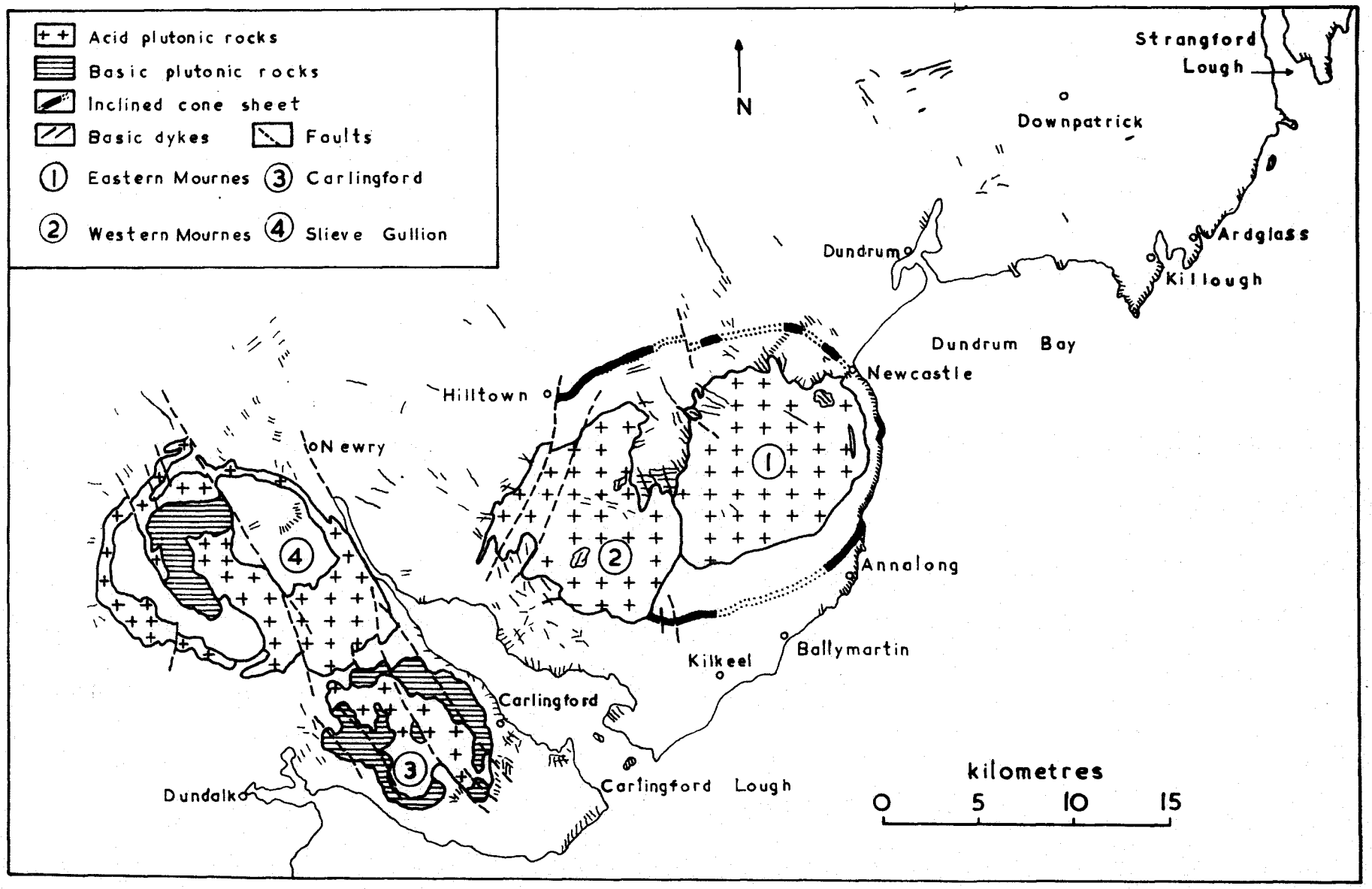
Acid plutonic rocks
Basic plutonic rocks
Inclined cone sheet
Basic dykes
Faults
1 Eastern Mournes
2 Western Mournes
3 Carlingford
4 Slieve Gullion
N
Strangford Lough
Downpatrick
Ardglass
Killough
Dundrum
Dundrum Bay
Newcastle
Hilltown
Newry
Annalong
Kilkeel
Ballymartin
Carlingford
Carlingford Lough
Dundalk
kilometres
0 5 10 15

with Kilkeel. A network of used and abandoned small quarry roads within the Eastern Mourne Mountains makes the area also easily accessible.

Field-work has been carried out for about two months in the summer 1968. More than 250 dyke and cone-sheet samples from both coastal and inland sections were collected for this study. In addition, 20 xenolithic core samples from these dykes were drilled out by means of a hand drill. 20 representative granite samples from the existing granite quarries within the Eastern Mournes and 20 dyke samples from the Killough-Ardglass dyke-swarm were also collected for comparative purposes.

b) Methods of investigation

More than 250 thin sections were cut in connection with this research, some of which are polished and carbon-coated for electron microprobe study.

The access to automatic X-ray fluorescence equipment (Philips PW 1212) made it possible to analyse more than 300 whole-rock samples for major and trace element constituents, and access to an electron microprobe (Cambridge, Geoscan Mk.2) permitted quantitative analyses of the major mineral components in a representative, selected suite of rocks. Computing of X-ray and microprobe output data was achieved by the use of data-processing facilities at Durham University.

The geochemistry of 308 whole-rock samples investigated by X-ray fluorescence spectrometry includes 288 samples from the Mourne area and 20 samples from the Killough-Ardglass dyke-swarm. Concentrations of the following 18 elements were determined, where present: Si, Al, Fe, Mg, Ca, Na, K, Ti, P, Mn, S (major elements), and Ba, Sr, Rb, Zr, Ni, Cu, Zn (trace elements). The operating conditions and computing

procedures used in the X-ray fluorescence analyses are described in Appendix, (A-2).

Ferrous iron was determined by the potassium permanganate method (cf. Appendix, A-3).

The following elements were determined in the minerals analysed by the electron microprobe: in olivines: Si, Fe, Mg, Ca, Mn; in pyroxenes: Si, Al, Fe, Mg, Ca, Na, Ti, Mn; in feldspars: Si, Al, Fe, Ca, Na, K, Sr, Ba; in opaque minerals: Si, Al, Fe, Mg, Ti, Mn, Cr, V. The operating conditions for the microprobe are described in Appendix (A-4).

In addition, detailed optical and X-ray diffraction studies have been carried out on a restricted sample of minerals for comparative purposes.

c) Previous works

The series of basic and intermediate dykes and acid cone-sheet of the Mourne swarm, which dip towards and partly surround the Tertiary granite massif of the Eastern Mourne Mountains has already received mention by several other authors. A number of geologists have visited and described the area, together with the neighbouring Tertiary intrusive centres of Slieve Gullion, Western Mournes and Carlingford.

The earliest record of the dykes was made by Patrickson (1833) who published a detailed list of these dykes later in 1837. Before him Berger (1816), recorded two varieties of granite in the Eastern Mournes, but only noted the uniform NW and SE direction and the parallelism of all the dykes of NE Ireland. In 1835, Griffiths' geological map of Ireland on a scale of 1/253440 was completed and published later in 1839. On it, with some alterations on subsequent editions up to 1855,

the boundary of the Mourne granite massif was accurately traced. The intrusions of Slieve Gullion and of Carlingford were also drawn in considerable detail. A series of NW trending dykes were indicated along the shore south of Newcastle, east of the Mourne granite, which, however, they did not penetrate. Griffiths was aware that the dykes were cut off by the granite margin, this fact was also recorded many years later by Hull (1881).

The detailed mapping of the area on a scale of 1/10560 was carried out by Traill during 1870 to 1873 (Unpublished sheets: Down 48, 49, 49A, 53 and 56). The important results obtained were published in a joint paper by Hull and Traill in 1871. The several one-inch sheets (scale 1/63360) covering the area were published in 1876 (Sheets 60, 61 and 71) followed by the explanatory Memoir (Hull, 1881). In this Memoir, a later set of basic dykes was found to be intruded into the granite. This later set was regarded as Tertiary, while the earlier dykes were placed with the Carboniferous. An intermediate Mesozoic age for the granite was therefore put forward.

Another contribution to the geology of the area was made by Haughton (1877), who, among many analyses of the rocks of the region, gave several of the dykes of the Eastern Mournes. Kinahan (1875) and Rutley (1877) have described a tachylitic margin of one of the dykes.

Since the publication of the Memoir in 1881, very few papers dealing with the dykes have appeared prior to Tomkeieff and Marshall's (1935) account. Among these, papers on the variolitic margins of NW dykes belonging to the Mourne pre-granite suite, given by Cole (1888, 1892, 1894a, 1894b), and the paper on the spherulitic rocks of the area by Hyland (1890) may be mentioned.

The detailed structural description of the Mourne granites was

made by Richey (1927), but was not concerned with the minor intrusions and the dyke-swarm.

A notable contribution to the petrology of the Mourne dyke-swarm was that made by Tomkeieff and Marshall (1935), who remapped the coastal section on a scale of 1/21120. Several outcrops were correlated, and the suggestion made that they represented a number of single, multiple and composite dykes and a cone-sheet which surrounds the ring-dyke complex of the Eastern Mournes. Although a limited number of chemical analyses were given by Tomkeieff and Marshall (op.cit. p.261, Table 2) they concluded that the majority of the Mourne pre-granite dykes were of intermediate composition which they attributed to the contamination of basaltic magma by an acid magma.

The age relationships between the Mourne granite and associated minor intrusions were investigated by Patterson (1946b), who pointed out that the late-stage veins belonged to the epi-magmatic and hydrothermal stages of the intruded magma (Patterson, 1946a, p.76).

Cook and Murphy (1952) conducted a gravity survey of NE Ireland and found a large positive anomaly in the Slieve Gullion - Carlingford - Mourne Mountain area, which they attributed to two large bodies of basic igneous rock, one beneath the Slieve Gullion and Carlingford area and the second beneath the southern border of the Mourne Mountains at a depth of 5 or 6 km. They suggest that although the surface outcrop of acid rock predominates, the total mass of basic rock under-lying the region must be at least one hundred times greater and would be sufficient to yield the visible acid intrusions by a process of differentiation. The investigation of the gravity anomalies associated with the Tertiary Igneous centres has been extended to include Skye, Mull, and Ardnamurchan where similarly large positive Bouguer anomalies

have more recently been discovered under nearly all the Tertiary igneous complexes of the Hebrides (Tuson, 1959; McQuillin and Tuson, 1963).

The other recent publications are mostly related to the granitic massif. Patterson (1953) studied the acid intrusive rocks of the Mourne Mountains and Slieve Gullion. Emeleus (1955) subdivided the Western Mourne granites into G-4 and G-5 and showed that they were emplaced by cauldron subsidence as in the case of the other three granites of the Eastern Mournes. Additional papers and articles on the Mourne granites have appeared in the past few years. Robbie (1955) described some basic and acid porphyritic dykes associated with a few composite intrusions met within the Slieve Bingian tunnel - an aqueduct in the Eastern Mournes. Some anomalous K/Rb ratios in the Western Mourne and Slieve Gullion igneous complexes were reported by Emeleus (cf. Taylor et al. 1956, p.226). Bailey and McCallien (1956), made some contributions to the mode of emplacement of the composite minor intrusions about the granite massif.

A few papers dealing with the Mourne granite itself have been published over the past decade. Of these, a further study of the granites (Brown, 1956), and some chemical data on G2 (Brown and Rushton, 1960) may be mentioned. The chemical compositions of a number of granite samples indicated a high degree of uniformity of the plutonic mass, which is also confirmed by the new X-ray fluorescence analyses made during the present research.

Finally, an absolute age determination of the Mourne granites was carried out by Brown and Miller (1963), by separating biotite from granite G-1, collected from the vicinity of Slievenagarragh on the eastern margin of the complex. Isotopic age determination by the K-Ar

method gave a result of 75 $\pm$ 7 million years (Brown and Miller, op.cit. p.93) which indicates, on the time scale of Kulp (1960), that the intrusion occurred at the beginning of the Tertiary period.

CHAPTER II

ROCK FORMATIONS

a) Pre-Tertiary country rocks

It is outside the scope of this investigation to discuss the nature and mode of occurrence of the pre-Tertiary sedimentary rocks of the area. No particular attempt has been made to collect representative samples and to give full descriptions of these rocks. However, a brief summary concerning the country rocks is presented as follows:

Sedimentary rocks occur in situ along the shore south of Newcastle as well as inland where they are seen to be intruded by the granite. Between Newcastle and Glasdrumman Port they have an outcrop 800 m. wide striking in NE-SW direction along the eastern flank of the Mourne granites. The belt widens beyond Newcastle northwards and beyond Glasdrumman Port southwards. The sedimentary strata are overlain and truncated by the Eastern Mourne granites on the west and on the north. The prevalent dip is to the SE. The amount of dip varies from place to place, and may have been slightly affected by the emplacement of the granites. The sedimentary rocks have been classified by the Geological Survey with the Llandovery (Egan, 1901). Lithologically, they consist of hard, compact, laminated grit and shales, often in alternating layers of different colour. The strata are often found to occur in isoclinal folds of small size, sometimes overturned, with the development of minute crumpling. Folding was not attributed to the intrusion of the granites (Richey, 1927), except possibly south of Newcastle.

The sedimentary rocks are cut by numerous dykes and a few cone-sheets, and locally reveal slight metamorphic effects such as bleaching

and induration of the grit and shales. Locally, at the granite contacts hornfelses are formed.

b) Rocks of the dyke-swarm

In general, dykes are closely associated with igneous activity in NE Ireland and the dyke-swarms (p.1) are believed to be the hypabyssal manifestations of the central plutonic complexes.

The intrusion of the pre-granitic NW dykes is the earliest known episode in the Tertiary igneous history of the Mourne area. Towards the north in the vicinity of Newcastle, and to the south of Annalong they become very sparse. Along a continuously exposed part of the coast from Glasdrumman Port for 4 km. northwards to the mouth of Bloody Bridge River, about one hundred dykes have been mapped by Traill. These dykes, in fact, constitute a swarm, comparable to the dyke-swarms of Scotland and Iceland, of which well-known Tertiary examples are those crossing Skye (Harker, 1904), Mull, Ardnamurchan and Arran (Bailey, et al., 1924) and Setberg (Sigurdsson, 1970).

The Mourne dykes do not extend in abundance far to the NW of the Mournes, as shown by the maps of the Geological Survey (cf. Map 1). They are thus developed in a narrow belt surrounding E-SE of the Eastern Mourne granites.

The rocks constituting the Mourne dyke-swarm are mainly basic and to some extent, intermediate in composition. The basic types include alkalic basalts, olivine basalts and dolerites, olivine-tholeiites and quartz-tholeiites. The intermediate rocks comprise tholeiitic andesites. With these, a few acid intrusions are associated, usually in the form of composite, inclined cone-sheets which surround the Eastern Mourne granites. These acid rocks are classified as felsites, granophyres and

quartz-feldspar porphyries.

The basic rocks represent 60% of the bulk volume of the Mourne dyke-swarm. Intermediate types form up to 30% by volume and the rest are mainly the acid members.

Although the prevailing type of intrusion is in the form of single dykes, some multiple and composite intrusions also occur throughout the swarm. Among them, multiple intrusions are of basic or intermediate composition, whereas in composite intrusions both acid and basic types are equally well represented.

In the composite intrusions the acid rocks are flanked by basic margins from which the acid centre is separated by a hybrid zone. Wherever they occur the composite intrusions usually form inclined sheets which are believed to represent different parts of a single, extensive cone-sheet surrounding the Eastern Mournes (Figure 2).

While the multiple intrusions are characterized by marginal chilling of successively intruded members of similar composition, in the case of composite intrusion there is no chilling between the earlier and the later intrusions, which are usually of widely different chemical and mineralogical composition.

c) Rocks of the Mourne granite massif

The Mourne dyke-swarm is closely associated with the Eastern Mourne igneous centre. Richey (1927) has pointed out that the massif included more than one granite intrusion, in fact at least four distinct intrusions, composed of different varieties of granite were known to exist in the area. Three of these which he called G-1 (feldspathic variety), G-2 (quartzose variety), and G-3 (aplitic variety) occur to the east, the fourth, G-4 (pink variety), to the west. The

last named variety has been subdivided into two different units (Emeleus, 1955), an earlier outer granite G-4, and a later inner granite G-5 (cf. Map 1). Thus, the Eastern Mourne centre, composed of the granites G-1, G-2 and G-3 in the chronological order, and the Western centre, composed of the granites G-4 and G-5, represent two closely synchronous granite emplacements in Silurian sediments by a process of ring-dyke formation and cauldron subsidence.

Twenty representative rock samples of the Eastern Mourne granites have been collected from the existing granite quarries scattered throughout the massif. The relationship between the granites and the acid cone-sheet surrounding them was studied chemically. According to the results obtained, some geochemical differences between the granites and acid rocks constituting the cone-sheet were revealed which will be discussed in the next chapter.

d) Auto-intrusions and post-granitic dykes within the plutonic massif

A number of post-granitic basic dykes occur within the Mourne massif, the dominant direction of which are WNW. About a dozen rock samples have been collected from different localities. From their chemical and mineralogical similarities, they are seen to belong to the oversaturated quartz-tholeiites of the Mourne dyke swarm.

On the other hand, a few acid intrusions, apparently dykes, are shown on the Geological Survey maps cutting the Mourne granites and extending for considerable distances. They have been designated by the Survey "elvan dyke", "felstone", etc. Richey (1927) has pointed out that some of them at least as mapped out by Traill have been confused with aplite auto-intrusions of varying width which are found everywhere throughout the Mourne granites. Occasionally, however, E-W

trending acid dykes occur in some places, differing from the aplites in their regular habit and in composition, but none of these could be traced far. Again, about a dozen rock samples have been collected from the suite, of which the three dykes slightly differ from the rest in chemical composition.

Wherever they occur the aplitic dykes are usually more or less irregular in habit, undulating or else running zig-zag with sharp bends indicating joint-control by the host-rock.

CHAPTER III

ACID ROCKS

a) Distribution and field characteristics of the acid rocks

The acid rocks include granophyres, felsites and quartz-feldspar porphyries. They form inclined sheets surrounding the Eastern Mourne granites and are usually composite in character.

Two good examples of the cone-sheet granophyre occur along the shore between Newcastle and Annalong, one at Glasdrumman Port and the other at the mouth of Bloody Bridge River (cf. Map 2). The Glasdrumman inclined sheet is displayed from Jenkins Point on the north to Sherby Rocks on the south (Tomkeieff and Marshall, 1935, p.270, fig. 4), and disappears inland under a cover of drift. Farther south it is again exposed in the bed of Annalong River.

The inner portions of the composite dykes Nos. 88, 89 and 90* (Tomkeieff and Marshall's numbers, 1935, p.286) are granophyres similar to that of Glasdrumman inclined sheet.

The Bloody Bridge cone-sheet extends from near to the mouth of Bloody Bridge River on the south to the Broad Cove on the north. Here again the inner portion of composite dyke No.30 is a granophyre similar to that of Bloody Bridge sheet, but of finer texture.

The limits of these two inclined sheets were accurately mapped by Traill (1871) and later by Tomkeieff and Marshall (1935).

Apart from the cone-sheets occurring along the shore and extending closely parallel to the outer margin of the Eastern Mourne granite

* dyke numbers are shown on Map 2.

massif, there are some other exposures of similar type of acid rocks occurring mainly inland. Of these, the acid rock of Knockree Hill which is located 3 km. NW of Kilkeel and probably the southerly continuation of the Glasdrumman Port - Annalong River inclined sheet, is a similar rock, but with smaller and less abundant phenocrysts and a well developed spherulitic groundmass (Tomkeieff and Marshall, 1935).

The second exposure of the same kind of rock can be traced on the NW side of the Mourne massif, and at a distance 5 km. ENE of Hilltown where it extends parallel to the northern margin of the Eastern Mourne granite and is cut off by a later normal fault trending NNE (cf. Map 1). Its spherulitic character makes it identical with the Knockree Hill rock.

During his investigation on the Western Mourne granites Emeleus (1955) has reported some other inclined sheets occurring at Gruggandoo and Slieve Roe on the west, and at Knockshee, Formal Hill and Cloghachorcha along the southern margin of the Western Mourne igneous complex. Of these sheets, the first two are porphyritic and spherulitic granophyres, identical with the Hilltown sheet, and the latter three are composite, inclined sheets similar to that exposed at Glasdrumman Port. According to Emeleus (op.cit. p.47), the sheets along the south dip northwards at an angle of 35° to 45°, and the Gruggandoo sheet has a similar dip to the SE. They all represent the western extension of the cone-sheet system.

The spherulitic granophyre of Gruggandoo is exposed about 3 km. SSW of Hilltown, and is cut off by the later Pink Granite G-4 (cf. Map 1). Owing to the similarity between this and the Hilltown rock, it is probably the southerly continuation of the Hilltown cone-sheet granophyre. It provides a conclusive evidence that the cone-sheets

of this system are earlier than the granites of the western centre. Specimens taken from the contact of an apophysis of G-4 and the sheet show granite chilled against spherulitic granophyre. The locality of this contact is about 600 m. NE of Gruggandoo summit, at 275 m. level, as reported by Emeleus (1955, p.47). Its southerly continuation is again represented by the same kind of rock on Slieve Roe, 2 km. SW of Gruggandoo.

The fifth inland exposure of the inclined sheets can be traced at Formal Hill, approximately 8 km. WNW of Kilkeel, where it has a composite character and dips towards north. The central member is a porphyritic granophyre with its larger and abundant rounded quartz and alkali feldspar phenocrysts set in a well developed spherulitic groundmass. The marginal rock is a dolerite, and there has been reaction between this and the acid centre. It thus very much resembles to the Glasdrumman Port composite sheet where similar relations can be seen. Again, its southwesterly continuation is traced on Knockshee Hill, 800 m. SW of Formal Hill, with the same type of composite intrusion (Emeleus, 1955, p.48).

The isolated outcrops of cone-sheet granophyre can thus be traced all round the Eastern and Western Mourne granite massifs. If these separate exposures of inclined sheets are joined by a continuous line, it will then be seen that they form a cone-sheet, surrounding the Eastern Mourne granites, and are cut off by the later granite, G-4 of the Western centre (cf. Map 1).

Everywhere, provided field conditions permitting, the sheets are seen to dip towards the granite at an angle of approximately 35°. Assuming the inclination of the sheet to be uniform at 35°, the calculated depth of the focus would be about 5 km., a figure in close

agreement with the geophysical evidence (Cook and Murphy, 1952), and that reached for the Scottish Tertiary igneous centres (Tuson, 1959).

The source of igneous activity has shifted with time in the Mourne area as in the case of the Scottish Tertiary centres. Within the Eastern Mournes, the sequence G-1 → G-2 → G-3 shows a change to the WSW, a direction which is continued in the change from the Eastern to the Western centre, and again within the latter in the sequence G-4 → G-5 as pointed out by Richey (1927) and Emeleus (1955). Significantly, the cone-sheet system of approximately elliptical outline, has its longer axis in the same direction (Figure 2).

In addition to the cone-sheet granophyres in the Mourne area, felsite is represented by dyke No.120. It occurs near Samuel's Port, about 2 km. SSW of Annalong, and trends NNE. Its thickness varies between 5-7 m. It is a pale buff or creamy coloured and fine-grained rock, with rough fracture and more or less curved jointing. A markedly well-developed fluxion structure is represented by dark-coloured mafic constituents as parabolic flow lines with apices directed to the SW.

Farther south near Murphy's Point, a porphyritic felsite occurs as an inner member of composite and multiple dyke No.124, trending NW with a total thickness of 13 m. The central porphyritic felsite is about 10 m. thick. It is pale brown or buff coloured rock with feldspar phenocrysts measuring up to 1 cm. in length. Some of these phenocrysts are altered and surrounded by ferruginous rims. Macroscopically no quartz grains are seen, although groundmass material can contain some quartz.

The Glasdrumman Port and Bloody Bridge inclined sheets have already been described in detail by Tomkeieff and Marshall (1935, p.271). While the former is a composite intrusion, the latter seems to be a single sheet or its basic margins may be concealed by the sea water on the

eastern flank of the intrusion.

The Bloody Bridge cone-sheet granophyre is exposed over about 360 m. of raised beach platform, and is a coarse grained porphyritic rock. It is rather resistant to weathering and has widely spaced joints. The most conspicuous constituents of the rock are the phenocrysts of alkali feldspar up to 1 cm. in length and rather smaller, rounded grains of quartz. The feldspar phenocrysts are also rounded and partly altered.

Grit and shale inclusions ranging in size from a few cm. to tens of centimetres are common, and many of them are almost completely digested or permeated by the granophyre.

Towards the southern extremity of the outcrop, near to the north of the mouth of Bloody Bridge River, where the rock emerges from beneath a steep scarp of raised beach deposits, the cone-sheet is traversed by a 30 cm. thick, fine-grained aplitic dyke trending NE. It displays a straight course across the sloping face of the granophyre. The downward prolongation of the dyke is roughly parallel to the walls of the main intrusion, although occasionally irregular and bifurcating. The contact against the granophyre is unchilled and tends to merge into it by the incoming of sporadic xenocrysts of alkali feldspar and quartz, obviously derived from the enclosing host-rock. No xenoliths of baked or digested country rock exist in the dyke, although they occur abundantly in the granophyre.

The Bloody Bridge cone-sheet cuts a basaltic dyke No.16 at right angles, some 100 m. north of this locality. This supports the view held by Emeleus (1955, p.48) that the basic and intermediate dykes of the Mourne swarm are older than the cone-sheet granophyres surrounding the Eastern and Western Mournes.

The Glasdrumman Port cone-sheet granophyre can be traced in the form of sinusoidal outcrop from north to south and disappears inland under a cover of raised beach deposits. Traill (1871) has delimited the exposure as bifurcating on the Geological Survey map (sheet 61), and later Tomkeieff and Marshall (1935, p.272) regarded the exposures as parts of a single, continuous outcrop separated by a slab of country rock. On the north, the inclined sheet again disappears under the sea and its continuation becomes rather obscure, but the similarity of the composite dykes Nos.88 and 89 to the sheet suggests a certain connection between the two. Although these dykes seem to be parted, they are probably faulted portions of one dyke. Their trend and thickness are identical, i.e., NNW, and 4 m. Both are externally bounded by a thin marginal basalt and owing to the chemical and mineralogical similarities which will be mentioned later in this chapter, there seems no reason to doubt that they are a contorted continuation of the Glasdrumman Port sheet, and all are more or less contemporaneous.

The central member of the Glasdrumman Port composite intrusion is a coarse grained, porphyritic, pale buff coloured rock with granophyric affinities. As in the case of the Bloody Bridge cone-sheet, the alkali feldspar phenocrysts are rounded and partly altered, measuring up to 1 cm. in length. Quartz grains are smaller than the feldspar phenocrysts and are more rounded.

The central granophyre reaches 11 m. in thickness and dips west at an angle of approximately 35°. No xenoliths of baked country rock are found in the granophyre, although they exist abundantly in the enclosing basaltic margins, xenoliths of which are often seen in the central member of the intrusion.

The SW continuation of the Glasdrumman Port inclined sheet is

exposed in Annalong River, at a distance of about 1 km. from the shore. It has a thickness of 9 m. and trends NE. Here the sheet is characterized by its drusy cavities and well developed porphyritic structure. The pink coloured alkali feldspar phenocrysts give a reddish-buff appearance to the rock. Their size varies between 1 - 2 cm. Quartz crystals are abundant but smaller in size and more rounded than the feldspar phenocrysts.

Finally, two acid dykes occur in the vicinity of the mouth of Bloody Bridge River, of which one is composite and the other is single in character.

The composite dyke No.30 is exposed some 450 m. to the south of Bloody Bridge River and is composed of an inner granophyre enclosed in marginal basalts. The central part is about 3 m. thick with a trend of NW. It resembles the Bloody Bridge cone-sheet chemically, but is finer grained, and contains inclusions of marginal basalt like the central granophyre of the Glasdrumman Port composite intrusion.

The dyke No.20 occurs 55 m. to the north of Bloody Bridge River. It is 1 m. thick, composed of dark coloured quartz and feldspar phenocrysts and trends NNE. Chemically it resembles the Bloody Bridge cone-sheet and may represent an off-shoot from it.

Although the great majority of acid rocks are in the form of inclined sheets surrounding the Eastern Mournes, there are, however, some acid intrusions within the granite massif itself. Of these, a felsitic dyke occurs on the southern slope of Round Seefin near the granite quarry (cf. Map 1). It is 1 m. thick and trends ENE. It very much resembles the Samuel's Port felsitic dyke No.120 of Annalong section in its general appearance. Macroscopically it has the same pale buff colour as in the case of No.120 dyke, and small globular

quartz grains with minute flakes of black mica.

To the west of this locality, on the southern slopes of Slieve Bingian, there occur two markedly thin acid dykes with 60 cm. thickness and ESE trend. Similar aplitic intrusions have also been traced on the north and NE side of Slieve Bingian. The occurrence of these dykes indicates that the older granites (i.e. G-2) in the vicinity of younger ones (i.e. G-3) are penetrated to some extent by aplites belonging to younger masses.

The majority of the acid intrusions within the granitic massif are non-porphyritic, although a few of them are porphyritic in habit. In the porphyritic types, rounded quartz phenocrysts are rather abundant with aggregates of black mica flakes. Conspicuous druses, on the other hand, are often found in non-porphyritic types containing well-developed quartz and orthoclase crystals.

On the north and NE side of Slieve Bearnagh, two acid porphry dykes differing from the aplites in their regular habit and in composition, trending WNW, lie in a conspicuous cleft. They contain alkali feldspar and abundant quartz phenocrysts, the latter often rounded, while the former are partly altered into kaolin.

Another aplitic auto-intrusion occurs in a granite quarry in the bed of Bloody Bridge River, at a distance of about 2 km. from the shore. Here the quartzose granite is penetrated by 15 cm. thick aplite, trending WNW. It is a non-porphyritic, gray coloured rock.

In addition to the acid intrusions, there are some greisen veins which are abundant within the outer margin of G-2 and run parallel to the granite margin. The best exposure of these veins can be seen in an old quarry south of Newcastle and north of Millstone Mountain (cf. Map 1; Nockolds and Richey, 1939).

b) Petrography of the acid rocks

In general, the acid rocks of the Mourne dyke-swarm are mainly composed of alkali feldspar and quartz, and minor amounts of sodic plagioclase, hornblende, biotite and opaque iron oxides set in a feldspathic and quartzose, cryptocrystalline groundmass.

The cone-sheet granophyre is a granitic rock superficially rather similar to the feldspathic granite of the Eastern Mournes (G-1 of Richey, 1927, p.659).

A description of the microscopic petrography of some of the granophyres has already been published (Tomkeieff and Marshall, 1935, p.267).

The feldspar phenocrysts consist principally of two kinds, namely, soda-orthoclase, and albite-oligoclase. The former has a wide range in size from 0.5 mm. to 1 cm. in length, while the latter is much smaller in size. They are often rounded, and partly altered into kaolinite and a fine aggregate of white mica (Plate 1).

Orthoclase is by far the most common porphyritic constituent of the granophyres. It is often associated with quartz and to a lesser extent with sodic plagioclase in the groundmass. Micrographic intergrowths of quartz and orthoclase are often seen in the matrix (Plate 2). Orthoclase is usually found as individual phenocrysts and as interstitial groundmass material. The phenocrysts are subhedral, but the groundmass orthoclase is anhedral giving a felsitic texture to the rock.

The composition of the alkali feldspar phenocrysts was determined on the basis of the three peak method (Wright, 1968). The results are tabulated in Table 1, the compositions range from $Or_{83}Ab_{17}$ to $Or_{67}Ab_{33}$ (Figure 3). In addition, analyses of a few single crystals of

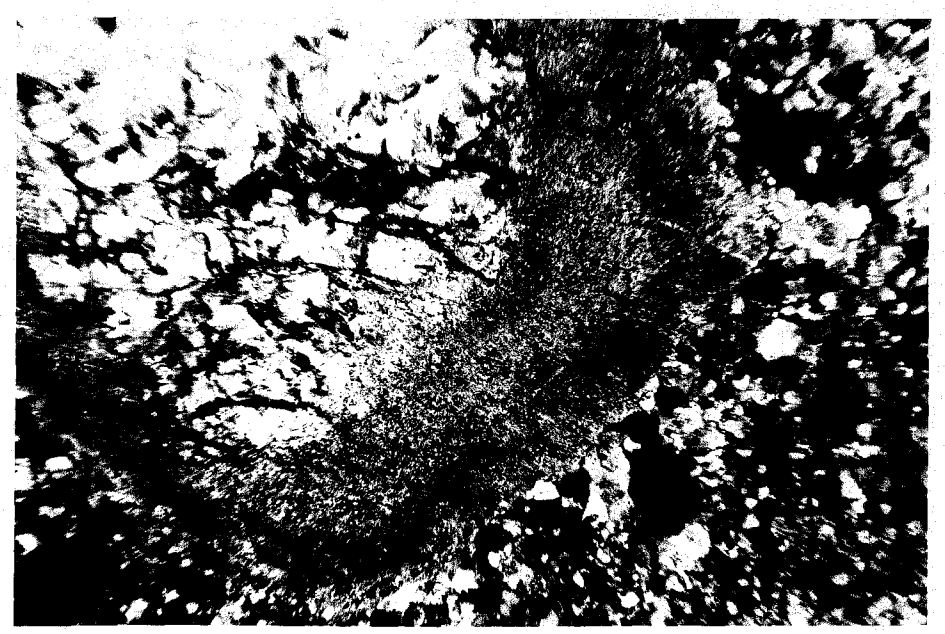

Plate 1: Phenocryst of orthoclase altered into kaolinite, in the Bloody Bridge cone-sheet granophyre (BBCS-3), x 45, crossed nicols.

Plate 2: Micrographic intergrowth of quartz and feldspar in the Bloody Bridge cone-sheet granophyre (BBCS-5), x 350, crossed nicols.

Table 1: Composition and structural state of alkali feldspar phenocrysts from the Mourne cone-sheet granophyres

Sample No.	hkl	2θ	Wt % Composition	Structural State	Locality
GPCS 14F	$\bar{2}01$	21.100	$Or_{80.5}$ $Ab_{19.5}$	P50 - 56F Orthoclase	Glasdrumman Port
	002	28.075			
	060	42.000			
	$\bar{2}04$	50.875			
GPCS 16F	$\bar{2}01$	21.180	$Or_{73.5}$ $Ab_{26.5}$	"	"
	002	27.750			
	060	41.905			
	$\bar{2}04$	50.870			
GPCS 19F	$\bar{2}01$	21.115	$Or_{79.2}$ $Ab_{20.8}$	"	"
	002	27.785			
	060	41.850			
	$\bar{2}04$	50.820			
GPCS 20F	$\bar{2}01$	21.125	$Or_{78.3}$ $Ab_{21.7}$	"	"
	002	27.705			
	060	41.925			
	$\bar{2}04$	50.895			
GPCS 21F	$\bar{2}01$	21.075	$Or_{82.7}$ $Ab_{17.3}$	"	"
	002	27.700			
	060	41.900			
	$\bar{2}04$	50.925			
GPCS 22F	$\bar{2}01$	21.135	$Or_{77.4}$ $Ab_{22.6}$	"	"
	002	27.650			
	060	42.015			
	$\bar{2}04$	50.940			
13325 F	$\bar{2}01$	21.100	$Or_{80.5}$ $Ab_{19.5}$	"	"
	002	27.750			
	060	41.875			
	$\bar{2}04$	50.850			
88-b F	$\bar{2}01$	21.075	$Or_{82.7}$ $Ab_{17.3}$	"	"
	002	28.100			
	060	41.975			
	$\bar{2}04$	50.970			
89-b F	$\bar{2}01$	21.095	$Or_{81.0}$ $Ab_{19.0}$	"	"
	002	27.725			
	060	41.920			
	$\bar{2}04$	50.825			
90-b F	$\bar{2}01$	21.210	$Or_{70.9}$ $Ab_{29.1}$	"	"
	002	27.750			
	060	41.905			
	$\bar{2}04$	50.950			

Table 1 continued:

Sample No.	hkl	2θ	Wt % Composition	Structural State	Locality
ARCS F	$\bar{2}01$	21.250	$Or_{67.4}$ $Ab_{32.6}$	P50 - 56 F Orthoclase	Annalong River
	002	27.800			
	060	42.000			
	$\bar{2}04$	50.925			
M 89 F	$\bar{2}01$	21.100	$Or_{80.5}$ $Ab_{19.5}$	"	Knockree Hill
	002	27.650			
	060	41.875			
	$\bar{2}04$	50.930			
11105 F	$\bar{2}01$	21.150	$Or_{76.1}$ $Ab_{23.9}$	"	Formal Hill
	002	27.700			
	060	41.850			
	$\bar{2}04$	50.890			
BBCS-1F	$\bar{2}01$	21.130	$Or_{77.9}$ $Ab_{22.1}$	"	Bloody Bridge
	002	27.625			
	060	41.910			
	$\bar{2}04$	50.900			
BBCS-2F	$\bar{2}01$	21.120	$Or_{78.8}$ $Ab_{21.2}$	Between P50 - 56F Orthoclase & Max-Microcline Low-Albite	"
	002	27.620			
	060	41.970			
	$\bar{2}04$	50.775			
BBCS-3F	$\bar{2}01$	21.175	$Or_{73.9}$ $Ab_{26.1}$	P50 - 56F Orthoclase	"
	002	27.675			
	060	41.925			
	$\bar{2}04$	50.925			
20 F	$\bar{2}01$	21.125	$Or_{78.3}$ $Ab_{21.7}$	"	"
	002	27.675			
	060	41.875			
	$\bar{2}04$	50.875			
30-b F	$\bar{2}01$	21.200	$Or_{71.7}$ $Ab_{28.3}$	"	"
	002	27.700			
	060	41.950			
	$\bar{2}04$	50.925			
11102 F	$\bar{2}01$	21.250	$Or_{67.4}$ $Ab_{32.6}$	"	"
	002	27.750			
	060	41.925			
	$\bar{2}04$	51.025			
11103 F	$\bar{2}01$	21.225	$Or_{69.5}$ $Ab_{30.5}$	"	"
	002	27.875			
	060	41.900			
	$\bar{2}04$	50.925			

Table 1 continued:

Sample No.	hkl	2θ	Wt. % Composition	Structural State	Locality
11100 F	$\bar{2}01$	21.175	$Or_{73.9}$ $Ab_{26.1}$	P50 - 56F	Gruggandoo
	002	27.700			
	060	41.925			
	$\bar{2}04$	50.905			
11101 F	$\bar{2}01$	21.175	$Or_{73.9}$ $Ab_{26.1}$	"	"
	002	27.655			
	060	41.875			
	$\bar{2}04$	50.880			

Equations relating $2\theta_{\bar{2}01}$ (x) and Or content (y) for complete series of alkali feldspars of constant structural state, where y = m x+b

Feldspar series	m	b
High sanidine - High albite	- 92.18	+ 2030.05
P50 - 56F Orthoclase	- 87.69	+ 1930.77
Maximum microcline - low albite	- 92.19	+ 2031.77

(Quoted from Wright, 1968, p.97)

orthoclase separated from the granophyres have been carried out by using the X-ray fluorescence spectrograph. Two additional microprobe analyses of the alkali feldspar phenocrysts have also been done for comparative purposes. From Table 2, it is seen that there is a fair agreement between these three methods.

Modally, alkali feldspar phenocrysts form up to 25% by volume. The ratio of alkali feldspar to plagioclase is high as it can be judged from the modal analyses of the granophyres (Table 3).

$2V_{\alpha}$ measurements in the alkali feldspar phenocrysts show erratic variations and can be grouped as follows:

a) angles between 52° and 55°,

b) angles between 60° and 62°,

c) angles between 65° and 67°.

When these are considered together with the chemical compositions the alkali feldspar phenocrysts fall inside the region orthoclase cryptoperthites (low albite-orthoclase series of Tuttle, 1952, p.557, fig.1). A plot relating the optic axial angle measurements and compositions of alkali feldspar phenocrysts from the Mourne cone-sheet granophyres is shown in Figure 4.

Plagioclase phenocrysts range in size from 0.3 to 1 mm. in length and are mainly found as individual crystals. Polysynthetic twinning of albite and combined Albite-Carlsbad twinning are common. Plagioclase compositions were estimated on the basis of maximum extinction angle on a (010) face and the measured extinction angles lie between

---

Fig. 3: Compositional variations of the alkali feldspar phenocrysts from the Mourne cone-sheet granophyres. (After Wright, 1968, p.93, fig. 4).

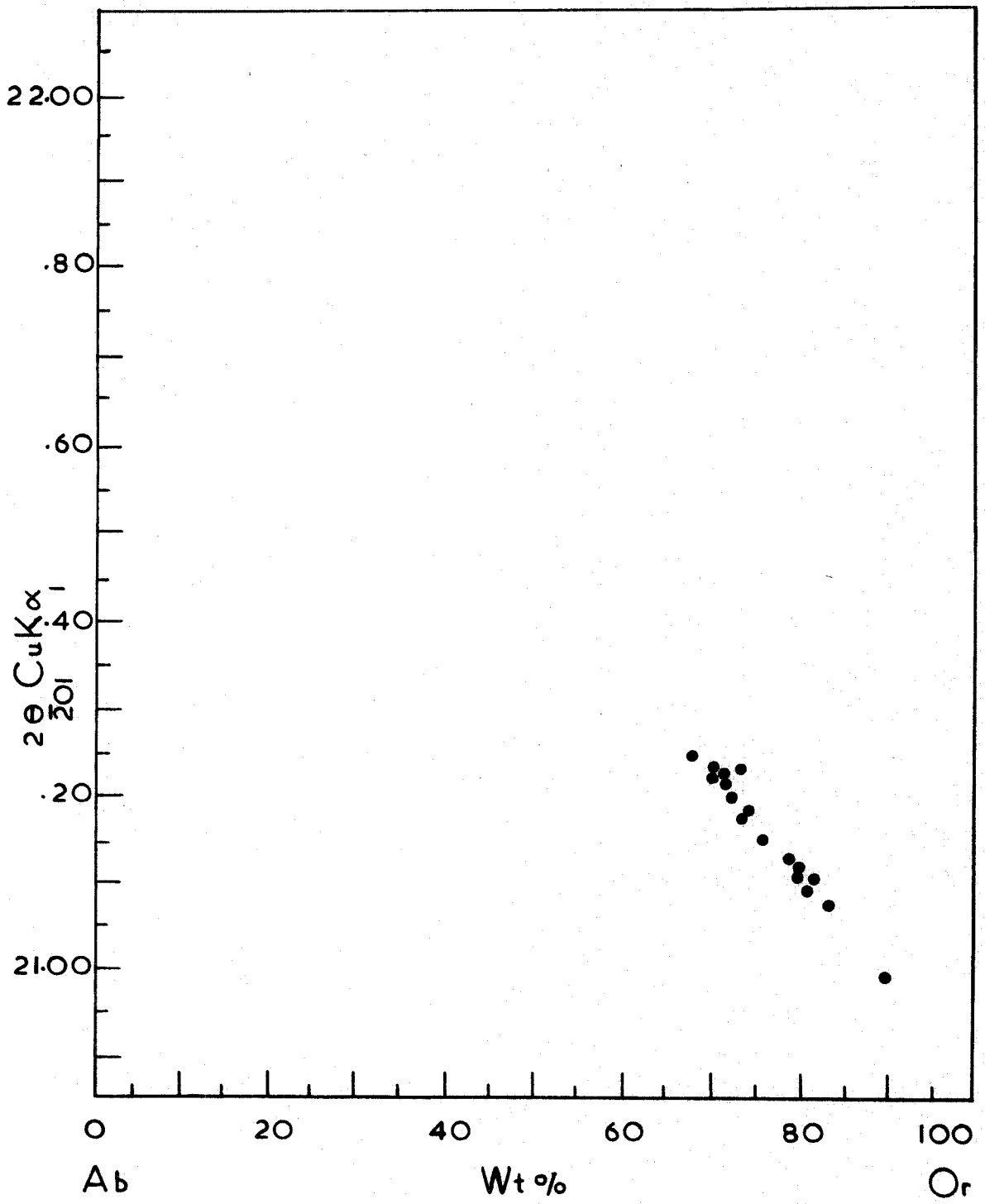
22.00
.80
.60
.40
.20
21.00
2θ CuKα1
201
0
20
40
60
80
100
Ab
Wt %
Or

Table 2: Comparison of XRD, XRF and electron-probe analyses of alkali feldspar phenocrysts in granophyric cone-sheets of Glasdrumman Port and Bloody Bridge River

Sample No.	XRD (Wt %)	XRF (Wt %)	Electron-probe (Wt %)
GPCS 16F	$Or_{73.5}\ Ab_{26.5}$	$Or_{75.3}\ Ab_{23.5}\ An_{1.2}$	$Or_{77.4}\ Ab_{21.6}\ An_{1.0}$
90-b F	$Or_{70.9}\ Ab_{29.1}$	$Or_{66.5}\ Ab_{30.5}\ An_{3.0}$	-
ARCS F	$Or_{67.4}\ Ab_{32.6}$	$Or_{62.1}\ Ab_{33.6}\ An_{4.3}$	-
11102 F	$Or_{67.4}\ Ab_{32.6}$	$Or_{65.9}\ Ab_{29.2}\ An_{4.9}$	-
11103 F	$Or_{69.5}\ Ab_{30.5}$	$Or_{67.7}\ Ab_{29.3}\ An_{3.0}$	-
BBCS 3 F	$Or_{73.9}\ Ab_{26.1}$	-	$Or_{72.1}\ Ab_{27.4}\ An_{0.5}$

Table 3: Modal analyses of the Mourne cone-sheet granophyres

Sample No.	Ground-mass	Alkali feldspar	Plagio-clase	Quartz	Ferromag-nesian	Inclu-sions
GPCS-16	59.6	25.2	4.1	6.0	4.6	0.5
GPCS-20	54.4	21.7	4.3	13.1	5.8	0.7
GPCS-19	56.2	19.3	4.1	14.8	5.4	0.2
GPCS-21	57.4	21.2	3.1	13.0	4.8	0.5
GPCS-22	58.5	20.7	3.6	12.0	4.7	0.5
13325	55.6	18.5	2.0	19.9	3.6	0.4
ARCS	55.0	20.1	3.2	16.5	4.7	0.5
88-b	58.4	22.3	3.3	12.0	3.6	0.4
89-b	57.3	20.8	3.7	13.4	4.5	0.3
90-b	61.5	17.9	9.8	7.2	3.6	-
BBCS-1	63.9	27.9	1.2	4.6	2.4	-
BBCS-2	64.6	26.5	1.3	5.2	2.4	-
11102	65.3	25.2	1.4	5.8	2.3	-
11103	82.7	11.7	-	4.9	0.7	-
BBCS-6	84.5	10.5	-	4.4	0.6	-
BBCS-7	86.4	9.3	-	3.8	0.5	-
BBCS-8	90.3	5.4	-	3.6	0.7	-
30-b	94.8	1.1	-	3.2	0.8	-

10° and 25° corresponding to the composition of albite and oligoclase. Plagioclase phenocrysts are also rounded and partly altered.

The quartz phenocrysts measure up to 3 mm. in diameter and their modal proportion varies between 3% and 20% of the rock. They are frequently rounded and eaten into, owing to the magmatic corrosion and have lost all crystal outlines. They sometimes contain inclusions of the groundmass material (Plate 3).

The great majority of the granophyres have a fine-grained groundmass. The modal proportion of the groundmass varies between 54% and 95% of the rock. The groundmass consists mainly of alkali feldspar and quartz, often intergrown as micropegmatite, together with subordinate amounts of sericite and iron ore. The texture of the groundmass is granophyric, including both micropegmatitic and microspherulitic, characterized by its micrographic intergrowths of feldspar and quartz and regular radiating aggregates of feldspar fibres. The spherulitic granophyres of Knockree Hill, Gruggandoo and Hilltown are of the cryptographic kind, giving a more or less distinct black cross between crossed nicols (Plate 4). The minute, radially arranged fibres of feldspar show characteristically a black cross, caused by extinction in those fibres which lie nearly parallel to one of the cross-wires. Sometimes spherulites occur isolated in a groundmass otherwise of simple microcrystalline texture, and more frequently they make up the chief part or whole of the groundmass. In this case the individual

---

Fig. 4: Variation of the optic axial angles and composition of alkali feldspar phenocrysts from the Mourne cone-sheet granophyres. The fields represent: 1) high albite-high sanidine, 2) high albite-anorthoclase-sanidine, 3) low albite-orthoclase, 4) low albite-microcline, and are taken from Tuttle (1952, p.557, fig. 1).

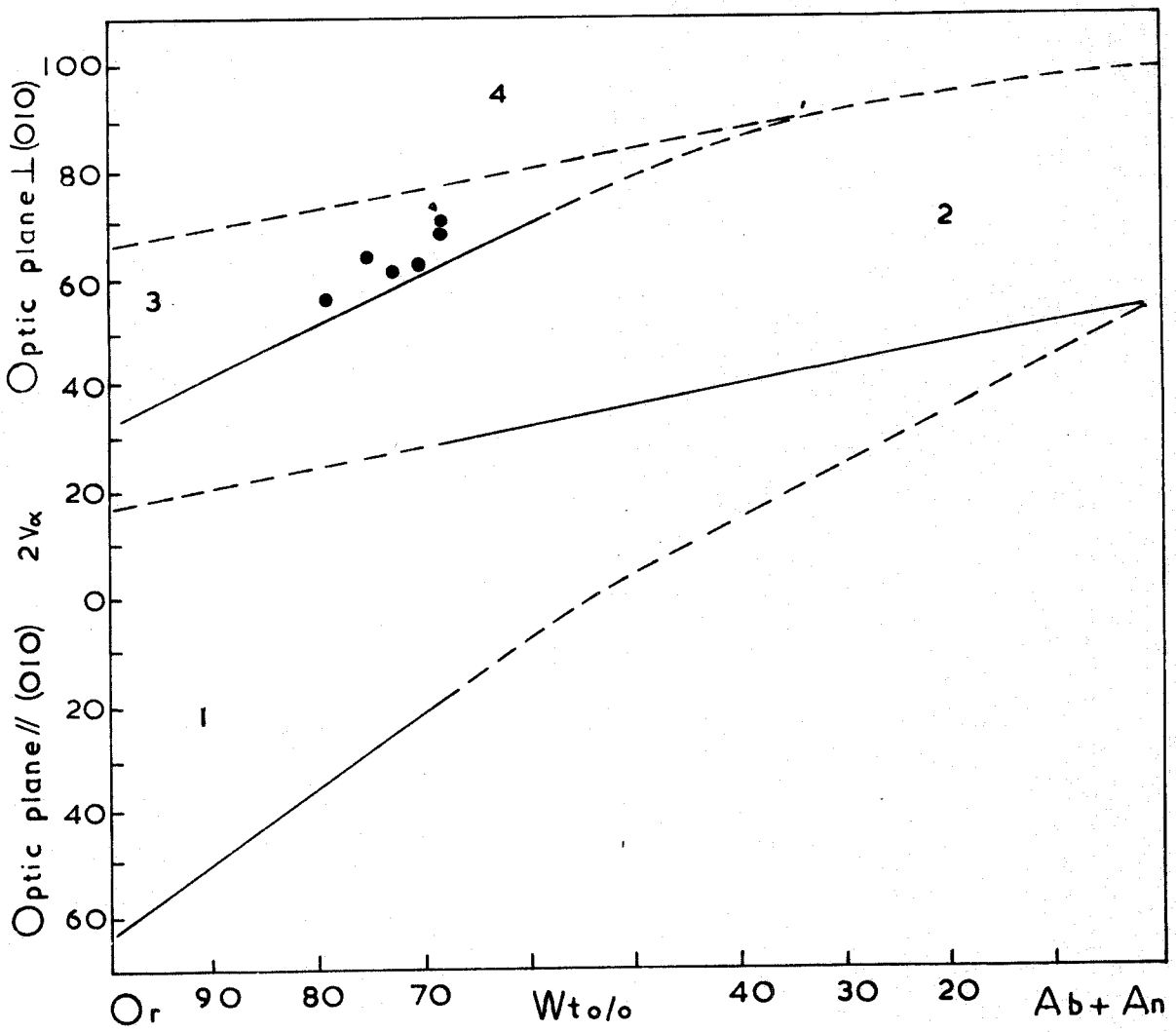
Optic plane ⊥ (010)
100
80
60
40
20
0
20
40
60
Optic plane // (010)
2Vα
4
3
2
1
Or
90
80
70
Wt o/o
40
30
20
Ab + An

Plate 3: Rounded and corroded phenocryst of quartz in the Glasdrumman cone-sheet granophyre (13325), x45, crossed nicols.

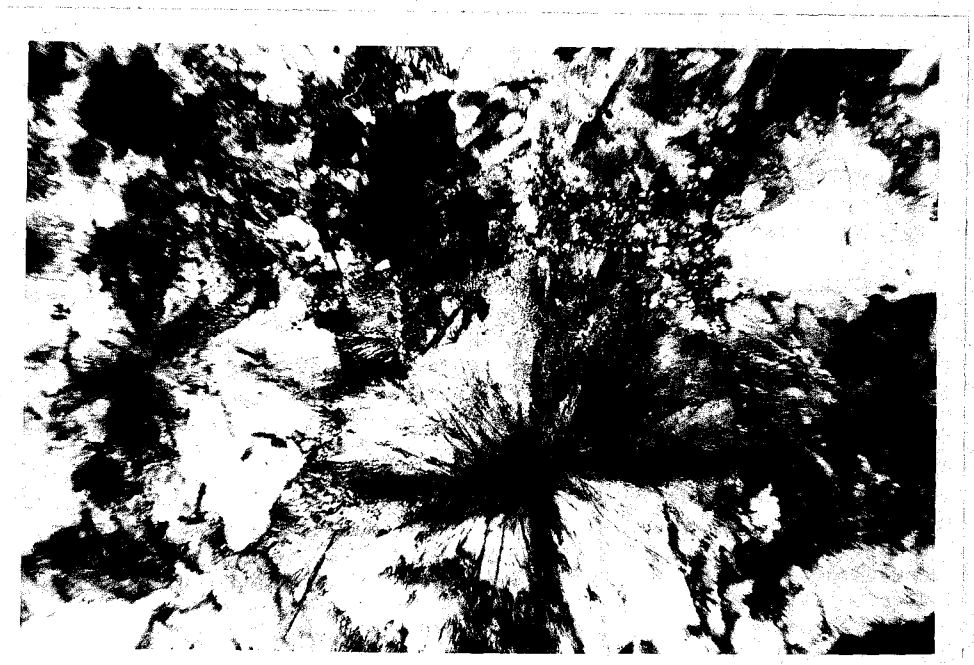

Plate 4: Spherulitic granophyre, (M90), from Knockree Hill cone-sheet, showing quartz and orthoclase phenocrysts with fringing alkali feldspar spherulites, x45, crossed nicols.

spherulites are sometimes sharply bounded against one another, with polygonal outlines due to mutual interference (Plate 4). Two good examples are the sheets at Knockree Hill and at Gruggandoo.

The ferromagnesian minerals in the cone-sheet granophyres of the Mourne area are usually brown biotite and hornblende. Biotite occurs as discrete grains measuring up to 0.5 mm. in length. It is generally idiomorphic and shows strong pleochroism, from Z = dark brown to X = brownish yellow. Chlorite is the common alteration product of biotite in the granophyres.

A greenish hornblende is also present in subordinate amounts as sub-idiomorphic grains up to 0.3 mm. long, bounded against the felsic constituents by a narrow fringe of iron ore grains. It is also altered into chlorite, thin threads or streaks of which are seen in the felsitic groundmass. The pleochroism of the hornblende is not so strong as in the case of biotite and is from Z = greenish brown to X = light green.

As accessory constituents, little apatite and granular sphene are rarely distributed, while the iron oxides are usually represented by minor amounts of magnetite. The secondary minerals include small amounts of kaolin, epidote and sericite.

c) Structural state of feldspars

The structural state of alkali feldspar and plagioclase phenocrysts has been determined by means of X-ray technique. The normative plagioclase content was calculated from the whole rock analysis because the method modified by Smith and Gay (1958) requires knowledge of normative plagioclase content.

Wright (1968) has developed a new X-ray method for the

determination of the structural state of alkali feldspars and these two methods were applied to the alkali feldspar and plagioclase phenocrysts of the Mourne cone-sheet granophyres.

c.1) Structural state of alkali feldspars

The study of the structural state of alkali feldspars in the granophyres was carried out for 22 specimens on a Philips (PW 1051) X-ray diffractometer, following the procedure described by Wright (1968). The 2θ values of the (060) and $(\bar{2}04)$ reflections obtained from powder films were plotted on a diagram shown in Figure 5. One out of 22 specimens falls in between P50-56F orthoclase and maximum microcline - low albite area and the other 21 are plotted on a straight line where P50-56F orthoclase series forms. In Table 1 the 2θ values of the two reflections are tabulated individually.

c.2) Structural state of plagioclase feldspars

The structural state of plagioclase feldspars was determined from the relative separations of the peaks 220, $1\bar{3}1$, and 131 on X-ray diffractometer patterns from the whole-rocks. These measurements give values of the function $\Gamma\,(2\theta_{131} + 2\theta_{220} - 4\theta_{1\bar{3}1})$.

The values have been plotted against the weight per cent An/An + Ab content of the whole-rocks defined by their normative compositions. The determinations have been carried out on 25 samples which give a functional value ranging between (-0.05) and (-0.22) and are given in Table 4. All the specimens are closely located within the area

---

Fig. 5: Structural state of alkali feldspar phenocrysts from the Mourne cone-sheet granophyres. (After Wright, 1968, p.91, fig. 2).

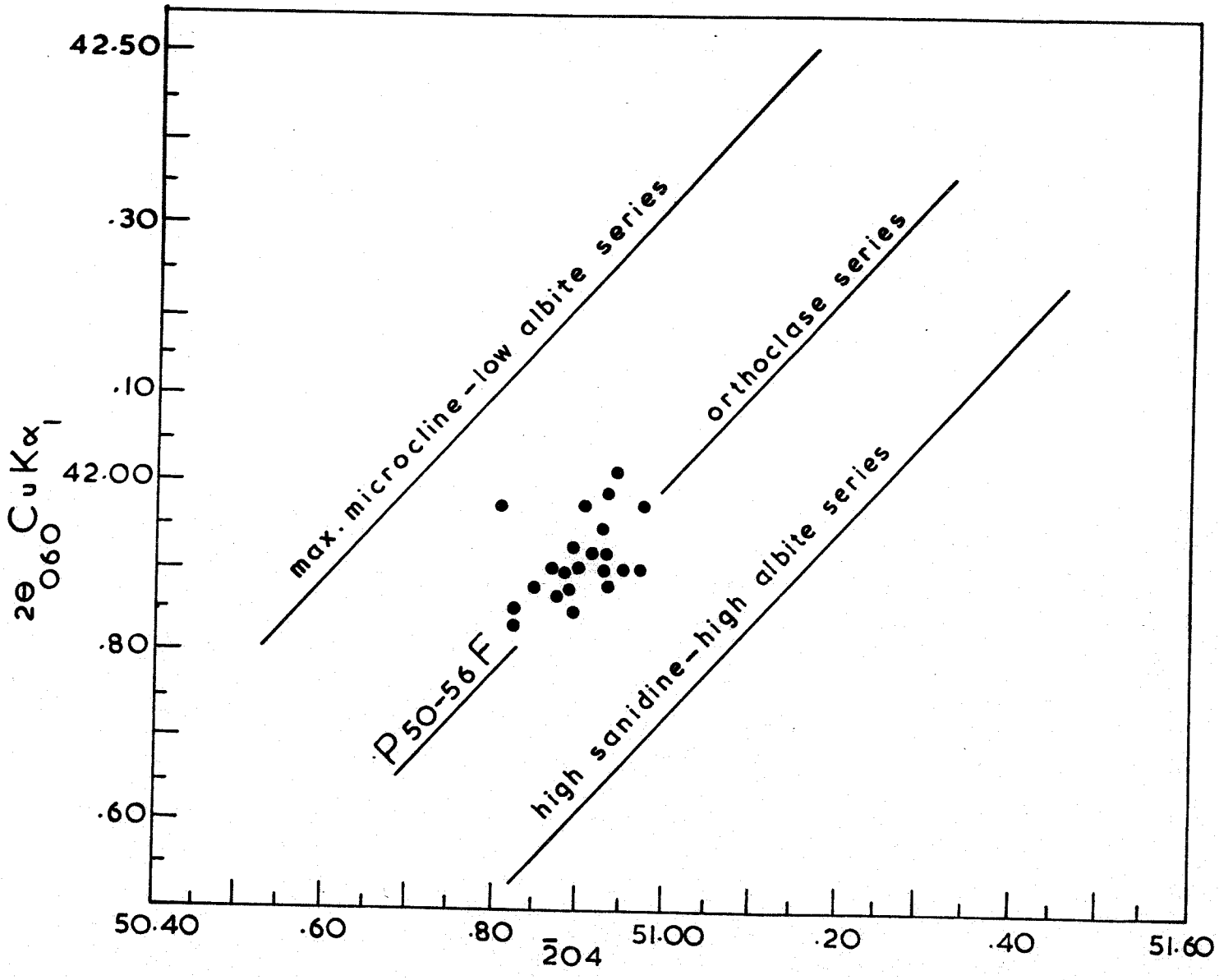
42·50
·30
·10
42·00
·80
·60
$2\theta_{060}$ Cu $K\alpha_1$
max. microcline–low albite series
orthoclase series
high sanidine–high albite series
P50-56F
50·40
·60
·80
$\bar{2}04$
51·00
·20
·40
51·60

Table 4: Measurements of the function $\Gamma (2\theta_{131} + 2\theta_{220} - 4\theta_{1\bar{3}1})$ of the plagioclase feldspars in the cone-sheet granophyres

Sample No.	$2\theta_{220}$	$2\theta_{1\bar{3}1}$	$2\theta_{131}$	Γ	Bulk composition wt. % An/Ab+An	Locality
GPCS 14	28.26	29.87	31.35	-0.13	20.2	Glasdrumman Port
GPCS 16	28.30	29.97	31.45	-0.19	10.5	"
GPCS 19	28.33	29.94	31.45	-0.10	12.4	"
GPCS 20	28.20	29.83	31.30	-0.16	5.6	"
GPCS 21	28.25	29.85	31.25	-0.20	14.8	"
GPCS 22	28.24	29.85	31.30	-0.16	1.1	"
13325	28.20	29.85	31.32	-0.18	5.2	"
88-b	28.26	29.89	31.37	-0.15	0.6	"
89-b	28.23	29.85	31.30	-0.17	0.9	"
90-b	28.33	29.89	31.33	-0.12	0.4	"
ARCS	28.26	29.93	31.43	-0.17	2.1	Annalong River
124-b'	28.24	29.90	31.42	-0.14	0.8	Murphy's Point
124-b"	28.15	29.75	31.20	-0.15	2.8	"
BBCS 1	28.33	29.90	31.35	-0.12	6.8	Bloody Bridge
BBCS 2	28.32	29.97	31.40	-0.22	5.6	"
BBCS 3	28.33	29.90	31.42	-0.05	17.6	"
BBCS 5	28.30	29.91	31.35	-0.17	7.7	"
BBCS 6	28.32	29.91	31.28	-0.22	8.6	"
BBCS 7	28.20	29.85	31.27	-0.23	2.2	"
BBCS 8	28.23	29.83	31.30	-0.13	1.2	"
BBCS 9	28.23	29.82	31.27	-0.14	0.5	"
20	28.27	29.87	31.30	-0.17	4.4	"
30-b	28.29	29.92	31.35	-0.20	17.1	"
11102	28.33	29.97	31.47	-0.14	21.9	"
11103	28.24	29.86	31.33	-0.15	9.1	"

defined for the hypabyssal (intermediate) structural state (Smith and Gay, 1958).

In connection with this structural state study, some 14 specimens from the Mourne granites have been run for the determination of their structural state. Their functional values were also plotted on the diagram shown in Figure 6, and are given in Table 5. All the granite samples fall inside the plutonic field.

The operating conditions for the X-ray diffractometer are described in Appendix (A-1).

d) Chemistry of the acid rocks

Altogether 64 acid rock samples representing both plutonic and hypabyssal types have been analysed for their major and trace element contents. The major element analysis of the acid rocks has been run on the Philips (PW 1212) automatic X-ray fluorescence spectrograph against the four international standards of W-1, G-1, S-1 and T-1, plus 28 secondary standards used in this department. The same samples were also analysed for 7 trace elements, using 29 additional trace element standards.

d.1) Major element contents of the acid rocks

From the chemical analyses of acid rocks tabulated in Tables 6, 7, and 8, it is seen that the most obvious feature of these analyses is their remarkable uniformity in certain oxides.

Fig. 6: Structural state of plagioclase phenocrysts from the Mourne cone-sheet granophyres and granites. (After Smith and Gay, 1958). Symbols denote: o cone-sheet granophyres, • Eastern Mourne granites.

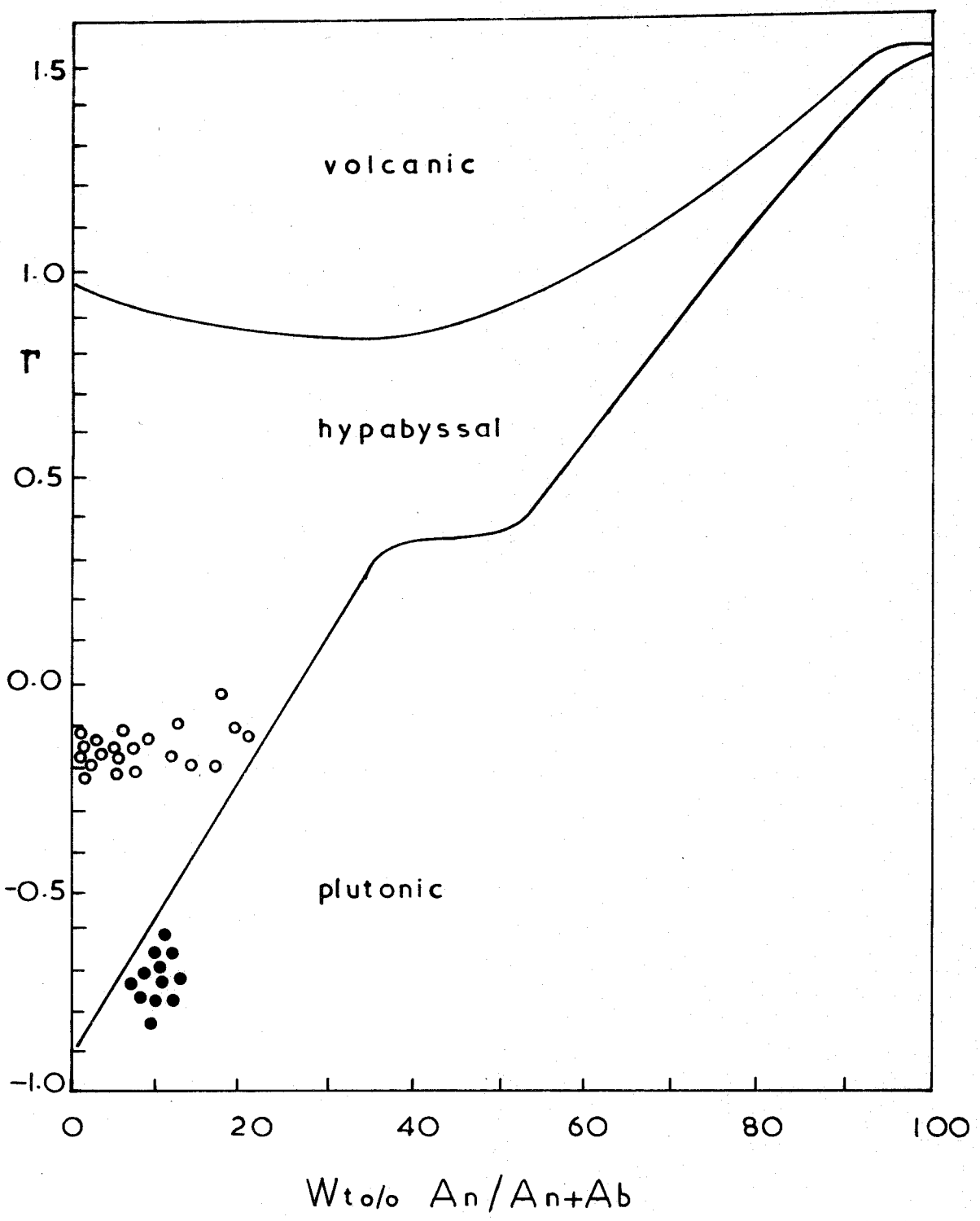
1.5
1.0
r
0.5
0.0
-0.5
-1.0
volcanic
hypabyssal
plutonic
0
20
40
60
80
100
Wt o/o An / An+Ab

Table 5: Measurements of the function $\Gamma (2\theta_{131} + 2\theta_{220} - 4\theta_{1\bar{3}1})$ of the plagioclase feldspars in the Mourne granites

Sample No.	2θ 220	2θ $1\bar{3}1$	2θ 131	Γ	Bulk composition wt. % An/Ab+An	Locality
MG-1	28.15	29.93	30.87	-0.84	9.8	Thomas Mt. G-2
MG-3	28.16	29.80	30.80	-0.64	9.3	" "
MG-5	28.25	29.90	30.85	-0.70	8.6	" "
MG-6	28.20	29.87	30.80	-0.74	10.0	" "
MG-8	28.21	29.90	30.82	-0.77	8.5	" "
MG-9	28.17	29.88	30.80	-0.79	8.8	" "
MG-10	28.26	29.97	30.90	-0.78	10.7	Millstone Mt. G-1
MG-11	28.21	29.86	30.88	-0.63	10.5	Bloody Bridge G-1
MG-12	28.15	29.84	30.77	-0.76	9.4	Chimney Rock Mt. G-1
MG-13	28.13	29.80	30.77	-0.70	9.5	Bloody Bridge G-2
MG-14	28.20	29.85	30.80	-0.70	6.9	" "
MG-15	28.23	29.86	30.83	-0.66	10.4	" "
MG-16	28.08	29.73	30.70	-0.68	11.5	Spences Mt. G-1
MG-22	28.23	29.87	30.77	-0.74	12.3	Ben Crom Dam G-3

Table 6: Chemical analyses and C.I.P.W. norms of the Mourne cone-sheet granophyres

Wt %	124-b'	124-b''	124-b'''	120-a	120-b	120-c	13338	13339
SiO_2	71.90	69.53	67.67	74.28	75.17	71.59	69.96	68.53
Al_2O_3	15.04	15.97	15.79	15.04	14.65	15.93	15.62	15.73
Fe_2O_3	1.80	2.84	2.20	0.75	0.47	0.83	2.16	1.58
FeO	0.79	0.94	2.40	1.22	0.91	1.65	1.38	2.48
MgO	0.53	0.84	2.89	0.56	0.45	0.73	0.70	2.03
CaO	0.11	0.29	0.30	0.02	0.32	0.02	0.30	0.24
Na_2O	3.17	2.96	2.54	3.78	2.69	4.59	2.84	2.45
K_2O	6.23	5.99	5.47	4.22	5.17	4.49	6.48	6.26
TiO_2	0.34	0.47	0.57	0.06	0.05	0.12	0.43	0.52
P_2O_5	0.05	0.11	0.09	0.01	0.01	-	0.07	0.09
MnO	0.01	0.02	0.03	0.02	0.02	0.02	0.02	0.03
S	-	-	-	-	0.12	-	-	-
Qz	28.67	27.76	26.38	34.51	37.87	25.57	27.06	25.82
Or	36.86	35.44	32.37	24.98	30.54	26.53	38.31	37.05
Ab	26.86	25.08	21.56	32.04	22.79	38.84	24.08	20.79
An	0.21	0.72	0.90	0.03	1.52	0.09	1.03	0.60
Cor	2.98	4.33	5.33	4.22	4.05	3.48	3.54	4.68
Hy	1.32	2.09	8.93	2.96	2.15	4.01	1.82	7.52
Mt	1.62	1.76	3.20	1.09	0.69	1.21	3.14	2.30
Hm	0.68	1.63	-	-	-	-	-	-
Ilm	0.64	0.89	1.08	0.11	0.09	0.22	0.81	0.99
Ap	0.11	0.26	0.21	0.02	0.02	-	0.16	0.21
Py	-	-	-	-	0.22	-	-	-
DI	92.40	88.29	80.32	91.53	91.21	90.95	89.45	83.67
SI	4.23	6.19	18.65	5.32	4.64	5.94	5.16	13.72

Table 6 continued:

Wt %	88-b	89-b	90-b	GPCS-14	GPCS-16	GPCS-19	GPCS-20	GPCS-21
SiO_2	76.40	75.88	76.56	69.00	71.18	70.99	75.72	71.33
Al_2O_3	13.60	13.69	13.79	14.24	14.76	14.80	13.73	14.95
Fe_2O_3	0.92	1.15	0.82	1.44	0.50	0.83	0.46	1.76
FeO	0.42	0.39	0.47	2.96	2.42	2.02	0.93	1.16
MgO	0.22	0.32	0.29	1.74	0.79	0.70	0.27	0.52
CaO	0.06	0.07	0.07	2.71	0.82	1.02	0.40	1.07
Na_2O	3.32	2.91	6.05	4.77	3.65	3.82	3.67	3.31
K_2O	4.91	5.41	1.78	2.42	5.38	5.32	4.64	5.44
TiO_2	0.09	0.11	0.09	0.48	0.34	0.33	0.11	0.31
P_2O_5	0.02	0.02	0.02	0.12	0.07	0.08	0.02	0.07
MnO	0.01	0.02	0.02	0.07	0.05	0.05	0.02	0.04
S	-	-	-	-	-	-	-	-
Qz	37.87	37.64	33.95	22.71	24.95	24.19	34.80	28.18
Or	29.03	32.00	10.53	14.35	31.83	31.47	27.46	32.20
Ab	28.11	24.64	51.24	40.43	30.89	32.33	31.10	28.05
An	0.16	0.21	0.21	10.24	3.62	4.55	1.85	4.85
Cor	2.75	2.96	1.82	-	1.60	1.08	1.97	1.82
Hy	0.54	0.79	0.80	6.96	5.54	4.32	1.86	1.54
Mt	1.15	1.03	1.19	2.09	0.72	1.21	0.67	2.55
Hm	0.12	0.44	-	-	-	-	-	-
Ilm	0.17	0.20	0.17	0.91	0.64	0.62	0.20	0.58
Ap	0.04	0.04	0.04	0.28	0.16	0.19	0.04	0.16
Py	-	-	-	-	-	-	-	-
DI	95.02	94.29	95.73	77.50	87.68	88.00	93.36	88.45
SI	2.25	3.14	3.08	13.05	6.20	5.52	2.71	4.27
				Includes 1.98% Di				

Table 6 continued:

Wt %	GPCS-22	ARCS	13325	13326	BBCS-1	BBCS-2	BBCS-3	BBCS-5
SiO_2	77.10	72.04	75.09	69.51	73.44	73.44	70.53	74.09
Al_2O_3	13.28	15.27	14.24	13.73	14.39	14.41	14.60	14.18
Fe_2O_3	0.42	1.31	0.56	1.62	0.51	1.18	0.87	0.54
FeO	1.04	1.65	0.95	2.13	1.64	1.15	2.63	1.45
MgO	0.29	0.34	0.31	1.14	0.30	0.29	0.47	0.18
CaO	0.11	0.22	0.40	4.20	0.47	0.43	1.36	0.51
Na_2O	4.98	3.09	4.01	6.69	3.38	3.73	3.35	3.41
K_2O	2.61	5.62	4.24	0.41	5.57	5.06	5.59	5.41
TiO_2	0.09	0.30	0.12	0.37	0.18	0.18	0.36	0.13
P_2O_5	0.01	0.08	0.02	0.10	0.04	0.04	0.11	0.02
MnO	0.04	0.04	0.02	0.06	0.04	0.05	0.08	0.04
S	-	-	-	-	-	-	-	-
Qz	36.74	31.04	33.69	20.61	29.98	30.62	24.61	31.25
Or	15.45	33.23	25.09	2.43	32.92	29.95	33.09	31.97
Ab	42.21	26.20	33.98	56.69	28.66	31.62	28.36	28.91
An	0.48	0.57	1.85	6.17	2.07	1.87	6.04	2.40
Cor	2.07	3.88	2.35	-	2.02	2.09	0.80	1.82
Hy	2.22	2.37	1.90	-	3.11	1.66	4.84	2.52
Mt	0.61	1.91	0.81	2.35	0.75	1.71	1.27	0.79
Hm	-	-	-	-	-	-	-	-
Ilm	0.17	0.57	0.22	0.70	0.34	0.34	0.68	0.24
Ap	0.02	0.18	0.04	0.23	0.09	0.09	0.26	0.04
Py	-	-	-	-	-	-	-	-
DI	94.41	90.48	92.78	79.73	91.58	92.20	86.07	92.13
SI	3.10	2.83	3.08	9.51	2.63	2.54	3.64	1.64
				Includes 10.06% Di				

Table 6 continued:

Wt %	BBCS-6	BBCS-7	BBCS-8	BBCS-9	11102	11103	20	30-b
SiO_2	75.16	74.91	75.35	75.57	70.05	75.84	75.89	72.03
Al_2O_3	13.34	13.78	13.85	13.96	14.91	13.56	13.62	14.00
Fe_2O_3	1.27	1.11	0.92	0.87	1.23	0.04	0.11	0.97
FeO	0.40	0.62	0.39	0.26	2.50	0.87	1.32	1.94
MgO	0.12	0.12	0.12	0.12	0.42	0.23	0.20	1.32
CaO	0.64	0.20	0.09	0.06	1.67	0.65	0.32	0.75
Na_2O	3.96	3.54	4.71	4.92	3.20	3.71	3.95	1.98
K_2O	5.02	5.59	4.54	4.18	5.41	5.00	4.47	6.60
TiO_2	0.05	0.07	0.02	0.02	0.38	0.05	0.05	0.28
P_2O_5	-	0.05	-	0.02	0.11	0.01	0.01	0.04
MnO	0.03	0.02	0.01	0.01	0.08	0.01	0.02	0.04
S	0.04	0.02	0.01	0.01	-	-	-	-
Qz	31.39	32.41	30.20	30.69	25.37	32.65	33.71	30.63
Or	29.66	33.01	26.84	24.72	32.01	29.59	26.46	39.05
Ab	33.49	29.97	39.85	41.62	27.08	31.44	33.49	16.80
An	3.13	0.66	0.47	0.19	7.59	3.16	1.52	3.46
Cor	0.25	1.66	1.02	1.27	0.99	0.86	2.31	1.70
Hy	0.29	0.40	0.29	0.29	4.14	2.08	2.79	5.67
Mt	1.12	1.61	1.22	0.79	1.79	0.06	0.16	1.41
Hm	0.49	-	0.08	0.32	-	-	-	-
Ilm	0.10	0.13	0.03	0.04	0.72	0.09	0.09	0.53
Ap	-	0.12	-	0.05	0.26	0.02	0.02	0.09
Py	0.07	0.03	0.02	0.02	-	-	-	-
DI	94.54	95.39	96.88	97.03	84.47	93.69	93.68	86.48
SI	1.11	1.09	1.12	1.16	3.29	2.34	1.99	10.30

Table 7: Chemical analyses and C.I.P.W. norms of the post-granitic minor acid intrusions

Wt %	MD-404	E-1	E-2	E-4	E-5	E-6	E-7	E-8	E-9	E-10	E-11
SiO_2	70.45	76.76	75.39	75.55	74.25	73.50	74.84	75.56	75.45	74.48	75.02
Al_2O_3	16.19	13.50	14.25	14.68	15.49	15.17	14.71	14.21	13.79	14.72	14.53
Fe_2O_3	1.21	1.07	0.74	0.40	0.65	1.77	0.92	1.64	1.73	0.50	0.50
FeO	0.95	0.26	0.29	0.72	0.20	0.27	0.49	0.31	0.32	0.77	0.71
MgO	0.12	0.12	0.12	0.12	0.11	0.44	0.12	0.46	0.44	0.12	0.12
CaO	1.09	0.13	0.51	0.15	0.17	0.49	0.22	0.43	0.16	0.30	0.40
Na_2O	3.37	3.39	3.95	3.53	4.28	1.76	3.28	2.98	0.83	3.72	3.52
K_2O	6.29	4.73	4.73	4.83	4.83	6.31	5.33	4.10	7.00	5.31	5.13
TiO_2	0.24	0.02	-	-	-	0.24	0.06	0.25	0.24	0.05	0.04
P_2O_5	0.04	-	-	-	-	0.03	-	0.03	0.02	-	-
MnO	0.05	0.02	0.02	0.03	-	0.02	0.03	0.02	0.02	0.02	0.03
S	0.01	0.01	0.01	0.01	0.01	0.01	0.01	0.01	0.01	0.01	0.01
Qz	24.21	38.48	33.02	35.57	30.29	37.50	34.67	40.96	42.87	31.25	33.50
Or	37.16	27.97	27.94	28.53	28.55	37.28	31.48	24.23	41.34	31.38	30.31
Ab	28.50	28.67	33.45	29.87	36.25	14.88	27.78	25.24	7.05	31.51	29.78
An	5.13	0.65	2.55	0.74	0.87	2.27	1.11	1.98	0.71	1.48	1.99
Cor	1.96	2.56	1.70	3.38	2.89	4.62	3.14	4.14	4.58	2.30	2.46
Hy	0.70	0.29	0.29	1.32	0.29	1.08	0.37	1.16	1.09	1.24	1.17
Mt	1.76	0.83	0.96	0.58	0.63	0.20	1.34	0.33	0.34	0.73	0.72
Hm	-	0.50	0.08	-	0.21	1.64	-	1.42	1.49	-	-
Ilm	0.45	0.04	-	-	-	0.46	0.11	0.47	0.46	0.10	0.07
Ap	0.10	-	-	-	-	0.06	-	0.06	0.04	-	-
Py	0.02	0.01	0.02	0.01	0.02	0.02	0.01	0.02	0.02	0.01	0.01
DI	89.87	95.12	94.41	93.97	95.09	89.65	93.93	90.44	91.26	94.14	93.58
SI	1.00	1.25	1.22	1.25	1.09	4.17	1.18	4.85	4.26	1.15	1.20

Table 8: Chemical analyses and C.I.P.W. norms of the Eastern Mourne granites

Wt %	MG-403	MG-1	MG-3	MG-5	MG-6	MG-8	MG-9	MG-10	MG-11	MG-12	MG-13
SiO_2	76.46	76.00	74.97	76.11	75.41	75.83	76.15	75.37	76.70	74.97	76.56
Al_2O_3	13.38	13.38	13.98	13.46	13.65	13.60	13.16	13.44	12.78	13.44	12.98
Fe_2O_3	0.86	0.55	0.86	0.66	0.70	0.54	0.37	0.68	0.44	0.56	0.40
FeO	0.55	0.75	0.52	0.54	0.73	0.73	0.91	0.77	0.90	0.94	0.92
MgO	0.24	0.17	0.12	0.12	0.12	0.12	0.12	0.12	0.12	0.12	0.12
CaO	0.26	0.63	0.63	0.62	0.70	0.57	0.60	0.75	0.68	0.77	0.59
Na_2O	2.97	3.40	3.55	3.90	3.74	3.60	3.63	3.70	3.39	4.14	3.34
K_2O	5.18	5.02	5.26	4.52	4.85	4.92	4.97	5.08	4.86	4.90	4.98
TiO_2	0.07	0.07	0.07	0.05	0.06	0.06	0.06	0.07	0.10	0.11	0.08
P_2O_5	-	-	-	-	-	-	-	-	-	0.01	-
MnO	0.03	0.03	0.03	0.03	0.03	0.03	0.03	0.03	0.03	0.04	0.03
S	0.01	-	0.01	0.01	0.02	0.02	0.01	0.01	0.01	0.02	0.01
Qz	38.34	34.99	32.58	34.45	33.11	34.25	33.98	32.32	36.22	29.86	36.07
Or	30.61	29.67	31.10	26.70	28.64	29.09	29.38	29.99	28.72	28.95	29.43
Ab	25.16	28.79	30.06	32.98	31.64	30.49	30.71	31.27	28.69	35.11	28.23
An	1.25	3.13	3.09	3.08	3.50	2.84	2.95	3.73	3.35	3.89	2.94
Cor	2.42	1.20	1.31	1.03	0.97	1.30	0.73	0.50	0.71	-	1.02
Hy	0.83	1.29	0.47	0.70	0.99	1.12	1.60	1.06	1.46	1.20	1.56
Mt	1.24	0.80	1.25	0.96	1.02	0.78	0.53	0.98	0.64	0.81	0.58
Hm	-	-	-	-	-	-	-	-	-	-	-
Ilm	0.13	0.13	0.13	0.09	0.10	0.10	0.12	0.14	0.18	0.22	0.14
Ap	-	-	-	-	-	-	-	-	-	0.01	-
Py	0.01	-	0.01	0.01	0.04	0.03	0.01	0.01	0.01	0.04	0.01
DI	94.11	93.45	93.73	94.13	93.39	93.83	94.06	93.58	93.63	93.92	93.74
SI	2.45	1.72	1.16	1.23	1.18	1.21	1.20	1.16	1.24	1.13	1.23

Table 8 continued:

Wt %	MG-14	MG-15	MG-16	MG-17A	MG-17B	MG-18	MG-19	MG-20	MG-21	MG-22
SiO_2	74.72	76.04	75.94	75.46	75.22	74.08	77.00	74.71	75.66	76.23
Al_2O_3	14.32	13.11	12.97	13.82	13.62	13.19	12.83	13.57	13.29	12.95
Fe_2O_3	0.22	0.57	0.59	0.49	0.51	0.45	0.57	0.76	0.74	0.73
FeO	0.79	0.91	1.00	0.75	0.89	1.00	0.64	0.95	0.76	0.75
MgO	0.12	0.12	0.12	0.12	0.12	0.12	0.12	0.16	0.12	0.12
CaO	0.55	0.68	0.77	0.59	0.65	0.89	0.51	0.87	0.60	0.78
Na_2O	4.33	3.44	3.44	3.70	3.95	4.94	3.20	3.52	3.60	3.25
K_2O	4.93	4.99	5.01	5.02	4.94	5.12	5.04	5.27	5.09	5.07
TiO_2	-	0.10	0.13	0.03	0.07	0.13	0.06	0.15	0.10	0.09
P_2O_5	-	-	-	-	-	0.02	-	-	-	-
MnO	0.03	0.03	0.03	0.03	0.03	0.03	0.02	0.04	0.04	0.03
S	0.01	0.01	0.01	0.01	0.01	0.03	0.01	0.01	0.01	0.01
Qz	28.73	34.83	34.41	32.90	31.26	24.81	37.53	31.54	33.48	35.79
Or	29.13	29.49	29.62	29.64	29.18	30.28	29.79	31.12	30.10	29.98
Ab	36.64	29.07	29.09	31.27	33.42	39.31	27.10	29.83	30.44	27.47
An	2.72	3.38	3.79	2.90	3.22	3.20	2.51	4.28	2.97	3.85
Cor	0.86	0.82	0.50	1.24	0.60	-	1.18	0.50	0.77	0.70
Hy	1.61	1.37	1.47	1.26	1.44	1.34	0.93	1.32	0.97	0.96
Mt	0.31	0.83	0.85	0.71	0.73	0.70	0.83	1.10	1.07	1.05
Hm	-	-	-	-	-	-	-	-	-	-
Ilm	-	0.20	0.25	0.06	0.13	0.25	0.12	0.28	0.19	0.17
Ap	-	-	-	-	-	0.06	-	-	-	-
Py	0.01	0.01	0.01	0.01	0.01	0.05	0.01	0.02	0.01	0.02
DI	94.49	93.39	93.12	93.81	93.86	94.39	94.42	92.49	94.02	93.24
SI	1.16	1.20	1.18	1.19	1.15	1.03	1.25	1.50	1.16	1.21

The Mourne cone-sheet granophyres are mainly characterized by their high SiO_2 content which shows only slight difference from sample to sample. Another characteristic feature is the excess of Al_2O_3 which is expressed as normative corundum varying between 0.25% and 5.33%. Almost all the cone-sheet granophyres have an overall low content of total iron oxides, CaO, MgO, TiO_2, P_2O_5, S and MnO. The Mourne granite samples, however, contain even lower proportions of these oxides which indicate that the larger intrusions are much more differentiated than the surrounding cone-sheet granophyres.

The variation in the K_2O content seems to be closely associated with the proportion of Na_2O except for the specimens 90-b and GPCS-22, in which K_2O content decreases to 1.78% and 2.61%, whereas the proportion of Na_2O increases to 6.05% and 4.98%, respectively.

On the other hand, in specimens 30-b, E-6 and E-9, the K_2O content amounts to 6.60%, 6.31% and 7.00%, while the Na_2O decreases to 1.98%, 1.76% and 0.83%, respectively.

Specimens GPCS-14 and 13326 which are hybrid in nature were also included in the table of chemical analyses in order to show and compare the degree of hybridization of samples 90-b and GPCS-22, all from the Glasdrumman Port cone-sheet granophyres. Thus, the decrease in K_2O content may be attributed to hybridization of acid rocks by surrounding basic material.

d.2) Chemical composition of the alkali feldspar phenocrysts from the Mourne cone-sheet granophyres

Five alkali feldspar phenocrysts of samples GPCS-16, 90-b, ARCS, 11102 and 11103 collected from the central parts of the composite cone-sheets were separated for chemical analysis which was carried

out by X-ray fluorescence spectrograph using the international and secondary standards. Iron, magnesium and other minor oxides were determined to be very low. Using the standard wet chemical methods neither combined water nor FeO could be detected. The results are given in Table 9. The values calculated for the Z group (Si, Al, Fe^{3+}) and X group (Mg, Ca, Na, K) on the basis of 32 oxygens are fairly close to the theoretical formula $(K, Na, Ca)_4 (Si, Al)_{16} O_{32}$. The general tendency is for a slight excess in the Z group with a varying range from 16.10 to 16.20, while the X group shows deficiency varying between 3.38 and 3.76, in comparison with the theoretical values of 16 and 4, respectively, indicating the alteration of alkali feldspar phenocrysts into kaolinite.

Two additional analyses of the alkali feldspar phenocrysts, carried out by electron microprobe were also included in Table 9 for comparative purposes.

d.3) Trace element contents of the acid rocks

42 granophyre samples including 10 specimens from post-granitic minor acid intrusions within the Eastern Mourne granite massif, and 21 granite samples have been analysed by the standard X-ray fluorescence method for their trace element content.

A rotating circular holder with Mylar window beneath aluminium cover top locked by a plastic cover was used as a powder holder during the analysis.

Analyses of 7 trace elements from the acid rocks of the Mourne area are tabulated in Tables 10, 11, and 12.

Table 9: Analyses of alkali feldspar phenocrysts from the porphyritic granophyre cone-sheets of Glasdrumman Port and Bloody Bridge River

	GPCS 16 F	90-b F	ARCS F	11102 F	11103 F	GPCS 16 F*	BBCS 3 F*
SiO_2	65.65	65.01	64.90	65.53	65.08	66.25	63.61
Al_2O_3	19.34	19.84	20.30	20.32	19.87	19.21	19.87
Fe_2O_3	0.25	0.29	0.39	0.40	0.29	0.19	0.18
FeO	-	-	-	-	-	-	-
MgO	0.11	0.11	0.11	0.11	0.11	-	-
CaO	0.23	0.54	0.81	0.86	0.56	0.18	0.10
Na_2O	2.54	3.35	3.59	2.92	3.18	2.32	3.41
K_2O	11.69	10.46	9.49	9.43	10.46	11.74	12.75
Total	99.81	99.60	99.59	99.57	99.55	99.79	99.92
2 V	52^o-53^o Includes 0.2% Ba	62^o-63^o Includes 0.4% Ba	67^o Includes 0.2 % Ba	65^o-67^o Includes 0.2% Ba	60^o Includes 0.2% Ba	52^o-53^o *Electron-Probe analyses	60^o
	Numbers of ions on the basis of 32 Oxygens						
Si	11.932	11.820	11.758	11.833	11.827	12.016	11.696
Al	4.133	4.245	4.329	4.313	4.255	4.092	4.303
Fe^{+3}	0.033	0.033	0.054	0.054	0.033	0.022	0.022
Mg	0.033	0.033	0.033	0. 033	0.033	-	-
Ca	0.044	0.109	0.152	0.162	0.109	0.033	0.022
Na	0.894	1.179	1.262	1.019	1.113	0.805	1.214
K	2.716	2.434	2.197	2.167	2.422	2.721	2.990
Z	16.10	16.10	16.14	16.20	16.11	16.13	16.02
X	3.69	3.76	3.64	3.38	3.68	3.56	4.22
Mol % (Or	74.3	65.4	60.8	64.7	66.5	76.5	70.8
Mol % (Ab	24.5	31.7	34.9	30.4	30.5	22.6	28.7
Mol % (An	1.2	2.9	4.2	4.8	3.0	0.9	0.5

Table 10: Trace element analyses of the pre-granitic cone-sheet granophyres

Sample No.	Ba(ppm)	Sr(ppm)	Rb(ppm)	Zr(ppm)	Ni(ppm)	Cu(ppm)	Zn(ppm)
124-b'	673	42	247	559	5	22	36
124-b''	878	50	239	502	7	23	43
124-b'''	1258	85	189	458	16	20	54
13338	857	56	258	509	7	11	54
13339	1474	81	203	459	10	11	59
120-a	244	26	165	522	5	9	50
120-b	341	14	193	520	5	8	34
120-c	374	27	174	557	5	8	31
88-b	274	24	187	492	5	9	33
89-b	287	26	235	516	5	8	32
90-b	286	22	66	496	5	8	44
GPCS-14	1300	149	179	442	12	8	60
GPCS-16	708	62	206	464	2	10	50
GPCS-19	785	68	202	477	7	9	48
GPCS-20	312	30	241	515	5	8	32
GPCS-21	734	65	207	479	5	10	54
GPCS-22	343	28	98	503	6	22	59
ARCS	771	58	168	487	7	8	58
13325	332	40	149	499	5	7	39
13326	1320	118	13	448	9	9	54
BBCS-1	817	64	238	541	5	9	39
BBCS-2	785	47	240	550	5	19	58
BBCS-3	1048	84	270	527	6	9	88
BBCS-5	342	25	234	488	4	8	50
BBCS-6	175	10	203	483	4	9	45
BBCS-7	265	21	275	474	5	10	32
BBCS-8	170	15	166	534	5	8	35
BBCS-9	216	17	192	534	5	7	35
11102	1122	90	231	520	6	9	81
11103	335	87	210	572	5	8	19
20	254	19	140	572	5	21	43
30-b	381	58	245	541	8	9	48
Average:	597	50	196	508	6	11	47

Table 11: Trace element analyses of the post-granitic minor acid intrusions

Sample No.	Ba(ppm)	Sr(ppm)	Rb(ppm)	Zr(ppm)	Ni(ppm)	Cu(ppm)	Zn(ppm)
Average:	210	7	511	210	5	8	30
E-1	148	2	543	178	5	8	9
E-2	132	1	472	107	5	8	20
E-4	135	2	830	254	5	9	27
E-5	137	2	571	213	5	8	12
E-6	400	18	343	272	5	9	35
E-7	136	3	470	186	5	8	41
E-8	356	25	325	284	5	8	51
E-9	374	16	492	287	4	10	57
E-10	147	3	533	172	5	8	24
E-11	142	1	530	151	5	7	25

Table 12: Trace element analyses of the Eastern Mourne granites

Sample No.	Ba(ppm)	Sr(ppm)	Rb(ppm)	Zr(ppm)	Ni(ppm)	Cu(ppm)	Zn(ppm)
MG403	178	19	445	151	5	8	28
MG-1	172	7	459	150	5	9	33
MG-3	219	6	467	184	6	8	39
MG-5	161	5	512	122	5	8	25
MG-6	171	6	544	171	6	6	30
MG-8	136	4	462	171	5	8	21
MG-9	165	3	470	161	5	7	23
MG-10	169	4	489	140	5	8	29
MG-11	203	13	382	166	5	8	29
MG-12	239	10	465	107	5	9	29
MG-13	176	5	414	148	5	8	25
MG-14	127	nil	715	275	2	8	16
MG-15	182	7	430	64	5	8	25
MG-16	230	11	404	178	5	9	24
MG-17A	134	3	454	176	5	7	25
MG-17B	170	11	455	144	5	8	28
MG-18	425	35	338	179	5	8	35
MG-19	175	4	393	149	5	8	27
MG-20	254	15	413	159	5	8	28
MG-21	178	8	510	158	5	8	21
MG-22	235	13	392	159	5	8	24
Average:	195	8	458	157	5	8	27

Barium:

There is a remarkable distinction between the Ba content of pre-granitic and post-granitic granophyres and that of the Eastern Mourne granites. With an average concentration of 597 ppm. the pre-granitic cone-sheet granophyres contain almost three times more Ba than the Eastern Mourne granites and the post-granitic acid intrusions. The depletion in Ba in the Eastern Mourne granites and minor acid intrusions is closely associated with the enrichment in Rb in these rocks. This depletion is also associated with similar depletion in Sr as will be seen below.

Strontium:

Like barium, this element shows relatively higher concentrations in the pre-granitic granophyres than the granites and post-granitic acid intrusions. While the latter have an arithmetic mean of 8 ppm. the former contain up to 50 ppm. on average.

Geochemically speaking, Sr and Ba are found in a close relation to each other and their behaviour has long been significant from the point of view of differentiation. The low Sr and Ba figures indicate that a highly differentiated magma was a source in forming the Eastern Mourne granites and post-granitic minor acid intrusions. This can be represented by a plot relating the differentiation index (DI of Thornton and Tuttle, 1960) and Sr content of the acid rocks. From Figure 7, it is seen that both granites and post-granitic acid

---

Fig. 7: A plot relating DI and Sr ratios in the Mourne acid rocks. Symbols denote: o pre-granitic cone-sheet granophyres, ⊕ post-granitic minor acid intrusions, • Eastern Mourne granites.

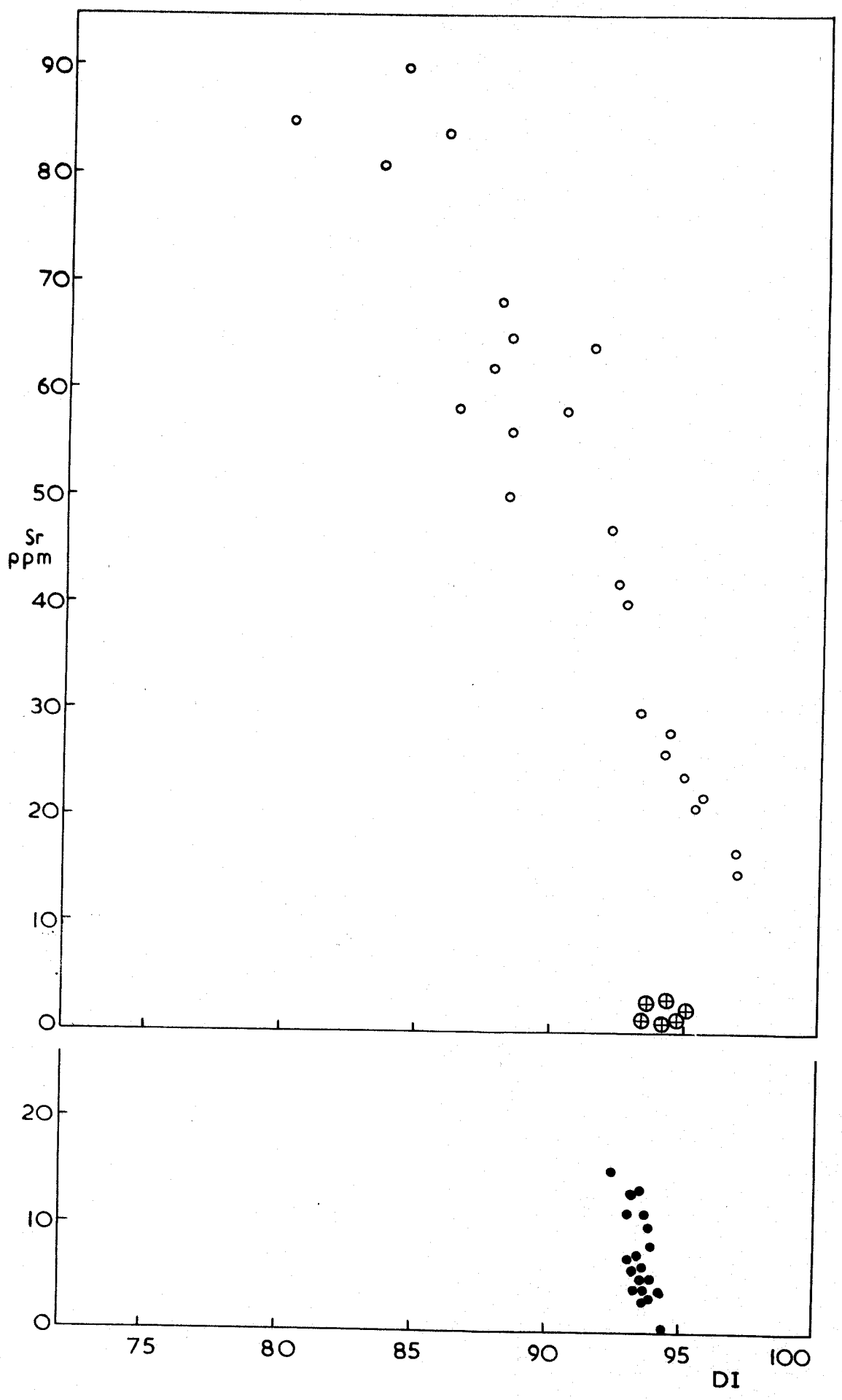
90
80
70
60
50
Sr
ppm
40
30
20
10
0
20
10
0
75
80
85
90
95
100
DI

intrusions have the similar trend, but the pre-granitic cone-sheet granophyres show comparatively different trend.

There is a relation between Sr and Ca contents of the granitic rocks as suggested by Nockolds and Allen (1953) on the variable behaviour of the Sr variation curve for different provinces. The difference is attributed to the amount of plagioclase remaining from the magma. If much plagioclase is removed, the Sr content will decrease in the residual liquid, whereas if relatively little is removed, Sr will tend to increase. Thus the low Ca content of the acid rocks may be held responsible for the low Sr concentrations in them. From the petrography of these rocks it is recalled that both modal and normative plagioclase content of the acid rocks are much less than those of the alkali feldspar content.

Rubidium:

The close association of K and Rb in igneous rocks has been widely recognized and proved that anomalously low K/Rb ratios are common in highly differentiated igneous rocks. By using the international standards W-1 and G-1, Rb content was determined in them. The standards gave 23 and 220 ppm. Rb respectively which are in good agreement with the recommended value for Rb in the former between 25 and 30 ppm., and 215 to 240 ppm. in the latter (Taylor et al., 1956). The analytical results are tabulated in Tables 13 and 14. It is seen from the tables that the average K/Rb ratio in the pre-granitic cone-sheet granophyre is 212, whereas it falls down to 93 in the granites and to 90 in the post-granitic minor acid intrusions.

Table 13: Geochemical data for the pre-granitic cone-sheet granophyres

Sample No.	%K	ppm Rb	K/Rb
124-b'	5.17	247	209
124-b''	4.97	239	208
124-b'''	4.53	189	240
13338	5.37	258	208
13339	5.19	203	256
120-a	3.50	165	212
120-b	4.28	193	222
120-c	3.72	174	214
88-b	4.08	187	218
89-b	4.49	235	191
90-b	1.48	66	224
GPCS-14	2.01	179	112
GPCS-16	4.46	206	217
GPCS-19	4.41	202	218
GPCS-20	3.85	241	160
GPCS-21	4.52	207	218
GPCS-22	2.17	98	221
ARCS	4.66	168	277
13325	3.52	149	236
13326	0.34	13	261
BBCS-1	4.62	238	194
BBCS-2	4.20	240	175
BBCS-3	4.63	270	172
BBCS-5	4.48	234	191
BBCS-6	4.17	203	205
BBCS-7	4.63	275	168
BBCS-8	3.77	166	227
BBCS-9	3.47	192	181
11102	4.48	231	194
11103	4.15	210	198
20	3.71	140	265
30-b	5.47	245	223
Average:	4.01	196	212

Table 14: Geochemical data for the post-granitic minor acid intrusions and the Eastern Mourne Granites

Sample No.	%K	ppm Rb	K/Rb
E-1	3.93	543	72
E-2	3.92	472	83
E-4	4.00	830	48
E-5	4.01	571	70
E-6	5.23	343	152
E-7	4.42	470	94
E-8	3.40	325	104
E-9	5.80	492	118
E-10	4.40	533	82
E-11	4.25	530	80
Average:	4.34	511	90
MG-1	4.16	459	91
MG-3	4.36	467	93
MG-5	3.75	512	73
MG-6	4.02	544	74
MG-8	4.08	462	88
MG-9	4.12	470	87
MG-10	4.21	489	86
MG-11	4.03	382	105
MG-12	4.06	465	87
MG-13	4.13	414	100
MG-14	4.09	715	57
MG-15	4.14	430	96
MG-16	4.15	404	103
MG-17A	4.16	454	92
MG-17B	4.09	455	90
MG-18	4.25	338	126
MG-19	4.18	393	106
MG-20	4.37	413	106
MG-21	4.22	510	83
MG-22	4.21	392	107
MG-403	4.30	445	97
Average:	4.15	458	93

Figure 8 shows the close association of K and Rb. The great majority of results fall within the limits of scatter in Figure 1 of Ahrens et al. (1952, p.240). They represent the pre-granitic cone-sheet granophyres. On the other hand, all the Eastern Mourne granites and the post-granitic minor acid intrusions fall beyond the limits of scatter. Those off-scatter samples display relative enrichment in Rb. In other words the normal K/Rb relation holds true for the pre-granitic cone-sheet granophyres, but the granites and the post-granitic minor acid intrusions show anomalously low K/Rb ratios.

The enrichment in Rb content of the igneous rock is a well-known feature in the crystallization products of late-stage small volume residual solutions, e.g., aplites, pegmatites (Rankama and Sahama, 1950, pp.436-439; Ahrens et al., 1952, p.239; Ahrens, 1953, p.11; Nockolds and Allen, 1953, p.137; Taylor et al., 1956, p.228). It is an unusual feature in normal igneous rock.

The low K/Rb ratios in the Eastern Mourne granites and the post-granitic acid intrusions suggests that these rocks have crystallized from a magma which had undergone differentiation to a degree typical of the pegmatitic phase rather than the less extreme differentiation common in normal acid igneous rocks. At this stage, the magma may have become impoverished in certain trace elements common in less highly differentiated acid rocks.

Fig. 8: K/Rb ratios in the Mourne acid rocks.

⤫ Limits of scatter (Ahrens et al., 1952, fig. 1). W_E-1, G_E-1: Analytical values reported in this study. W_A-1, G_A-1: Analytical values quoted from Taylor et al. (1956). Symbols refer to: o pre-granitic cone-sheet granophyres, ⊕ post-granitic minor acid intrusions, ● Eastern Mourne granites.

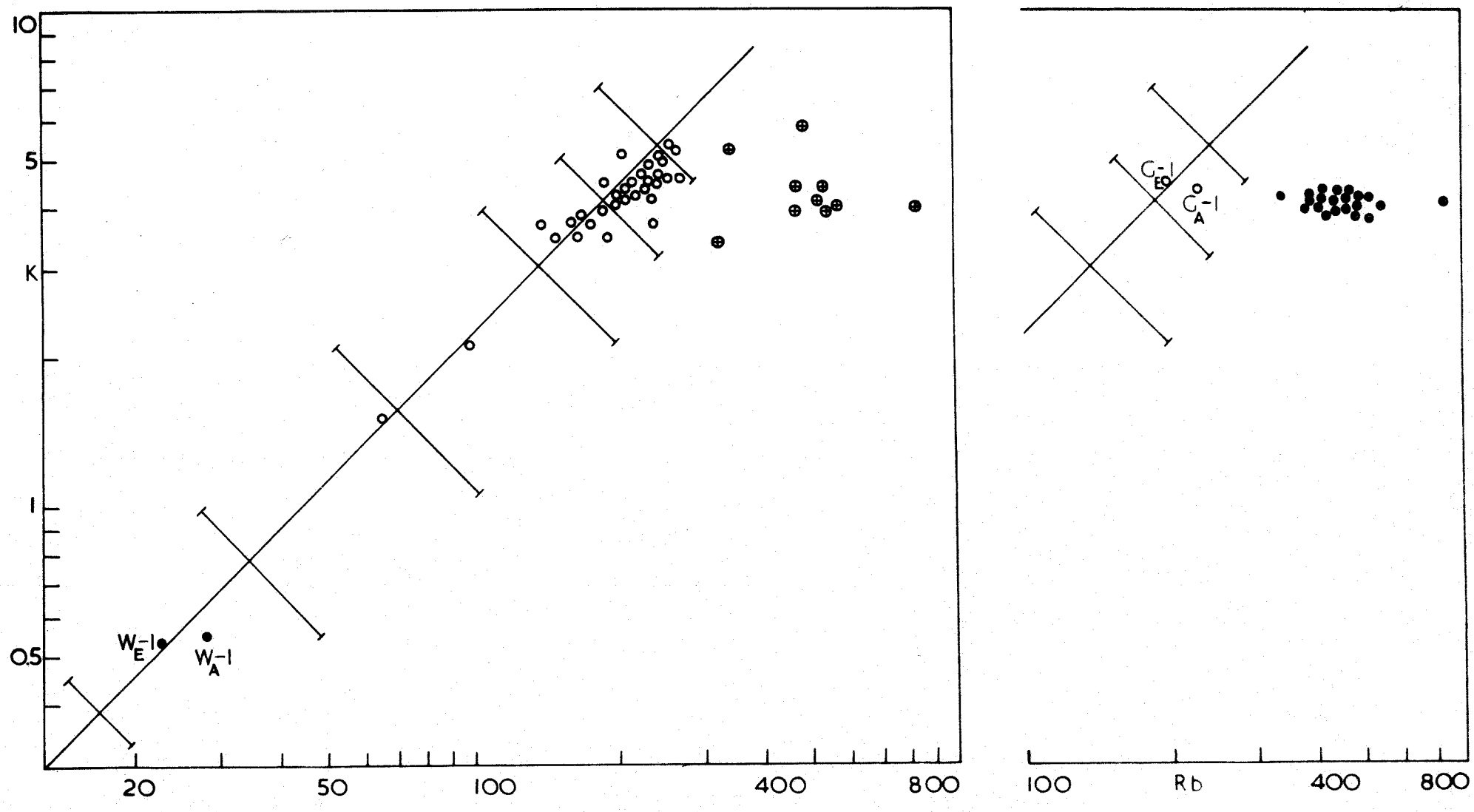
10
5
K
1
0.5
W_E-1
W_A-1
20
50
100
400
800
G_{EO}-1
G_A-1
100
Rb
400
800

Table 15 gives comparison of the arithmetical means of 42 determinations of Ba, Sr and Zr in the North American granites, the mean of end products of the Western Mourne and St. Austell granites and the mean of the 21 Eastern Mourne granites. From the table it is seen that these elements are markedly less abundant than the granite averages with an only exception of Zr in the Western Mourne granites. For Skye granites and granophyres similar depletion in Ba and Sr has been found at the extreme acid end of the differentiation sequence (Taylor et al., 1956, p.228).

Zirconium:

Like barium the Zr content of the pre-granitic cone-sheet granophyres is more than that of the value found in the Eastern Mourne granites and the post-granitic acid intrusions. The average Zr concentration is 508 ppm. in the former rocks in comparison with 157 ppm. and 210 ppm. in the latter, respectively. In other words, the mean is more than three times the mean of 42 North American and 21 Eastern Mourne granites. The depletion of Zr is closely associated with the concomitant depletions in Ba and Sr.

Nickel and copper:

Among the 7 trace elements determined in the acid rocks from the Mourne area, Ni and Cu do not display any significant difference between the amounts found in these rocks. As a whole the amount of Cu is slightly higher than the Ni concentration in the acid rocks.

Although Cu is geochemically chalcophile, it is probable that in some instances, it also enters into the structures of the rock-forming silicates (Rankama and Sahama, 1950), but the present study

Table 15: Arithmetical means of some trace element content of different granite suites for comparison

Sample Source	Ba	Sr	Zr	Reference Source
St. Austell granites	105	60	47	Taylor et al., 1956.
Western Mourne granites	230	45	310	Taylor et al., 1956.
Eastern Mourne granites	195	<10	157	Present study.
North American granites	1300	180	170	Taylor et al., 1956.

gives no evidence to substantiate this view. The reported Cu content for an average acid igneous rock is 38 ppm. (Rankama and Sahama, 1950), as compared with the crustal abundance of Cu being about 60 to 70 ppm. As a whole the Cu concentration in the acid rocks from the Mourne area keeps constant throughout the region and is about 9 ppm. on average.

Ni shows no variation regardless of Fe^{2+} and Mg^{2+}. The Mg content is very low in the acid rocks from the Mourne area, and like Cu, Ni amount keeps constant throughout the acid igneous complex. The average Ni content is 5 ppm. in all the acid rocks from the Mourne area, while its value reaches as much as 100 ppm. in the upper lithosphere (Goldschmidt, 1954).

Zinc:

The crustal abundance of Zn is 40 ppm. (Goldschmidt, 1954). An average value of 47 ppm. has been found in the pre-granitic cone-sheet granophyres and it drops down to 30 and 27 ppm. in the post-granitic minor acid intrusions and the granites, respectively. Geochemically there is no significance of this slight difference in Zn content between the pre- and post-granitic acid rocks.

CHAPTER IV

BASIC ROCKS

a) Classification of the basic rocks

In studies of the basic rocks where the chemical composition of a magma is the principal concern, it is convenient to adopt a normative (i.e. indirect chemical) classification rather than a modal (mineralogical) classification (Green, 1969, p.410; 1970, p.221).

The widely used CIPW normative classification of Yoder and Tilley (1962) is such an indirect chemical classification in the reference basalt tetrahedron (Figure 9). By virtue of their position within this tetrahedron, basalts are termed tholeiites, olivine-tholeiites and alkalic basalts. The objective grouping of this classification is desirable, but tends to create artificial clarity, particularly in the case of olivine-tholeiites.

Poldervaart (1964) showed that some Hy-normative basalts do not possess olivine reaction relationships, i.e., those falling in the volume Di-Fo-Ab-X in the reference basalt tetrahedron (Figure 9). The volume Di-Fo-Ab-SiO_2 should be, according to Yoder and Tilley (1962), alien to alkalic basalts at low pressures, and is indeed so to Ne-normative basalts when these are plotted in the basalt tetrahedron. But here also an area exists where there is no reaction relationship between olivine and orthopyroxene; the area between the

---

Fig. 9: Reference basalt tetrahedron in the system silica-nepheline-diopside-forsterite. (After Poldervaart, 1964, p.230, fig.1).

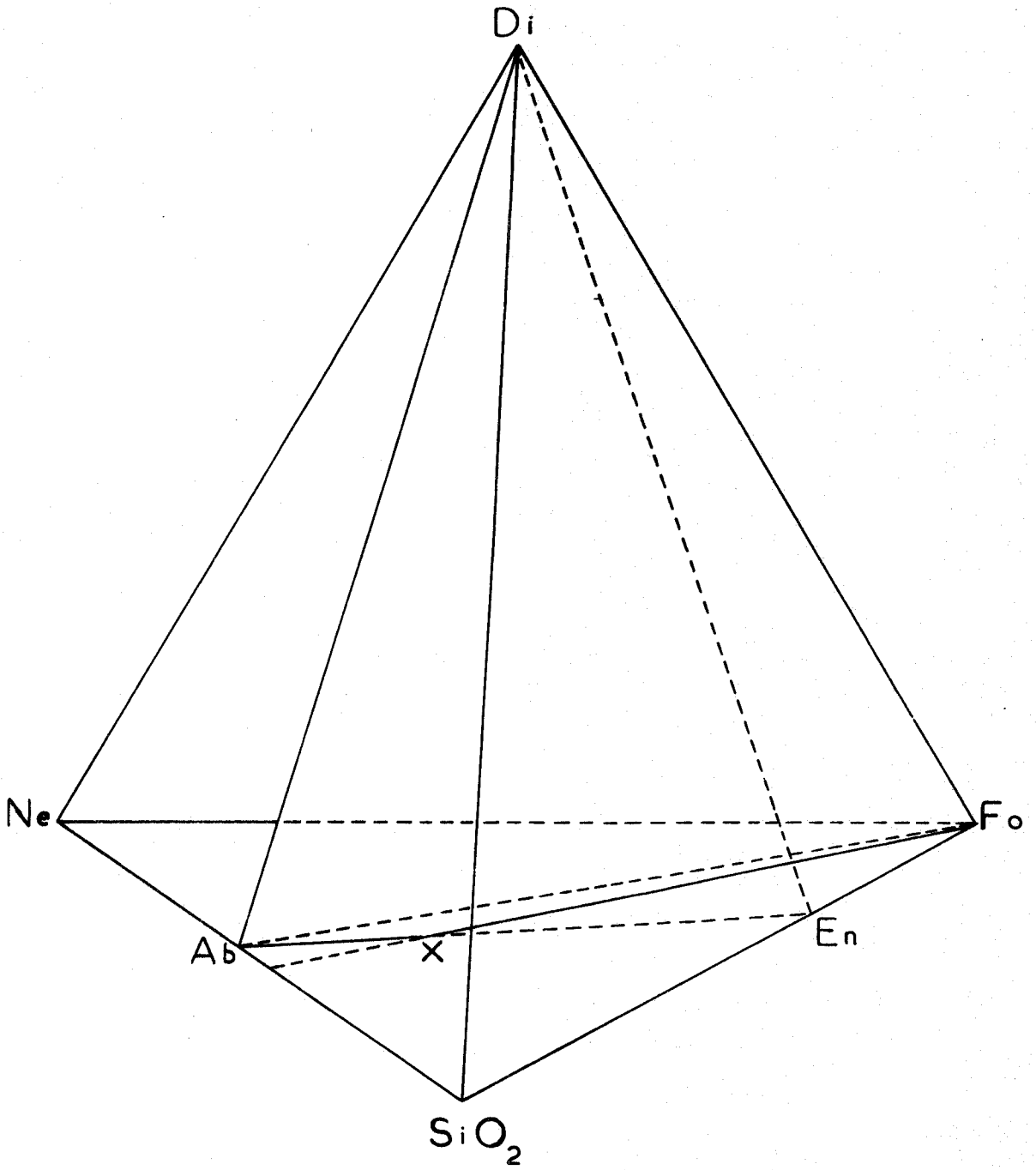
Di
Ne
Fo
Ab
X
En
SiO2

Fo-Di join and a line drawn from the Fo corner to the thermal divide on the Di-Opx join. Basalts plotting in this wedge-shaped area of the tetrahedron (Figure 9) are petrographically alkalic basalts, as shown by Poldervaart (1964, p.231), although Hy-normative. The presence of such basalts is not accounted for in the classification of Yoder and Tilley, where they would be placed together under the heading "olivine-tholeiites" (containing normative Ol and Hy), thus often giving the false impression of a tholeiitic parentage.

The term olivine basalt which formerly spanned a considerable range of basalt compositions, as applied in common usage, was allocated by Yoder and Tilley to basalts with normative Ol only. As pointed out by MacDonald and Katsura (1964), this reduces the olivine basalts almost to a vanishing point, as very few olivine basalts indeed have neither Ne nor Hy in the norm.

A classification scheme for the basic rocks of the Mourne area must serve to identify and separate the two basaltic series, alkalic basalts on the one hand and tholeiites on the other. To this end a chemical classification is adopted based on a number of factors. The main factors employed are the differentiation index of Thornton and Tuttle (1960, DI : sum of normative Qz, Ab, Or and Ne when present), the weight percentage of various oxides, the CIPW normative mineralogy, the solidification index of Kuno (1968, SI: $MgO \times 100/MgO + FeO + Fe_2O_3 + Na_2O + K_2O$), and the trace element data, particularly the concentration of strontium.

The division of the basaltic types within each rock series is facilitated by the value of the solidification index which is a more sensitive measure of the chemical variation in basaltic rocks than the index of differentiation which is better suited to intermediate and

acid rocks.

In the present study, the classification outlined by Yoder and Tilley (1962), based on the reference basalt tetrahedron is followed broadly, but for the definition of olivine basalts, which here is expanded on the basis suggested by Poldervaart (1964), to include the volume of some of the olivine-tholeiites.

The following terms are used to define the principal basic rock types in the Mourne area:

Quartz-tholeiite: basalt with normative Hy and Qz.

Tholeiite: basalt lying close to the plane of silica saturation, i.e., with Di, Hy and Pl as the principal normative constituents and very little Qz or Ol.

Olivine-tholeiite: basalt with normative Ol and Hy, but where Ab - 2 En (Hy) - 1.5 Fs (Hy) < 0. This value, quoted from Poldervaart (1964, p.232), serves to demarcate the olivine basalts and the olivine-tholeiites, and is referred to as the Poldervaart Index (PI). Ab is the normative content of albite, En and Fs are the normative contents of enstatite and ferrosilite in hypersthene, respectively. The Poldervaart Index is positive for the olivine basalts but negative for the olivine-tholeiites.

Olivine basalt: with normative Ol and Hy, but Poldervaart Index Ab - 2 En (Hy) - 1.5 Fs (Hy) > 0.

Alkali olivine basalt: with normative Ol and Ne, but with the latter less than 5%; no normative Hy.

Basanite: basalt with normative Ol and Ne, but with the latter more than 5%.

High-alumina basalt: aphyric basalt with normative Ol and either normative Hy or low normative Ne contents, but with Al_2O_3 content

distinctly higher (ca. 18-20%) than the normal olivine-tholeiites or alkali olivine basalts of similar silica and alkali contents.

The main pitfall of the normative classification is the question of post-magmatic oxidation which will, of course, shift the rock composition towards the silica corner in the normative, reference basalt tetrahedron.

Post-magmatic oxidation is common among the basic rocks of the Mourne area, and some oxidation has even demonstrably taken place during the fine grinding of the samples (Fitton and Gill, 1970, p.523).

b) Distribution and field characteristics of the basic rocks

The basic rocks comprise the bulk of the Mourne dyke-swarm and include undersaturated alkali basalts, olivine basalts and olivine-tholeiites; saturated tholeiites; and oversaturated quartz-tholeiites. They are fine to medium grained, dark coloured hypabyssal rocks with typically non-porphyritic, holocrystalline texture.

The dykes become very sparse towards the north near Newcastle, and to the south near Annalong, and thus are best developed to the east and SE of the Eastern Mourne granite massif. There are, however, a few outcrops in the Glen River and Shimna River, north of the granites (cf. Map 1).

Sand dunes fringing the whole of Dundrum Bay separate the Killough-Ardglass dyke swarm, which is located some 15 km. NE of Newcastle, from the Mourne swarm (Figure 2). Similar alkali basalt dykes are abundant at either end of this shore and there may therefore be further representatives beneath the sands.

The basic rocks of the Mourne dyke-swarm can be subdivided into two main groups:

1) alkali basalts (Plateau Magma type of Mull),

2) tholeiites (Non-Porphyritic Central Magma type of Mull, Bailey et al., 1924).

In the northern part of the Mourne area the dykes belong exclusively to the group of alkali basalts, whereas tholeiitic rocks make their appearance towards the south in the densest part of the swarm. The distinction between the two groups is by no means an easy task in the field. The alkali basalts reappear in the Killough-Ardglass dyke swarm, especially at its southern exposures near St. John's Point area (Figure 2).

In thickness, the Mourne dykes vary from a few cm. to 9 m. but the majority do not exceed 3 m. The average thickness is 2 m. They occur as upstanding walls, as troughs, or level with the country rock, depending upon their resistance to weathering. Jointing is developed both parallel with, and at right angles to, the contacts with the country rock. When developed at right angles to the cooling face, the dyke assumes a columnar habit, often to a marked degree. Some of these joints pass out of the dykes into the country rocks where they are often marked by chloritic and epidotic veinlets and streaks. The dykes are frequently sinuous and often exhibit thinning out, forking, swelling, and abruptly terminating with echelon structure.

The expansion of the earth's crust due to the intrusion of the dykes amounts to 2.5%, a figure considerably less than that obtained for the Arran swarm (6.9%) and the Mull swarm (3.8%), but more than that for the Killough-Ardglass dyke swarm (0.77%), (Tomkeieff and Marshall, 1940).

c) Petrography of the basic rocks

The basic rocks of the Mourne area are mainly composed of augite and plagioclase with subordinate amounts of olivine, opaque Fe-Ti oxide minerals and chlorite, set in a fine-grained holocrystalline groundmass.

Many of the thick dykes have a doleritic central portion and a basaltic marginal zone. They are either olivine dolerite-olivine basalt or dolerite-basalt without olivine. The somewhat thinner dykes are independently formed by olivine basalts and tholeiites.

c.1a) Alkali basalts:

The plagioclase of the alkali basalts occurs as moderately large phenocrysts and as groundmass, lath-shaped microlites. The size of the phenocrysts varies between 0.5 mm. and 1 mm. whereas microlites have much smaller dimensions ranging from 0.03 mm. to 0.1 mm. in length. The plagioclase phenocrysts have a strong tendency to idiomorphism, with columnar or sometimes tabular habit. Twinning on the albite law is quite common, and is often combined with Carlsbad twinning. On the other hand, groundmass plagioclase laths are usually too narrow to show repeated twinning. Zoning in the phenocrysts is not very common, although one example (No.128) exhibits a wide compositional range from core (An_{75}) to margin (An_{45}).

Modally, plagioclase phenocrysts form up to 6-7% by volume, but groundmass plagioclase microlites are very much higher in proportion (35-50%). Normative plagioclase content of the alkali basalts varies between 40% and 55%.

Chemically, the plagioclase phenocrysts are bytownite to labradorite in composition, ranging between An_{75} and An_{65}. The compositions are expressed in terms of weight per cent, unless otherwise stated, and

are derived from the electron microprobe analyses.

Groundmass plagioclase is generally of An_{50-45} composition. The normative plagioclase composition in the average alkali basalts is An_{62-52}.

Augite forms scattered, relatively coarse phenocrysts in most of the alkali basalts. It is, however, always present as a major ferromagnesian mineral in the groundmass, forming purplish-brown tinted crystals which are commonly titaniferous and are invariably more abundant than the groundmass olivine. The augite phenocrysts often have good crystal forms, but the augite of the groundmass is either in little idiomorphic prisms or in granules. The size of the groundmass pyroxene is about 0.04 to 0.06 mm. whereas phenocrysts of augite sometimes reach 0.7 mm. in length. The groundmass pyroxenes show good ophitic texture as seen in thin section, being moulded around or between the columnar crystals of plagioclase which show more or less elongated sections with no law of arrangement (Plate 5).

The augite phenocrysts of alkali basalts are all Ca-rich varieties, and have a compositional range from $Wo_{46}\ En_{34}\ Fs_{20}$ to $Wo_{39}\ En_{36}\ Fs_{25}$. All the compositions given are again based on the electron microprobe analyses, and are expressed in terms of molecular per cent.

The modal analyses of some of the alkali basalts show 16 to 32% augite phenocrysts, although normative pyroxenes are in the range from 10 to 25% with compositions of $Wo_{50}\ En_{30}\ Fs_{20}$.

On the whole, olivine-bearing dykes are scarce and in only a few cases (Nos. 129, 128 and 102) are the olivine microphenocrysts partly fresh. They do, however, occur as a groundmass phase. On the other hand, all the analysed undersaturated basic rocks, especially alkali basalts constantly show 12 to 30% olivine in their norms, having an

Plate 5: Textural features of the Mourne basic rocks: ophitic texture showing plagioclase laths surrounding augite (No: 128), x70, crossed nicols.

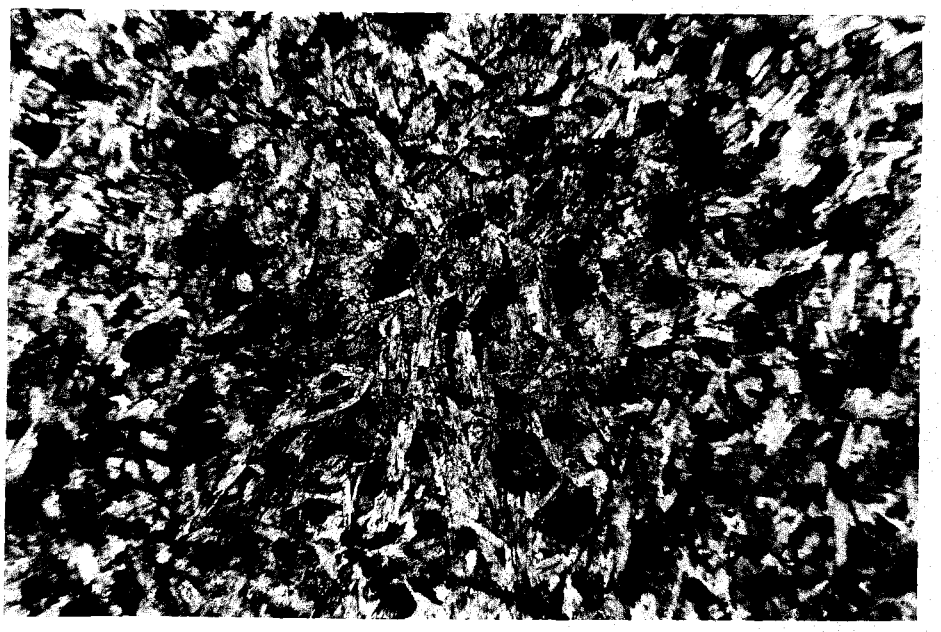

Plate 6: Textural features of the Mourne basic rocks: Intergranular texture showing plagioclase laths with olivine, pyroxene and magnetite grains (No.: 102), x45.

average of 21%.

The relatively uncommon olivine crystals have sometimes well defined crystal outlines, but in most cases, they are more or less rounded and often largely or completely serpentinized. Serpentine strings follow cleavage or other cracks formed in the crystals. The larger microphenocrysts have more magnesian cores of up to Fo_{82} (as determined by the electron microprobe and expressed in terms of molecular per cent). Analyses of olivine microphenocrysts and groundmass phases give a composition of Fo_{67-57}. The normative composition of olivine in the average alkali basalts is Fo_{67}.

The olivine crystals range in size from 0.02 mm. to 0.3 mm. Olivine to orthopyroxene reaction relationships have never been observed in the alkali basalts. The relative modal proportions of olivine microphenocrysts together with other constituent minerals in the basic rocks from the Mourne area are shown in Table 16.

Nepheline has not been positively identified in any of the alkali basalts in spite of its presence in the norm.

The iron-titanium oxide minerals include magnetite and ilmenite. A somewhat titaniferous magnetite, usually restricted to the groundmass, rarely forms euhedral microphenocrysts. Ilmenite is also present, being in the form of skeletal crystals. In some cases, the ilmenite shows alteration into leucoxene.

Chlorite is usually present as an alteration product of pyroxene.

c.1b) Olivine basalts:

Olivine dolerites and basalts are readily distinguished from alkali basalts by the absence of nepheline in their norms and in general, a very slightly Hy-normative character. The division of alkali basalts

Table 16: Modal analyses of the basic rocks from the Mourne area

Sample No.	Ground-mass	Plagio-clase laths	Plagio-clase pheno-crysts	Augite	Olivine	Fe-Ti Oxides	Chlorite (and others)
128	7.9	51.1	5.7	16.4	12.0	6.3	0.6
124-c	15.8	45.5	-	31.6	-	4.8	2.3
112-b	28.7	37.2	-	19.0	-	9.8	5.3
102	46.2	17.2	2.2	16.5	14.1	2.5	1.3
55-a	34.1	33.8	-	19.2	10.4	2.5	-
37-b	23.2	41.2	-	29.0	-	6.6	-
26-b	26.9	46.0	-	20.0	-	7.1	-
25-b	25.2	32.9	-	18.5	-	12.0	11.4
23	30.5	39.5	-	20.8	-	9.2	-
14	35.5	33.5	-	25.8	-	5.2	-
414	14.8	40.3	-	26.4	-	18.4	0.1

Key to the analyses:

Nos. 124-c, 112-b, 102 and 55-a: Olivine-tholeiites,

Nos. 37-b, 26-b, 23 and 14: Alkali basalts,

Nos. 25-b and 414: Quartz-tholeiites,

Nos. 128: Olivine basalt.

and olivine basalts is based on the solidification index, as well as on the normative characters.

Plagioclase forms phenocrysts which are sometimes zoned from An_{70} cores to An_{50-45} margins and the groundmass plagioclase is An_{45-50}.

Purplish augite is the sole pyroxene phase, forming somewhat large phenocrysts which, in most cases, is the major ferromagnesian groundmass mineral.

Olivine, although rare, occurs as microphenocrysts having the compositions of Fo_{78} to Fo_{70}.

Magnetite is more abundant than in the alkali basalts, forming irregular microphenocrysts.

No pigeonite was found to be present in the olivine basalts.

Chlorite often forms patches around the plagioclase phenocrysts as an alteration product of augite.

c.2) Tholeiites:

The rocks belonging to the tholeiitic group are well represented in the Mourne area, forming more than one-third of the total number of dykes. They include many varieties ranging from undersaturated to oversaturated types.

The mineral assemblage consists of plagioclase from bytownite to calcic andesine-sodic labradorite, pale brown augite, pigeonite, chlorite and opaque iron ore.

c.2a) Olivine-tholeiites:

Almost all the olivine-tholeiites are fine grained rocks (Nos. 100, 101, 102, 104, 105, 112, 115, 116, 117, 118, 119, 121, 124, 125,

126 and 127) with subophitic to intergranular texture in a groundmass consisting essentially of augite granules, plagioclase laths, magnetite and chlorite.

Plagioclase phenocrysts are generally present as moderately large euhedral and calcic grains (An_{80-70}), whereas groundmass plagioclase is An_{60-45}. The normative plagioclase content of the olivine-tholeiites is about 50% with the composition of An_{60-70}. The size of the phenocrysts is around 0.8 mm. in length, although the groundmass laths, being 0.05 mm., are much smaller in size.

In most cases, augite distinctly wraps round the plagioclase laths, and often forms plates of some extent, enclosing many of the plagioclase crystals. This may be due to the simultaneous crystallization of the two minerals. In other cases, the augite tends to form more or less rounded grains embedded in a network of lath shaped plagioclases, adjacent grains not being parts of one crystal but showing different orientations (Plate 6). This kind of intergranular texture (e.g. No. 102) is less common than the ophitic texture of the Mourne olivine-tholeiites. In both types, olivine, when present, is almost idiomorphic towards the augite, but is sometimes penetrated by the plagioclase laths. The commonest decomposition products of augite are pale green, fibrous or scaly aggregates of serpentinuous and chloritic substances. In many cases, patches of green chloritic material surrounds some of the groundmass plagioclase laths.

Occasional Ca-poor clinopyroxenes are sometimes present in the groundmass of the olivine-tholeiites (No. 93), as identified by their small optic axial angle.

Olivine, although rare, forms small irregular patches, largely serpentinized due to the alteration. Ovoidal, serpentinuous areas

may represent pseudomorphs after olivine microphenocrysts.

The groundmass of the olivine-tholeiites consists of intergranular augite and basic andesine or labradorite microlites, with interstitial iron ore and chlorite.

Iron-titanium oxides are mainly confined to the groundmass, although they occasionally form some euhedral microphenocrysts scattered throughout the rock.

c.2b) Pre-granitic quartz-tholeiites:

Plagioclase phenocrysts are sporadically present in the pre-granitic quartz-tholeiites of the Mourne dyke-swarm, with labradorite composition, but the majority of the plagioclase are in the form of lath shaped microlites confined to the groundmass.

Augite forms rare phenocrysts with large optic axial angle, but is usually found as a groundmass material. The texture is either subophitic or, with more abundant pyroxene, intergranular. Typical tholeiites with a distinct glassy groundmass are also present. The groundmass is often chloritized which may or may not have been glassy.

Iron-titanium oxides are abundant, forming euhedral microphenocrysts which range in size down to a groundmass fraction.

The contact facies of the tholeiites are very fine-grained. The margins of the moderately large dykes assume an aphanitic texture with a few microphenocrysts of plagioclase and augite, and only a thin tachylytic film with fluidal and microspherulitic texture at the actual contact.

c.2c) Post-granitic quartz-tholeiites:

Comparatively few basic dykes cut the Mourne granites. They are

sub-ophitic in texture, with euhedral labradorite laths enclosed by brownish augite.

Quartz-tholeiite dykes are either aphyric or contain scattered phenocrysts of plagioclase, An_{58-53}, zoned to An_{48} margins. Groundmass plagioclase has a composition in the range An_{50-40}. Thus the plagioclase phenocrysts and groundmass microlites are less calcic than those of the olivine-tholeiites.

Clinopyroxene forms microphenocrysts of augite, 0.1 - 0.3 mm. in diameter with moderate to high optic axial angle. Electron microprobe analyses of 3 grains from one of the post-granitic quartz-tholeiites (No.414) show almost a constant composition $Wo_{39}\ En_{37}\ Fs_{24}$ and $Wo_{40}\ En_{34}\ Fs_{26}$. In addition to augite microphenocrysts, there also exists a Ca-poor phase, mainly confined to the groundmass. Its composition is given as $Wo_{12}\ En_{54}\ Fs_{34}$, a magnesian pigeonite, with very small optic axial angle.

Iron-titanium oxides form abundant euhedral microphenocrysts as in the case of pre-granitic quartz-tholeiites, and are often enclosed by augite. Abundance in Fe-Ti oxides is clearly reflected by their normative contents as contrasted with the olivine-tholeiites.

All the quartz-tholeiite dykes are devoid of olivine, but contain interstitial quartz in the groundmass. Occasional xenocrysts of quartz, measuring 0.05 - 0.3 mm. in diameter, are highly corroded and embayed and invariably rimmed by prismatic clinopyroxene grains. Xenocrysts of alkali feldspar are also present in the groundmass in addition to quartz, representing small fragments of an acid rock, probably a granite, through which later more basic material was injected.

The quartz-tholeiites within the granitic massif are frequently altered, as shown by the presence of abundant chlorite.

d) Chemistry of the basic rocks

Tables 17 - 21 show the chemical compositions and the CIPW norms of the basic rocks from the Mourne area. Among them, the alkali basalts are typified by a high content of magnesia and consequently a high solidification index, which is combined with relatively low total iron and high total alkali contents. They all contain considerable amount of normative nepheline within the range of 0.3 to 5%, except in the case of Nos. 2, 3, 10, 54 and 504 which are basanites in the normative speaking.

Most of the pre-granitic dyke rocks in the southern part of the Mourne area show tholeiitic affinities. These rocks are typically low in combined alkalis and titania, but high in lime, resembling in this respect the so-called "primitive" olivine-tholeiites from ocean floors. They are also characterized by their high MgO content and high solidification index, but their total alkalis are very much lower than those of the alkali basalts.

More differentiated than the olivine-tholeiites, the tholeiites have differentiation indices ranging from 27 to 36 and are either very slightly Qz-normative or Ol-normative. There is a steady increase in total alkalis, silica and titania with decreasing MgO going from the olivine-tholeiites to the tholeiites and quartz-tholeiites of the southern Mourne region.

Prevailing high Al_2O_3 content in the alkali basalts and olivine-tholeiites places some of them in the high-alumina basalt type, characteristically displayed by the diagrams plotted in Figure 10. Basalts with Al_2O_3 content higher than 18% are termed high-alumina basalts in the present study, and there is only one basic rock having Al_2O_3 content more than 18% (No. 97; 19.53% Al_2O_3) which is an aphyric

Table 17: Chemical analyses and C.I.P.W. norms of the Mourne alkali basalts

Wt %	503	504	505	511	512	513	516
SiO_2	47.05	42.98	43.12	45.67	46.98	46.31	46.53
Al_2O_3	15.60	16.67	18.97	16.63	15.55	16.90	16.93
Fe_2O_3	3.59	5.04	4.26	3.38	2.18	1.60	4.54
FeO	8.06	8.62	8.97	7.67	7.66	8.56	7.26
MgO	10.20	9.27	6.47	12.56	11.83	9.48	10.33
CaO	10.65	10.31	14.09	9.59	10.78	12.02	9.32
Na_2O	2.71	3.49	1.54	2.98	2.75	2.78	3.14
K_2O	0.40	1.50	0.48	0.38	0.83	0.64	0.44
TiO_2	1.36	1.73	1.66	0.93	1.03	1.25	1.17
P_2O_5	0.17	0.20	0.22	0.06	0.14	0.17	0.14
MnO	0.21	0.20	0.22	0.14	0.18	0.21	0.20
S	-	0.01	0.02	0.02	0.09	0.08	-
Or	2.22	8.89	2.86	2.22	4.88	3.77	2.60
Ab	22.53	5.55	9.09	17.82	15.33	13.10	24.24
An	29.19	25.30	43.39	30.86	27.52	31.69	30.86
Ne	0.28	12.92	2.15	3.98	4.26	5.68	1.14
Di	18.31	19.89	20.46	13.10	20.29	21.84	11.55
Ol	19.25	16.38	12.18	25.15	22.07	18.70	20.42
Mt	5.20	7.31	6.17	4.90	3.16	2.32	6.58
Ilm	2.59	3.28	3.15	1.77	1.96	2.37	2.28
Ap	0.41	0.46	0.51	0.14	0.33	0.39	0.34
Py	-	0.02	0.04	0.04	0.17	0.15	-
DI	25.03	27.36	14.10	24.02	24.47	22.55	27.98
SI	40.86	33.20	29.79	46.57	46.85	41.11	40.18

Table 17 continued:

Wt %	2	3	10	11	14	18	19
SiO_2	45.60	45.26	44.94	45.44	45.88	45.59	43.89
Al_2O_3	16.13	16.29	16.16	16.20	17.51	16.38	15.21
Fe_2O_3	3.62	2.52	3.69	4.41	2.83	3.35	4.79
FeO	9.60	10.41	8.11	7.58	8.47	8.90	8.76
MgO	9.79	10.02	11.13	11.06	9.84	11.13	10.54
CaO	8.59	8.24	9.76	10.68	9.75	9.32	12.75
Na_2O	3.31	3.36	3.06	2.43	3.05	3.14	1.32
K_2O	1.48	2.08	1.39	0.37	0.67	0.40	0.89
TiO_2	1.53	1.49	1.44	1.47	1.57	1.35	1.43
P_2O_5	0.13	0.13	0.12	0.17	0.18	0.16	0.20
MnO	0.21	0.20	0.19	0.19	0.20	0.19	0.22
S	0.02	0.02	0.01	0.01	0.07	0.09	0.01
Or	8.89	12.23	7.78	2.19	3.93	2.36	5.29
Ab	15.72	9.96	11.53	18.99	19.29	20.43	8.96
An	24.74	23.35	26.41	32.25	32.08	29.75	32.93
Ne	6.53	9.94	7.67	0.85	3.55	3.12	1.19
Di	13.68	13.54	16.93	15.97	12.19	12.53	23.34
Ol	21.95	24.15	21.18	20.36	21.32	23.90	18.15
Mt	5.25	3.65	5.35	6.26	4.10	4.84	6.94
Ilm	2.91	2.84	2.74	2.72	2.98	2.56	2.71
Ap	0.31	0.31	0.30	0.40	0.43	0.34	0.46
Py	0.03	0.o3	0.02	0.02	0.13	0.18	0.02
DI	31.14	32.13	26.98	22.03	26.77	25.91	15.44
SI	35.21	35.29	40.65	42.78	39.58	41.34	40.07

Table 17 continued:

Wt. %	22	23	24	26-a	26-b	33	37-b
SiO_2	46.57	45.55	47.15	45.71	45.93	47.92	48.52
Al_2O_3	16.25	16.46	17.44	16.14	17.33	17.61	17.32
Fe_2O_3	0.87	1.15	2.43	1.39	1.70	1.19	1.59
FeO	9.86	9.23	7.72	9.16	8.46	8.76	8.22
MgO	9.43	13.28	8.76	12.25	12.58	8.74	8.46
CaO	11.14	8.78	10.94	10.42	9.05	9.79	10.11
Na_2O	2.97	3.14	3.13	2.48	3.03	3.45	3.33
K_2O	0.66	0.63	0.64	0.67	0.24	0.81	0.90
TiO_2	1.85	1.32	1.43	1.37	1.20	1.37	1.21
P_2O_5	0.22	0.18	0.17	0.17	0.20	0.16	0.15
MnO	0.18	0.16	0.19	0.24	0.16	0.20	0.18
S	-	0.13	-	-	0.13	-	0.01
Or	3.89	3.48	3.78	3.89	1.67	4.79	5.56
Ab	15.98	15.72	19.91	13.70	19.39	21.35	22.00
An	28.91	29.19	31.69	30.86	32.80	30.30	29.47
Ne	4.97	5.68	3.41	3.98	3.41	4.05	3.41
Di	20.36	10.95	17.50	16.13	8.93	14.24	16.24
Ol	20.61	30.13	17.08	26.41	28.45	20.58	18.38
Mt	1.26	1.67	3.52	2.02	2.37	1.73	2.30
Ilm	3.50	2.51	2.72	2.61	2.28	2.61	2.30
Ap	0.52	0.43	0.40	0.40	0.47	0.36	0.35
Py	-	0.24	-	-	0.24	-	0.01
DI	24.84	24.88	27.10	21.57	24.47	30.19	30.97
SI	39.64	48.41	38.62	47.21	48.37	38.08	37.60

Table 17 continued:

Wt. %	45-a	45-b	46	54	54-b	56
SiO_2	47.74	47.75	47.68	47.05	45.68	48.61
Al_2O_3	15.43	16.02	15.61	16.94	15.54	16.67
Fe_2O_3	2.62	2.30	1.82	1.06	3.66	1.42
FeO	8.12	8.44	8.43	8.66	7.41	8.35
MgO	10.82	9.50	10.64	10.40	13.22	9.20
CaO	9.86	9.20	9.87	9.80	10.03	10.08
Na_2O	3.04	3.02	2.91	3.34	2.33	3.26
K_2O	0.42	1.93	1.59	1.35	0.60	0.96
TiO_2	1.35	1.43	1.17	1.06	1.15	1.07
P_2O_5	0.22	0.21	0.11	0.15	0.19	0.17
MnO	0.18	0.20	0.17	0.19	0.18	0.21
S	0.20	-	-	-	0.02	-
Or	2.78	11.12	9.45	7.78	3.55	5.56
Ab	24.63	17.29	15.11	13.62	17.29	22.01
An	26.97	24.46	24.74	27.25	30.02	28.08
Ne	0.57	4.54	5.11	7.95	1.42	2.84
Di	16.52	15.98	19.06	16.65	14.83	17.13
Ol	21.30	19.96	21.42	22.85	24.99	19.87
Mt	3.79	3.34	2.63	1.54	5.31	2.06
Ilm	2.56	2.72	2.22	2.01	2.12	2.03
Ap	0.52	0.50	0.26	0.35	0.45	0.40
Py	0.37	-	-	-	0.03	-
DI	27.98	32.95	29.67	29.35	22.26	30.41
SI	43.24	37.71	41.90	41.92	48.57	39.67

Table 17 continued:

Wt. %	GPCS-1	GPCS-2	86	103	13340*
SiO_2	46.66	47.52	47.56	47.35	46.16
Al_2O_3	15.50	15.57	17.88	17.06	14.55
Fe_2O_3	4.01	4.17	1.37	3.06	2.97
FeO	9.50	9.14	9.53	8.03	6.29
MgO	8.95	8.49	8.18	7.11	13.00
CaO	8.14	7.92	9.42	12.22	12.79
Na_2O	3.85	3.80	2.80	2.90	1.92
K_2O	0.98	0.99	1.57	0.39	0.53
TiO_2	1.67	1.70	1.30	1.43	1.24
P_2O_5	0.51	0.48	0.12	0.09	0.34
MnO	0.20	0.21	0.20	0.27	0.16
S	0.01	0.02	0.03	0.09	0.03
Or	5.56	5.56	9.33	2.32	3.15
Ab	25.94	29.34	18.24	21.00	13.09
An	22.24	22.80	31.53	32.35	29.46
Ne	3.55	1.42	2.97	1.90	1.73
Di	11.92	11.25	11.79	22.50	25.23
Ol	20.57	19.36	21.27	12.32	19.76
Mt	5.80	6.03	1.99	4.44	4.31
Ilm	3.18	3.23	2.48	2.72	2.35
Ap	1.21	1.00	0.28	0.21	0.81
Py	0.02	0.02	0.05	0.17	0.05
DI	35.05	36.32	30.54	25.22	17.97
SI	32.80	31.93	34.88	33.08	52.61

*Murphy's Point

Table 18: Chemical analyses and C.I.P.W. norms of the Mourne olivine basalts

Wt. %	129-b	128	124-d	113	110-a'	87-a	12	502	506
SiO_2	46.52	47.12	47.02	47.79	45.42	47.60	48.27	47.94	47.46
Al_2O_3	14.10	17.78	14.94	17.66	17.80	16.14	17.77	16.60	16.30
Fe_2O_3	4.12	0.74	3.32	3.21	1.17	1.88	1.21	2.81	2.47
FeO	8.38	9.05	5.86	6.95	12.94	8.24	9.59	7.34	9.33
MgO	9.50	11.32	12.24	9.34	8.25	10.23	9.06	8.87	8.55
CaO	9.37	9.70	12.35	10.37	8.22	11.41	8.10	11.53	10.95
Na_2O	3.01	2.60	1.96	2.78	2.57	2.12	2.75	2.08	2.16
K_2O	0.95	0.18	0.53	0.19	0.57	0.57	1.16	1.09	0.95
TiO_2	3.08	1.02	1.22	1.29	2.46	1.29	1.61	1.39	1.39
P_2O_5	0.56	0.16	0.33	0.12	0.22	0.20	0.25	0.17	0.19
MnO	0.24	0.17	0.15	0.19	0.24	0.17	0.17	0.18	0.21
S	0.22	0.22	0.05	0.12	0.18	0.18	-	0.01	0.07
Or	5.61	1.07	3.15	1.13	3.36	3.40	6.87	6.41	5.59
Ab	25.46	22.00	16.62	23.56	21.78	17.96	23.29	17.56	18.24
An	22.13	36.26	30.37	35.10	35.28	32.78	32.70	32.76	31.99
Di	16.48	8.71	22.80	12.47	3.32	18.12	4.78	18.81	17.12
Hy	1.45	1.52	1.98	6.44	4.63	4.81	6.49	4.65	4.80
Ol	15.28	26.59	17.02	13.64	24.36	16.89	20.39	12.67	15.43
Mt	5.97	1.07	4.81	4.66	1.69	2.72	1.76	4.07	3.58
Ilm	5.85	1.94	2.33	2.45	4.67	2.45	3.07	2.65	2.65
Ap	1.33	0.38	0.78	0.28	0.53	0.47	0.59	0.40	0.46
Py	0.41	0.41	0.09	0.22	0.34	0.34	-	0.02	0.14
DI	31.07	23.07	19.78	24.69	25.14	21.36	30.17	23.97	23.83
SI	36.59	47.38	51.19	41.57	32.35	44.40	38.12	39.97	36.45

Table 19: Chemical analyses and C.I.P.W. norms of the Mourne olivine-tholeiites

Wt. %	127-a	127-c	127-d	126-a	126-b	125	124-c	124-e"
SiO_2	49.59	49.57	47.26	48.06	47.27	46.53	47.98	46.80
Al_2O_3	15.47	15.82	17.55	17.28	17.21	16.51	17.96	17.52
Fe_2O_3	3.77	2.95	4.27	2.48	2.73	3.33	1.82	3.12
FeO	7.85	8.19	6.42	8.43	8.60	7.17	7.63	6.79
MgO	7.61	9.88	11.26	9.00	7.90	11.79	10.09	9.89
CaO	10.19	9.03	9.47	10.11	11.60	11.18	10.50	11.89
Na_2O	2.74	2.12	1.63	2.33	2.29	1.45	2.11	1.84
K_2O	0.38	0.30	0.59	0.26	0.23	0.59	0.21	0.26
TiO_2	1.74	1.57	1.13	1.57	1.71	1.02	1.28	1.46
P_2O_5	0.25	0.29	0.15	0.13	0.14	0.13	0.16	0.16
MnO	0.24	0.21	0.19	0.22	0.20	0.18	0.18	0.19
S	0.22	0.05	0.07	0.15	0.15	0.14	0.09	0.09
Qz	0.17	0.28	-	-	-	-	-	-
Or	2.26	1.79	3.51	1.55	1.37	3.51	1.25	1.55
Ab	23.16	17.95	13.82	19.75	19.42	12.29	17.85	15.62
An	28.74	32.73	38.78	35.88	35.93	36.74	38.88	38.72
Di	16.23	8.19	5.72	10.85	16.78	14.29	9.79	15.35
Hy	19.60	30.97	22.70	15.90	8.84	11.71	15.15	10.55
Ol	-	-	6.60	8.87	9.81	14.09	11.42	10.34
Mt	5.47	4.27	6.19	3.59	3.96	4.83	2.65	4.52
Ilm	3.31	2.99	2.16	2.99	3.24	1.93	2.43	2.77
Ap	0.59	0.69	0.35	0.31	0.33	0.31	0.38	0.38
Py	0.41	0.09	0.13	0.28	0.28	0.26	0.17	0.17
DI	25.60	20.03	17.33	21.31	20.79	15.81	19.10	17.17
SI	34.05	42.15	46.59	40.00	36.52	48.46	46.16	45.16

Table 19 continued:

Wt. %	124-e'''	119-b	118	117	116	112-a	112-b	107-a
SiO_2	47.51	48.52	47.60	49.01	48.48	48.22	47.88	48.00
Al_2O_3	16.74	17.12	16.55	16.87	16.61	17.85	17.13	17.48
Fe_2O_3	3.15	3.22	2.20	2.81	2.09	2.79	3.17	2.50
FeO	7.27	6.84	6.99	6.69	7.94	7.57	7.13	9.01
MgO	11.22	9.34	13.10	10.40	11.65	10.49	11.07	11.25
CaO	10.33	10.84	10.55	10.18	9.41	8.71	9.45	7.86
Na_2O	1.65	2.10	1.65	2.23	2.06	2.63	2.36	1.78
K_2O	0.18	0.48	0.20	0.33	0.26	0.30	0.18	0.31
TiO_2	1.55	1.11	0.75	1.08	1.05	0.93	1.24	1.41
P_2O_5	0.17	0.14	0.12	0.15	0.15	0.18	0.15	0.23
MnO	0.17	0.16	0.18	0.16	0.16	0.16	0.18	0.11
S	0.03	0.17	0.12	0.10	0.18	0.23	0.04	0.03
Qz	-	-	-	-	-	-	-	-
Or	1.07	2.86	1.19	1.96	1.55	1.79	1.07	1.85
Ab	14.00	17.75	14.00	18.86	17.43	22.30	19.98	15.06
An	37.72	35.83	37.12	35.02	35.26	35.93	35.59	37.48
Di	9.93	13.62	11.50	11.58	8.36	4.87	8.26	-
Hy	23.25	16.50	15.78	18.76	20.15	14.69	15.92	32.64
Ol	6.01	5.97	15.24	7.10	11.49	13.72	11.75	5.53
Mt	4.56	4.67	3.19	4.07	3.04	4.05	4.60	3.63
Ilm	2.95	2.10	1.43	2.06	1.99	1.76	2.35	2.69
Ap	0.40	0.33	0.28	0.35	0.35	0.43	0.35	0.55
Py	0.05	0.32	0.22	0.18	0.34	0.43	0.07	0.05
DI	15.07	20.61	15.19	20.82	18.98	24.09	21.05	16.92
SI	47.80	42.49	54.27	46.30	48.54	44.11	46.30	45.27

Table 19 continued:

Wt. %	105	104	102	101	96	55-a	6
SiO_2	48.48	46.02	48.30	47.89	48.36	45.55	46.64
Al_2O_3	16.14	17.43	17.02	15.81	16.62	16.92	15.04
Fe_2O_3	3.99	2.15	1.47	2.81	2.96	1.62	3.59
FeO	7.00	9.45	7.96	6.84	6.54	7.95	6.93
MgO	8.39	11.16	11.71	14.31	12.54	14.60	10.99
CaO	11.95	9.99	9.46	9.24	8.84	10.22	13.81
Na_2O	2.01	1.85	2.19	1.46	2.01	1.31	1.36
K_2O	0.18	0.18	0.32	0.41	0.49	0.49	0.31
TiO_2	1.42	1.39	1.17	0.88	1.11	0.94	1.01
P_2O_5	0.15	0.05	0.17	0.11	0.20	0.16	0.13
MnO	0.18	0.19	0.18	0.14	0.18	0.18	0.18
S	0.11	0.16	-	0.10	0.20	-	-
Qz	0.14	-	-	-	-	-	-
Or	1.07	1.07	1.91	2.44	2.91	2.91	1.83
Ab	17.07	15.67	18.54	12.37	17.06	11.11	11.47
An	34.43	38.68	35.64	35.34	34.80	38.83	34.03
Di	19.13	8.53	8.19	7.78	6.13	8.66	26.90
Hy	19.06	10.97	15.05	23.37	21.24	7.51	6.63
Ol	-	18.85	15.86	12.45	10.57	26.40	11.69
Mt	5.79	3.12	2.14	4.07	4.30	2.36	5.21
Ilm	2.70	2.65	2.22	1.68	2.10	1.80	1.93
Ap	0.35	0.11	0.40	0.26	0.47	0.38	0.31
Py	0.20	0.30	-	0.18	0.37	-	-
DI	18.29	16.75	20.45	14.82	19.98	14.02	13.30
SI	38.90	45.02	49.51	55.40	51.10	56.22	47.41

Table 20: Chemical analyses and C.I.P.W. norms of the pre-granitic quartz-tholeiites

Wt. %	127-b	124-e'	123	122	121-a	121-b	111-b	108
SiO_2	53.37	52.92	53.42	53.05	52.80	54.35	51.61	53.96
Al_2O_3	15.90	15.59	16.40	14.99	15.03	14.94	16.08	15.33
Fe_2O_3	3.11	3.41	2.30	4.08	3.48	3.14	4.69	2.79
FeO	5.24	6.45	7.05	5.02	5.79	5.64	5.87	5.29
MgO	9.21	6.98	8.20	7.79	8.15	7.54	6.15	7.70
CaO	8.91	8.68	6.94	9.16	8.95	8.38	10.02	10.22
Na_2O	1.98	3.06	2.06	2.21	2.37	2.36	2.18	1.93
K_2O	1.23	0.96	1.96	1.85	1.62	2.01	1.13	1.51
TiO_2	0.74	1.35	1.26	1.26	1.30	1.19	1.77	0.91
P_2O_5	0.09	0.30	0.20	0.26	0.26	0.24	0.19	0.14
MnO	0.15	0.23	0.15	0.17	0.18	0.16	0.23	0.15
S	0.05	0.06	0.01	0.21	0.04	0.01	0.05	0.06
Qz	4.53	3.25	3.86	4.78	3.19	4.99	6.28	5.72
Or	7.31	5.71	11.62	10.94	9.58	11.90	6.72	8.92
Ab	16.78	25.93	17.50	18.73	20.11	20.03	18.49	16.35
An	30.81	25.91	29.67	25.44	25.54	24.18	30.69	28.70
Di	10.20	12.22	2.78	14.48	13.71	12.66	14.19	16.86
Hy	24.09	18.61	28.30	16.27	19.61	18.79	12.88	17.19
Ol	-	-	-	-	-	-	-	-
Mt	4.52	4.94	3.34	5.91	5.04	4.55	6.80	4.04
Ilm	1.41	2.56	2.39	2.39	2.48	2.27	3.36	1.74
Ap	0.21	0.71	0.47	0.61	0.62	0.57	0.45	0.33
Py	0.09	0.11	0.01	0.39	0.07	0.01	0.09	0.11
DI	28.63	34.90	32.99	34.45	32.89	36.93	31.50	31.00
SI	44.34	33.46	38.00	37.18	38.07	36.44	30.72	40.06

Table 20 continued:

Wt. %	99	91	76	68	57-a	57-b	54-a	30-a
SiO_2	49.63	53.59	51.15	53.63	53.64	52.61	55.48	55.21
Al_2O_3	17.04	15.96	16.23	16.01	16.38	15.48	16.14	15.24
Fe_2O_3	3.81	2.26	0.74	2.15	3.27	3.03	2.89	2.48
FeO	7.48	7.53	10.13	7.60	6.64	7.15	6.18	6.98
MgO	7.80	6.50	6.74	6.53	5.74	7.95	5.41	6.27
CaO	7.14	8.22	9.03	7.89	7.95	8.70	7.73	8.08
Na_2O	3.07	2.44	2.46	2.50	2.71	1.85	2.34	2.50
K_2O	0.97	1.62	1.04	1.95	1.76	1.29	2.31	1.48
TiO_2	2.12	1.39	1.79	1.29	1.39	1.41	1.09	1.24
P_2O_5	0.40	0.22	0.27	0.18	0.19	0.18	0.16	0.26
MnO	0.17	0.21	0.27	0.19	0.19	0.19	0.17	0.18
S	0.61	0.03	0.20	0.06	0.19	0.20	0.07	0.07
Qz	-	4.40	0.03	3.16	5.06	5.62	7.70	7.63
Or	5.72	9.60	6.16	11.57	10.42	7.63	13.70	8.76
Ab	25.96	20.67	20.83	21.18	22.95	15.71	19.87	21.16
An	29.72	27.78	30.10	26.64	27.27	30.06	26.64	25.98
Di	2.36	9.43	10.64	9.24	8.82	9.59	8.65	10.07
Hy	24.39	21.59	26.71	22.05	17.25	23.47	16.62	19.66
Ol	0.17	-	-	-	-	-	-	-
Mt	5.51	3.28	1.07	3.12	4.73	4.39	4.19	3.60
Ilm	4.02	2.64	3.40	2.45	2.64	2.68	2.08	2.35
Ap	0.95	0.52	0.64	0.43	0.45	0.43	0.38	0.62
Py	1.15	0.05	0.37	0.11	0.35	0.37	0.13	0.13
DI	31.69	34.68	27.03	35.93	38.45	28.97	41.27	37.57
SI	33.72	31.94	31.93	31.50	28.53	37.37	28.28	31.81

Table 20 continued:

Wt. %	30-c	29	25-a	25-b	25-c	508	510
SiO_2	53.45	54.66	50.11	50.73	49.56	49.13	51.90
Al_2O_3	14.98	15.77	15.33	15.98	15.55	14.72	14.85
Fe_2O_3	3.11	2.20	3.96	4.36	4.19	4.10	5.69
FeO	7.05	6.30	7.98	7.26	7.82	9.95	6.28
MgO	6.53	6.81	6.30	6.50	6.53	6.73	7.10
CaO	8.90	8.33	9.13	7.72	8.53	7.85	7.90
Na_2O	2.20	2.30	3.26	3.21	2.14	2.71	2.25
K_2O	2.00	2.40	1.17	1.37	2.82	1.58	1.77
TiO_2	1.28	0.90	2.01	1.97	2.08	2.37	1.63
P_2O_5	0.25	0.11	0.35	0.52	0.46	0.61	0.30
MnO	0.20	0.15	0.29	0.28	0.27	0.21	0.18
S	0.01	0.01	0.11	0.09	0.01	0.09	0.30
Qz	4.64	3.67	-	1.01	-	-	6.16
Or	11.86	14.23	6.92	8.11	16.70	9.33	10.42
Ab	18.69	19.53	27.61	27.15	18.11	22.89	19.02
An	25.02	25.57	23.70	25.13	24.47	23.33	25.14
Di	14.20	12.19	15.64	7.85	11.99	9.49	9.58
Hy	18.00	19.57	12.77	19.23	15.31	21.84	17.08
Ol	-	-	2.72	-	2.24	1.07	-
Mt	4.51	3.19	5.75	6.32	6.07	5.94	8.24
Ilm	2.43	1.72	3.81	3.75	3.95	4.50	3.10
Ap	0.59	0.26	0.83	1.24	1.10	1.44	0.70
Py	0.01	0.01	0.20	0.17	0.01	0.17	0.56
DI	35.20	37.45	34.53	36.28	34.82	32.22	35.60
SI	31.26	34.03	27.79	28.63	27.79	26.84	30.75

Table 21: Chemical analyses and C.I.P.W. norms of the post-granitic quartz-tholeiites

Wt. %	405	406	408	409	410	411	414
SiO_2	54.14	54.56	54.50	54.46	49.52	53.64	52.07
Al_2O_3	15.83	16.43	16.89	15.92	16.85	15.45	16.03
Fe_2O_3	4.25	4.31	4.12	4.32	5.95	5.32	3.48
FeO	5.90	5.73	5.74	5.42	6.15	6.17	5.75
MgO	6.59	6.53	6.39	6.07	8.59	6.23	8.99
CaO	7.51	6.63	6.56	7.08	8.01	7.54	9.04
Na_2O	2.49	2.48	2.37	3.48	2.28	2.03	1.74
K_2O	1.87	1.98	2.20	1.91	0.99	1.84	1.22
TiO_2	0.98	0.99	0.90	0.94	1.21	1.36	1.16
P_2O_5	0.21	0.18	0.19	0.21	0.24	0.20	0.22
MnO	0.18	0.17	0.16	0.16	0.20	0.20	0.23
S	0.09	0.01	0.01	0.04	0.01	0.03	0.03
Qz	6.53	7.36	7.06	3.46	2.18	9.44	4.66
Or	11.04	11.71	12.99	11.28	5.83	10.88	7.26
Ab	21.04	21.01	20.05	29.45	19.30	17.18	14.74
An	26.49	27.84	28.95	22.17	32.83	27.60	32.28
Di	7.54	3.09	1.91	9.27	4.25	6.81	8.89
Hy	18.68	20.43	20.93	15.74	24.08	17.26	24.29
Ol	-	-	-	-	-	-	-
Mt	6.17	6.24	5.97	6.27	8.62	7.72	5.05
Ilm	1.86	1.88	1.71	1.78	2.30	2.58	2.21
Ap	0.49	0.43	0.44	0.49	0.57	0.46	0.52
Py	0.17	0.02	0.01	0.08	0.02	0.05	0.05
DI	38.61	40.08	40.09	44.20	27.31	37.51	26.67
SI	31.23	31.05	30.69	28.63	35.85	28.86	42.45

olivine-tholeiite. Rocks plotting in the high-alumina basalt fields in the diagrams are not high-alumina basalts in the strict sense, owing to the presence of some plagioclase phenocrysts scattered throughout the groundmass.

For comparative purposes, the two main basic rock types in the Mourne swarm are plotted on the alkali vs. silica diagram (Figure 11), along with the Hawaiian alkalic series (MacDonald and Katsura, 1964) and the tholeiitic series of Thingmuli (Carmichael, 1964). Analyses of the Killough dyke rocks are also plotted to show the similarity between these and the alkali basalts from the northern part of the Mourne dyke-swarm. The Killough rocks fall on or fairly near the Hawaiian alkalic series trend, however, are seen to be more differentiated than the Mourne alkali basalts.

The Mourne alkalic rocks, on the other hand, are plotted in a rather restricted area, the majority fall in the silica range between 45 to 47%. In spite of this limitation, the Mourne tholeiitic suite shows a typical differentiation trend, characteristically similar to that of Thingmuli tholeiitic series, ranging in silica content continuously from 47 to 60%.

The chemical compositions of some of the Killough dyke rocks are given in Table 22-A, along with their norms. Samples have been

---

Fig. 10: Silica-total alkalis-alumina (weight %) relation of the tholeiitic and alkalic basalts from the Mourne and Killough dyke-swarms with silica range 45 to 55%. (After Kuno, 1960, p.130, fig.5). Symbols refer to: o Mourne tholeiites, • Mourne alkali basalts, ⊕ Killough alkali basalts. (1) Tholeiite field, (2) High-alumina basalt field, (3) Alkali basalt field.

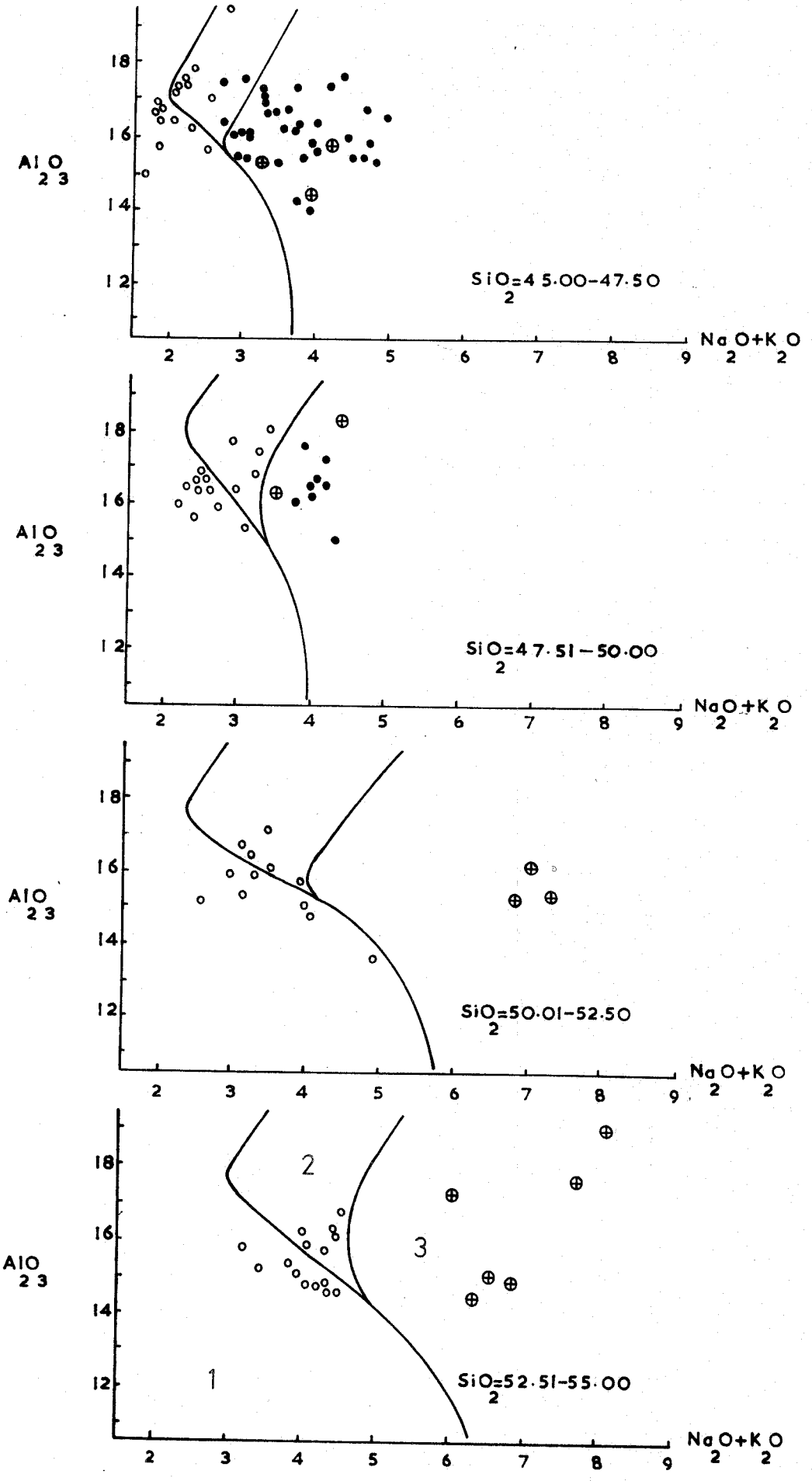
Al2O3
18
16
14
12
SiO2=45.00-47.50
2 3 4 5 6 7 8 9
Na2O+K2O
Al2O3
18
16
14
12
SiO2=47.51-50.00
2 3 4 5 6 7 8 9
Na2O+K2O
Al2O3
18
16
14
12
SiO2=50.01-52.50
2 3 4 5 6 7 8 9
Na2O+K2O
Al2O3
18
16
14
12
2
3
1
SiO2=52.51-55.00
2 3 4 5 6 7 8 9
Na2O+K2O

Table 22-A: Chemical analyses and C.I.P.W. norms of the Killough dyke rocks

Wt. %	KD 46	KD 47	KD 53A	KD53B	KD 56	KD 57	KD 59
SiO_2	49.24	50.17	50.34	53.02	50.36	48.24	46.08
Al_2O_3	14.95	17.26	15.73	19.02	15.31	18.54	15.45
Fe_2O_3	5.62	5.26	6.69	4.63	6.34	3.04	7.22
FeO	7.59	7.71	5.38	4.32	5.31	9.19	5.97
MgO	7.52	3.27	6.00	3.64	7.71	5.76	11.92
CaO	6.61	5.54	5.17	4.89	4.86	8.54	7.74
Na_2O	3.86	3.08	4.07	4.73	3.45	4.18	2.94
K_2O	1.62	4.12	3.40	3.43	3.38	0.27	0.29
TiO_2	2.33	2.22	2.24	1.65	2.40	1.74	1.88
P_2O_5	0.47	1.18	0.72	0.49	0.70	0.25	0.23
MnO	0.15	0.13	0.20	0.15	0.16	0.17	0.17
S	0.06	0.09	0.10	0.08	0.04	0.15	0.25
Qz	-	0.20	-	-	-	-	-
Cor	-	0.47	-	-	-	-	-
Or	9.59	24.31	20.08	20.28	19.96	1.58	1.70
Ab	32.67	26.06	34.42	39.97	29.19	34.10	24.83
An	18.65	19.79	14.60	20.53	16.30	31.01	28.08
Ne	-	-	-	-	-	0.68	-
Di	8.83	-	4.94	0.42	2.56	7.96	6.90
Hy	7.13	14.37	2.09	0.95	11.20	-	12.15
Ol	9.33	-	8.02	6.72	5.32	16.09	11.32
Mt	8.15	7.62	9.70	6.71	9.19	4.41	10.45
Ilm	4.42	4.22	4.26	3.14	4.55	3.31	3.56
Ap	1.11	2.78	1.71	1.15	1.65	0.59	0.54
Py	0.11	0.17	0.19	0.14	0.08	0.27	0.48
DI	42.27	50.58	54.50	60.25	49.14	36.35	26.53
SI	28.69	13.95	23.49	17.54	29.44	25.67	42.06

collected from St. John's Point where the swarm reaches its densest part. All the analysed rocks show alkaline affinities. They are mainly characterized by their variable silica content from 46 to 53%, and total alkalis from 4 to 8%.

For comparative purposes, some chemical analyses of the Killough dyke rocks were also quoted from Tomkeieff and Marshall (1940, pp. 331-334), and are shown in Table 22-B. Tomkeieff and Marshall (op.cit.) referred to some of them (e.g. Nos. 53A, 53B and 68 in Table 22-B) as "trachybasalts". They, however, reported the existence of oligoclase in the groundmass, and the association of an intermediate plagioclase (mainly in phenocrysts) with alkali feldspar (orthoclase or anorthoclase). These are characteristic features of "mugearites" as defined by Harker (1904, p.264).

The Killough alkali basalts have solidification indices varying from 42 to 26. Mugearites, on the other hand, are characterized by very low solidification indices ranging between 15 and 10. Their differentiation indices, however, are distinctly higher (50 to 60) than those of the alkali basalts (26 to 36) of the Killough-Ardglass dyke-swarm.

As it is seen from Table 17 that no alkali basalt from the Mourne area with differentiation index higher than 36 exists. This indicates

---

Fig. 11: A plot of $Na_2O + K_2O$ versus SiO_2 (weight %) of the Mourne and Killough dyke rocks with comparisons. The diagonal line represents the line of demarcation between Hawaiian alkalic and tholeiitic series (MacDonald and Katsura, 1964).

Symbols refer to: o Mourne tholeiitic series, • Mourne alkali basalts, ⊕ Killough alkalic series.

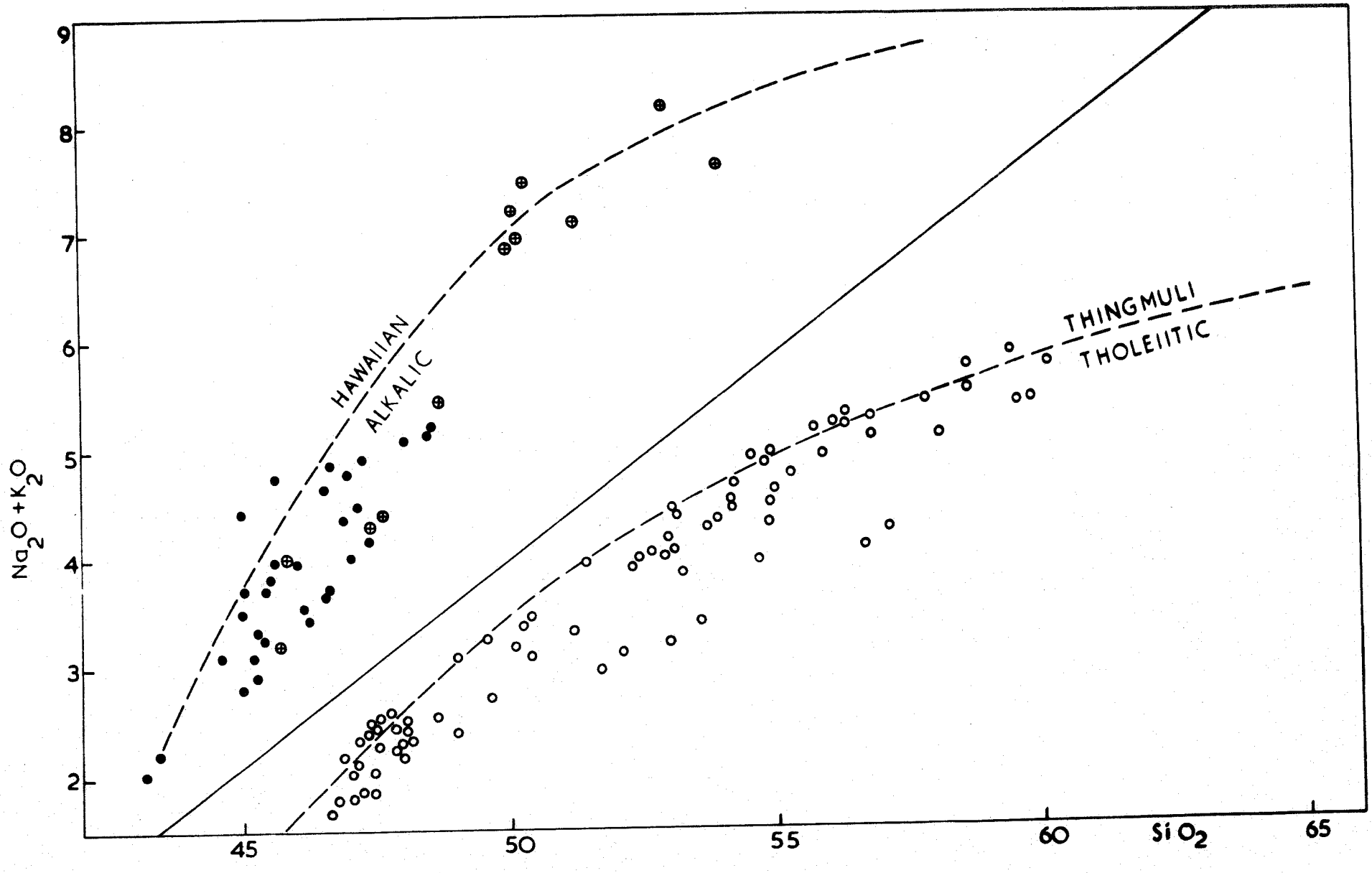
HAWAIIAN
ALKALIC
THINGMULI
THOLEIITIC
Na_2O+K_2O
SiO_2
9
8
7
6
5
4
3
2
45
50
55
60
65

Table 22-B: Chemical analyses and C.I.P.W. norms of the Killough dyke rocks (Quoted from Tomkeieff and Marshall, 1940)

Wt. %	14	27	53A	53B	68
SiO_2	47.39	45.86	50.14	51.26	53.98
Al_2O_3	15.56	14.29	16.42	20.04	17.78
Fe_2O_3	3.91	3.99	4.15	2.67	3.96
FeO	6.43	8.11	6.48	5.31	4.87
MgO	7.91	6.73	3.63	2.64	1.92
CaO	9.03	9.51	5.76	6.05	4.99
Na_2O	3.07	3.13	3.44	4.56	3.69
K_2O	1.23	0.88	3.48	2.52	3.92
TiO_2	2.51	1.98	1.94	1.18	1.03
P_2O_5	0.33	0.26	0.72	0.36	0.73
S	-	-	-	0.21	-
MnO	0.31	0.21	0.14	0.13	0.11
BaO	0.06	0.03	0.13	0.08	-
CO_2	0.21	3.96	0.29	0.59	0.26
H_2O^+	1.53	1.61	1.47	1.99	2.03
H_2O^-	0.61	0.59	1.70	0.50	0.59
Qz	-	2.11	-	-	4.38
Cor	-	-	-	-	0.10
Or	7.30	5.15	20.55	14.92	23.31
Ab	25.95	26.50	29.10	38.60	31.20
An	25.03	22.30	19.10	26.75	20.03
Di	13.26	-	2.55	-	-
Hy	5.70	22.90	13.13	1.62	8.20
Ol	8.86	-	-	7.22	-
Mt	5.66	5.80	6.05	3.90	5.75
Ilm	4.75	3.75	3.70	2.25	1.95
Ap	0.77	0.65	1.70	0.85	1.70
Cc	0.48	8.55	0.66	1.31	0.50
H_2O	2.14	2.20	3.17	2.49	2.62
DI	33.25	33.76	49.65	53.52	58.90
SI	35.08	29.47	17.14	14.92	10.46

that there are no differentiation products of alkali basalts in the Mourne dyke-swarm. Various other diagrams also show that the alkali basaltic differentiates are not represented in the Mourne region.

One of such diagrams is the AFM plot which shows that the Mourne alkali basalts only occupy the earlier stages of the Hawaiian alkalic trend and do not extend far beyond the intermediate types (Figure 12-A). By contrast, the Killough alkalic rocks follow the main part of the trend of Hawaiian mugearites and trachytes (MacDonald and Katsura, 1964).

The continuum of the tholeiitic trend from basic to acid end is clearly demonstrated in the Mourne tholeiitic series (Figure 12-B). Absolute iron enrichment of the intermediate rocks is the greatest in the tholeiitic series of the Mourne area, paralleling the Thingmuli tholeiitic trend (Carmichael, 1964), and progressively much less in the alkalic rocks of the Mourne and Killough dyke-swarms.

The AFM diagram also shows a steady increase in the total iron content of the Mourne tholeiitic and alkalic suites, before alkali enrichment becomes predominant. In both suites, the course of the main trend of evolution is impoverishment first in magnesia, and then in both magnesia and iron. However, the depletion in magnesia and

---

Fig. 12: Total iron-total alkalis-magnesia (atomic %) variation diagram of the Mourne and Killough alkalic (A), and the Mourne tholeiitic (B) rocks. The crystallization trends of the Hawaiian alkalic (MacDonald and Katsura, 1964) and the Thingmuli tholeiitic (Carmichael, 1964) series are also indicated.
Symbols denote: o Mourne tholeiitic series, • Mourne alkali basalts, ⊕ Killough alkalic series.

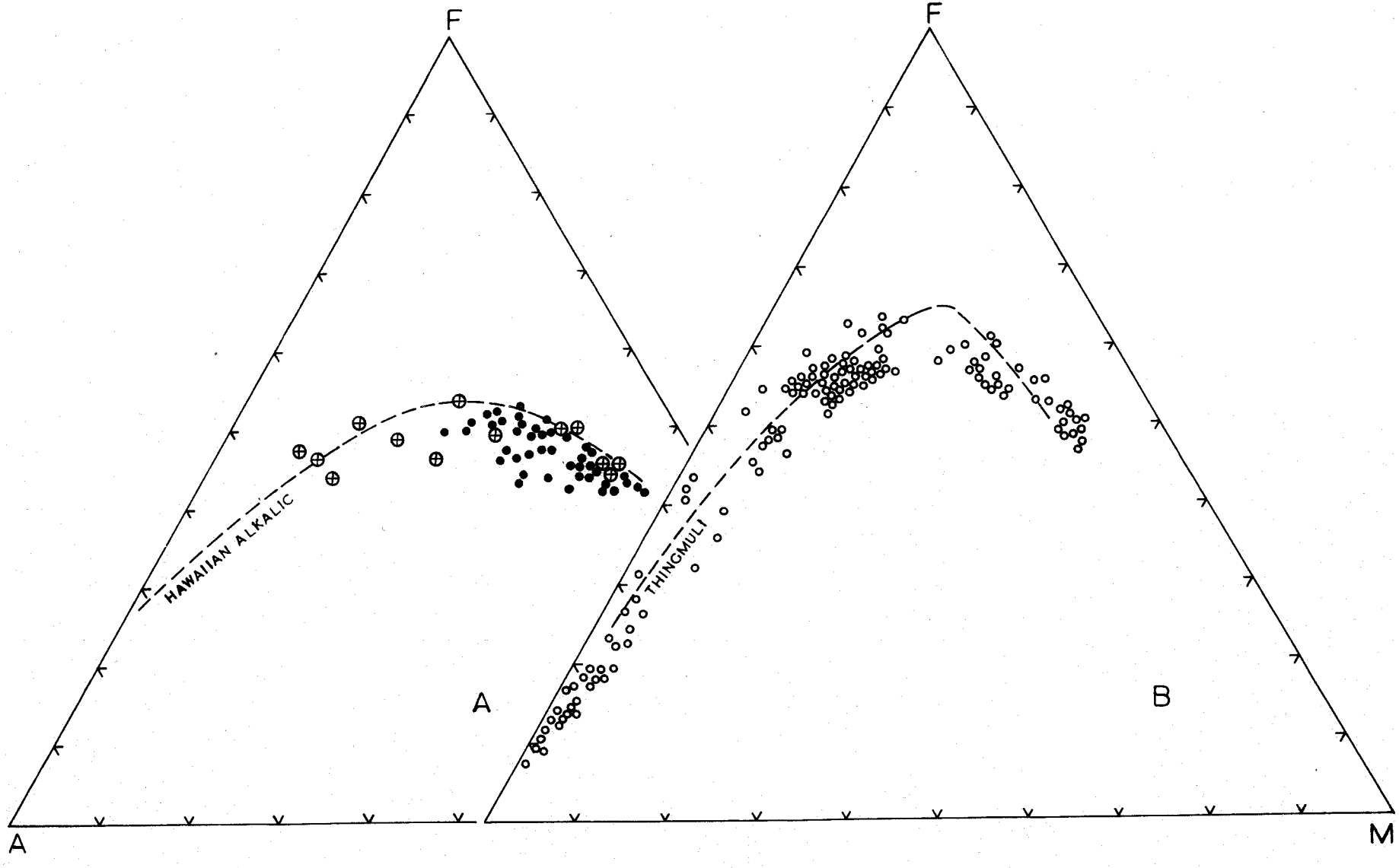
F
HAWAIIAN ALKALIC
A
A
F
THINGMULI
B
M

iron is more strikingly displayed in the later acid differentiates of the Mourne tholeiitic series than in the alkalic rocks of the Mourne and Killough dyke-swarms. In this respect, the end-stage products of the Mourne tholeiitic suite very much resemble the extreme differentiates of the Thingmuli tholeiitic series (either rhyolite or a granophyre).

From Figure 12, it will be noted that each suite shows two distinctly different evolutionary trends; the tholeiitic one leads first to iron enrichment and then to enrichment in alkalis, possibly as a result of different partial pressures of oxygen in the magma chamber (deduced by Osborn, 1959), and the alkalic trend leads to enrichment in iron, though to a lesser extent but with greater enrichment in alkalis than in the case of the tholeiitic trend.

Trend of the Hawaiian alkalic rocks could be accounted for largely by the removal of ferromagnesian minerals, initially controlled by the subtraction of olivine and pyroxene, in more or less equal amounts and later joined by calcic plagioclase (MacDonald and Katsura, 1964, p.108). On the other hand, the trend of the Thingmuli tholeiitic rocks depends on the movement of olivine crystals and the progressive enrichment of iron relative to magnesium throughout the successive liquids of this series is halted during an intermediate stage (Figure 12-B), as magnetite becomes an early crystallizing phase (Carmichael, 1964, p.435).

From this evidence, the same factors governing the movements and separations of olivine, pyroxene, plagioclase and magnetite crystals within the magma chambers which yielded Hawaiian alkalic and Thingmuli tholeiitic rock suites, could be applied to the Mourne tholeiitic and alkalic rocks as well as to the Killough alkalic series, if they are largely the results of fractional crystallization. Variations within

each of the two distinctly different suites appear, therefore, to be largely controlled by crystal fractionation, although the operation of other factors to a lesser degree is not ruled out. The evidence is not conclusive, but the present writer considers that the balance of that presently available indicates that the Mourne tholeiitic series could have been derived by a process of fractionation from a basaltic parent (probably an olivine-tholeiite), similar to that of the tholeiitic suite of Thingmuli (Carmichael, 1964).

The relative proportions of potassium, sodium and calcium as atomic percentages in the tholeiitic and alkalic rocks from the Mourne area are plotted in Figure 13, along with the tholeiitic trend of Brito-Arctic (Thulean) and the Hawaiian alkalic series (Nockolds and Allen; 1956, 1954). Again, some of the Killough dyke rocks are plotted on the Hawaiian alkalic diagram to show their affinity with the Mourne alkalic rocks.

The Mourne alkali basalts are Ca-rich in nature and closely follow the Hawaiian alkalic trend at the initial stages. The Killough rocks, however, plot with more basic equivalents of the Mourne suite at the beginning of the curve, but they are scattered and somewhat deflected from the main trend at the intermediate stages towards the K-apex (Figure 13-A).

Fig. 13: Variation diagram of the K : Na : Ca (atomic %) ratios in the Mourne and Killough alkalic (A), and the Mourne tholeiitic (B) rocks. The main trends of the Hawaiian alkalic (Nockolds and Allen, 1954) and the Thulean tholeiitic (Nockolds and Allen, 1956) series are also indicated.

Symbols refer to: o Mourne tholeiitic series, • Mourne alkali basalts, ⊕ Killough alkalic series.

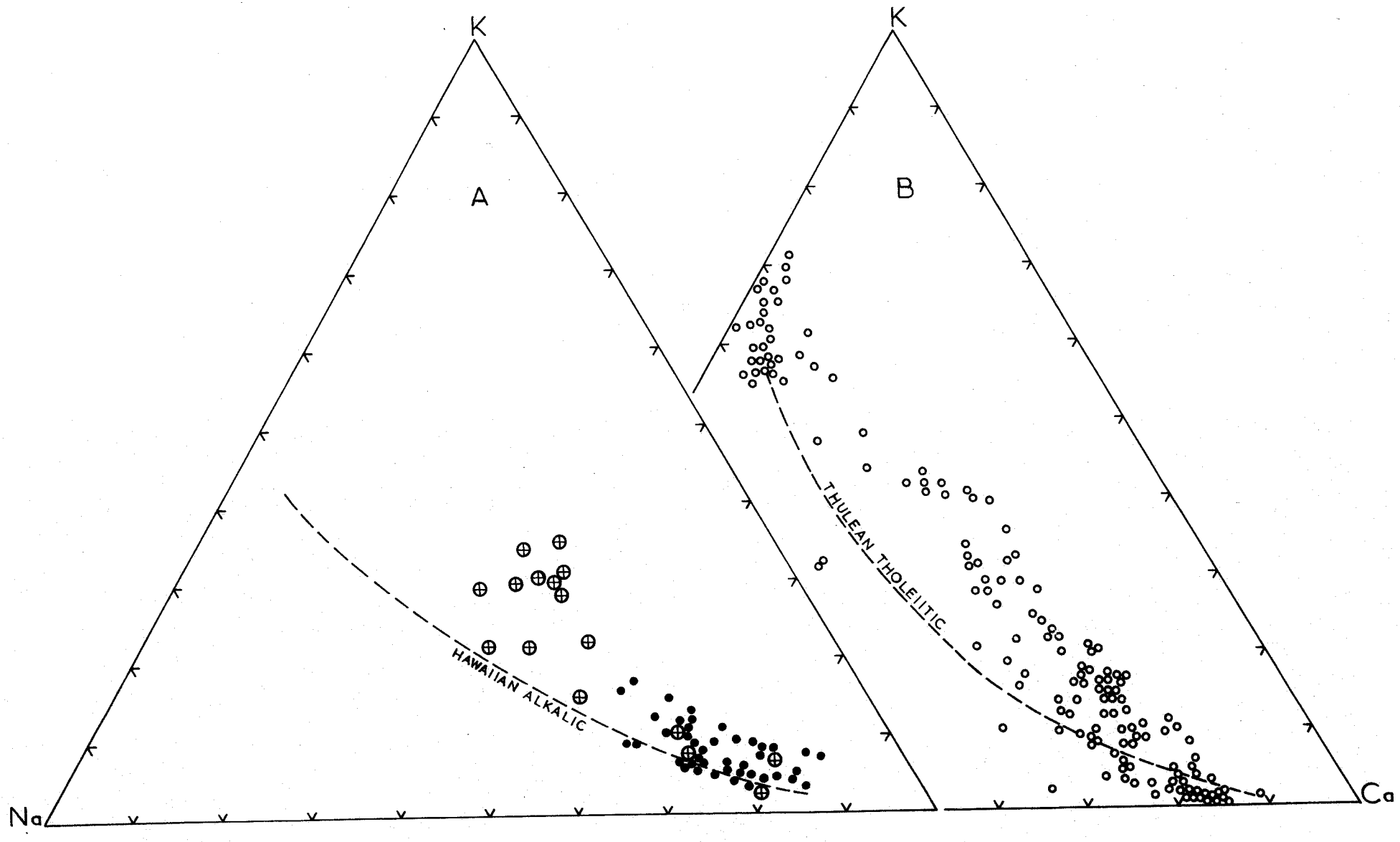
K
A
Na
HAWAIIAN ALKALIC
K
B
Ca
THULEAN THOLEIITIC

The relatively Na-rich character of the Ca-Na-K trend in the Mourne alkali basalts shows itself in the form of nepheline making its appearance in their norms. One of the alkali basalts from the St. John's Point area is also Ne-normative in character (Table 22-A, No.57).

The Mourne tholeiitic series, on the other hand, closely approaches a straight line in the Ca-Na-K variation diagram as shown in Figure 13-B. Its deviation from the main curve of the Thulean tholeiitic trend towards the K-end can be explained by the overall predominance of K_2O over Na_2O throughout the intermediate varieties of the Mourne tholeiitic suite.

A plot relating total iron oxides to magnesia for the Mourne tholeiitic and alkalic suites is shown in Figure 14. The Hawaiian alkalic (MacDonald and Katsura, 1964) and the Thingmuli tholeiitic (Carmichael, 1964) trends are also presented to illustrate the two extremes, along with the Killough alkalic series which parallels the Hawaiian alkalic trend, although somewhat less differentiated. The similarity between the two groups of alkali basalts from the Mourne and Killough dyke-swarms is clearly demonstrated in Figure 14-A.

The tholeiitic series of the Mourne swarm shows no notable difference from the Thingmuli tholeiitic trend in the maintenance of a

---

Fig. 14: Total iron versus magnesia (weight %) variation diagram for the Mourne and Killough alkalic (A), and the Mourne tholeiitic (B) rocks. The Hawaiian alkalic (MacDonald and Katsura, 1964) and the Thingmuli tholeiitic (Carmichael, 1964) trends are also indicated. Symbols refer to: o Mourne tholeiitic series, • Mourne alkali basalts, ⊖ Killough alkalic series.

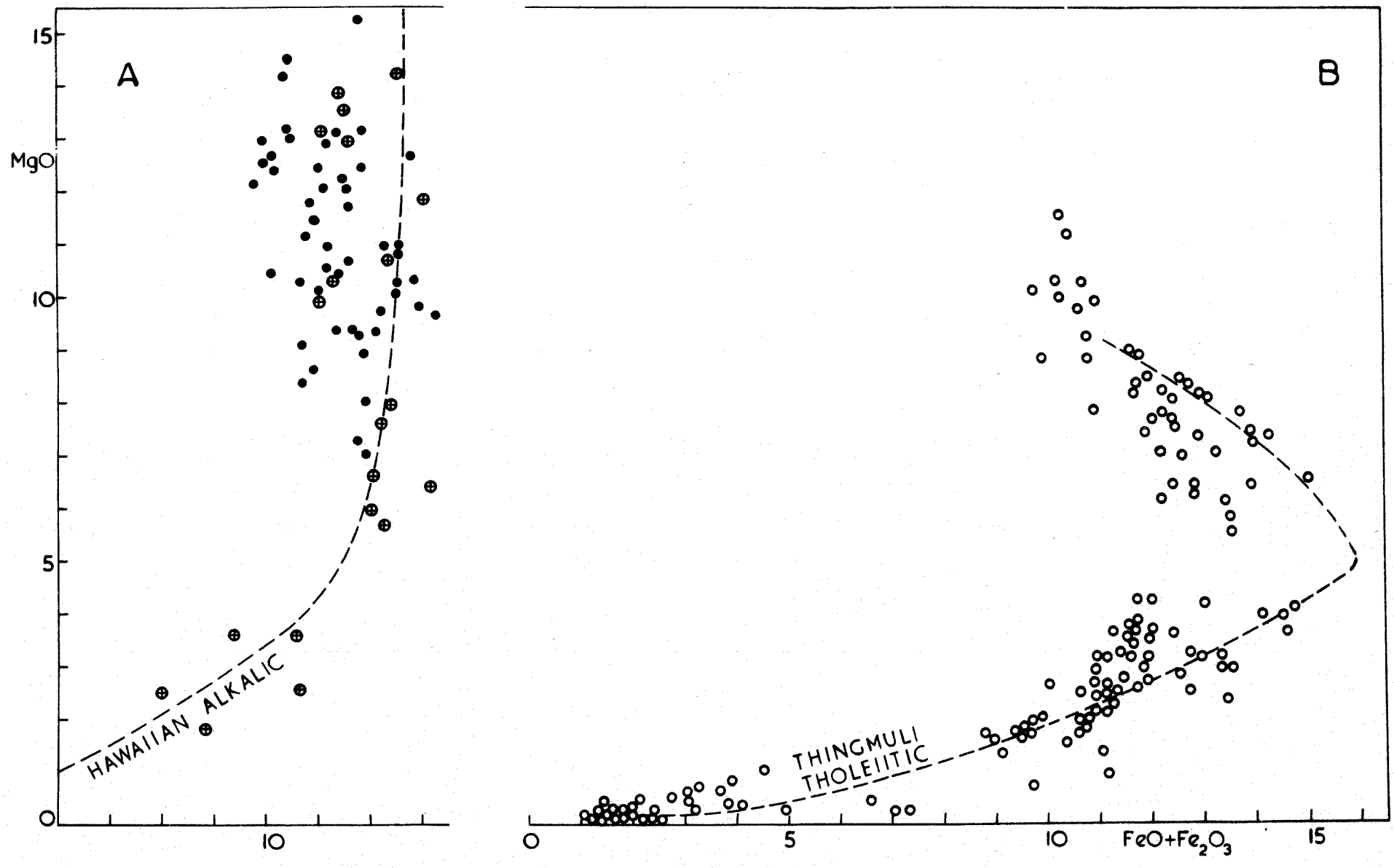
A
B
MgO
15
10
5
0
10
HAWAIIAN ALKALIC
THINGMULI
THOLEIITIC
0
5
10
15
FeO+Fe2O3

high iron content in the more differentiated, magnesia-poor intermediate members (Figure 14-B). The depletion of iron and thus the deviation from the Skaergaard trend of the Thingmuli tholeiitic andesites (Icelandites) has been attributed to precipitation and early removal of magnetite from the tholeiitic magma (Carmichael, 1964).

Phosphorus reaches a maximum in the mugearites of the Killough swarm (solidification index : 15) where apatite appears in the norm, being more than 2%. The basaltic members of the alkalic series have higher P_2O_5 content than their tholeiitic equivalents, and show a gradual increase in phosphorus with decreasing solidification index, reaching its maximum at about 1% in the intermediate members of the Killough-Ardglass dyke-swarm (cf. Table 22-A, No.47). It is probable that this value approaches the saturation point of phosphorus in the magma, at which level apatite becomes a cumulus phase.

In their discussion of phosphorus enrichment in rocks of the Upper Zone of the Skaergaard intrusion, Wager and Brown (1968, p.166, fig.114-B) indicate that apatite precipitates when 97% of the initial liquid is solid, from a residual liquid with 1.75% P_2O_5.

e) Chemical compositions of the major constituent minerals in the tholeiitic and alkalic rock suites from the Mourne area

An electron-probe X-ray microanalyser (Cambridge Instruments Mk II Geoscan), equipped with two spectrometers, was utilized for quantitative analysis of a number of elements in alkali feldspars, plagioclases, pyroxenes and olivines, as well as in some opaque iron-titanium oxide minerals. Analyses were carried out on both microphenocrysts and groundmass phases in a selected suite of rocks. The secondary minerals, chlorite (an alteration product of pyroxene), and serpentine (an

alteration product of olivine) have not been analyzed.

In most instances, complete analyses were carried out, using closely comparable standards where possible. The analytical techniques and subsequent correction procedures are dealt with in Appendix (A-4).

e.1) Olivines

The analyses of the olivines in the Mourne alkali basalts and olivine-tholeiites are shown in Table 23. They have been recalculated into the various olivine molecules and the summation in terms of weight per cent of the four olivine end-members indicates that the analyses are satisfactory.

The CaO and MnO contents, expressed as the larnite (La) and tephroite (Tp) molecules, show no significant variation in the recalculated mineral compositions. However, CaO and MnO slightly increase with increasing iron content in the olivine microphenocrysts of the Mourne olivine-tholeiites (Table 23).

CaO is always above the level of 0.10 wt. % which Simkin and Smith (1966, p.203; 1970, p.304) consider separates olivines of the deep-seated rocks from those which have crystallized in an extrusive or hypabyssal environment.

The low amount of Ca-substitution in the forsteritic olivines of the Mourne alkali basalts is a reflection of the much greater ionic radius of Ca^{2+} (0.99 Å) relative to the Mg^{2+} ion (0.66Å). However, with increasing iron content, increasing substitution or admission of Ca^{2+} and Mn^{2+} becomes possible.

The composition of each of the olivines has been plotted in Figure 15, to show their relationship to the co-existing pyroxenes. The orientation of their tie-lines in Figure 15-B is more or less

Table 23: Electron probe analyses of olivine microphenocrysts from the Mourne basic dykes

Wt. %	102A	102B	102C	102D	102E	102F	128A	128B	128C	128D
SiO_2	38.16	38.26	38.81	39.30	38.54	38.53	39.45	38.89	38.88	39.98
FeO	23.30	27.83	27.65	23.46	24.51	27.01	15.76	19.45	16.28	15.55
MgO	34.71	31.73	30.98	34.30	33.61	31.44	41.83	39.04	42.80	41.89
CaO	0.39	0.37	0.34	0.39	0.38	0.32	0.32	0.24	0.26	0.25
MnO	0.31	0.38	0.38	0.33	0.32	0.39	0.20	0.22	0.19	0.26
Total	96.87	98.23	98.16	97.78	97.36	97.69	97.56	97.84	98.41	97.93
	Numbers of ions on the basis of 4 Oxygens									
Si	1.027	1.034	1.050	1.045	1.037	1.045	1.016	1.016	0.997	1.023
Fe^{+2}	0.524	0.627	0.623	0.520	0.549	0.611	0.338	0.424	0.348	0.332
Mg	1.403	1.285	1.258	1.370	1.357	1.280	1.616	1.532	1.646	1.608
Ca	0.011	0.011	0.010	0.011	0.011	0.010	0.009	0.006	0.008	0.006
Mn	0.006	0.008	0.008	0.008	0.006	0.008	0.005	0.005	0.005	0.006
Z	1.02	1.03	1.05	1.04	1.03	1.04	1.01	1.01	1.00	1.02
X	1.94	1.93	1.90	1.91	1.92	1.91	1.97	1.97	2.00	1.95
Mg	72.8	67.2	66.9	72.5	71.2	67.7	82.7	78.3	82.5	82.9
Fe^{+2}	27.2	32.8	33.1	27.5	28.8	32.3	17.3	21.7	17.5	17.1
Fo	64.0	57.8	57.4	63.6	62.2	58.4	76.0	70.8	75.9	76.3
Fa	34.9	41.1	41.5	35.2	36.7	40.6	23.2	28.5	23.3	22.9
La	0.6	0.6	0.5	0.6	0.6	0.5	0.5	0.3	0.4	0.3
Tp	0.4	0.5	0.5	0.4	0.4	0.5	0.3	0.3	0.3	0.4
Mol %										
Fo	72.2	66.5	66.2	71.8	70.6	67.0	82.1	77.9	82.0	82.4
Fa	27.0	32.5	32.8	27.2	28.6	32.0	17.2	21.6	17.3	17.0
La	0.6	0.6	0.5	0.6	0.6	0.5	0.5	0.3	0.4	0.3
Tp	0.3	0.4	0.4	0.4	0.3	0.4	0.3	0.3	0.2	0.3

Key to the analyses:

Nos. 102 A - F Olivine-tholeiites

Nos. 128 A - D Alkali basalts.

similar to comparable phases in the Thingmuli tholeiitic series (Carmichael, 1967, p.1826, fig.5-b).

e.2) Clinopyroxenes

Augite is the sole pyroxene phase in all alkali basalts and in most of the tholeiites from the Mourne area. Optical determinations indicate that there are very few Ca-poor pyroxenes in the Mourne tholeiites in contrast to the Thingmuli tholeiitic rocks (Carmichael, 1967, p.1824).

In the analysed olivine-tholeiites, no evidence of Ca-poor groundmass pyroxene has been found with the electron-probe, however, in one of the quartz-tholeiites (No.414), pigeonite has been identified.

The analyses of the clinopyroxene phenocrysts and co-existing groundmass phases of the Mourne alkali basalts and tholeiites are given in Table 24A and B, and plotted in Figure 15, in terms of Ca, Mg, and Fe+Mn as atomic percentages.

The valency of iron is unknown in the case of microprobe analysis, and all iron is taken as FeO. However, Fe_2O_3 is arbitrarily recalculated by allotting equivalent molecular amounts of Fe_2O_3 to Na_2O.

Na_2O shows little variation in the analysed pyroxenes as a whole,

---

Fig. 15: A plot of clinopyroxene analyses (atomic %) from the Mourne alkalic (A) and the tholeiitic (B) rocks. The analyses of the co-existing olivines are also plotted on the base. Filled circles represent groundmass phases and open circles represent phenocrysts. The Thingmuli pyroxene trend is indicated by dashed line (Carmichael, 1967, p.1826, fig.5-B). The solid continuous line represents calcic augite trend of alkali olivine-basalt magma (Wilkinson, 1956, p.727, fig.2).

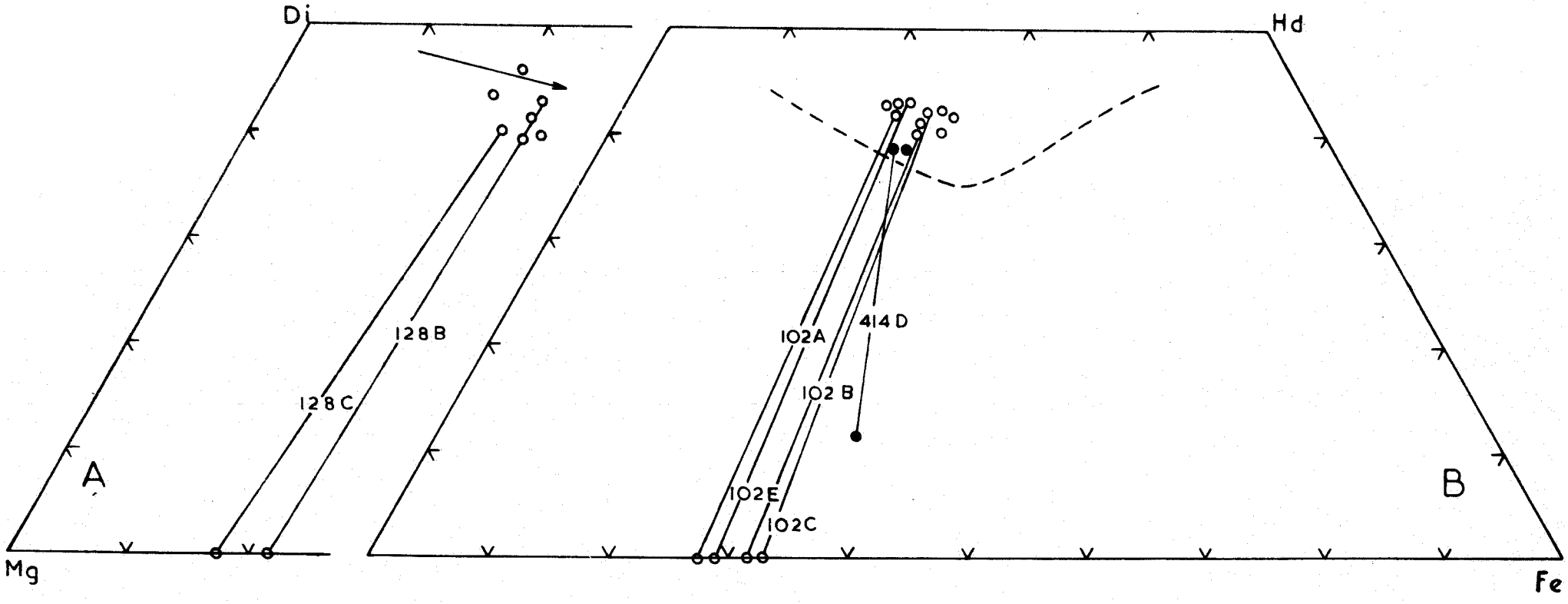
Di
Hd
128B
128C
102A
414D
102B
102E
102C
A
B
Mg
Fe

Table 24A: Analyses of clinopyroxenes from alkali basalts of the Mourne dyke-swarm

Wt. %	128A	128B	128C	128D	37b	26bA	26bB
SiO_2	48.16	47.17	47.88	48.37	47.75	47.06	48.10
Al_2O_3	3.70	4.73	3.88	3.20	5.37	5.71	5.36
TiO_2	1.82	2.31	1.96	1.29	1.86	2.60	1.70
Fe_2O_3	1.27	1.27	1.27	1.27	0.24	0.14	0.24
FeO	13.35	12.15	11.53	12.62	13.08	11.60	10.57
MnO	0.47	0.34	0.36	0.55	0.28	0.19	0.23
MgO	11.95	11.75	13.13	12.83	11.23	11.28	12.26
CaO	18.61	19.06	19.12	18.84	20.04	21.28	19.84
Na_2O	0.49	0.49	0.50	0.50	0.09	0.08	0.09
Total	99.82	99.27	99.63	99.47	99.94	99.94	98.39
	Numbers of ions on the basis of 6 oxygens						
Si	1.842	1.808	1.823	1.847	1.818	1.788	1.836
Al	0.158	0.192	0.174	0.144	0.182	0.212	0.164
Al	0.008	0.021	-	-	0.058	0.043	0.077
Ti	0.052	0.066	0.056	0.037	0.053	0.074	0.049
Fe^{3+}	0.036	0.036	0.036	0.036	0.007	0.004	0.007
Fe^{2+}	0.425	0.388	0.366	0.402	0.415	0.367	0.336
Mn	0.015	0.011	0.011	0.018	0.009	0.006	0.007
Mg	0.685	0.675	0.750	0.735	0.641	0.643	0.702
Ca	0.762	0.783	0.780	0.771	0.818	0.866	0.811
Na	0.036	0.036	0.036	0.037	0.007	0.006	0.007
Z	2.00	2.00	2.00	2.00	2.00	2.00	2.00
X+Y	2.02	2.01	2.03	2.03	2.01	2.01	2.00
Mg	35.6	35.6	38.6	37.5	33.9	34.1	37.7
Fe	24.8	23.0	21.3	23.2	22.8	20.0	18.8
Ca	39.6	41.4	40.1	39.3	43.3	45.9	43.5

Table 24B: Analyses of clinopyroxenes from the tholeiitic basalts of the Mourne dyke-swarm

Wt. %	112bA	112bB	112bC	102A	102B	102C
SiO_2	50.74	50.32	51.00	48.91	49.55	49.12
Al_2O_3	3.24	2.54	3.09	3.48	2.73	2.97
TiO_2	1.29	2.23	1.20	1.65	1.30	1.45
Fe_2O_3	0.12	0.38	0.24	0.34	0.60	0.24
FeO	12.95	12.30	13.28	13.02	14.25	14.72
MnO	0.32	0.39	0.40	0.47	0.39	0.49
MgO	11.38	11.39	10.88	11.81	10.93	11.42
CaO	19.85	19.73	19.76	19.87	19.60	19.39
Na_2O	0.07	0.16	0.09	0.12	0.23	0.09
Total	99.96	99.44	99.94	99.67	99.58	99.89
	Numbers of ions on the basis of 6 oxygens					
Si	1.918	1.913	1.930	1.869	1.903	1.883
Al	0.082	0.087	0.070	0.131	0.097	0.117
Al	0.062	0.027	0.068	0.025	0.026	0.017
Ti	0.037	0.064	0.034	0.047	0.037	0.042
Fe^{3+}	0.003	0.011	0.007	0.009	0.017	0.007
Fe^{2+}	0.408	0.390	0.419	0.415	0.456	0.470
Mn	0.010	0.013	0.013	0.015	0.013	0.016
Mg	0.645	0.649	0.618	0.672	0.625	0.652
Ca	0.804	0.803	0.801	0.813	0.806	0.796
Na	0.005	0.012	0.007	0.009	0.017	0.007
Z	2.00	2.00	2.00	2.00	2.00	2.00
X+Y	1.97	1.97	1.97	2.00	2.00	2.00
Mg	34.5	34.8	33.3	34.9	32.6	33.6
Fe	22.5	22.2	23.6	22.8	25.4	25.4
Ca	43.0	43.0	43.1	42.3	42.0	41.0

Table 24B continued:

Wt. %	124cA	124cB	124cC	414A	414B*	414C*	414D*
SiO_2	50.58	51.26	50.48	51.30	52.49	52.35	50.98
Al_2O_3	2.70	2.69	3.18	3.03	3.20	3.38	1.25
TiO_2	1.44	1.85	2.02	1.80	1.80	1.29	0.55
Fe_2O_3	0.17	0.79	0.95	0.93	1.26	0.80	0.30
FeO	14.86	14.52	14.08	13.30	11.90	13.18	21.20
MnO	0.40	0.42	0.39	0.38	0.43	0.36	0.47
MgO	10.22	10.11	9.31	10.88	11.37	11.19	19.10
CaO	19.51	17.62	17.99	17.67	16.76	16.96	5.92
Na_2O	0.08	0.30	0.38	0.36	0.49	0.30	0.11
Total	99.96	99.56	98.78	99.65	99.70	99.81	99.88
	Numbers of ions on the basis of 6 oxygens						
Si	1.929	1.950	1.937	1.939	1.962	1.963	1.930
Al	0.071	0.050	0.063	0.061	0.038	0.037	0.056
Al	0.050	0.070	0.081	0.074	0.103	0.112	-
Ti	0.041	0.053	0.058	0.051	0.050	0.036	0.016
Fe^{3+}	0.005	0.023	0.027	0.026	0.035	0.022	0.009
Fe^{2+}	0.472	0.460	0.450	0.419	0.371	0.412	0.669
Mn	0.013	0.014	0.013	0.012	0.014	0.011	0.015
Mg	0.585	0.577	0.536	0.617	0.638	0.629	1.085
Ca	0.797	0.718	0.740	0.716	0.671	0.681	0.240
Na	0.006	0.022	0.028	0.026	0.035	0.022	0.008
Z	2.00	2.00	2.00	2.00	2.00	2.00	2.00
X+Y	1.97	1.94	1.94	1.94	1.92	1.93	2.03
Mg	31.2	32.2	30.4	34.5	36.9	35.8	53.8
Fe	26.3	27.7	27.7	25.5	24.3	25.4	34.3
Ca	42.5	40.1	41.9	40.0	38.8	38.8	11.9

*groundmass phases

although it slightly increases in augites of the Mourne alkali basalts (Table 24A, No.128). Na detection, however, is poor on the probe used and figures of low concentration need treating with caution.

The Al_2O_3 content of pyroxenes varies according to pressure and temperature of crystallization and the type of magma involved, and where two pyroxenes (i.e. Ca-rich and Ca-poor) are present it is higher in the Ca-rich phase (Brown, 1967, p.123). The augites of the Mourne olivine-tholeiites (Figure 15-B) contain, on the average, about 3% Al_2O_3 (Table 24-B), whereas the content in calcic augites of some of the Mourne alkali basalts is more than 5% (Table 24-A). Both Kushiro (1960, p.548) and Le Bas (1962, p.267) have shown a marked increase in Al for the Na-poor clinopyroxenes from tholeiitic, through alkaline, to peralkaline assemblages (Figures 3, 5 of Le Bas, 1962).

The augites of the Mourne alkali basalts are rich in the Wo molecule and tend towards a calcic augite-salite trend (a characteristic feature of the alkalic series). This is comparable to the early trend of pyroxenes in the alkali olivine-basalt magma of the Gunnedah Sill (Wilkinson, 1956). Ca-poor pyroxenes are absent from the alkali basalts of the Mourne area.

The Ca-rich nature of the augites from undersaturated basalts, the absence of Ca-poor pyroxenes and the abrupt termination of the augite trend has been discussed by Brown (1967, p.129). As undersaturated liquids in the system Fo-Di-SiO_2 (Kushiro and Schairer, 1963, fig.25) are in equilibrium with diopside and forsterite only, more calcium will be taken up by the clinopyroxenes.

The presence of two co-existing pyroxene phases in the groundmass of one of the quartz-tholeiites (No.414) suggests that a metastable subcalcic augite is not present in the Mourne tholeiites.

e.3) Plagioclase compositions

Plagioclase is the only feldspar found either as a phenocryst or as a predominant groundmass constituent in the Mourne alkali basalts and tholeiites.

Many of the plagioclase phenocrysts are zoned and therefore their bulk composition is not easy to determine, and would require the analysis of numerous crystals from core to margin. Approximately six crystals in each selected rock with extensive zoning in the plagioclase have been analysed with the microprobe (Table 25-A). The plagioclase analyses, expressed as weight % An, Ab and Or (Table 25-B) are plotted in Figure 16.

The concentration of iron has been determined in all analysed plagioclases. In keeping with conventions and the evidence from chemically analysed feldspars (Deer et al., 1963, vol.4, p.107; Brown, 1967, p.109), all the iron is assumed to be in the trivalent state and consequently is expressed as weight % Fe_2O_3.

Strontium and barium have also been determined to show possible ion substitution between Ca^{2+} and Sr^{2+}. Recent work on the partition of Sr and Ca in plagioclases from basic rocks, carried out by Brooks (1968) and by Berlin and Henderson (1968) has shown that Sr enters more readily into the plagioclase structure than does Ca, contradicting earlier concepts.

The probe analyses show a consistent silica excess (1-3% in terms

---

Fig. 16: The variation in composition of plagioclase feldspars in the basic rocks from the Mourne area, represented in terms of wt. % of the components An, Ab and Or. Filled circles refer to microprobe analyses, open circles represent normative feldspars of the host-rock.

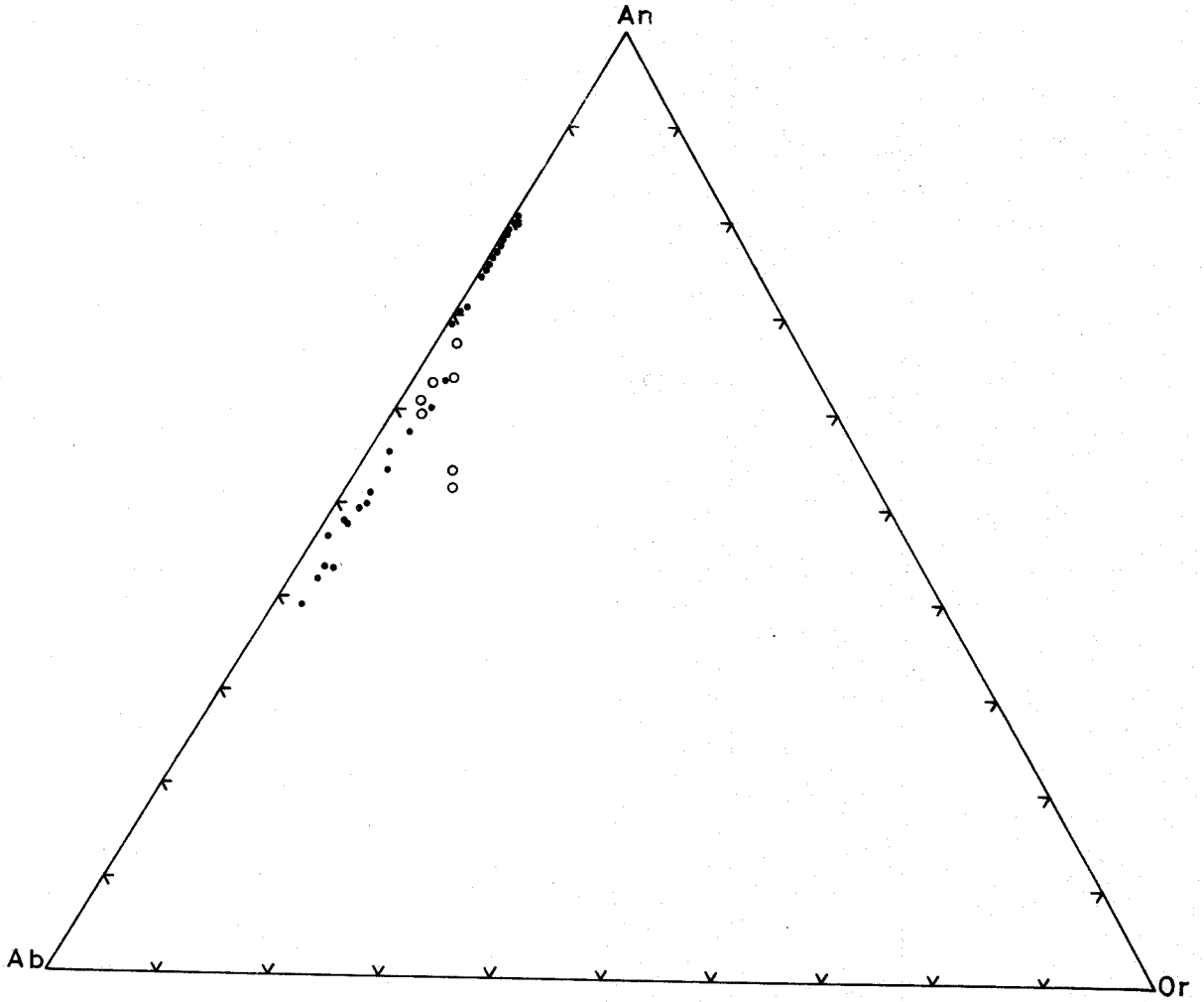
An
Ab
Or

Table 25-A: Analyses of plagioclase feldspars from the Mourne alkalic and tholeiitic basalts. Groundmass compositions are indicated by an asterisk.

Wt. %	128A	128B	128C	128D	128E*	128F	37b	33
SiO_2	50.08	51.65	56.56	51.52	56.69	50.77	49.57	50.55
Al_2O_3	31.56	29.82	27.33	29.78	27.22	29.73	31.84	31.34
Fe_2O_3	0.44	0.60	0.22	0.60	0.23	0.62	0.55	0.32
CaO	14.88	13.83	9.16	15.12	9.55	15.12	15.34	14.90
Na_2O	2.80	3.59	6.15	2.77	5.48	2.95	2.45	2.76
K_2O	0.03	0.05	0.20	0.02	0.44	0.10	0.14	0.05
Sr	0.03_7	0.04_7	0.03_7	0.04_4	0.03_9	0.03	0.01_9	0.02_8
Ba	-	-	-	0.00_5	-	0.00_4	0.00_1	0.00_2
Total	99.83	99.59	99.66	99.86	99.65	99.32	99.91	99.95
	Numbers of ions on the basis of 32 oxygens							
Si	9.161	9.449	10.200	9.415	10.220	9.344	9.074	9.220
Al	6.791	6.420	5.798	6.401	5.775	6.439	6.855	6.725
Fe^{3+}	0.066	0.077	0.032	0.077	0.032	0.088	0.077	0.044
Ca	2.918	2.711	1.774	2.959	1.849	2.982	3.010	2.911
Na	0.987	1.273	2.142	0.975	1.914	1.049	0.868	0.974
K	0.007	0.011	0.046	0.004	0.102	0.023	0.033	0.012
Sr	0.003	0.004	0.003	0.005	0.004	0.003	0.002	0.003
Z	16.02	15.95	16.03	15.89	16.03	15.87	16.00	15.99
X	3.92	4.00	3.97	3.94	3.87	4.06	3.91	3.90
Mol % Ab	25.2	31.8	54.0	24.8	49.6	25.9	22.2	25.0
Mol % An	74.6	67.9	44.8	75.1	47.8	73.6	77.0	74.7
Mol % Or	0.2	0.3	1.2	0.1	2.6	0.5	0.8	0.3
	Core	Intermediate	Margin					

Table 25-A continued:

Wt. %	124cA	124cB	124cC	112bA	112bB	112bC*	112bD*	KD53C†
SiO_2	49.81	49.69	49.58	49.87	49.85	55.34	57.03	57.92
Al_2O_3	31.12	31.34	31.13	31.17	31.83	27.80	26.45	24.36
Fe_2O_3	0.27	0.26	0.29	0.44	0.21	0.50	0.54	1.69
CaO	16.03	15.68	16.10	15.56	15.00	10.92	9.56	8.00
Na_2O	2.45	2.57	2.58	2.62	2.86	4.90	5.89	5.97
K_2O	0.06	0.06	0.05	0.05	0.04	0.40	0.41	1.49
Sr	0.02_4	0.03_5	0.02_4	0.03_4	0.02_6	0.03_3	0.03_1	0.10
Ba	-	0.00_3	0.00_2	-	-	0.00_1	-	0.07
Total	99.76	99.64	99.76	99.74	99.82	99.89	99.91	99.60
	Numbers of ions on the basis of 32 oxygens							
Si	9.140	9.120	9.103	9.144	9.117	10.001	10.277	10.478
Al	6.717	6.768	6.722	6.724	6.846	5.912	5.612	5.190
Fe^{3+}	0.037	0.036	0.040	0.061	0.029	0.068	0.074	0.239
Ca	3.149	3.084	3.168	3.059	2.940	2.115	1.849	1.553
Na	0.870	0.914	0.915	0.930	1.009	1.714	2.054	2.085
K	0.014	0.014	0.012	0.012	0.009	0.092	0.094	0.347
Sr	0.002	0.003	0.002	0.003	0.002	0.003	0.003	0.011
Z	15.90	15.92	15.87	15.93	15.99	15.98	15.96	15.91
X	4.04	4.02	4.10	4.00	3.96	3.92	4.00	3.99
Mol % Ab	21.6	22.8	22.3	23.2	25.5	43.7	51.4	52.3
Mol % An	78.1	76.9	77.4	76.5	74.3	53.9	46.3	39.0
Mol % Or	0.3	0.3	0.3	0.3	0.2	2.4	2.3	8.7

† Specimen KD53C was collected from St. John's Point area, Killough, and was analysed by XRF method. Analysis includes 0.13% MgO, 0.20% TiO_2, 0.07% P_2O_5, 0.02% Mn, 19 ppm. Rb, 34 ppm. Zr, 9 ppm. Ni, 9 ppm. Cu and 9 ppm. Zn.

Table 25-A continued:

Wt. %	102A	102B	102C	102D*	102E*	102F*	26bA	26bB*
SiO_2	48.84	49.79	48.90	51.85	52.16	54.90	51.00	56.54
Al_2O_3	31.41	32.16	31.96	30.09	29.92	28.28	31.09	27.15
Fe_2O_3	0.80	0.53	0.66	0.36	0.47	0.40	0.34	0.37
CaO	16.25	13.71	15.89	12.60	12.03	10.29	13.96	9.80
Na_2O	2.37	3.38	2.29	3.96	4.31	5.45	3.28	5.49
K_2O	0.04	0.06	0.05	0.55	0.58	0.47	0.17	0.45
Sr	0.02_8	0.03_4	0.02_3	0.03_5	0.03_1	0.02_9	0.02_7	0.02_4
Ba	-	0.00_2	0.00_1	0.00_4	-	-	0.00_2	0.00_1
Total	99.74	99.67	99.77	99.45	99.50	99.82	99.87	99.82
	Numbers of ions on the basis of 32 oxygens							
Si	8.996	9.107	8.982	9.485	9.532	9.936	9.299	10.187
Al	6.808	6.924	6.910	6.477	6.436	6.027	6.674	5.753
Fe^{3+}	0.111	0.072	0.091	0.050	0.065	0.054	0.044	0.050
Ca	3.205	2.688	3.130	2.470	2.357	1.998	2.724	1.893
Na	0.840	1.196	0.816	1.405	1.524	1.911	1.160	1.914
K	0.009	0.014	0.012	0.128	0.135	0.109	0.039	0.104
Sr	0.002	0.003	0.002	0.003	0.002	0.003	0.003	0.002
Z	15.92	16.10	15.98	16.01	16.03	16.02	16.02	15.99
X	4.06	3.90	3.96	4.00	4.02	4.02	3.93	3.91
Ab	20.7	30.7	20.6	35.1	38.0	47.6	29.6	48.9
Mol % An	79.1	69.0	79.1	61.7	58.7	49.7	69.4	48.4
Or	0.2	0.3	0.3	3.2	3.3	2.7	1.0	2.7
	Core	Margin						

Table 25-A continued:

Wt. %	414A*	414B*	414C*	84A/	84B/	82A/	82B/
SiO_2	55.47	55.20	55.87	56.95	57.07	58.14	57.13
Al_2O_3	27.66	27.94	27.44	27.11	26.87	26.33	26.39
Fe_2O_3	0.46	0.55	0.45	0.27	0.72	0.77	0.43
CaO	10.55	11.14	9.80	8.57	8.29	7.61	8.72
Na_2O	5.10	4.53	6.00	6.29	6.47	6.63	6.46
K_2O	0.50	0.46	0.40	0.62	0.43	0.46	0.48
Sr	0.02_1	0.02_7	0.03	0.04_2	0.03_8	0.04_7	0.02_7
Ba	-	0.00_3	-	-	-	-	0.00_3
Total	99.76	99.85	99.99	99.85	99.89	99.99	99.64
	Numbers of ions on the basis of 32 oxygens						
Si	10.039	9.983	10.086	10.256	10.272	10.424	10.316
Al	5.885	5.946	5.828	5.749	5.692	5.551	5.602
Fe^{3+}	0.063	0.076	0.061	0.037	0.097	0.103	0.059
Ca	2.046	2.159	1.896	1.653	1.599	1.463	1.690
Na	1.786	1.584	2.096	2.194	2.258	2.302	2.254
K	0.115	0.106	0.092	0.143	0.098	0.105	0.111
Sr	0.002	0.002	0.003	0.004	0.004	0.005	0.002
Z	15.99	16.00	15.98	16.04	16.06	16.08	15.98
X	3.95	3.85	4.09	3.99	3.96	3.88	4.06
Mol % Ab	45.2	41.1	51.3	55.0	57.1	59.5	55.6
Mol % An	51.8	56.1	46.4	41.4	40.4	37.8	41.7
Mol % Or	3.0	2.8	2.3	3.6	2.5	2.7	2.7

/ Refers to analysis of groundmass plagioclase laths in the Mourne intermediate rocks.

Table 25B: Recalculated plagioclase compositions in terms of wt. % of the three feldspar components and normative feldspar of the host-rock

Wt. %	128A	128B	128C	128D	128E	128F	128 Norm	124cA	124cB	124cC
Ab	24.1	30.6	52.6	23.9	47.9	25.0	37.1	20.6	21.8	21.4
An	75.7	69.1	46.2	76.0	49.4	74.5	61.1	79.1	77.9	78.3
Or	0.2	0.3	1.2	0.1	2.7	0.5	1.8	0.3	0.3	0.3
	124c Norm	112bA	112bB	112bC	112bD	112b Norm	102A	102B	102C	102D
Ab	30.8	22.1	24.4	42.3	50.0	35.3	19.8	29.4	19.6	33.7
An	67.0	77.6	75.4	55.4	47.8	62.8	80.0	70.2	80.1	63.0
Or	2.2	0.3	0.2	2.3	2.2	1.9	0.2	0.4	0.3	3.3
	102E	102F	102 Norm	84A	84B	84 Norm	82A	82B	82 Norm	37b
Ab	36.6	46.1	33.0	53.4	55.5	26.6	58.0	54.1	29.4	21.2
An	60.0	51.1	63.6	42.9	41.9	40.8	39.2	43.1	40.0	78.0
Or	3.4	2.8	3.4	3.7	2.6	32.6	2.8	2.8	30.6	0.8
	37b Norm	33	33 Norm	26bA	26bB	26b Norm	414A	414B	414C	414 Norm
Ab	38.6	23.9	37.8	28.3	47.5	36.0	43.8	39.7	49.9	27.2
An	51.7	75.8	53.7	70.7	49.8	60.9	53.4	57.5	47.8	59.5
Or	9.7	0.3	8.5	1.0	2.7	3.1	2.8	2.8	2.3	13.3

Alkalic basalts: 128, 37b, 33, 26b;

Tholeiitic basalts: 124c, 112b, 102 (olivine-tholeiites); 414 (Quartz-tholeiite); 84,82 (Tholeiitic andesite-Dunmore Type).

of normative quartz), when recalculated in terms of molecular proportions of the three feldspar end-members. Whether this is a function of the quality of the analysis of the particular probe standard employed, or inherent in the correction methods applied to the probe data or, thirdly a real silica excess in the plagioclases is not fully known. However, this may probably be related to a small, constant analytical error in the probe determination of SiO_2.

A fairly continuous range of plagioclase compositions, from bytownite to andesine, exists in the basic rocks from the Mourne area, with a slight increase in Or content towards the sodic end of the feldspar trend (Figure 16).

The plagioclase phenocrysts in the Mourne olivine-tholeiites are similar in composition to those phenocrysts found in the alkali basalts; their outer rims correspond in composition with the associated groundmass plagioclases. The Mourne olivine-tholeiites contain calcic plagioclase phenocrysts (An_{80}) with K_2O at or below detection limit, but a gradual increase in the orthoclase molecule takes place with increasing albite content, with 2 and 4% Or in plagioclases of An_{50} and An_{40}, respectively, in the more differentiated quartz-tholeiites and tholeiitic andesites from the Mourne area.

The normative feldspar content for each of these rocks is invariably more potassic than the modal feldspar, and is frequently more sodic as well (Table 25-B).

A possible complete solidus fractionation path of the Mourne tholeiitic series is represented in Figure 17-B which illustrates a progressive enrichment in the potassium and sodium components of feldspar, from basic to acid end (Carmichael, 1963, p.99, fig.2).

e.4) Iron-titanium oxide minerals

Opaque iron-titanium oxide minerals exist throughout the two rock suites from the Mourne dyke-swarm and they appear as a microphenocryst phase, especially in the intermediate stages of the tholeiitic series.

In general, a titaniferous magnetite partially enclosing groundmass plagioclase and pyroxene in the olivine-tholeiites is in the form of interstitial ragged grains, whereas in the tholeiitic andesites it forms more or less euhedral crystals.

Ilmenite occurs as a discrete phase crystallizing directly from the liquid and forms beautiful skeletal crystals disseminated throughout the rock (Plate 7). Exsolution or heterogeneity has not been positively observed in any ilmenite examined with the microprobe.

The microprobe analyses of titaniferous magnetites and ilmenites are presented in Tables 26 and 27 respectively. Both sets of analyses of the iron-titanium oxides have been recalculated to check their quality (Carmichael, 1967b, p.40), and as may be seen from the Tables 26 and 27, the totals of the spinel phases are quite satisfactory either on the ilmenite basis of calculation or on the ulvospinel basis. The totals of the recalculated rhombohedral phases are also satisfactory.

Fig. 17: Compilation of the feldspar data for the Mourne and Killough alkalic (A), and the Mourne tholeiitic (B) rocks, based on the normative anorthite, albite, and orthoclase (weight %) components. The dashed line represents the limit of ternary solid solution in natural feldspars (After Smith and MacKenzie, 1958, p.874, fig.1). Symbols refer to: o Mourne tholeiitic series, • Mourne alkali basalts, ⊕ Killough alkalic series.

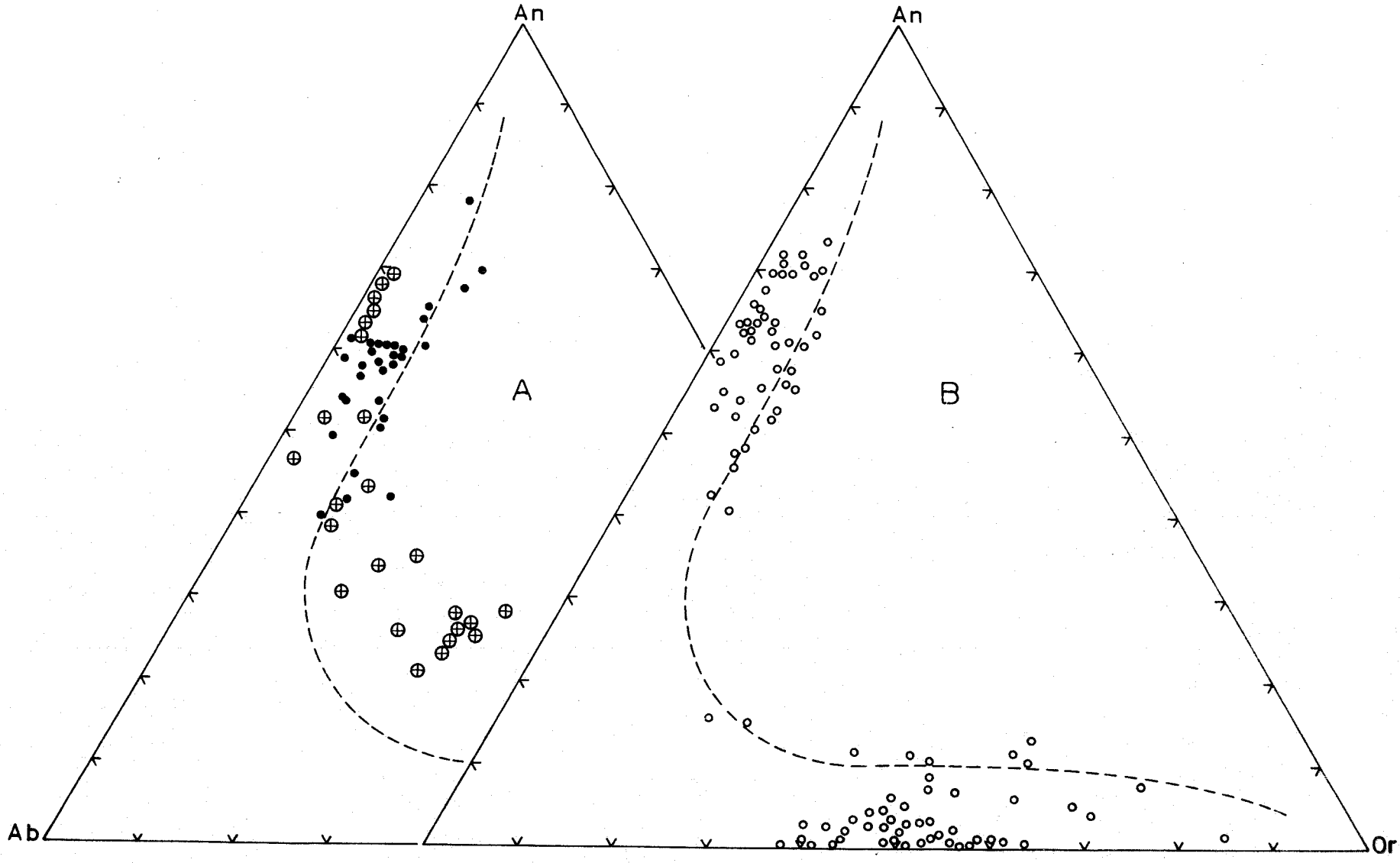
An
An
A
B
Ab
Or

Table 26: Analyses of titaniferous magnetites from the Mourne tholeiitic and alkalic rocks*

Wt. %	128	124c	112b	102	84A	84B	82
SiO_2	0.12	0.11	0.09	0.12	0.65	0.10	0.24
TiO_2	12.58	21.30	19.45	15.10	11.36	11.13	9.19
Al_2O_3	1.17	1.10	0.98	0.80	0.97	0.33	0.34
Cr_2O_3	0.03	0.02	0.02	0.02	0.02	0.04	0.03
V_2O_3	0.44	0.57	0.34	0.20	1.44	1.72	1.22
FeO	79.37	72.41	73.09	78.12	79.89	79.81	83.57
MnO	0.89	1.18	0.99	0.97	0.48	0.93	0.57
MgO	0.97	0.47	0.40	0.44	0.70	1.29	0.24
Sum	95.6	97.2	95.4	95.8	95.5	95.3	95.4
Recalculated analyses							
Ilmenite basis							
Fe_2O_3	51.5	40.0	41.7	48.5	51.2	53.3	55.7
FeO	33.0	36.3	35.5	34.4	33.7	31.8	33.4
Total	100.7	101.0	99.5	100.5	100.5	100.6	100.9
Ulvospinel basis							
Fe_2O_3	44.9	27.3	30.0	39.7	44.4	48.2	50.0
FeO	38.9	47.8	46.0	42.4	39.9	36.4	38.5
Total	100.0	99.8	98.3	99.7	99.9	100.1	100.3
Mol % Ulvo-spinel	29.7	57.4	53.0	39.3	31.0	23.4	24.5

* Specimen numbers as in Table 25-B.

Table 26 continued:

Wt. %	80	37bA	37bB	33	26bA	26bB	414
SiO_2	0.60	0.60	0.13	0.13	0.18	0.10	0.65
TiO_2	11.01	9.79	9.46	12.85	9.26	7.95	13.51
Al_2O_3	0.30	2.02	0.34	0.94	0.83	0.70	1.43
Cr_2O_3	0.02	n.d.	n.d.	0.02	n.d.	n.d.	n.d.
V_2O_3	1.22	n.d.	n.d.	0.80	n.d	n.d.	n.d.
FeO	80.81	81.57	84.39	79.25	81.51	84.82	78.74
MnO	0.98	0.83	1.01	1.07	1.20	0.99	1.16
MgO	0.29	0.85	n.d.	1.03	1.48	0.12	0.24
Sum	95.2	95.6	95.3	96.1	94.4	94.6	95.7
			Recalculated analyses				
Ilmenite basis							
Fe_2O_3	52.5	54.0	56.7	51.4	56.5	58.0	49.1
FeO	33.6	32.9	33.3	32.9	30.6	32.6	34.5
Total	100.5	101.0	100.9	101.1	100.0	100.5	100.6
Ulvospinel basis							
Fe_2O_3	45.7	48.8	51.0	44.9	53.1	53.6	40.7
FeO	39.7	37.6	38.4	38.8	33.7	36.6	42.1
Total	99.8	100.5	100.3	100.5	99.8	100.0	99.8
Mol % Ulvo-spinel	30.0	23.9	24.3	29.5	15.7	19.3	37.4

Table 27: Analyses of ilmenites from the Mourne tholeiitic and alkalic rocks

Wt. %	128	124c	112b	102	84A	84B	82
SiO_2	0.06	0.03	0.04	0.08	0.07	0.63	0.57
TiO_2	45.65	48.90	49.27	44.75	49.65	49.89	50.23
Al_2O_3	0.15	0.16	0.09	0.27	0.34	0.29	0.70
Cr_2O_3	n.d.	0.02	n.d.	0.06	n.d.	n.d.	n.d.
V_2O_3	n.d.	0.30	n.d.	0.55	0.46	0.58	0.52
FeO	49.81	46.34	47.05	51.34	47.97	46.93	46.56
MnO	1.15	0.82	0.98	0.70	0.90	0.95	0.63
MgO	2.21	2.61	1.65	1.17	o.26	0.36	0.58
Sum	99.0	99.2	99.1	98.9	99.6	99.6	99.8
			Recalculated analyses				
Fe_2O_3	15.3	8.6	7.4	15.3	5.1	3.2	2.6
FeO	36.0	38.5	40.4	37.5	43.4	44.0	44.2
Total	100.5	99.9	99.8	100.4	100.2	99.9	100.3
Mol % R_2O_3	16.9	10.0	8.1	17.0	6.0	4.2	3.9
Temp °C	880	995	950	960	735	665	675
fO_2 atm.	$10^{-11.5}$	$10^{-10.8}$	$10^{-11.6}$	$10^{-10.5}$	$10^{-16.3}$	$10^{-18.7}$	$10^{-18.7}$

	80	37bA	37bB	33	26bA	26bB	414
SiO_2	0.06	0.05	0.06	0.02	0.09	0.07	0.09
TiO_2	49.90	44.35	44.85	44.92	39.51	39.27	44.10
Al_2O_3	0.70	0.17	0.19	0.05	0.20	0.19	0.18
Cr_2O_3	0.02	n.d.	n.d.	n.d.	n.d.	n.d.	n.d.
V_2O_3	0.50	n.d.	n.d.	n.d.	n.d.	n.d.	n.d.
FeO	47.21	50.75	50.82	51.11	54.65	54.90	52.30
MnO	0.70	1.33	1.27	0.75	0.71	0.70	0.68
MgO	0.47	1.28	1.16	1.54	2.02	2.12	0.91
Sum	99.6	97.9	98.3	98.4	97.2	97.3	98.3
			Recalculated analyses				
Fe_2O_3	4.2	16.0	15.3	15.7	25.9	26.7	16.5
FeO	43.4	36.3	37.0	37.0	31.3	30.9	37.4
Total	99.9	99.5	99.8	100.0	99.7	100.0	99.9
Mol % R_2O_3	5.6	17.4	16.5	16.8	28.3	29.2	17.5
Temp °C	750	850	800	880	925	980	950
fO_2 atm.	$10^{-16.6}$	$10^{-12.0}$	$10^{-13.0}$	$10^{-11.5}$	$10^{-9.2}$	$10^{-8.8}$	$10^{-10.5}$

The estimated temperatures ($\bar{+}30^{o}C$) of the iron-titanium oxide equilibration are given in Table 27 together with the oxygen fugacities ($10^{\bar{+}1}$).

The compositions of the co-existing iron-titanium oxide phases in terms of the molecular percent of ulvospinel in the magnetite and the molecular percent of R_2O_3 (the sum of Al_2O_3, Cr_2O_3, V_2O_3 and Fe_2O_3) in the ilmenite have been plotted in Figure 18.

The spinel phases show a range of 57 to 24 molecular percent ulvospinel in the Mourne tholeiitic rocks, but the associated rhombohedral phases show only a small range in composition from 4 to 10% R_2O_3. In the alkali basalts, on the other hand, the TiO_2 content of both phases is distinctly lower than in the tholeiites. This may be due to the titaniferous character of the pyroxenes found in the alkali basalts. Since more TiO_2 was taken up by the early formed calcic augites the liquid may have become impoverished in TiO_2 before the later formation of oxide phases.

The ilmenites in the alkali basalts contain up to 29% R_2O_3 and the magnetites contain as little as 16% ulvospinel molecule (e.g. No.26b in Tables 26 and 27). Thus, it seems in a general way that there is a correspondence between the composition of the oxide phases and the co-existing ferromagnesian minerals, because the silicates, particularly pyroxene compete for TiO_2 or for the other components in the liquid.

Fig. 18: A plot relating the analyses of the co-existing iron-titanium oxides in the Mourne alkalic and tholeiitic rocks, in terms of the mol % Usp in the magnetite and of R_2O_3 in the ilmenite. Filled circles represent oxide phases in alkali basalts, open circles refer to those phases in the tholeiitic rocks.

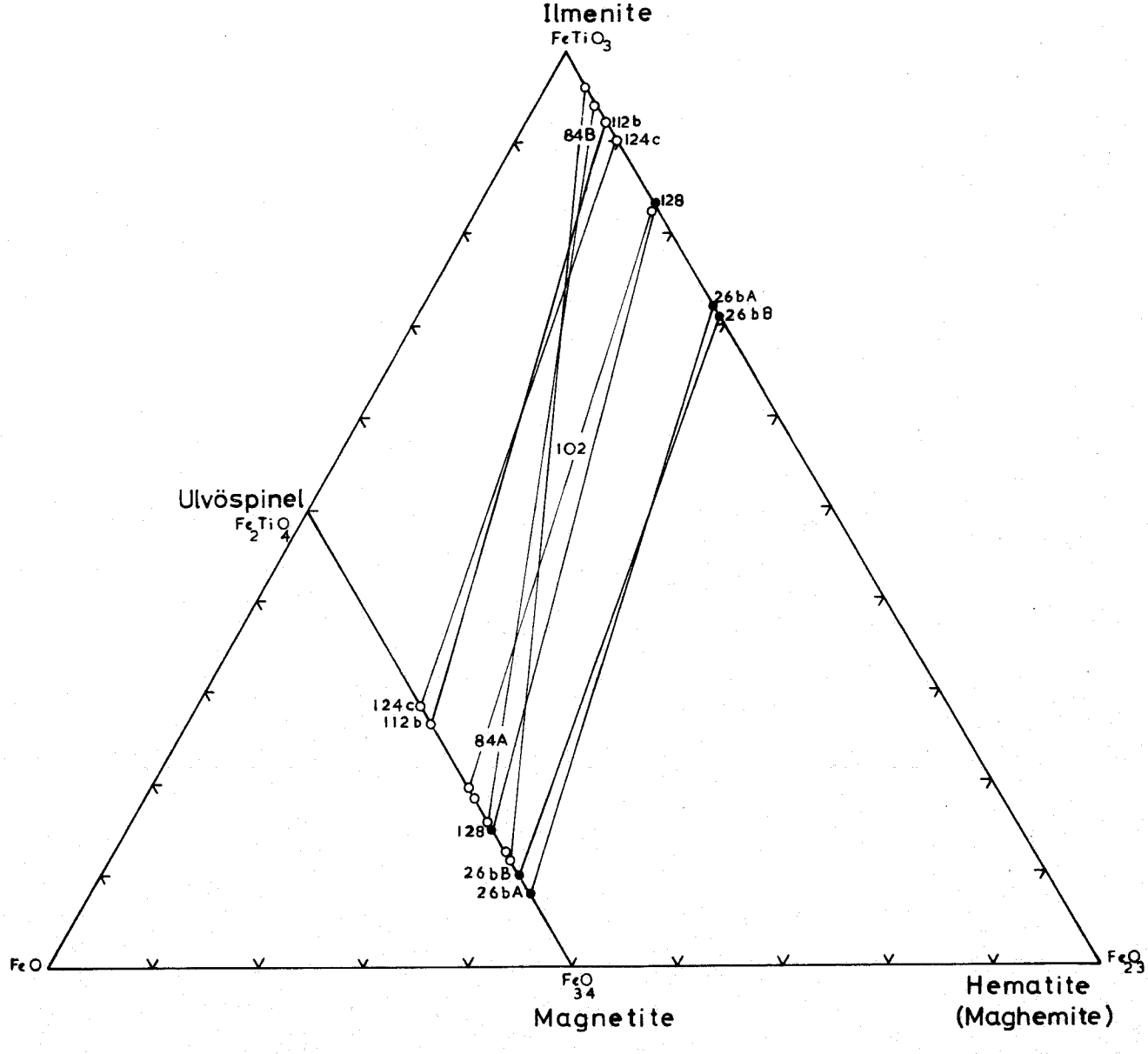
Ilmenite
$FeTiO_3$
112b
84B
124c
128
26bA
26bB
102
Ulvöspinel
Fe_2TiO_4
124c
112b
84A
128
26bB
26bA
FeO
$Fe_{34}O$
Magnetite
$Fe_{23}O$
Hematite
(Maghemite)

The oxide phases are sensitive to environmental conditions as shown by Buddington and Lindsley (1964, p.354).

Buddington and Lindsley (1964) have experimentally determined the composition of magnetite in equilibrium with ilmenite for a wide range of temperatures and oxygen fugacities and have also developed a method to estimate these two parameters (op.cit., p.316, fig.5). Although the co-precipitation of a ferromagnesian phase containing Ti, Fe^{3+} and Fe^{2+} may modify to some extent the applicability of this method, it has been used in the determination of estimated temperatues and oxygen fugacities of the Mourne alkalic and tholeiitic rocks, following the procedure described by Carmichael (1967b), and the results are plotted in Figure 19.

The Mourne tholeiitic rocks have equilibration data which plot very near the curve of the synthetic buffer fayalite-magnetite-quartz. The oxide assemblages in the alkali basalts, on the other hand, fall above the QFM curve.

The general conclusion drawn from the spinel-ilmenite phase equilibration data is that there is a smooth and progressive decrease in oxygen fugacity from the olivine-tholeiites to tholeiitic andesites throughout the Mourne series (Figure 19, Nos. 124-c, 112-b, and Nos. 84-A, 84-B, 82 and 80 respectively), the values of which are essentially

---

Fig. 19: A plot relating the values of the temperature and oxygen fugacity ($-\log_{10}$) of the Fe-Ti oxide equilibration curve for the Mourne alkalic and tholeiitic rocks. The curve QFM represents the variation of the fugacity of oxygen with temperature for the buffer fayalite - magnetite-quartz at 1 atm. total pressure. The curve WM is the curve for wustite-magnetite buffer at 1 atm. (Eugster and Wones, 1962). Symbols as in Figure 18.

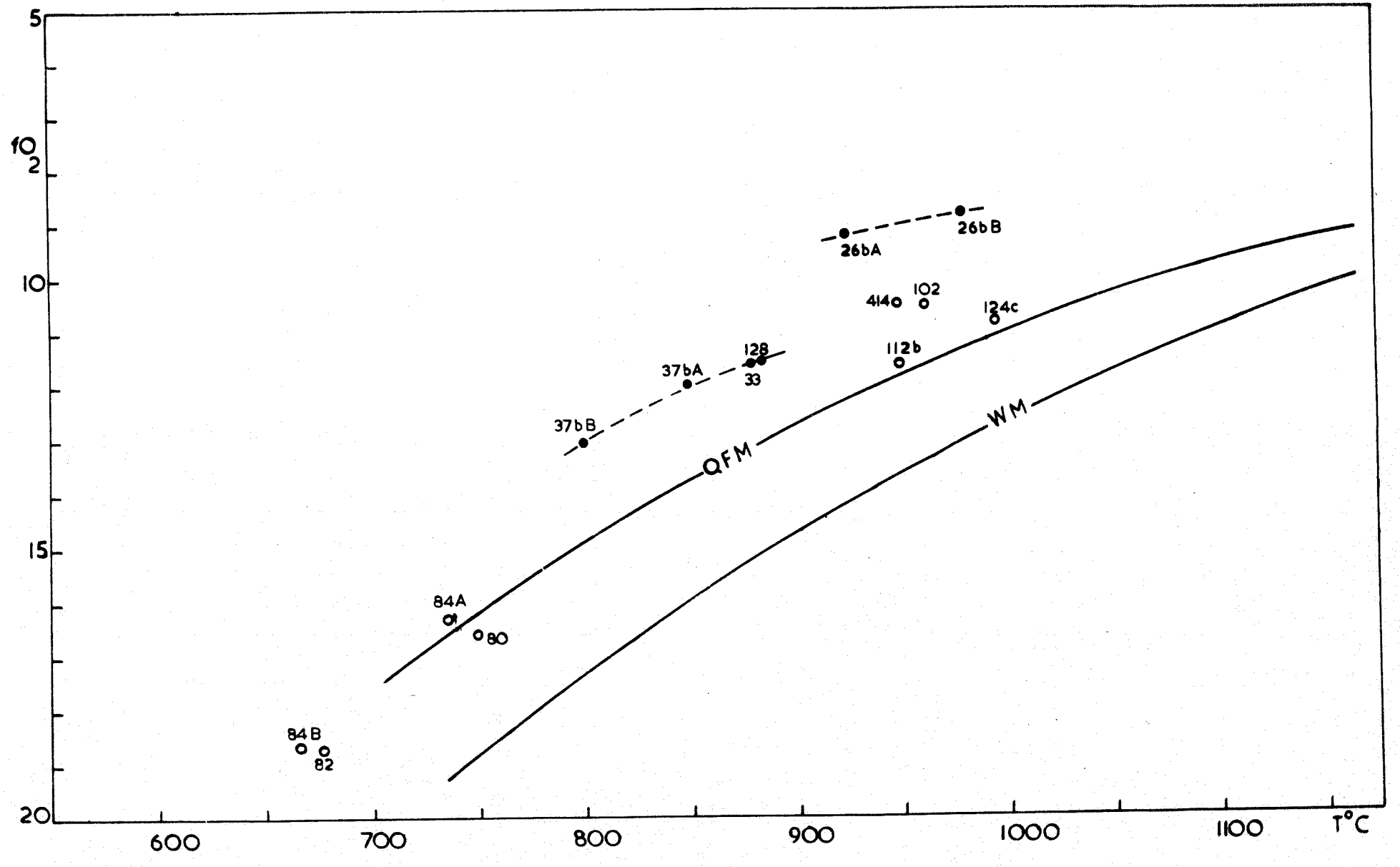
5
10
2
10
15
20
600
700
800
900
1000
1100
T°C
26bA
26bB
414o
102
124c
112b
128
33
37bA
37bB
QFM
WM
84A
80
84B
82

those of the synthetic fayalite-magnetite-quartz buffer at the appropriate temperatures.

Osborn (1959) has suggested that the Skaergaard intrusion and non-orogenic tholeiitic liquids which show a similar and progressive absolute iron-enrichment have fractionated with a low, fixed oxygen content. If the evidence of this course of fractionation is conveyed to the hypabyssal products, then the data from the Mourne tholeiitic series are in accord with Osborn's hypothesis.

Although the chemical analyses presented here, may shed some light on the composition of Fe-Ti oxide minerals in both rock suites from the Mourne area, the examination has been only cursory and the quantitative data on these minerals are not enough to represent the whole picture. The shortage of data on the iron-titanium oxides is a serious omission, particularly with regard to the potential of these minerals as indicators of physical conditions in the magma at the time of crystallization. A systematic examination and analysis of all the Fe-Ti oxide minerals found in the Mourne rocks would, therefore, be worthwhile.

After all the microprobe work had been completed and the above comments had been written, it was discovered that some of the magnetite crystals show minute exsolution grains of ilmenite (Plate 8). Some other grains, on the other hand, are spotted by tiny patches of ilmenite scattered throughout the grain. Unfortunately no reflected light microscopy studies had been carried out prior to the microprobe work and therefore all the analyses have been done without taking this effect into account, and assuming that all the magnetite grains are more or less homogeneous in composition. However, in most cases, two analyses of the magnetite from the same polished section have been

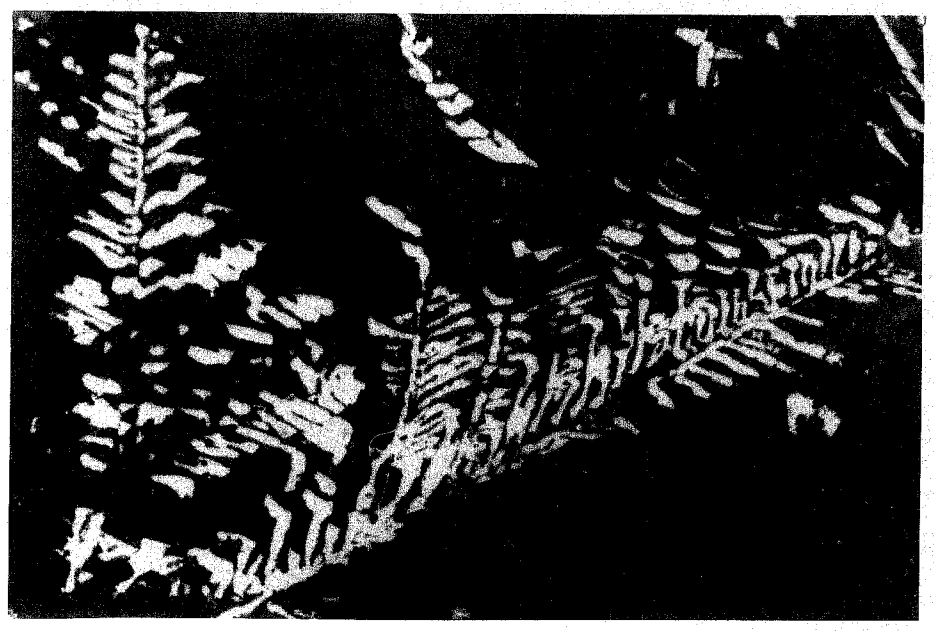

Plate 7: Dendritic ilmenite in dyke No: 84, x330, reflected light.

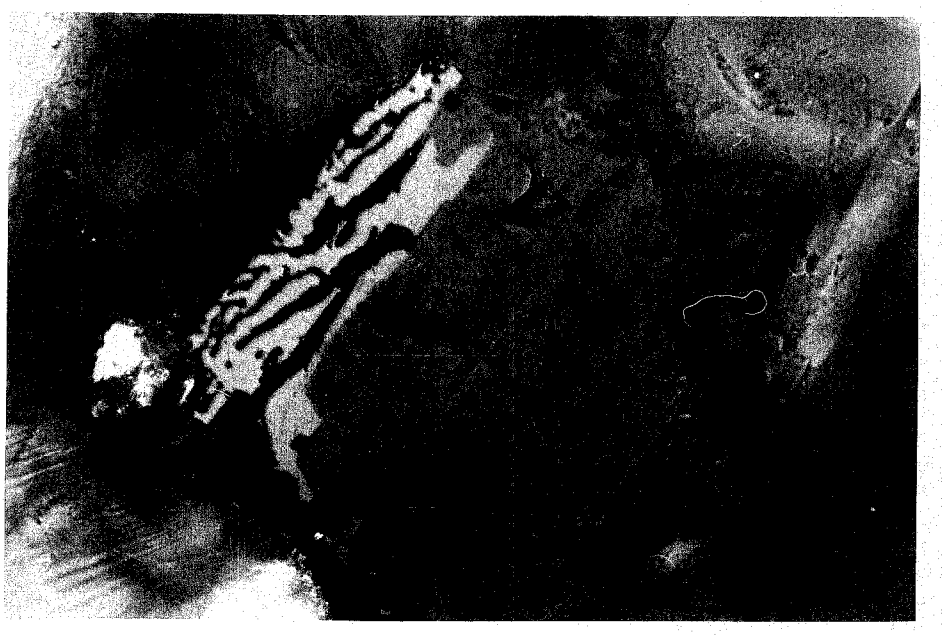

Plate 8: Magnetite (dark gray) showing exsolution grains of ilmenite (white) in dyke No: 112-b, x520, reflected light.

given in Table 26, and their close similarity to the theoretical value indicates that the majority of the analysed magnetite grains are unmixed.

f) Trace element analyses of the basic rocks

72 alkali basalts including 11 samples from St. John's Point area of the Killough-Ardglass dyke-swarm, 41 olivine-tholeiites, 32 quartz-tholeiites and 9 post-granitic basic dykes within the Eastern Mourne granites have been analysed for Ba, Sr, Rb, Zr, Ni, Cu and Zn (Tables 28 to 33; see Appendix, A-2, for the method). Variations of these elements are shown graphically for all the analysed rocks in Figures 20 to 28, along with the intermediate and acid members in order to show complete variation curves from basic to acid end.

Barium:

Ba is highly enriched in the differentiated intermediate members of the Mourne and Killough dyke rocks (Figure 20), although the degree of enrichment varies with the rock series. With an average concentration of 1926 ppm. the Killough mugearites show the highest Ba enrichment (Table 30). The Ba/K ratio for the alkalic rocks is higher than that for the tholeiitic series, but varies little with differentiation except in the very last stages of the tholeiitic trend.

Fig. 20: Distribution of barium (ppm) in the Mourne and Killough rocks. The ellipsoidal field represents compositional range found in the Eastern Mourne granites.

Symbols represent: o Mourne tholeiitic series; • Mourne alkali basalts ⊖ Killough alkalic series; Δ Eastern Mourne granites.

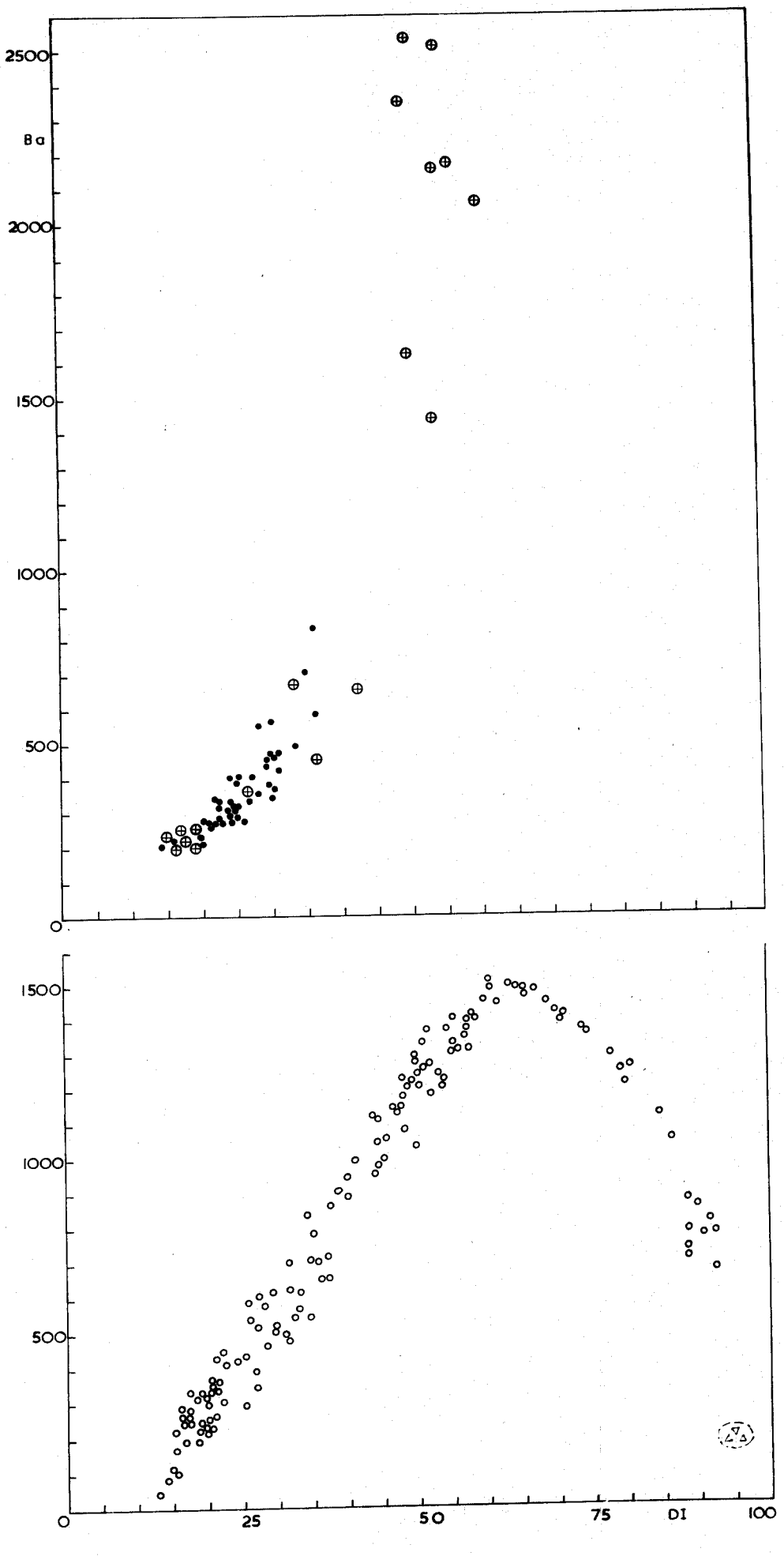
2500
Ba
2000
1500
1000
500
0
1500
1000
500
0
25
50
75
DI
100

Table 28: Trace element analyses of the Mourne alkali basalts

Sample No.	Ba (ppm)	Sr (ppm)	Rb (ppm)	Zr (ppm)	Ni (ppm)	Cu (ppm)	Zn (ppm)
129-a	462	341	24	200	73	91	108
129-b	470	322	22	212	44	82	131
128	275	140	6	77	236	217	52
124-d	230	317	7	80	136	122	55
113	304	205	12	74	96	106	72
110-a'	306	276	10	165	68	73	105
103	405	267	11	98	135	131	75
90-a	520	231	41	143	63	113	135
88-a	624	262	50	155	54	84	127
87	277	209	8	120	226	146	80
87-a	266	194	5	123	188	172	84
86	247	153	50	91	95	107	95
GPCS-1	712	231	24	172	70	89	76
GPCS-2	588	232	38	175	64	68	105
GPCS-3	571	254	60	162	50	58	114
GPCS-4	494	218	43	126	55	96	82
GPCS-5	470	234	39	144	60	103	89
GPCS-6	469	230	58	139	65	79	130
GPCS-8	558	202	54	149	68	68	169
13328	423	227	38	139	66	100	126
13329	508	225	51	151	53	72	136
56	368	195	41	177	117	73	184
54	442	147	29	175	118	462	235
54-b	331	178	7	79	208	140	149
46	387	185	93	180	190	232	236
46-a	279	196	13	120	232	164	88
45-a	254	187	7	124	222	239	86
45-b	366	190	50	119	227	134	244
37-b	424	263	40	191	104	104	99
36-a	214	248	65	178	107	121	92
33	338	190	17	124	73	89	100
28	843	207	69	188	39	78	130
27	701	185	44	189	40	76	132

Table 28 continued:

Sample No.	Ba (ppm)	Sr (ppm)	Rb (ppm)	Zr (ppm)	Ni (ppm)	Cu (ppm)	Zn (ppm)
26-a	343	133	7	88	311	285	147
26-b	278	174	6	94	216	138	169
24	257	241	20	114	93	115	94
23	280	135	16	94	256	157	90
22	287	185	7	146	97	118	82
21	206	143	13	96	294	268	114
19	224	259	9	93	326	262	197
18	270	195	8	99	209	188	163
15	269	274	21	128	132	93	141
14	335	329	31	151	100	105	118
12	299	226	54	161	97	112	82
11	211	157	10	125	148	145	94
10	270	138	20	121	137	119	116
3	316	120	66	123	150	94	93
2	322	121	44	121	130	93	102
502	407	292	11	93	138	156	109
503	394	213	7	106	132	164	119
504	407	343	16	110	112	237	177
505	207	316	10	126	102	171	179
506	338	238	10	91	45	78	104
507	230	134	10	94	183	204	97
509	262	175	7	86	354	86	146
511	293	122	15	67	211	194	75
512	320	180	9	81	183	126	78
513	318	204	5	81	227	191	109
516	351	154	12	97	109	163	86
13340	470	309	12	78	157	117	66
XB-1	425	301	12	64	156	119	60
Average:	372	215	25	125	138	137	116

Table 29: Trace element analyses of the Killough alkali basalts

Sample No.	Ba (ppm)	Sr (ppm)	Rb (ppm)	Zr (ppm)	Ni (ppm)	Cu (ppm)	Zn (ppm)
KD 48	263	147	2	76	257	179	63
KD 49	258	140	1	91	299	181	55
KD 51	226	124	4	82	292	215	70
KD 52	232	95	1	66	396	178	56
KD 54	242	101	2	71	271	171	43
KD 55	229	95	8	71	398	194	62
KD 57	456	295	5	159	70	91	75
KD 58	673	288	9	171	57	98	80
KD 59	360	239	4	126	87	123	62
KD 60	203	111	4	66	336	197	59
KD 61A	233	119	6	76	318	187	69
Average:	307	159	4	96	253	165	63

Table 30: Trace element analyses of the Killough mugearites

Sample No.	Ba (ppm)	Sr (ppm)	Rb (ppm)	Zr (ppm)	Ni (ppm)	Cu (ppm)	Zn (ppm)
KD 46	657	397	30	218	25	79	94
KD 47	2354	295	106	447	5	57	113
KD 53A	2510	467	112	319	10	36	94
KD 53B	2067	698	86	366	5	29	73
KD 56	2349	530	109	303	11	39	106
KD 61B	1620	485	88	236	8	92	104
KD 62	2173	421	105	308	3	50	117
KD 63	2162	418	112	314	7	25	122
KD 64	1442	402	90	293	7	26	117
Average:	1926	457	93	312	9	48	104

Table 31: Trace element analyses of the Mourne olivine-tholeiites

Sample No.	Ba (ppm)	Sr (ppm)	Rb (ppm)	Zr (ppm)	Ni (ppm)	Cu (ppm)	Zn (ppm)
127-a	592	270	5	116	80	103	95
127-c	219	258	4	127	92	104	90
127-d	279	195	10	74	149	110	65
126-a	335	205	3	88	82	103	82
126-b	337	223	2	95	81	162	75
125	294	212	11	64	213	128	58
124-c	226	207	2	107	104	104	75
124-e''	253	239	2	110	99	108	64
124-e'''	221	208	1	114	99	109	75
121-c	276	164	7	59	199	121	64
119-a	337	149	9	54	257	128	65
119-b	367	234	6	71	106	109	73
118	172	163	2	51	274	113	59
117	363	244	3	73	106	111	77
116	333	186	2	98	160	110	63
115	430	181	6	105	124	106	75
112-a	289	209	3	78	96	112	65
112-b	264	185	2	76	107	103	72
110-a''	252	200	7	118	35	72	91
109-a''	363	263	10	103	67	91	95
109-a'''	450	176	12	105	67	92	108
107-a	273	255	3	126	160	108	62
107-c	513	239	10	153	96	85	90
105	317	289	1	78	123	126	65
104	196	205	1	91	133	112	67
102	256	184	3	114	304	188	82
101	114	147	5	51	215	116	60
100-a	326	135	10	47	223	116	60
100-b	244	141	7	48	188	106	60
97	405	139	10	54	236	123	72
96	302	242	6	86	108	90	71
95	267	247	5	153	85	93	81
94-b	418	214	9	99	178	99	88
93	293	145	8	122	81	125	90
76-b	576	257	10	143	67	88	108
62	191	135	10	79	246	127	62
55-a	92	151	6	85	266	125	93
47	251	225	8	70	88	152	118
6	44	198	3	56	254	129	93
4	238	201	14	127	182	168	88
514	538	159	18	179	54	101	98
Average:	305	202	6	94	143	114	78

Table 32: Trace element analyses of the pre-granitic quartz-tholeiites

Sample No.	Ba (ppm)	Sr (ppm)	Rb (ppm)	Zr (ppm)	Ni (ppm)	Cu (ppm)	Zn (ppm)
127-b	464	163	37	101	114	89	60
127-e	996	135	97	148	84	65	62
124-a	524	217	76	165	39	77	78
124-e'	513	322	49	213	51	66	121
123	613	198	84	158	56	72	87
122	453	232	70	155	51	88	69
121-a	571	236	61	150	60	76	72
121-b	718	227	76	154	57	78	68
114	1122	321	63	275	26	68	98
111-a	417	135	86	164	32	93	69
111-b	703	208	22	186	63	79	109
109-a'	435	139	75	177	65	51	65
108	493	160	60	119	107	68	74
99	481	253	28	255	67	88	101
91	463	149	62	195	60	64	97
76	515	134	26	191	48	105	119
68	435	149	62	198	62	72	97
67	763	194	115	182	53	53	84
57-a	656	193	49	167	46	54	85
57-b	614	220	48	162	63	97	96
54-a	305	135	76	167	64	62	85
37-a	687	277	51	225	25	60	125
31	486	178	57	245	75	51	75
30-a	495	217	49	241	52	86	92
30-c	546	186	79	245	54	87	85
29	451	179	99	150	64	80	85
25-a	711	216	33	194	46	79	116
25-b	649	225	26	201	46	66	108
25-c	687	167	73	201	42	102	121
16	532	272	47	317	26	62	125
508	541	253	71	325	26	69	52
510	1030	356	45	185	54	92	95
Average:	596	207	61	194	55	75	90

Table 33: Trace element analyses of the post-granitic quartz-tholeiites

Sample No.	Ba (ppm)	Sr (ppm)	Rb (ppm)	Zr (ppm)	Ni (ppm)	Cu (ppm)	Zn (ppm)
401	419	173	30	94	71	102	80
405	907	191	103	166	51	71	83
406	945	181	118	162	56	79	92
408	896	176	119	159	45	78	86
409	976	197	88	167	52	53	77
410	692	183	56	132	72	104	115
411	971	145	125	200	53	88	113
412	388	204	51	125	73	99	99
414	504	180	42	119	43	96	86
Average:	744	181	81	147	57	85	92

Barium increases with increasing differentiation indices and reaches its peak value in the intermediate rocks of both series.

For comparative purposes, Ba concentrations in the Eastern Mourne granite specimens have also been plotted in Figure 20.

The Mourne alkali basalts also show a gradual increase in Ba with increasing DI, but this increase is more spectacular in the alkalic series of the Killough dyke-swarm (Figure 20). The variation of Ba in the Killough alkalic series follows a pattern similar to that of many other alkalic series, being comparable to the alkalic lavas of St. Helena (Baker, 1969, p. 1303, fig.12), and to the alkalic series of Setberg area (Sigurdsson, 1970, p.230, fig.51) in terms of Ba enrichment.

Baker (op.cit., p.1297) considers the initial removal of Sr with its smaller ionic radius (1.12 Å) into feldspars in preference to the larger Ba ions (1.34 Å), thus further enriching the intermediate rocks of St. Helena in Ba. The work of Berlin and Henderson (1969, p.253) shows that Ba is depleted in plagioclase relative to Ca and enriched in the residual liquid relative to K. This gains support from an analysis of a plagioclase phenocryst from the St. John's Point mugearite (No. KD 53-C, Table 25-A), where the andesine phenocryst and the whole rock contain 706 and 2510 ppm. Ba, respectively. A somewhat similar relationship has been reported by Sigurdsson (op.cit., p.228) in the Setberg alkalic lavas and the evidence indicates that in the intermediate rocks, Ba is more enriched in the liquid rather than in the individual feldspar phenocrysts.

Berlin and Henderson (op.cit., p.251) further showed that with differentiation the alkali feldspars show decreasing Ba/Sr and Sr/Ca ratios, i.e., during crystallization the alkali feldspars are enriched in Ba relative to Sr and in Sr relative to Ca, thus depleting the

residual liquid in Ba. Baker (op.cit., p.1297) also supports this view by giving evidence of Ba entering the alkali feldspars once the Sr concentration becomes low, thus greatly impoverishing the final liquid, and hence the late highly differentiated rocks in Ba. This is again supported by the analyses of the Mourne cone-sheet granophyres and their alkali feldspar phenocrysts. Analyses show that there are high concentrations of Ba in the individual alkali feldspar phenocrysts (Table 9) and relatively low Ba content in the host-rocks (Table 10).

It is seen that the evidence from the Mourne area supports the general view that Ba is likely to be more readily incorporated by the alkali feldspars rather than the plagioclases.

Strontium:

The variation diagram of Sr in the Mourne and Killough rocks is illustrated in Figure 21. There is a remarkable difference between the Sr distribution for the tholeiitic series and that in the alkalic rocks.

Sr shows a fairly continuous decrease with differentiation in the tholeiitic series of the Mourne dyke-swarm. A similar pattern has been reported by Sigurdsson (1970, p.237) in the tholeiitic rocks of the Setberg area. The average Sr concentration in the Mourne tholeiites is about 200 ppm. (Tables 31 and 32), but it decreases down to 50 ppm. in the late-stage acid members of this series (Table 10). The depletion of Sr with differentiation can be attributed to the amount of plagioclase remaining from the original liquid, and the low concentration of Sr in the late-stage differentiates may be held responsible for the

---

Fig.21: Distribution of strontium (ppm) in the Mourne and Killough rocks. Symbols as in Figure 20.

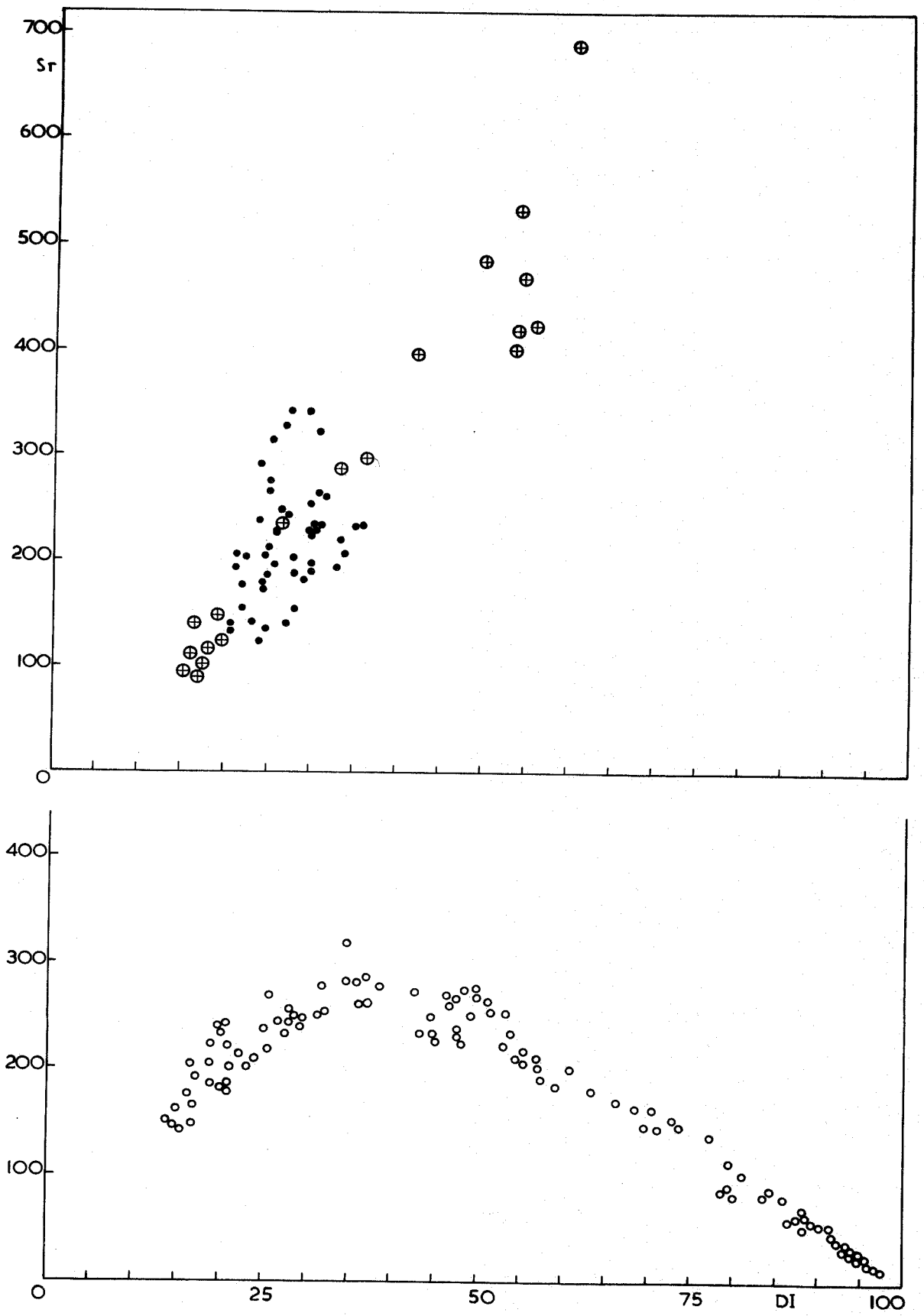
700
Sr
600
500
400
300
200
100
0
400
300
200
100
0
25
50
75
DI
100

low calcium content of these rocks. Patterson (1952, p.296) suggests that Sr^{2+} replaces Ca^{2+} rather than K^{1+} and the increase in Sr can be correlated with its entry into the plagioclase feldspars while its decrease in the acid rocks is consistent with the fall in the proportion of lime feldspars in these rocks. The evidence given by Brooks (1968, p.15) and by Berlin and Henderson (1968, p.80) shows that Sr enters more readily into the plagioclase structure and thus supports the above view.

The alkalic rocks, on the other hand, especially the Killough alkalic series show a remarkable Sr enrichment with differentiation. The basic members of this series contain as little as 159 ppm. Sr on average (Table 29), whereas intermediate alkalic rocks attain the highest Sr concentration among all the analysed specimens, with an average value of 457 ppm. (Table 30). Baker (1969, p.1297) reports that the St. Helena trachytes have never been greatly enriched in Sr because of the occurrence of alkali feldspars in these late derivatives. He claims that in the St. Helena trachytes Sr enters potassium-bearing minerals at DI = 60 corresponding with the appearance of discrete alkali feldspar phenocrysts in the more salic rocks. However, the more basic members of St. Helena display a similar enrichment of Sr (Baker, 1969, p.1302, fig.10) as in the case of Killough alkalic series, and Sigurdsson (1970, p.231, fig.52) shows a trend of Sr - enrichment in the alkalic series of the Setberg region.

Rubidium:

Rb shows a very steady increase with differentiation in both alkalic and tholeiitic rocks (Figure 22), ranging from an average value of 6 ppm. in the Mourne olivine-tholeiites to 196 ppm. in the late-stage acid members (Tables 31 and 10). Alkalic rocks, however, contain

higher amounts of Rb as compared with the tholeiitic rocks (cf. Table 28).

The correlation between Rb and K is good in both rock suites (Figures 23 and 24) with a strong grouping about K/Rb ratio of 230. The great majority of the values fall within the limits of scatter in fig.1 of Ahrens et al. (1952, p.240).

Similar Rb/DI relationships have been shown by Baker (1969, p.1303, fig.12) and by Sigurdsson (1970, p.232, fig.53; p.241, fig.58).

Zirconium:

Like Rb, Zr behaves in a similar manner in both rock suites from the Mourne and Killough area, and increases from approximately 100 ppm. in the basic members to 350 ppm. in the intermediate rocks of both alkalic and tholeiitic series (Tables 28, 29, 30, 31 and 35). It further increases to 508 ppm. on average in the acid rocks of the tholeiitic suite (Table 10).

The variation diagram of Zr in the Mourne and Killough rocks is illustrated in Figure 25. Similar enrichment in Zr with differentiation in many other igneous provinces have been reported by a number of

---

Fig. 22: Distribution of rubidium (ppm) in the Mourne and Killough rocks. Symbols as in Figure 20.

Fig. 23: Potassium-rubidium ratios in the Mourne and Killough alkalic rocks. Symbols as in Figure 20.

⨯ Limits of scatter (Ahrens et al., 1952, fig.1). W_E-1, G_E-1: Analytical values reported in this study. W_A-1, G_A-1: Analytical values quoted from Taylor et al. (1956).

Fig. 24: Potassium-rubidium ratios in the Mourne tholeiitic series. Symbols as in Figures 20 and 23.

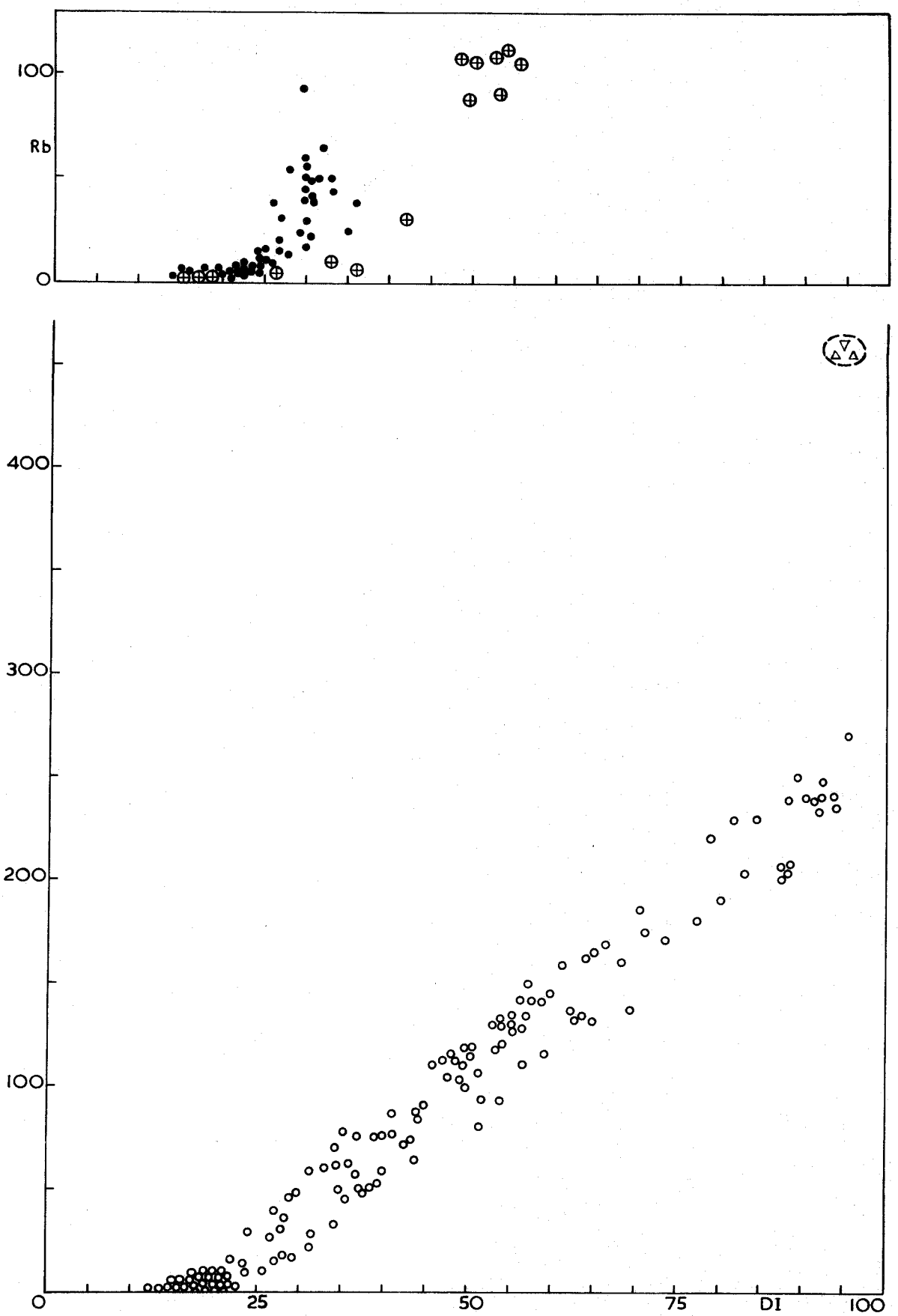
100
Rb
0
400
300
200
100
0
25
50
75
DI
100

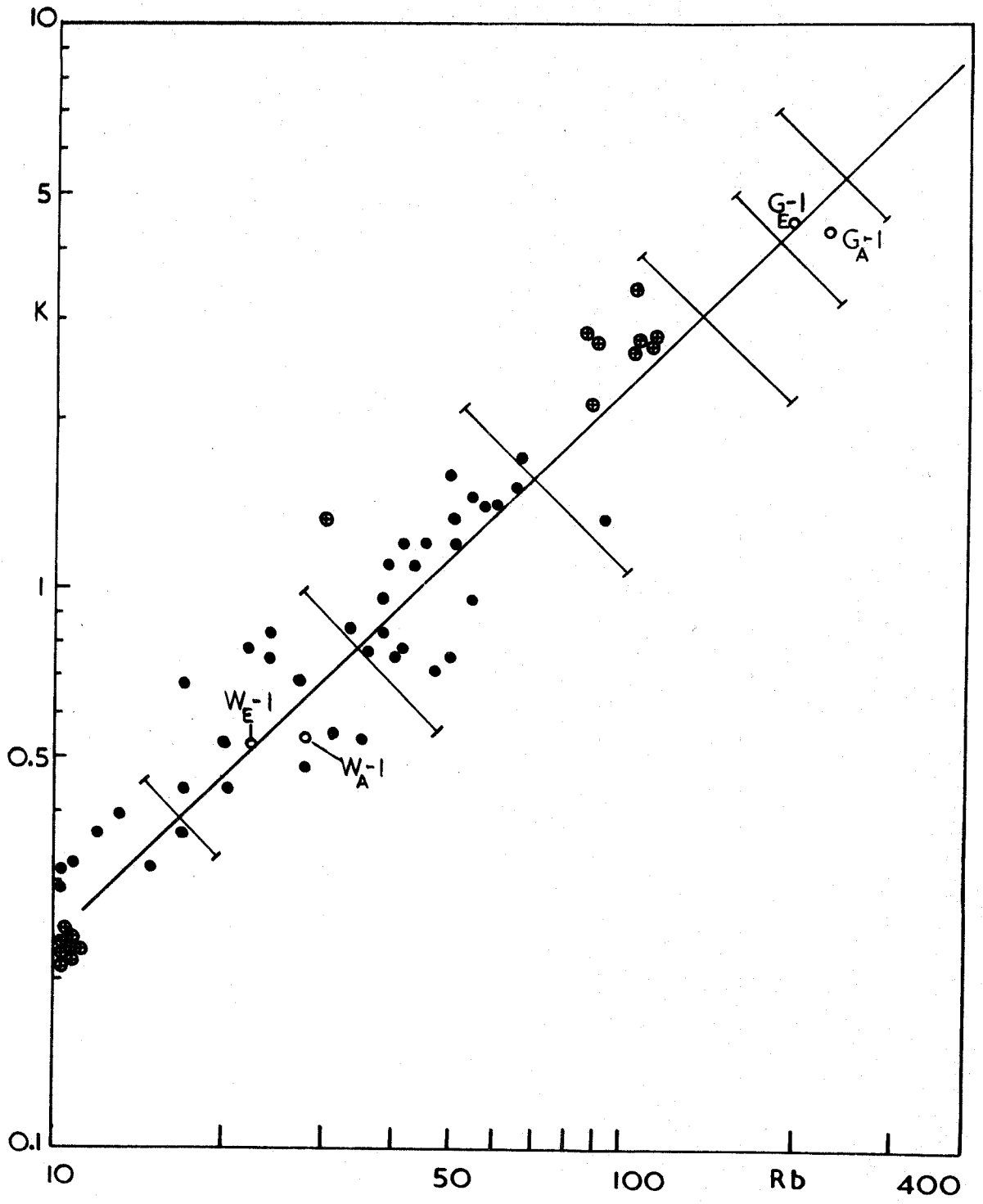
10
5
K
1
0.5
0.1
10
50
100
Rb
400
G-1
Eo
G_A-1
W_E-1
W_A-1

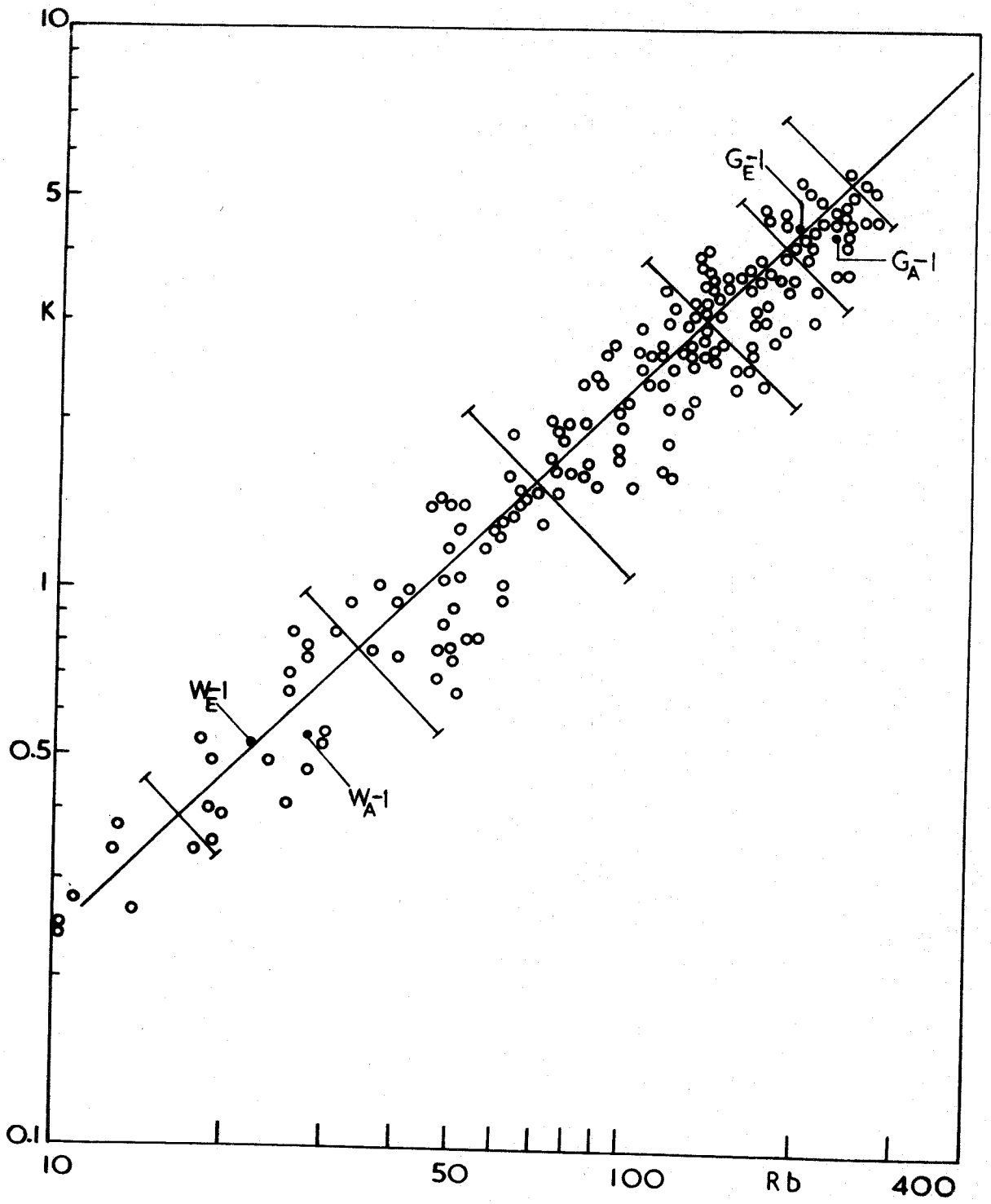
10
5
K
1
0.5
0.1
10
50
100
Rb
400
G_E-1
G_A-1
W_E-1
W_A-1

authors (e.g. Wager and Mitchell, 1951, p.192; Patterson, 1952, p.295; Baker et al., 1964, p.524, fig.16; Engel et al., 1965, p.726; Baker, 1969, p.1304, fig.13; and Sigurdsson, 1970, p.234, fig.55).

Nickel:

Ni shows a sharp decrease in the initial stages of fractionation in the Mourne and Killough rock series (Figure 26). This is the normal trend found in many other fractionated basaltic magmas (Wager and Mitchell, 1951, p.187; Cox et al., 1967, p.1465, fig.5; Sigurdsson, 1970, p.233, fig.54).

The average Tertiary olivine-tholeiite of the Mourne swarm contains 143 ppm. Ni (Table 31) and the alkali basalts have an average Ni content of 138 ppm. (Table 28), while the Mourne quartz-tholeiites only contain 55 ppm. Ni (Tables 32 and 33). The alkali basalts of the Killough area attain the highest Ni concentration among all the other rocks analysed, having an average value of 253 ppm. (Table 29). Ni is near the detection limit in the rest of the rocks from the Mourne and Killough swarms. The intermediate members of the tholeiitic and alkalic series contain as little as 12 ppm. and 9 ppm. Ni respectively (Tables 35 and 30). It has about the same concentration in the acid rocks of the tholeiitic series (Table 10). The very low Ni content in the intermediate and acid members of the Mourne tholeiitic suite may conceivably be accounted for by invoking a long process of olivine

---

Fig. 25: Distribution of zirconium (ppm) in the Mourne and Killough rocks. Symbols as in Figure 20.

Fig. 26: Distribution of nickel (ppm) in the Mourne and Killough rocks. Symbols as in Figure 20.

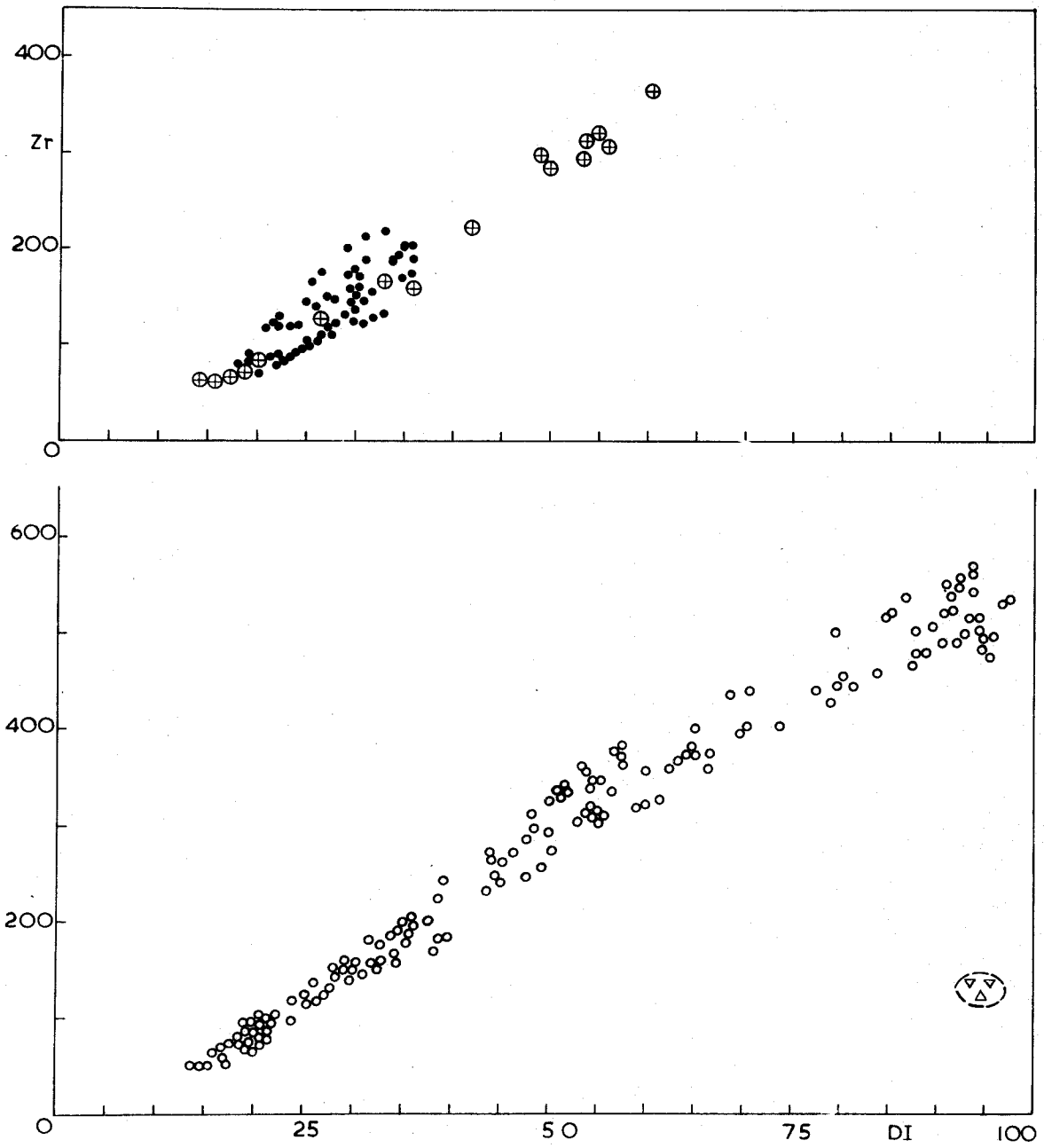
400
Zr
200
0
600
400
200
0
25
50
75
DI
100

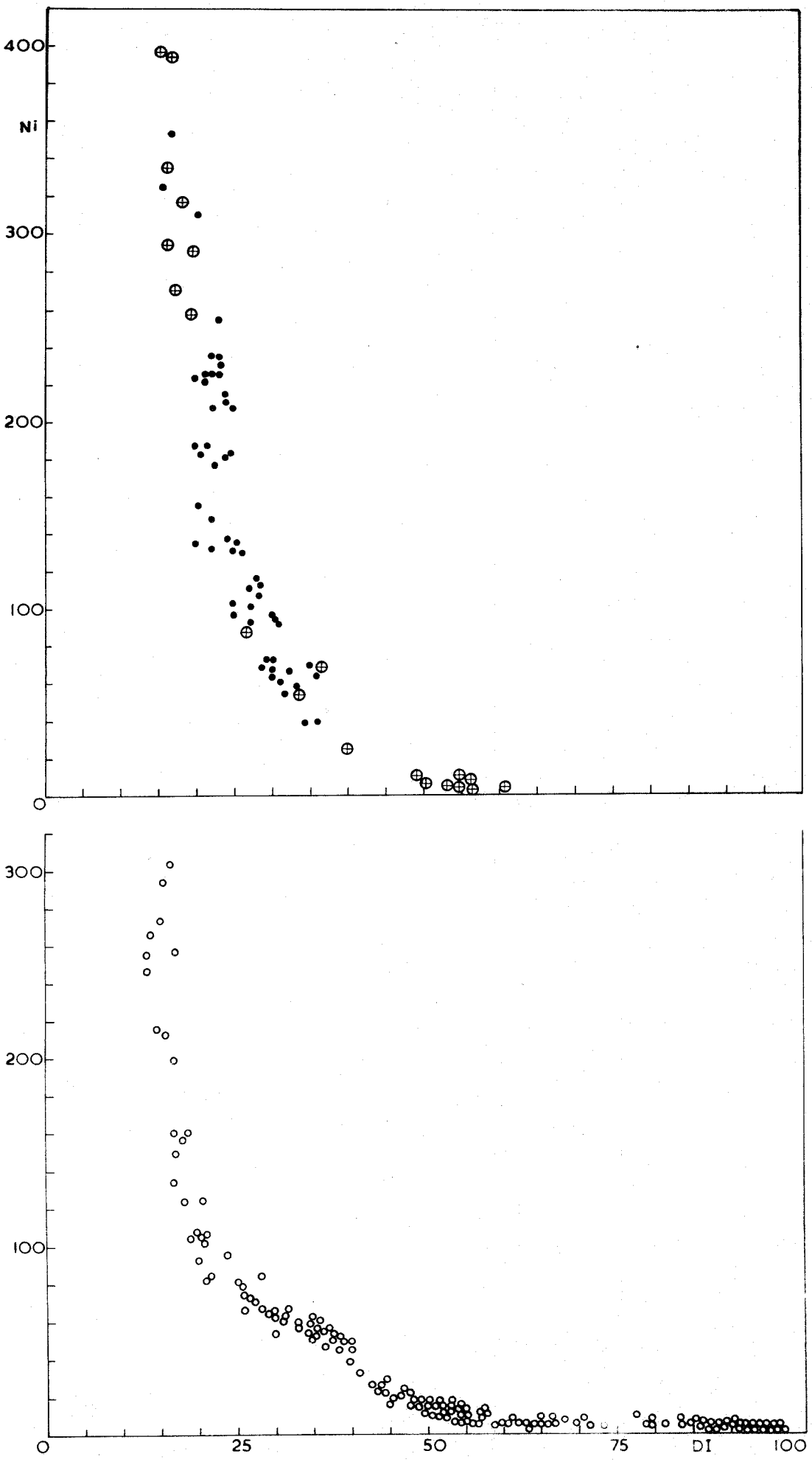
400
Ni
300
200
100
0
300
200
100
0
25
50
75
DI
100

extraction at the initial stages of fractionation of this series.

A fairly similar trend of Ni distribution has been shown by Sigurdsson (1970, p.240) in the alkalic and tholeiitic rocks of the Setberg volcanic region. Another comparable example has been given by Baker (1969, p.1301, fig.9) on the St. Helena alkalic lavas.

Several opinions have been suggested by a number of authors on the ease of entry of Ni into the crystal lattices of the early formed ferromagnesian minerals during crystal fractionation (e.g. Vogt, 1923; Goldschmidt, 1937, 1954; Wager and Mitchell, 1951, and Ringwood, 1955).

According to Vogt (1923, p.323), Ni normally occurs in Mg-silicates and the amount of Ni tends to increase with increasing Mg content and to decrease with increasing Fe content.

The Ni-Mg diadochy in the early formed ferromagnesian minerals has been questioned by Ringwood (1955, p.198) and it was claimed that Ni^{2+} enters crystal lattices at the expense of Fe^{2+} rather than Mg^{2+}. Once attributed to diadochy between Ni^{2+} and Mg^{2+}, with similar ionic radii (Goldschmidt, 1937, p.661), the Ni^{2+} in natural olivines is now believed to be camouflaged by Fe^{2+} with a similar electronegativity value (Ni^{2+} : 1.7; Fe^{2+} : 1.54; Mg^{2+} : 1.2; Brown, 1967, p.140).

Wager and Mitchell (1951, p.188) showed that during the strong fractionation process of the Skaergaard magma, the smaller amounts of Ni in the later ferromagnesian minerals were caused by a decrease in the concentration of Ni in the residual magma due to the abundant entry of this element into earlier fractions. The present study substantiates this view by providing evidence of Ni-depletion in the intermediate and late-stages of fractionation in the Mourne tholeiitic series (Figure 26).

Copper:

Rankama and Sahama (1950) showed that a large part of Cu contained in most igneous rocks occurs as sulphides. However, Wager and Mitchell (1951, p.190) have demonstrated that during the earlier stages of crystallization of a basic magma, Cu occurs free in the liquid and thus becomes incorporated in silicate minerals. The Cu^{1+} (0.96Å) is camouflaged by Na^{1+} (0.98Å) in plagioclases, and Cu^{2+} (0.72Å) is camouflaged by Fe^{2+} (0.74Å) in ferromagnesian minerals. Their results, however, prove that Cu does not enter crystal lattices as readily as Na and Fe^{2+}, and is therefore concentrated in residual magmas until a concentration is reached which is sufficient to precipitate $CuFeS_2$ (chalcopyrite).

Ringwood (1955, p.196) supports this opinion by giving evidence on the electronegativities of Cu, Na, and Fe^{2+}. Because of the relative weakness of Cu-O bonds, Cu does not readily enter silicate minerals, but accumulates in the residual liquid until a concentration sufficient to yield $CuFeS_2$ is reached.

Reflected light microscopy reveals the fact that some of the basic rocks in the Mourne area contain minute specks of primary chalcopyrite in polished sections (e.g. No.128), and the high Cu values for the Mourne and Killough series reflect a high content in the parent magma.

Cu shows a decrease with differentiation in the Mourne and Killough rock series (Figure 27), paralleling the trends of the St. Helena (Baker, 1969, p.1301, fig.9), and Setberg volcanic rocks (Sigurdsson, 1970, p.235, fig.56).

The Mourne tholeiitic rocks show a decrease from approximately

---

Fig. 27: Distribution of copper (ppm) in the Mourne and Killough rocks. Symbols as in Figure 20.

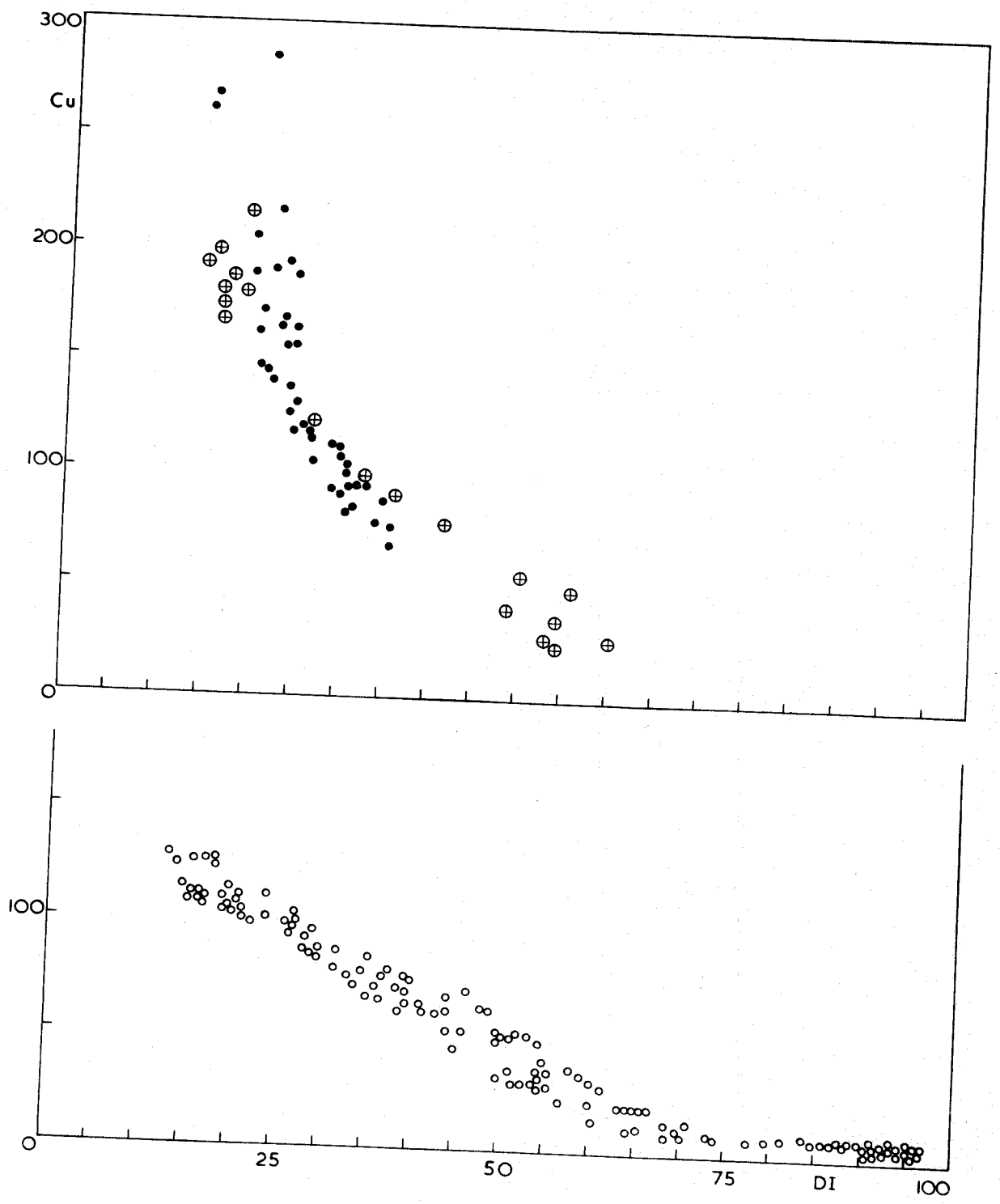
300
Cu
200
100
0
100
0
25
50
75
DI
100

114 ppm. Cu in the olivine-tholeiites (Table 31) to 37 ppm. in the intermediate tholeiitic rocks (Table 35) and then to 11 ppm. in the late-stage cone-sheet granophyres (Table 10).

The Mourne alkalic rocks, on the other hand, have higher Cu values than those of the tholeiitic equivalents, with an average content of 137 ppm. (Table 28). The Killough alkali basalts have even higher concentrations of Cu, being 165 ppm. on average, but their intermediate members are depleted in this element down to 48 ppm. (Tables 29 and 30).

The extraction of Cu from the Mourne and Killough liquids has thus in all probability not been affected by removal of the major precipitating silicate phases, but more likely by the separation of sulphide or oxide phases, such as has been demonstrated for the St. Helena volcanic suite (Baker, 1969, p.1296).

Zinc:

The ionic radii of Zn^{2+} and Fe^{2+} are similar (0.74Å), consequently Zn is camouflaged in minerals containing ferrous iron. Wedepohl (1953, p.122) demonstrated that the Zn content in basic rocks is greater than in acid rocks; however, the Zn/Fe ratio appears to increase during differentiation. The latter finding is in full accord with the present results (Figure 28).

The Mourne olivine-tholeiites contain an average Zn content of 78 ppm. (Table 31), and this amount increases to 90 ppm. in the quartz-tholeiites (Table 32), and then to 108 ppm. in the intermediate members of this series (Table 35). The acid rocks of the Mourne tholeiitic

---

Fig. 28: Distribution of zinc (ppm) in the Mourne and Killough rocks. Symbols as in Figure 20.

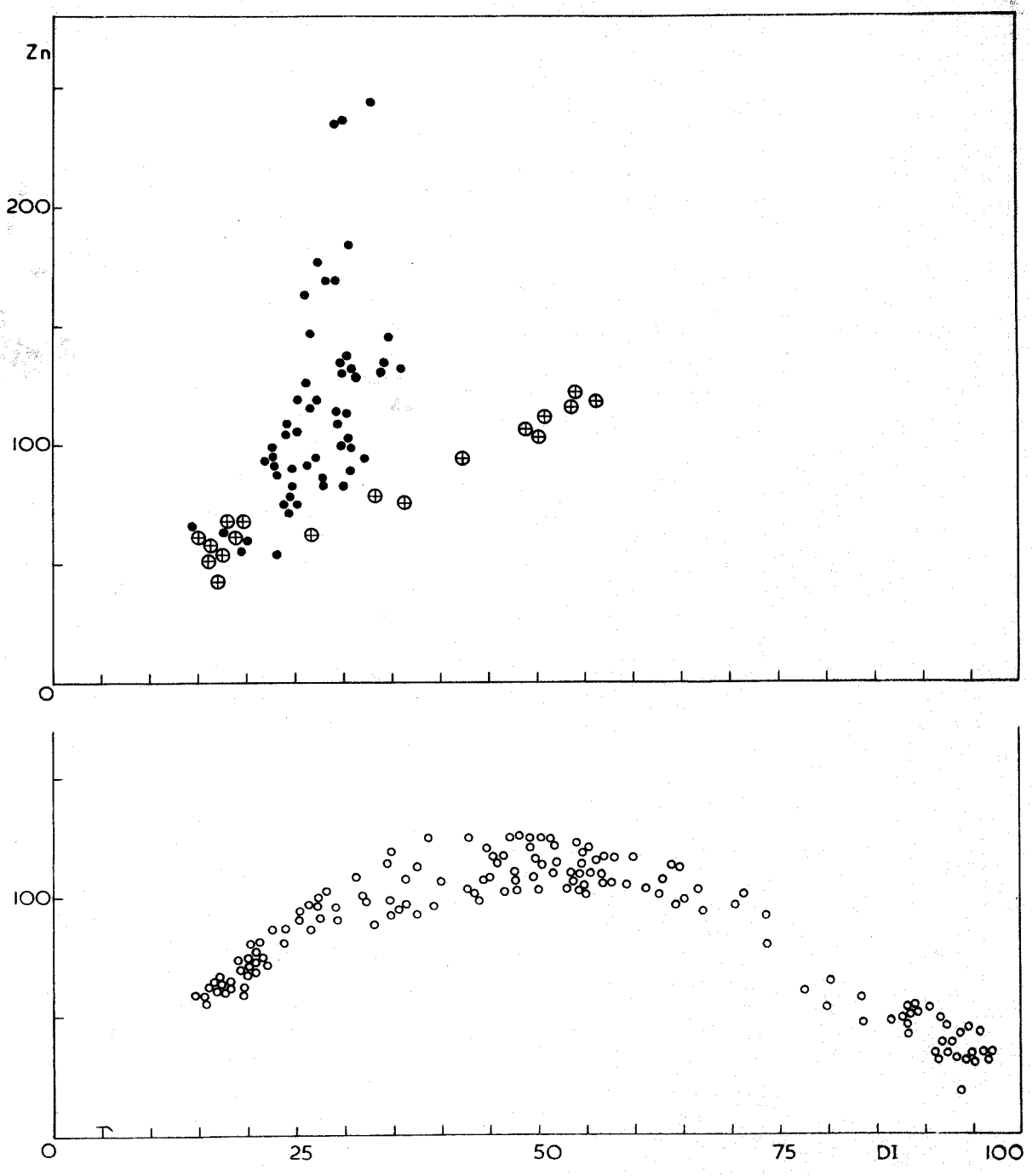
Zn
200
100
0
100
T
0
25
50
75
DI
100

suite show depletion in Zn with an average value of 47 ppm. (Table 10), notably those with low iron content.

The tendency of Zn to become depleted in residual magmas relative to ferrous iron was explained by Ringwood (1955, p.200), due to the higher electronegativity of Zn over Fe^{2+} (1.70 and 1.65 respectively).

The alkalic rocks of the Mourne area show greater concentration of Zn, as compared to the values obtained for the tholeiitic equivalents (116 ppm. Table 28). The Killough alkali basalts, on the other hand, contain 63 ppm. Zn on average (Table 29), but their intermediate members attain as high as 104 ppm. (Table 30), showing increase in Zn with differentiation as pointed out earlier.

A fairly similar pattern of Zn variation has been illustrated by Sigurdsson (1970, p.236, fig.57) in the Setberg volcanic region. There again, the intermediate rocks of the tholeiitic series show the highest concentration in Zn, and the depletion in this element is shown by some of the acid rocks with very low iron content.

CHAPTER V

INTERMEDIATE ROCKS

a) Distribution and field characteristics of the intermediate rocks in the Mourne area

The statistical evidence of distribution of the intermediate rocks in the Mourne dyke-swarm is rather significant. The dykes of this type appear to be concentrated in the middle zone of the 13 km. long swarm and to die out both to north and south. The densest exposures of the intermediate rocks are therefore mainly confined to the area between Green Harbour and Dunmore Head (see Map 2). However, a few occurrences of dykes of intermediate composition have been found at the northern outskirts of the Eastern Mourne granites along the section through Shimna River (Nos. 515, 517, 518, 520, 522, and 523). They are believed to be the continuation of the intermediate dykes cropping out on the shore, near Dunmore Head (cf. Map 1).

The average thickness of these dykes is between 0.5 and 2 m. and very few dykes are more than 2 m. thick. The rocks belonging to this group are generally very fine-grained, being almost glassy in some cases, especially at the marginal zones of the dykes.

There are many textural variations among the intermediate rocks. Variolitic, tachylytic and vesicular varieties are well represented in the Mourne area. Variolitic andesites (Nos. 34, 36-b, 40-b, 52, 55-d, 66, 69, 71, 72, 74, 75, 76-a, and 77) are often characterized by minutely spherulitic appearance with tachylytic margins near the contacts with the wall-rock. The others (Nos. 55-b, 55-c, 518, and 520) contain vesicles varying in size from a few mm. up to 4 cm. in length.

These vesicles are usually orientated and elongated parallel to the dyke walls and are filled with secondary quartz, epidote, chlorite and calcite (Plate 9).

It is interesting to note that the rocks of intermediate composition contain numerous acid and basic xenoliths. The angular outline of the inclusions and the sharp line of separation suggest that they are fragments of pre-existing rock caught up by the rising magma (Plates 15 and 16).

b) Petrography of the intermediate rocks

The intermediate rocks of the Mourne dyke-swarm are mainly tholeiitic andesites which are characterized by plagioclase laths, microlites and dendrites of either pyroxene or of hornblende in certain cases, opaque iron-titanium oxide minerals in the form of rods, composite spindles, and skeletal microlites, and patches of chlorite set in a microcrystalline to glassy groundmass with minute grains of interstitial quartz and alkali feldspar. Xenocrysts of alkali feldspar and quartz are also present in the rocks of this group.

The tholeiitic andesites are well represented among the Mourne dykes (Nos. 48, 58, 59, 60, 61, 63, 70, 73, 78, 79, 80, 81, 82, 83, 84, 85, and 98), especially in the vicinity of Dunmore Head. They range in texture from relatively medium-grained (0.5 mm.), sub-ophitic dyke rocks (Nos. 73, 78, 80, and 81) to very fine-grained, intergranular marginal varieties (Nos. 84-a, 85-a).

These exceedingly compact, almost black and fine-grained rocks are typified by numerous plagioclase laths, ranging in size from 0.05 mm. to 0.5 mm. in length, set in a fine-grained hypohyaline groundmass similar in texture to the matrix of the variolitic andesites (Plate 10).

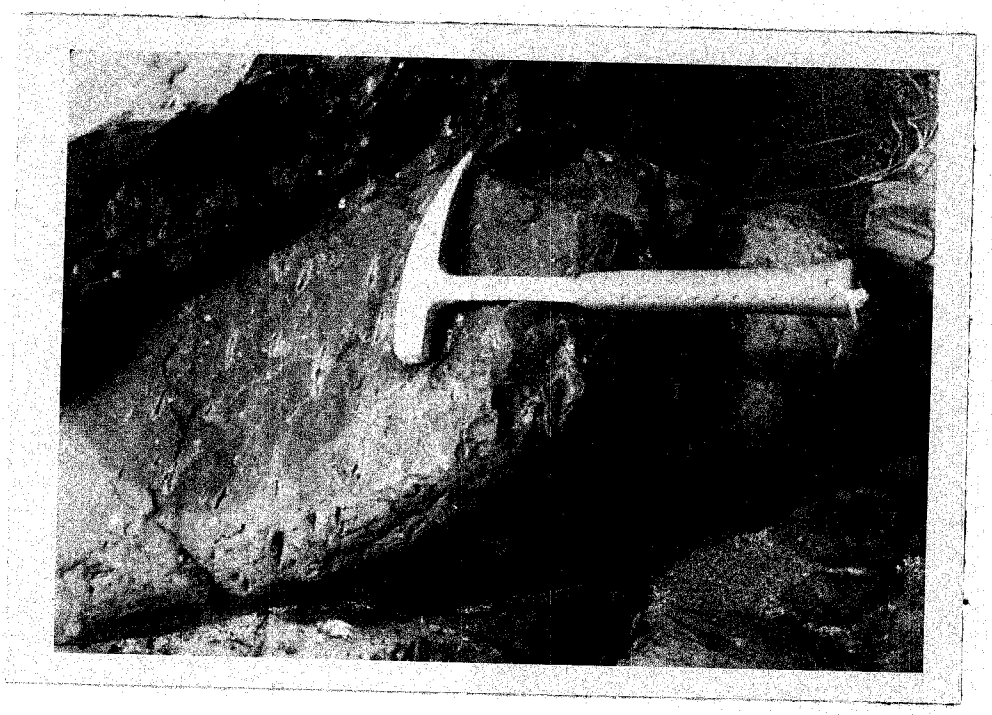

Plate 9: Vesicular variolite dyke from Green Harbour (No: 55-b), trending W.N.W.

Plate 10: Textural features of the Mourne intermediate rocks: Variolitic texture in dyke No: 76-a, x 45.

The plagioclase is predominantly andesine (An_{40-45}) with a subordinate proportion of acid labradorite (An_{50}), as determined optically and confirmed chemically. The plagioclase laths have been analysed by electron-probe and the composition was found to be An_{39-43} (Nos. 82, 84 in Table 25-B) in terms of weight percent. Albitic twinning is common in these laths, however, some microlites are too small to exhibit twinning. The plagioclase laths usually have ragged margins and are sometimes skeletal with abrupt termination. They are commonly bent and fractured and cemented by the groundmass. Zoning is rare. The modal proportion of the plagioclase laths is approximately 25% in the tholeiitic andesites, however, there is a quite considerable amount of this mineral in the glassy groundmass, mainly as tiny microlites of a shadowy nature.

Hornblende often occurs in the form of small microlites, laths and tufts of indefinite outline merging into the hypohyaline matrix. Pyroxene is not common in these rocks, but in some dykes, microlites and dendrites of brown augite are developed (Plate 11). They are partly transformed into green fibrous hornblende. Possibly the major part of the hornblende is an alteration product of pyroxene. Small hornblende laths occur in druses in one of the more siliceous type of the tholeiitic andesites (No. 76-a, Plate 12).

Iron-titanium oxide minerals are abundant in the intermediate rocks of the Mourne area, in the form of euhedral microphenocrysts and skeletal crystals. They are often bent and dendritic (Plate 7). Some of them are arranged parallel to the feldspar laths, the others are quite unoriented. These opaque minerals are of at least two generations, one being earlier than the feldspar. The chemical compositions of some of the opaque iron-titanium oxide minerals in the Mourne intermediate

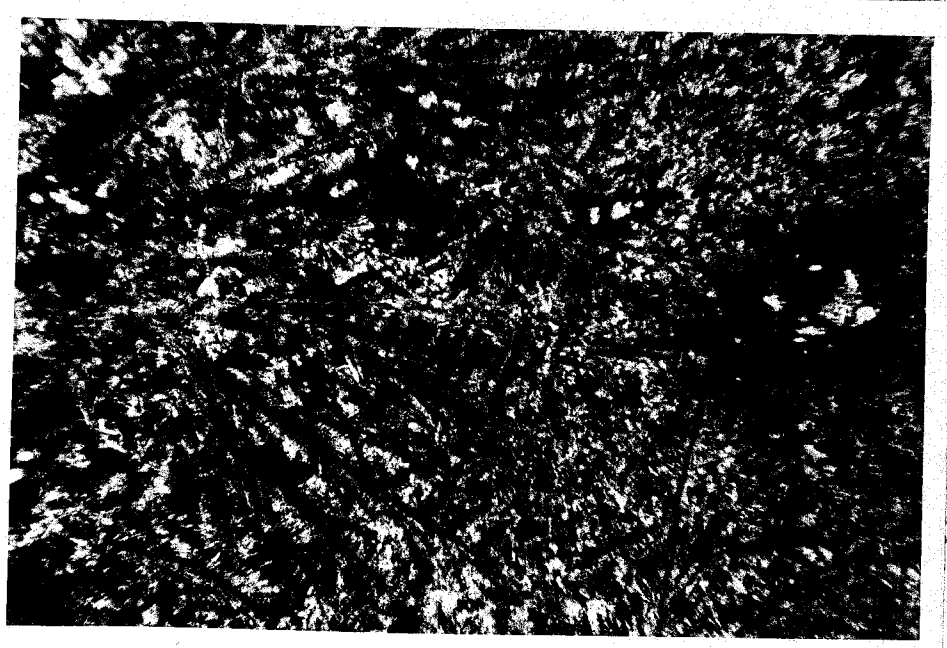

Plate 11: Microlites and dendrites of pyroxene in dyke No: 76-a, x 45.

Plate 12: Hornblende showing basal cleavage, in the vesicles of a tholeiitic andesite (No: 76-a), x 350.

rocks are given in Tables 26 and 27.

The continuous (only very occasionally patchy) groundmass is composed of a brown glass with irregular microlites of plagioclase, hornblende, some interstitial quartz and alkali feldspar. Epidote, chlorite and hornblende together with quartz are frequently found in vesicles showing mosaic texture (Plate 12).

The variolitic andesites differ from the tholeiitic andesites only texturally. They are hypohyaline rocks with spheroidal or radiating aggregates of feldspar and pyroxene microlites (Plate 10). In this respect they are analogous to the variolitic rocks of Mull and Ardnamurchan (Bailey et al., 1924, p.305, fig.51; Richey and Thomas, 1930, p.170, fig.22-B). Xenocrysts of corroded quartz and alkali feldspar are commonly present. Vesicles with infillings of hornblende and quartz are numerous. The altered glass forming the groundmass of the variolitic andesites is usually brownish and partly chloritized. Opaque iron oxide minerals form dusty aggregates around the feldspar fibres.

Towards the contacts of the intermediate dykes, the variolites pass into compact tachylytes of brown glass with fluidal texture and microscopic spherulites (Plate 13).

Besides normal variolites, there are a few examples of vesicular varieties (No. 55-b, Plate 9). These vesicles are filled with aggregates of green hornblende and, occasionally, with quartz as well. The microscopic characters of the vesicular varieties are the same as in the case of variolitic types.

Another type of intermediate rocks occurring in the Mourne dyke-swarm are the "leidleites". This is a local term used by Thomas and Bailey (1915, p.207) to describe the rocks of intermediate composition

Plate 13: Textural features of the Mourne intermediate rocks: Tachylytic margin of dyke No: 75, x 45, crossed nicols.

Plate 14: Anorthoclase phenocrysts in the xenolith XM, from dyke No: 80, x 45, crossed nicols.

in Mull. It is used elsewhere in the British Tertiary Igneous Provinces by some other authors (e.g. Anderson and Radley, 1915). Leidleites are also known in the form of sills and dykes elsewhere in Mull and Morvern, and near Kielder Head, Northumberland (Thomas and Bailey, op.cit.).

Leidleites (Nos. 39, 64, 65) are composed of laths of andesine with irregular outlines, pyroxene microlites and opaque iron oxides in a glassy groundmass. The plagioclase laths are simply twinned. Pyroxenes are commonly grouped in a roughly stellate fashion showing sub-variolitic texture (cf. Plate 10). Opaque iron oxide minerals occur as strings and minute rods in the groundmass. The matrix consists of devitrified glass with interstitial cloudy alkalifeldspar and quartz, resulting from the crystallization of the original glass. Occasional xenocrysts of quartz and alkali feldspar are also present in the groundmass.

c) Chemistry of the intermediate rocks

The intermediate rocks of the Mourne dyke-swarm have a differentiation index in the range of 45 to 70, SiO_2 of 55-65%, and typically very high total iron (9 to 15%) and high TiO_2 contents (between 2 and 3%, Table 34). They are further characterized by relatively low CaO (2-6%) and MgO (1-4%), and predominance of K_2O over Na_2O. They have a solidification index ranging from 8 to 20.

The chemical compositions of the intermediate rocks give a fairly clear idea about the mineralogy of these rocks. The high iron-titanium oxide content is reflected by abundant magnetite and ilmenite crystals dispersed throughout the groundmass. The absolute iron-enrichment, as in the case of Thingmuli tholeiitic intermediate rocks (Carmichael,

Table 34: Chemical analyses and C.I.P.W. norms of the intermediate rocks from the Mourne area

Wt. %	98	95-b	94	87-b	86-a	86-b	85	85-a	84	84-a
SiO_2	56.83	64.81	63.32	58.71	58.53	56.51	57.96	57.49	56.54	60.09
Al_2O_3	15.46	15.73	14.49	14.98	15.15	14.46	15.37	14.67	15.63	14.24
Fe_2O_3	2.78	1.70	2.06	2.23	1.51	4.99	1.89	2.39	1.46	2.45
FeO	7.67	7.18	6.08	8.00	8.72	7.03	8.19	8.29	9.50	6.81
MgO	3.67	2.02	1.85	2.47	2.44	2.48	2.51	3.24	3.72	2.69
CaO	4.76	1.88	2.70	5.10	4.82	4.89	4.63	5.48	5.17	5.35
Na_2O	2.24	3.20	3.51	3.24	2.74	3.03	2.23	1.58	1.82	2.89
K_2O	3.34	2.07	4.35	1.93	2.79	3.55	3.82	3.63	3.20	2.56
TiO_2	2.45	0.80	1.00	2.52	2.57	2.20	2.52	2.45	2.36	2.14
P_2O_5	0.47	0.31	0.38	0.49	0.46	0.67	0.54	0.45	0.30	0.51
MnO	0.26	0.23	0.15	0.27	0.21	0.17	0.28	0.27	0.26	0.22
S	0.04	0.01	0.09	0.03	-	0.02	-	0.01	-	-
Qz	12.91	27.05	15.09	15.36	14.28	11.51	13.71	15.06	12.03	17.11
Cor	0.62	5.52	-	-	-	-	0.43	-	0.48	-
Or	19.75	12.28	25.72	11.40	16.48	20.94	22.56	21.49	18.96	15.13
Ab	18.96	27.15	29.75	27.44	23.18	25.66	18.89	13.42	15.41	24.48
An	20.54	7.31	10.89	20.62	20.81	15.36	19.44	22.16	23.67	18.29
Di	-	-	-	1.21	0.06	3.69	-	1.73	-	4.07
Hy	17.30	15.90	12.54	14.68	16.97	9.79	16.10	16.89	22.09	12.04
Mt	4.03	2.47	2.99	3.23	2.19	7.24	2.74	3.46	2.11	3.55
Ilm	4.66	1.53	1.91	4.79	4.89	4.18	4.79	4.66	4.49	4.07
Ap	1.12	0.74	0.90	1.17	1.10	1.59	1.29	1.07	0.71	1.21
Py	0.07	0.01	0.16	0.05	-	0.04	-	0.01	-	-
DI	51.63	66.48	70.57	54.21	53.95	58.12	55.17	49.98	46.41	56.73
SI	18.63	12.49	10.36	13.82	13.40	11.76	13.46	16.94	18.88	15.46

Table 34 continued:

Wt. %	83	82	81	80	79	78	77	76-a	75	74
SiO_2	57.39	55.56	57.15	56.41	56.94	58.20	60.77	60.51	58.39	56.04
Al_2O_3	14.82	16.27	15.21	15.18	15.18	15.45	14.60	14.73	15.19	16.55
Fe_2O_3	1.91	0.91	1.62	1.44	1.58	1.98	2.56	1.50	1.66	1.64
FeO	8.33	9.99	8.44	9.18	8.89	7.79	7.04	8.25	8.51	9.04
MgO	3.20	3.76	3.28	3.46	3.28	2.52	1.58	2.07	2.64	3.69
CaO	5.87	5.04	5.20	5.73	5.50	5.05	4.43	4.56	4.36	4.77
Na_2O	2.29	1.98	2.23	2.26	2.12	2.92	2.36	1.90	2.03	1.97
K_2O	3.05	2.96	3.60	3.03	3.30	2.92	3.88	3.61	3.83	3.42
TiO_2	2.39	2.73	2.41	2.51	2.41	2.26	1.88	1.94	2.59	2.29
P_2O_5	0.43	0.34	0.46	0.48	0.47	0.62	0.59	0.63	0.45	0.23
MnO	0.27	0.35	0.27	0.27	0.26	0.23	0.25	0.24	0.28	0.30
S	-	0.12	0.13	0.01	0.02	-	-	-	-	0.03
Qz	12.65	11.04	11.26	10.68	11.78	12.99	18.32	19.43	15.09	10.92
Cor	-	1.44	-	-	-	-	-	0.91	0.85	1.48
Or	18.03	17.48	21.26	17.93	19.54	17.30	22.95	21.37	22.63	20.21
Ab	19.41	16.80	18.90	19.18	17.97	24.77	19.97	16.07	17.19	16.69
An	21.14	22.77	20.82	22.27	22.11	20.36	17.76	18.49	18.69	22.17
Di	4.29	-	1.59	2.52	1.73	0.49	0.31	-	-	-
Hy	16.11	22.89	17.84	19.36	18.79	15.41	11.96	16.32	17.09	21.16
Mt	2.77	1.31	2.36	2.09	2.30	2.87	3.72	2.18	2.42	2.38
Ilm	4.54	5.19	4.58	4.76	4.59	4.29	3.58	3.68	4.93	4.36
Ap	1.02	0.81	1.10	1.15	1.12	1.48	1.40	1.50	1.07	0.55
Py	-	0.22	0.24	0.01	0.03	-	-	-	-	0.05
DI	50.09	45.32	51.43	47.80	49.30	55.07	61.24	56.88	54.93	47.83
SI	17.04	19.18	17.11	17.86	17.11	13.90	9.07	11.94	14.14	18.67

Table 34 continued:

Wt. %	73	72	70	69	66	65	64	61-a	61-b	61-c
SiO_2	55.95	60.12	55.56	56.04	56.23	58.90	59.64	57.87	56.03	56.97
Al_2O_3	16.44	14.58	15.31	15.13	15.38	14.88	14.89	15.18	18.43	15.82
Fe_2O_3	1.49	1.72	1.43	1.68	1.99	2.66	2.21	1.32	1.83	1.72
FeO	9.28	8.12	9.17	9.22	8.65	6.42	6.70	9.31	6.52	9.13
MgO	3.91	1.91	3.85	3.26	3.52	2.03	1.78	2.67	2.75	3.07
CaO	5.19	4.66	6.71	5.04	5.85	4.86	4.76	4.29	6.64	4.57
Na_2O	1.77	1.99	2.54	2.05	2.00	2.49	2.72	1.98	2.83	1.69
K_2O	3.03	3.94	2.44	4.31	3.40	5.03	4.58	4.00	2.81	3.67
TiO_2	2.39	2.01	2.27	2.44	2.32	1.73	1.72	2.61	1.60	2.63
P_2O_5	0.25	0.62	0.34	0.51	0.34	0.78	0.74	0.42	0.31	0.38
MnO	0.25	0.29	0.30	0.25	0.26	0.17	0.20	0.29	0.20	0.29
S	-	-	-	-	-	-	-	0.02	-	0.03
Qz	12.16	17.47	8.22	8.40	10.57	11.64	12.65	13.44	7.94	14.53
Cor	1.41	0.05	-	-	-	-	-	0.79	-	1.67
Or	17.93	23.28	14.46	25.46	20.13	29.72	27.11	23.68	16.62	21.70
Ab	14.98	16.84	21.57	17.37	16.93	21.06	23.03	16.78	23.97	14.29
An	24.09	19.06	23.11	19.34	22.91	14.56	14.86	18.51	29.26	20.17
Di	-	-	6.64	1.94	3.23	3.72	3.26	-	1.37	-
Hy	22.08	15.48	18.75	19.14	18.06	10.26	10.81	18.84	14.36	19.15
Mt	2.16	2.49	2.07	2.43	2.89	3.86	3.20	1.92	2.66	2.49
Ilm	4.55	3.81	4.32	4.64	4.41	3.29	3.27	4.95	3.04	4.99
Ap	0.59	1.48	0.81	1.22	0.81	1.86	1.76	1.00	0.74	0.91
Py	-	-	-	-	-	-	-	0.03	-	0.05
DI	45.08	57.60	44.26	51.25	47.65	62.43	62.80	53.91	48.54	50.53
SI	20.07	10.80	19.81	15.89	18.00	10.89	9.89	13.85	16.43	15.92

Table 34 continued:

Wt. %	60-a	60-b	59	58	55-b	55-c	53	52	48	44
SiO_2	56.90	58.91	57.22	57.63	59.29	61.26	56.51	62.17	54.53	59.90
Al_2O_3	14.94	14.73	15.18	15.34	13.57	14.52	15.25	15.83	14.09	14.62
Fe_2O_3	1.57	1.45	1.84	1.81	4.50	1.73	1.88	2.03	2.91	1.71
FeO	9.29	8.52	8.21	8.19	7.94	8.42	8.62	6.18	9.47	8.08
MgO	2.71	2.18	2.99	2.71	1.60	1.40	2.85	1.63	2.92	1.79
CaO	4.98	4.90	5.17	5.16	3.59	3.19	5.66	2.51	6.22	4.49
Na_2O	2.86	3.02	2.32	2.53	2.86	3.00	2.69	3.38	3.20	2.55
K_2O	3.16	3.30	3.98	3.48	4.05	3.93	3.38	4.89	3.38	4.09
TiO_2	2.71	2.06	2.33	2.33	1.52	1.53	2.24	1.14	2.17	1.85
P_2O_5	0.53	0.64	0.50	0.49	0.79	0.74	0.63	-	0.91	0.61
MnO	0.30	0.24	0.21	0.24	0.28	0.23	0.22	0.18	0.20	0.24
S	0.02	-	-	0.06	0.02	-	0.04	0.01	0.01	-
Qz	10.10	12.19	10.40	11.69	15.38	16.46	9.27	12.21	4.83	14.27
Cor	-	-	-	-	-	1.31	-	0.37	-	-
Or	18.71	19.53	23.52	20.59	23.92	23.23	20.01	28.94	19.97	24.17
An	24.22	25.57	19.66	21.45	24.16	25.39	22.75	28.65	27.08	21.62
Ab	18.54	16.85	19.24	20.17	12.23	10.95	19.52	12.49	14.08	16.35
Di	2.23	2.74	2.60	1.85	0.33	-	3.69	-	9.09	1.63
Hy	17.43	15.54	16.25	15.87	12.68	15.43	16.15	12.15	14.44	14.45
Mt	2.28	2.11	2.67	2.63	6.52	2.50	2.72	2.95	4.22	2.48
Ilm	5.14	3.91	4.43	4.43	2.88	2.91	4.26	2.18	4.11	3.52
Ap	1.27	1.53	1.19	1.17	1.88	1.77	1.50	-	2.15	1.45
Py	0.03	-	-	0.11	0.03	-	0.07	0.01	0.02	-
DI	53.04	57.29	53.59	53.75	63.46	65.09	52.04	69.81	51.88	60.07
SI	13.83	11.80	15.46	14.47	7.63	7.57	14.67	9.00	13.34	9.82

Table 34 continued:

Wt. %	43-a	43-b	40-a	40-b	39	38	38*	36-b	35	34
SiO_2	60.24	60.84	60.32	60.19	59.64	60.71	60.20	59.25	58.28	58.00
Al_2O_3	14.76	15.03	14.79	15.04	15.03	14.94	14.82	15.07	14.81	14.70
Fe_2O_3	2.37	1.63	2.83	2.69	1.66	2.46	1.90	2.14	2.69	2.46
FeO	6.58	6.96	6.17	6.12	8.19	7.39	7.93	8.06	7.46	7.88
MgO	1.85	1.75	1.80	1.82	2.07	1.77	1.34	2.09	2.66	2.47
CaO	4.39	3.86	4.20	3.80	3.99	4.22	4.25	4.85	5.45	4.97
Na_2O	2.99	3.10	2.91	3.15	2.13	2.10	2.40	2.20	2.45	2.20
K_2O	4.40	4.43	4.46	4.73	4.40	3.71	4.15	3.38	3.26	4.32
TiO_2	1.58	1.60	1.67	1.62	2.13	1.77	1.05	2.12	2.14	2.14
P_2O_5	0.67	0.54	0.59	0.59	0.45	0.69	0.73	0.50	0.54	0.55
MnO	0.12	0.19	0.21	0.19	0.26	0.17	0.26	0.30	0.22	0.26
S	-	-	-	-	-	-	-	-	0.01	-
Qz	12.91	12.59	13.86	11.91	15.16	20.39		16.78	14.41	12.34
Cor	-	-	-	-	0.59	1.42		0.17	-	-
Or	26.02	26.23	26.37	27.98	26.03	21.94		19.99	19.26	25.54
Ab	25.33	26.29	24.63	26.68	18.03	17.84		18.63	20.75	18.63
An	13.81	13.95	14.10	12.90	16.82	16.42		20.75	19.76	17.47
Di	3.00	1.40	2.39	1.76	-	-		-	3.09	2.97
Hy	10.84	12.80	9.92	10.35	15.80	13.35		15.31	13.42	14.06
Mt	3.44	2.37	4.10	3.91	2.41	3.57		3.10	3.90	3.57
Ilm	3.00	3.04	3.17	3.08	4.04	3.37		4.02	4.06	4.06
Ap	1.59	1.29	1.40	1.40	1.07	1.64		1.19	1.29	1.31
Py	-	-	-	-	-	-		-	0.01	-
DI	64.27	65.12	64.88	66.57	59.23	60.19		55.42	54.43	56.52
SI	10.17	9.79	9.90	9.83	11.22	10.15		11.69	14.36	12.78

*Analysis of a variolitic andesite quoted from Tomkeieff and Marshall (1935), where H_2O^- = 0.50%, H_2O^+ = 0.60%, H_2O (total) = 1.10%. C.I.P.W. norm and DI, SI not calculated.

Table 34 continued:

Wt. %	5	515	517	518	520	522	523
SiO_2	55.44	54.30	53.92	57.48	56.80	54.70	54.44
Al_2O_3	15.33	14.16	14.94	13.94	14.50	13.75	13.99
Fe_2O_3	4.06	4.16	5.36	5.18	4.70	6.71	7.51
FeO	8.60	9.01	8.52	6.04	8.72	7.98	7.09
MgO	2.89	3.97	4.06	3.07	2.37	3.63	3.89
CaO	5.06	5.74	4.51	4.73	4.33	5.18	4.75
Na_2O	1.98	2.10	1.96	2.32	1.90	2.23	2.67
K_2O	3.25	3.39	3.15	4.36	3.64	2.70	2.59
TiO_2	2.62	2.46	2.84	1.87	2.47	2.28	2.22
P_2O_5	0.43	0.42	0.42	0.78	0.35	0.54	0.53
MnO	0.28	0.27	0.29	0.22	0.22	0.29	0.30
S	0.14	0.02	0.05	0.01	0.01	0.02	0.02
Qz	13.71	9.11	12.73	13.71	16.10	14.33	13.17
Cor	0.37	-	1.11	-	0.38	-	-
Or	19.20	20.06	18.63	25.75	21.51	15.92	15.31
Ab	16.71	17.78	16.57	19.61	16.11	18.83	22.58
An	22.31	19.17	19.61	14.75	19.23	19.57	18.54
Di	-	5.44	-	2.91	-	2.10	1.24
Hy	15.58	16.72	17.11	10.33	14.34	13.89	12.76
Mt	5.89	6.03	7.76	7.51	6.81	9.72	10.88
Ilm	4.97	4.68	5.39	3.55	4.69	4.32	4.21
Ap	1.01	0.99	1.00	1.86	0.82	1.29	1.27
Py	0.26	0.03	0.09	0.02	0.02	0.04	0.04
DI	49.62	46.95	47.93	59.07	53.72	49.08	51.06
SI	13.90	17.54	17.61	14.64	11.11	15.61	16.38

1964, p.435), indicates the early separation and crystallization of the magnetite phase.

The high silica content gives a considerable amount of normative quartz (cf. CIPW norms in Table 34), and this mineral frequently occurs interstitially in the groundmass and as occasional xenocrysts.

The predominance of K_2O over Na_2O in the majority of the intermediate rocks from the Mourne area can be accounted for by the presence of interstitial alkali feldspar in the groundmass. This mineral also occurs as xenocrysts.

The phosphorus content in the intermediate rocks is the highest among all the other members of the Mourne tholeiitic series (Table 34). A similar enrichment in P_2O_5 has been reported by Sigurdsson (1970, p.217) in the intermediate rocks of the Setberg tholeiitic suite.

In general, the chemical analyses of the intermediate rocks show that chemically this type belongs to the group of tholeiitic andesites comparable in a way to the type leidleite of Mull (Bailey et al., 1924). A chemical analysis of one of the Mull leidleites is similar to the analyses of some intermediate rocks from the Mourne area (Anderson and Radley, 1915, p.212, analysis No. 1-b). The other closely comparable examples have been reported by a number of authors from different localities. McDougall (1962) has reported unusually high content of potassium compared to sodium in the differentiated Tasmanian dolerite-granophyre association (op.cit., p.305, Table 13, analysis No. M336P). The high K and low Na values are reflected in the normative feldspar which is rich in both An and Or molecules. Other examples are given by Walker (1953) in the Karroo dolerite-granophyre succession (op.cit., p.50, Table 3, analysis No.15), by Holmes and Harwood (1929) in the tholeiitic dykes of the North of

England (op.cit., p.39, analysis No.402), and by Sigurdsson (1970) in the Setberg tholeiitic series (op.cit., p.300, Table 14, analysis No. 338 - a basaltic andesite).

The Mourne intermediate rocks, with silica percentage ranging from 55 to 65 (Table 34) are chemically unlike, for example, the average Cascade andesites (Anderson, 1941; Williams, 1932, 1935 and 1942; Yoder and Tilley, 1962), being poorer in alumina, and richer in iron. In order to avoid confusion with the typical orogenic andesites of known calc-alkaline origin (Green and Ringwood, 1968), with their varied assemblages of phenocryst minerals, the present writer feels that it is perhaps better to call the Mourne tholeiitic andesites by the name "icelandite" as defined by Carmichael (1964, p.442) in view of their similar mineralogical, chemical and field characteristics and, in particular, their fine-grained nature.

For comparative purposes, duplicate analyses of a variolitic intermediate rock (No.38) are given in Table 34. Although they were carried out by different methods, both analyses show close similarity. The wet-chemical analysis (quoted from Tomkeieff and Marshall, 1935, p.261, Table 2, analysis No.3, dyke No.38 - a variolite) includes 1.10% total H_2O, and can be compared with XRF analysis of the same specimen (carried out on water-free basis) to show that the water content of the Mourne tholeiitic andesites has little significance in the analysis and is therefore negligible.

The trace element concentrations of the Mourne intermediate rocks are given in Table 35. The reader is referred to section (f) in Chapter IV for their diagrammatic distribution in the Mourne area.

Table 35: Trace element analyses of the Mourne intermediate rocks

Sample No.	Ba (ppm)	Sr (ppm)	Rb (ppm)	Zr (ppm)	Ni (ppm)	Cu (ppm)	Zn (ppm)
98	1181	190	79	348	18	53	122
95-b	1116	119	171	358	10	21	106
94	1089	164	187	444	9	16	97
87-b	916	326	121	322	17	28	102
86-a	1366	236	155	323	7	36	109
86-b	1400	336	187	357	16	28	117
85	1329	207	131	316	15	36	121
85-a	1240	248	135	338	18	49	116
84	1141	270	127	273	21	73	117
84-a	1368	345	128	384	9	17	110
83	1202	277	121	372	12	52	103
82	1053	227	90	264	19	30	117
81	1265	255	106	346	9	30	110
80	1230	233	105	244	19	81	104
79	1297	251	104	257	20	30	126
78	1400	330	83	349	7	30	121
77	1447	202	167	327	10	30	104
76-a	1400	264	133	388	13	11	118
75	1307	209	136	305	16	51	99
74	1176	238	148	323	18	35	107
73	997	234	162	241	18	45	108
72	1410	192	143	370	14	38	106
71	701	105	152	444	5	9	93
70	1045	405	84	275	22	62	108
69	1365	266	216	341	18	52	124
66	1147	268	128	289	22	36	109
65	1187	339	136	358	6	36	102
64	1304	353	132	367	7	33	108
63	1123	237	163	235	22	32	102
61-a	1374	182	120	318	16	36	104
61-b	1206	278	114	297	19	63	92
61-c	1333	192	119	276	18	26	115
60-a	1240	223	136	304	17	52	103

Table 35 continued:

Sample No.	Ba (ppm)	Sr (ppm)	Rb (ppm)	Zr (ppm)	Ni (ppm)	Cu (ppm)	Zn (ppm)
60-b	1310	212	160	382	15	34	105
59	1206	274	172	369	18	30	110
58	1222	259	135	368	19	35	110
55-b	1497	141	133	392	11	21	106
55-c	1489	113	131	400	11	22	99
55-d	1242	85	236	422	5	22	94
53	1432	326	93	267	18	30	115
52	1400	146	136	394	5	44	116
48	1401	346	180	450	12	44	104
44	1514	273	145	359	5	32	119
43-a	1496	301	163	376	5	11	97
43-b	1381	280	193	376	5	12	117
40-a	1474	295	166	379	5	23	114
40-b	1494	299	198	377	5	23	94
39	1459	183	116	318	5	22	105
38	1485	319	177	319	5	14	86
36-b	1306	217	128	316	7	52	110
35	1476	328	92	343	7	50	114
34	1350	301	142	334	6	23	116
5	1279	202	111	427	16	29	109
515	1134	260	115	387	25	53	105
517	1083	225	138	376	20	63	106
518	1083	420	140	452	4	38	104
519	1018	97	172	450	5	41	95
520	960	185	212	466	4	83	107
521	1472	144	175	451	4	73	103
522	1220	388	133	391	10	68	121
523	1260	320	118	394	9	36	124
13342	1215	87	222	507	5	21	114
Average:	1270	246	142	355	12	37	108

d) Acid and basic xenoliths in the Mourne intermediate rocks

d.1) Distribution of the xenoliths

As pointed out earlier in this chapter (p.75), some intermediate rocks of the Mourne dyke-swarm are characterized by many fragments of rocks of varying compositions from basic to acid. There are only 7 dykes in which xenoliths of pre-existing rocks have been found in the Mourne area (Nos. 60, 61, 63, 80, 82, 85 and 124).

The light-coloured xenoliths are readily distinguished in the contrasting black host-rock. They have been collected most thoroughly by means of a hand-drill. The most abundant xenoliths consist of white or light-gray, dense granitic fragments, averaging 3-20 cm. in diameter (Plates 15 and 16) which have suffered slight partial fusion in the basaltic magma (XE, XF of No.85; XI, XK of No.82 and XM of No.80 near Dunmore Head, cf. Map 2). The other xenoliths are anorthositic in character (those rich in calcic plagioclases are XN of dyke No.63; XP, XR of No.61; and XS, XT of No.60 near Green Harbour, cf. Map2).

Two more xenoliths (XA and XB-2 from dyke No.124 near Murphy's Point, cf. Map 2) represent the gabbroic inclusions in the Mourne dyke-swarm and indicate the presence of a mass of basic rock beneath the Eastern Mourne granite massif, and thus could lend support the view held by Cook and Murphy (1952) on the Mourne gravity field (Chapter I, p.6).

d.2) Petrography of the xenoliths

The acid xenoliths consist essentially of anhedral to subhedral quartz and feldspar grains, ranging in size from 0.5 to 3 mm. in diameter, usually forming a granophyric texture with rare micrographic intergrowths of these two minerals. The texture implies slight

crushing or granulation under plutonic conditions at high temperatures. The dominant feldspar of all the acid xenoliths is orthoclase. Grains of acid plagioclase-anorthoclase (Plate 14) are also present in subordinate amounts. The feldspars often exhibit turbidity and embayment of crystal outlines. Quartz grains have also become corroded and embayed. The hydrous ferromagnesian constituents, such as biotite and amphibole have been partly or completely digested.

Another group of leucocratic xenoliths are the fragments of anorthositic material (Plate 21). They consist mainly of glomeroporphyritic clusters of calcic plagioclase with compositions ranging from labradorite (An_{50}) to bytownite (An_{70}) as determined optically. The plagioclase phenocrysts form hypidiomorphic rectangular prisms, ranging in size from 5 mm. to 2 cm. in length, which interlock and interpenetrate each other (Plates 17 and 18). Very small amounts of ferromagnesian minerals are irregularly distributed, often occurring in aggregates.

A third type of xenolith is represented by gabbroic inclusions. They have a coarse-grained troctolitic aspect, and are composed of highly altered labradorite crystals (optically determined) with subordinate amounts of pyroxene and olivine. Pyroxene (purplish brown augite) forms pegmatitic intergrowth with the plagioclase. A comparatively large, allotriomorphic or hypidiomorphic olivine (completely serpentinized) usually occupies the area between plagioclase and augite. Opaque minerals are present only in small quantities, mostly as pyrite.

One characteristic feature of the gabbroic xenoliths from the

---

Plate 17: Photomicrograph of the anorthositic xenolith XS in dyke No.60 near Green Harbour, x9, crossed nicols.

Plate 26: Pillow-like body of doleritic xenolith contained in the basified granophyre of the Glasdrumman Fort composite cone-sheet.

Plate 27: Angular xenolith of basified (hybrid) granophyre in the marginal dolerite of the Glasdrumman composite cone-sheet.

Plate 15: Acid xenolith XM in dyke No: 80
near Dunmore Head.

Plate 16: Acid xenolith XE in dyke No: 85
near Dunmore Head.

Plate 21: Anorthositic xenolith XS in dyke No: 60 near Green Harbour.

Plate 22: Sedimentary xenolith (Silurian shale) in the marginal dolerite of the Glasdrumman composite cone-sheet.

Plate 24: Eastern contact between marginal dolerite and central granophyre in the Glasdrumman composite cone-sheet.

Plate 25: Rectangular block of marginal dolerite in the inner granophyre near the southern dolerite-granophyre contact in the Glasdrumman Port cone-sheet.

Mourne area is their saussuritization. The replacement, particularly of labradorite by a fine-grained aggregate of white mica (sericite) is frequently accompanied by chloritization of the pyroxene and serpentinization of olivine.

d.3) Chemistry of the xenoliths

12 representative samples from the acid and basic inclusions have been analysed for major and some minor elements and their compositions are given in Tables 36 and 37.

Inspection of the five analyses of the Mourne anorthositic xenoliths (XN to XT in Table 36) shows that they are very rich in Al_2O_3 and CaO. In general, the chemical compositions of the anorthositic xenoliths do not differ greatly from the plagioclase of labradorite composition (Table 36; cf. Table 16 of Deer et al., 1963, vol.4, pp.116-117).

The sodic character of the feldspar in the more acid zenoliths (XE and XF in Table 36) is reflected in their norms.

Due to the strong saussuritization of the labradorite phenocrysts in the gabbroic xenoliths (XA and XB-2 in Table 36), the chemical analyses indicate unusually high K_2O content which is attributed to the presence of tiny sericitic flakes disseminated throughout the plagioclase.

The minor element contents of the Mourne xenoliths (Table 37) reflect the major chemical variations from acid to basic compositions, and the trace element concentration generally varies sympathetically with the associated major elements.

The correlation of rubidium with potassium is shown in Figure 29. The correlation is generally satisfactory except in the gabbroic

---

Plate 18: Photomicrograph of the anorthositic xenolith XN in dyke No.63 near Green Harbour, x9, crossed nicols.

Table 36: Chemical analyses and C.I.P.W. norms of the Mourne acid and basic xenoliths

Wt. %	XT	XS	XR	XP	XN	XM	XK	XI	XF	XE	XB-2	XA
SiO_2	54.41	53.00	55.37	54.86	55.75	72.66	74.13	72.57	74.92	69.18	48.93	48.06
Al_2O_3	21.17	21.68	24.24	22.11	23.51	14.75	14.55	15.13	14.66	15.17	24.29	22.77
Fe_2O_3	1.92	1.98	0.58	1.78	0.64	0.52	0.24	0.59	0.10	1.39	2.92	3.32
FeO	3.30	3.37	0.89	1.85	1.23	1.44	0.72	1.20	0.96	3.29	2.39	3.33
MgO	1.29	3.56	0.25	0.82	0.69	0.59	0.40	0.59	0.46	1.39	8.32	9.44
CaO	11.06	10.97	13.37	13.07	12.07	2.09	1.15	1.21	0.58	1.72	5.41	7.55
Na_2O	4.18	3.18	4.19	4.08	4.43	3.25	2.43	2.97	5.29	6.06	1.17	0.94
K_2O	1.33	1.42	0.69	0.79	1.21	4.37	6.14	5.44	2.89	1.22	5.64	4.14
TiO_2	0.98	0.58	0.27	0.37	0.20	0.24	0.20	0.18	0.08	0.36	0.30	0.20
P_2O_5	0.24	0.14	0.10	0.15	0.21	0.04	0.01	0.07	0.03	0.11	0.05	0.06
MnO	0.12	0.12	0.05	0.11	0.05	0.04	0.03	0.05	0.02	0.11	0.09	0.13
S	0.01	0.01	0.01	0.03	0.02	0.01	0.01	0.01	0.03	0.02	0.97	0.13
Qz	2.64	1.68	3.64	3.82	2.20	30.94	33.12	30.51	30.49	21.72	-	-
Cor	-	-	-	-	-	0.98	1.85	2.33	1.82	1.00	6.52	3.17
Or	7.84	8.41	4.08	4.70	7.15	25.83	36.27	32.17	17.06	7.22	33.17	24.42
Ab	35.32	26.89	35.48	34.53	37.51	27.46	20.54	25.13	44.80	51.31	9.88	7.93
An	35.10	40.68	45.28	39.64	40.68	10.10	5.63	5.52	2.73	7.82	26.34	37.02
Di	12.66	10.35	2.81	7.21	6.47	-	-	-	-	-	-	-
Hy	-	7.67	-	-	-	3.36	1.82	2.96	2.70	7.94	9.53	10.46
Wo	1.20	-	7.11	6.41	4.16	-	-	-	-	-	-	-
Mt	2.79	2.87	0.84	2.58	0.92	0.76	0.35	0.85	0.14	2.01	4.21	4.81
Ilm	1.86	1.11	0.52	0.69	0.37	0.45	0.39	0.34	0.15	0.68	0.57	0.39
Ap	0.56	0.33	0.23	0.37	0.50	0.09	0.03	0.17	0.06	0.25	0.13	0.15
Py	0.02	0.01	0.02	0.05	0.05	0.03	0.01	0.03	0.05	0.03	1.81	0.23
DI	45.80	36.98	43.19	43.05	46.86	84.24	89.92	87.81	92.34	80.25	43.05	32.35
SI	10.73	26.35	3.79	8.80	8.41	5.80	4.03	5.47	4.74	10.41	40.70	44.59
											Includes 7.8% Ol	Includes 11.4% Ol

Table 37: Trace element analyses of the Mourne acid and basic xenoliths

ppm	XT	XS	XR	XP	XN	XM	XK	XI	XF	XE	XB-2	XA
Ba	437	313	96	218	339	1660	4632	1260	585	344	697	685
Sr	432	348	441	461	519	237	334	205	201	244	142	134
Rb	36	37	19	26	36	91	124	112	62	31	304	278
Zr	115	46	-	11	-	113	143	128	24	259	13	21
Cu	8	7	22	9	7	8	20	10	7	16	34	24
Ni	8	18	6	9	7	7	8	5	6	7	205	201
Zn	89	109	23	41	39	31	25	38	25	97	33	48

Table 38: The normative feldspar content of the Mourne acid and basic xenoliths

Wt. %

Or	10.0	11.0	4.8	6.0	8.4	40.7	58.0	51.2	26.4	10.9	47.8	35.2
Ab	45.1	35.4	41.8	43.8	44.0	43.3	33.0	40.0	69.4	77.3	14.2	11.4
An	44.9	53.6	53.4	50.2	47.6	16.0	9.0	8.8	4.2	11.8	38.0	53.4

Table 39: The normative salic constituents (less anorthite) of the Mourne acid and basic xenoliths

Qz	5.8	4.5	8.4	8.9	4.7	36.7	36.8	34.7	33.0	27.0	-	-
Or	17.1	22.7	9.4	10.9	15.3	30.7	40.3	36.6	18.5	9.0	77.0	75.5
Ab	77.1	72.8	82.2	80.2	80.0	32.6	22.8	28.6	48.5	64.0	23.0	24.5

Key to the analyses: XT, XS: xenoliths from dyke No.60; XR, XP: xenoliths from dyke No.61; XN: xenolith from dyke No.63; XM: xenolith from dyke No.80; XK, XI: xenoliths from dyke No.82; XF, XE: xenoliths from dyke No.85; XB-2, XA: xenoliths from dyke No.124.

xenoliths where Rb shows strong enrichment due to the isomorphous replacement between this element and potassium in the fine-grained white mica (sericite).

It is interesting to note that three acid (XM, XK and XI) and two basic xenoliths (XA and XB-2 in Table 36) contain nearly the same amount of K_2O (ca. 5%), although their trace element chemistry is entirely different. The former inclusions are enriched in Ba averaging 2500 ppm. while the latter contain only 685 ppm. Ba on average. This indicates that Ba is strongly incorporated with alkali feldspars in the acid xenoliths, supporting the view mentioned earlier (Chapter IV, p.65).

Concentration of strontium, on the other hand, would result from the formation of calcic plagioclase. The anorthositic xenoliths contain the highest Sr amount (averaging 450 ppm.) among all the Mourne xenoliths.

The other trace elements show little or no variation in the acid and basic xenoliths from the Mourne area, except in Ni which is highly enriched in the gabbroic inclusions due to the greater abundance of ferromagnesian minerals, such as olivine and pyroxene (Table 37).

d.4) Genesis of the xenoliths

It is significant that all the anorthositic xenoliths are found in dykes situated in the vicinity of the Big-Feldspar Basalt (dyke No. 57-b, near Green Harbour, cf. Map 2 and Plate 19), with which the inclusions show a certain genetic connection. The mineralogical and chemical composition and texture of the anorthositic xenoliths place

---

Fig. 29: Rubidium (ppm) versus K_2O (wt %) for the Mourne xenoliths.

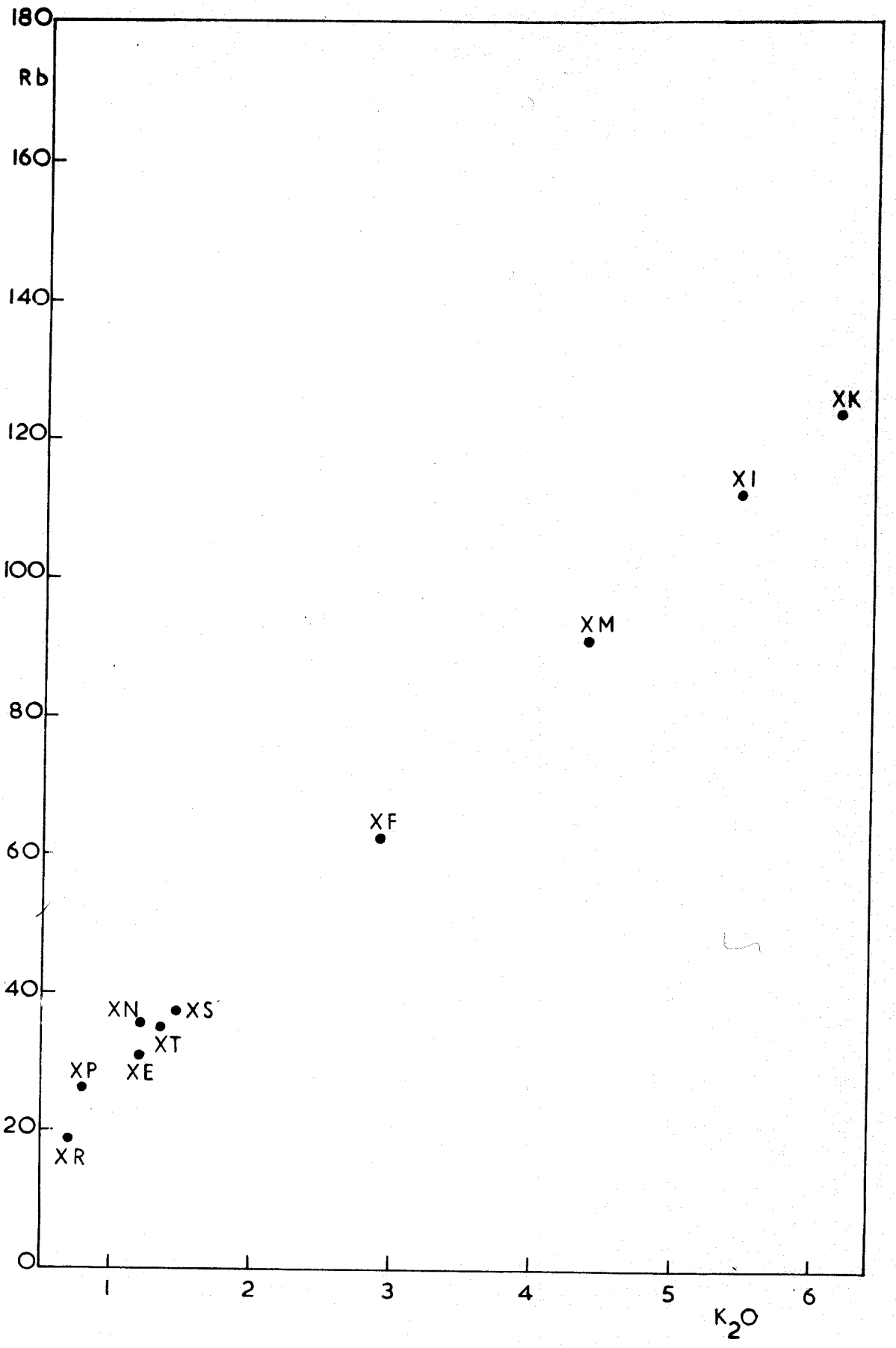
180
Rb
160
140
120
100
80
60
40
20
0
1
2
3
4
5
6
K_2O
XK
XI
XM
XF
XN
XS
XT
XE
XP
XR

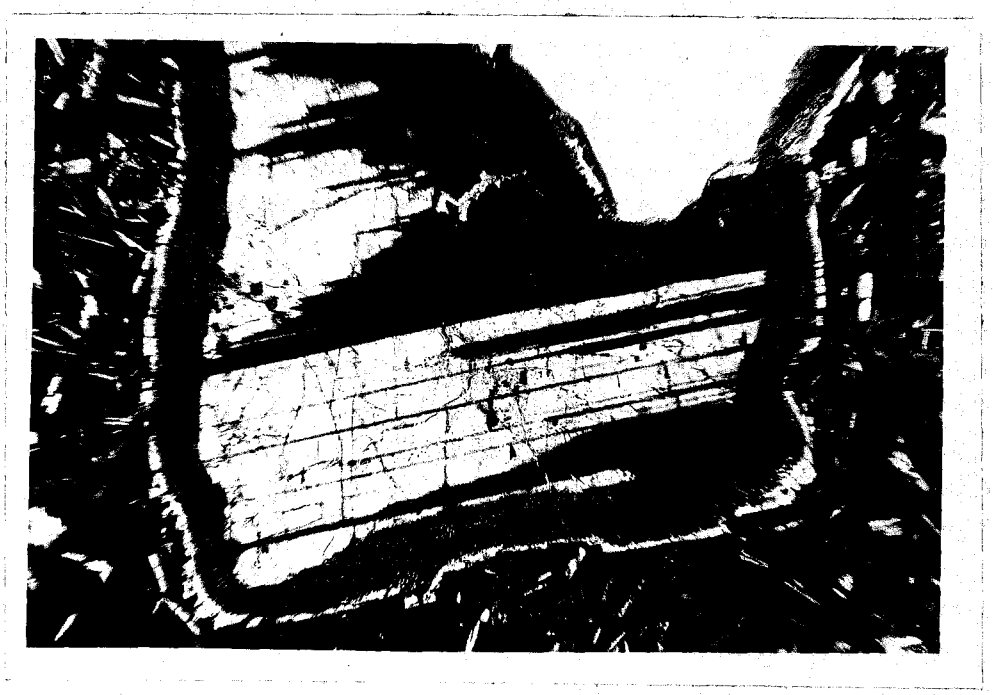

Plate 19: Plagioclase phenocryst in the Big-Feldspar Basalt, dyke No: 57-b, near Green Harbour, x 45, crossed nicols.

Plate 20: Finger-print texture on margin of labradorite phenocryst in the Big-Feldspar Basalt, with an outer rim of oligoclase (dyke No: 57-b), x 140.

them in the group of feldspar-phyric basalts occurring elsewhere in the British Tertiary Igneous Provinces (see, for example, Bailey et al., 1924, p.151, fig.21-B, and p.163, fig.23-A). They belong to the Porphyritic Central Magma type of Mull (Bailey et al., op.cit., p.24, Table 6; p.146 : Big-Feldspar Basalt type).

Bowen (1928, p.170) considered several types of monomineralic rocks to be the result of crystal sorting. Rocks believed to result from crystal settling were described by him as "accumulative rocks"; this term has since been shortened to "cumulates" (Wager et al., 1960, p.73).

The plagioclase phenocrysts which constitute the Mourne anorthositic xenoliths (Plates 17 and 18), although very much larger in size, are in many ways analogous to the unzoned calcic plagioclase crystals in the igneous cumulates from Rhum (Brown, 1956, plate 5, fig.38).

For the process of enlargement of the cumulus crystals by addition of material of the same composition the term "adcumulus growth" has been proposed by Wager, Brown and Wadsworth (1960, p.77). Rocks in which there has been much adcumulus growth have been called "adcumulates" (Wager et al., op.cit., p.78).

The large size of the plagioclase phenocrysts and very small amounts of intercumulus material in the Mourne anorthositic inclusions (cf. Plates 17 and 18) can be accounted for by the growth of the cumulus crystals as a result of slow diffusion to them of the required material of the same composition and the displacement of the intercumulus liquid by a mechanical effect (Wager and Brown, 1967, p.64).

The normative feldspar components of the Mourne acid xenoliths are plotted in Or-Ab-An ternary diagram (Figure 30). It is seen from the diagram that the acid xenoliths lie in the region between Ab-Or

join and the limit of naturally occurring feldspar solid-solution series. They may, therefore, have been derived ultimately from a basic magma through a process of fractional crystallization. Similar acid xenoliths from Surtsey, Iceland, have been described by Sigurdsson (1968, p.443) which have resulted from fractionation of a basaltic liquid.

The normative salic constituents (less anorthite) of the Mourne acid xenoliths are tabulated in Table 39 and plotted in the system $NaAlSi_3O_8$-$KAlSi_3O_8$ -SiO_2 (Figure 31).

The majority of the bulk compositions of the Mourne acid xenoliths, expressed in terms of normative wt % Qz-Ab-Or, plot near the experimentally determined cotectic boundary curves separating the silica and feldspar fields in the system Ab-Or-SiO_2-H_2O at 1000 kg/cm^2 and 3000 kg/cm^2 water-vapour pressures. The greater abundance of quartz and alkali feldspar phenocrysts in the acid xenoliths (e.g. XI, XK and XM) shows that the liquids had reached such a boundary curve (i.e. 1000 kg/cm^2 PH_2O) before coming to the surface, suggesting an immediate derivation for the acid material from a depth of the order of 5 to 6 km., which is not in excess of that expected on geological grounds.

The acid xenoliths may also have a bearing on the origin of the

---

Fig. 30: Ternary feldspar diagram, showing normative feldspar components of the Mourne acid xenoliths in terms of weight percent. The limit of ternary solid-solution in natural feldspars (dashed line) is taken from Smith and MacKenzie (1958) and Tuttle and Bowen (1958). The alkali feldspar minimum (M) and the minimum for the calcium bearing alkali feldspars (m) are also taken from Tuttle and Bowen.

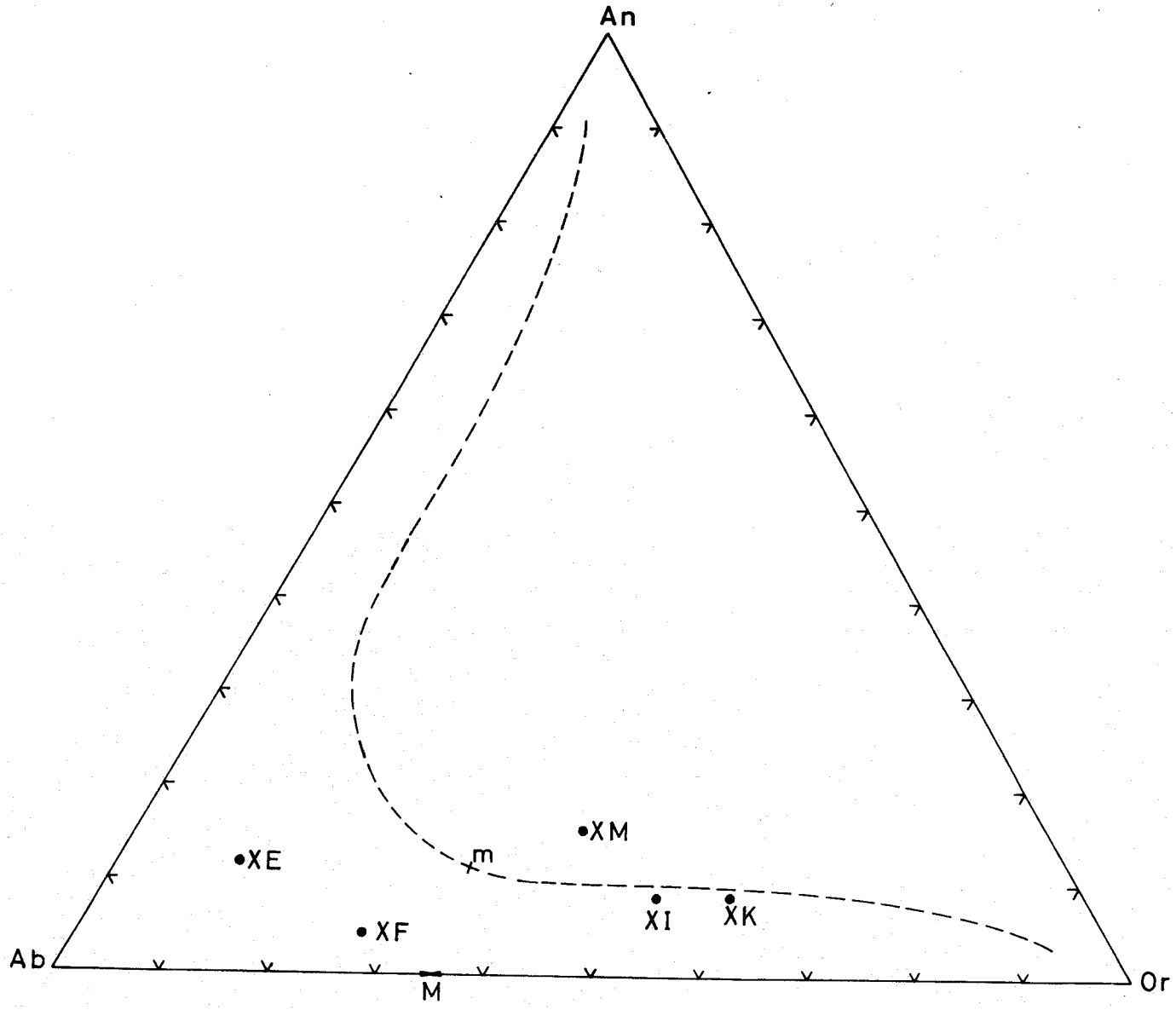
An
Ab
Or
M
m
XE
XF
XM
XI
XK

acid rocks in the Mourne dyke-swarm. The question has often been raised as to whether the cone-sheet granophyres of the Mourne area could be solely the product of differentiation from a basic parent magma or whether sialic fusion or contamination were operative. Petrological and chemical evidence favours differentiation as a more likely source of the cone-sheet granophyres.

As shown above, the chemical composition of the acid xenoliths can be attributed to crystal fractionation from a basic parent magma and, furthermore, their mineralogy is similar to many of the cone-sheet granophyres cropping out at the surface. It is interesting to note that the acid xenoliths are found in dykes situated in the vicinity of the Glasdrumman cone-sheet granophyres with which the inclusions shows a certain genetic relation.

Sigurdsson (1968, p.452), in his study of the acid xenoliths from Surtsey, has reached a similar conclusion that Icelandic xenoliths represented fragments of granophyres exposed at the surface and were ultimately formed by fractional crystallization of a basic parent magma which produced bulk of the acid material in Eastern Iceland.

e) Composite minor intrusions in the Mourne area

e.1) General statement

The term "composite minor intrusion" is here used in the sense

---

Fig. 31: The normative salic constituents (less anorthite) of the Mourne acid xenoliths plotted in the system $NaAlSi_3O_8$-$KAlSi_3O_8$-SiO_2 (weight %). The experimental boundary curves and minima at 500 and 3000 kg/cm^2 P_{H_2O} are taken from Tuttle and Bowen (1958).

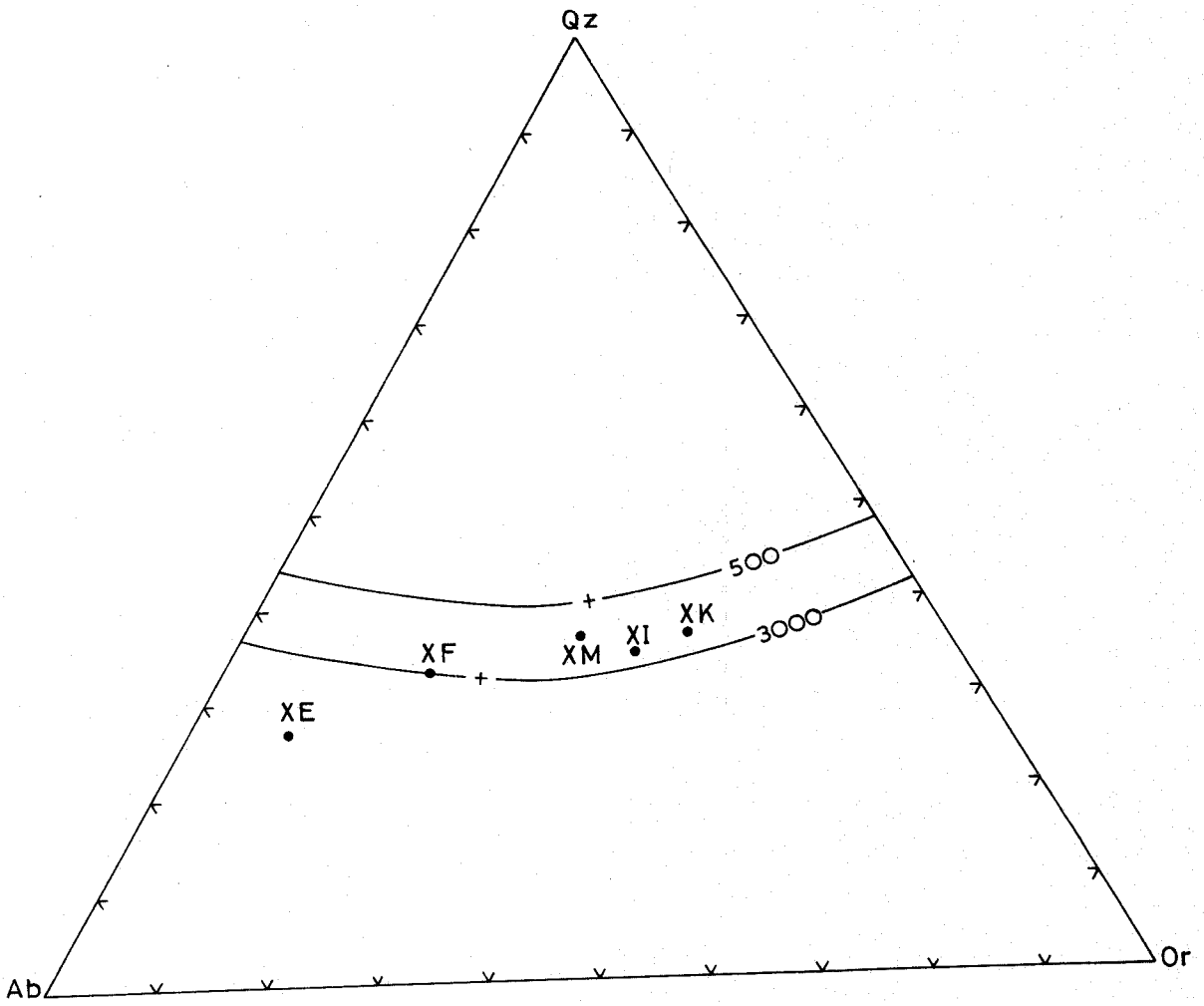
Qz
Ab
Or
500
3000
XE
XF
XM
XI
XK

given to it by Bailey and McCallien (1956, p.467). According to them, every composite minor intrusion has a combination of four distinct characteristics as outlined below:

1. The margins differ in composition from the interior.
2. The margins chill against country rock.
3. The interior is somewhat later than the margins.
4. The interior does not chill against the margins.

Composite minor intrusions, predominantly sills and cone sheets, though dykes are also known, are characteristic features of the British Tertiary Igneous Province from western Scotland to NE Ireland. They have long been the subject of debate by British geologists (e.g. Harker, 1904; Bailey et al., 1924; Richey and Thomas, 1930). A recent account is that by Bailey and McCallien (1956).

The other world-wide known composite intrusions come from different geological regions, in particular, from Iceland (Guppy and Hawkes, 1925; Gibson and Walker, 1963; Blake et al., 1965; Sigurdsson, 1970) and from North America (e.g. Gardiner River Complex, Wyoming: Fenner, 1938, 1944; Wilcox, 1944; Hawkes, 1945; Boyd, 1961; and Mount Desert Island, Maine: Chapman, 1962).

e.2) Field relations and microscopical characters

Basaltic, intermediate and acid magmas have been available throughout the intrusive history of the Mourne ring-dyke and cone-sheet swarm. No systematic order of intrusion of magma types can be observed, and, indeed, the contemporaneous availability of the magmas is best demonstrated by a number of composite dykes and sheets, where both basic and acid magma often appear to have been intruded simultaneously in the fluid state.

The composite minor intrusions of the Mourne area occur either as dykes (Nos. 30, 88, 89 and 90) or as inclined cone-sheets (Formal Hill, Knockree Hill and Glasdrumman Port, cf. Map 1). The two composite dykes (Nos. 88 and 89) are probably faulted portions of a single dyke. The rocks are in each case identical - an outer dolerite and an inner granophyre. It is quite possible that this dyke is closely related to the Glasdrumman cone-sheet.

Most examples of the composite minor intrusions from the British Tertiary Igneous Province have relatively thin basic margins and thicker acid interiors (Bailey and McCallien, 1956, p.467).

The type just illustrated above is well-developed as an inclined cone-sheet along the shore near Glasdrumman Port where a thick central granophyre, measuring 10 m. in width is flanked by 1 - 1.5 m. thick marginal dolerite dipping 30^{o} west. The basic rock forming the outer part of the composite sheet presents chilled contacts against the Silurian sedimentary strata, numerous angular xenoliths and rectangular blocks of which are contained in the marginal dolerite (Plate 22).

The petrographical character of the dolerite has already been described (cf. Chapter IV, section c). However, a few additions can be made to this end. The most interesting feature of this rock is its xenocrystic structure, particularly near the contact of the dolerite with inner granophyre (Plate 23). The xenocrysts are sparsely distributed, except in the main mass of the dolerite and in the xenoliths of dolerite in the granophyre (cf. Plates 28, 29 and 30). They consist of quartz and alkali feldspar with varying size from 2 mm. up to 1 cm. The alkali feldspar xenocrysts are usually turbid and rounded. There is no doubt that they were derived from a granophyre.

The central granophyre is characterized by a great abundance of

basic fragments and lobate or pillow-like bodies of dolerite, a few cm. to tens of cm. in diameter, becoming more numerous towards the dolerite-granophyre contact (Plates 24, 25 and 26).

An intimate mixing of the basic envelope and the felsic magma occurs in places, with stringers and irregular apophyses running from one rock type into the other. At the time of solidification the result of this mixing was a rather basified granophyre littered with basic pillows (Plate 26).

There are, however, rare examples of xenoliths of hybrid granophyre in the dolerite matrix near the contacts between granophyre and dolerite (Plate 27).

The basified (hybrid) granophyre forms marginal zones on either side of the central granophyre and separates it from the marginal dolerite. The rock is similar to the normal granophyre except for a much darker groundmass. The phenocrysts of the two rocks are identical, but the groundmass of the hybridized granophyre is richer in hornblende and biotite. The immediately observable effect of slight contamination on the composition of the groundmass of the basified granophyre, with no corresponding effect on its phenocrysts, is regarded as an indication that the groundmass of the granophyre was in a vulnerable chemical condition at the time of contact suggesting that both magmas were in liquid state. A further evidence substantiating this view is provided

---

Plate 23: Photomicrograph of dolerite-granophyre contact in the Glasdrumman composite cone-sheet. The contact is unchilled and a xenocryst of alkali feldspar is seen in the dolerite (right) which indicates that both the granophyre and dolerite co-existed in their liquid phases, x9.

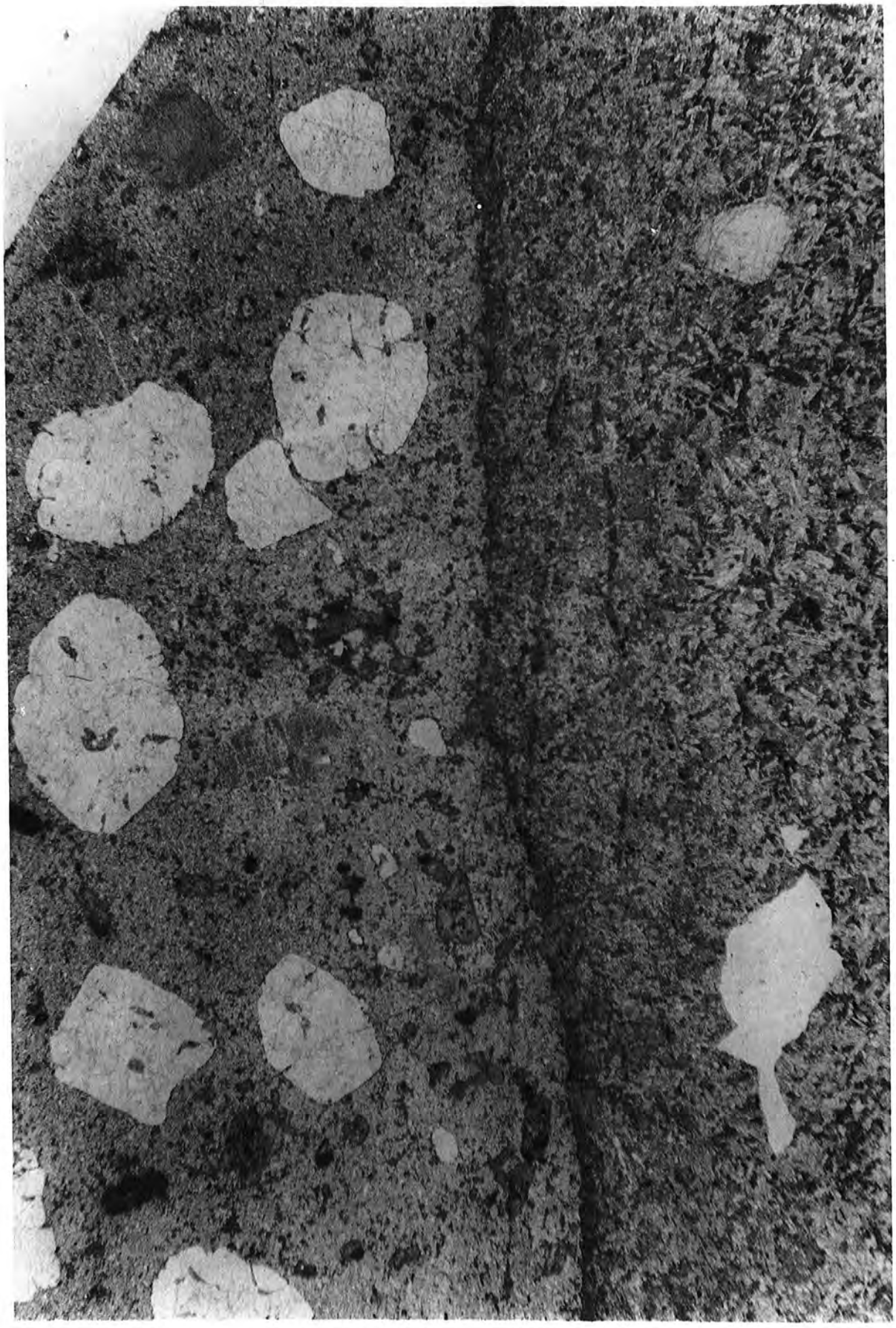

by the examination of the microscopical characters of the contact zone which shows no sign of chilling between the basic and the acid members of the composite sheet (Plate 23). Instead of a chilled contact, a narrow melanocratic zone composed of small crystals of pyroxene and hornblende, measuring up to 0.5 mm. in width was developed at the junction of basic margin and acid interior.

e.3) Mechanism of intrusion

Geologists who have studied composite intrusions in Scotland, Ireland and Iceland are agreed that the evidence suggests that somewhat later acid magma having followed the basic magma before the latter had completely solidified in the fissure, or at any rate before it had appreciably cooled.

Richey and Thomas (1930, p.63), in the Ardnamurchan Memoir, suggested that the origin of composite sills and dykes appeared to be the result of simultaneous availability of two compositionally different magmas and of their co-existence in the same magma reservoir, one magma following upon the other along the same fissure after a very short interval of time, before the first had an opportunity to solidify completely.

Harker (1904, p.230), on the evidence of the composite intrusions of Skye, considered it beyond doubt that the magmas responsible co-existed in subterranean reservoirs, and that the denser basic magma was overlain by the lighter acid one. Harker's suggestion has since been widely approved and adopted by a number of authors (e.g. Wilcox, 1944; Hawkes, 1945; Bailey and McCallien, 1956; Blake et al., 1965) in different geological regions.

Blake and co-workers (op.cit., p.40) attempted to show a possible

situation in which a composite intrusion could originate and how they may be related to one another structurally. Their diagrammatic representation is given in Figure 32, where (a) represents a basic dyke transecting a body of acid magma. The dyke is able to do this if the acid material is so viscous that it fractures under the action of rapidly applied stress. Then the acid magma adjacent to the dyke has been heated up by the basic magma and its viscosity is reduced to a degree that the basic material can no longer pass through it in the form of a dyke but instead forms pillows (Figure 32-b). Further, the mobilized acid material now starts to rise along the hot and still liquid centre of the basic dyke. The continued uprise of the basic magma into the acid magma results in the mobilization of more acid material and the pillows of basic magma are carried to the surface (Figure 32-c).

The present writer is in favour of the above described mechanism, since the pillow-like bodies of dolerite are frequently found near the contact between the central granophyre and marginal dolerite of the Glasdrumman Port composite, inclined cone-sheet (Plate 26).

The xenoliths of the hybrid granophyre included in the marginal dolerite, although not much abundant as in the case of doleritic ones, are considered to be caught up by the rising basic magma at the initial stages of composite intrusion when the basic magma was passing through the acid material above, and the movement of quartz and alkali feldspar xenocrysts into the marginal dolerite is assumed to have taken

---

Fig. 32: Diagrammatic representation of the possible relationship between, and origin of a composite dyke feeding a composite lava-flow (Quoted from Blake et al., 1965, p.41, fig.2).

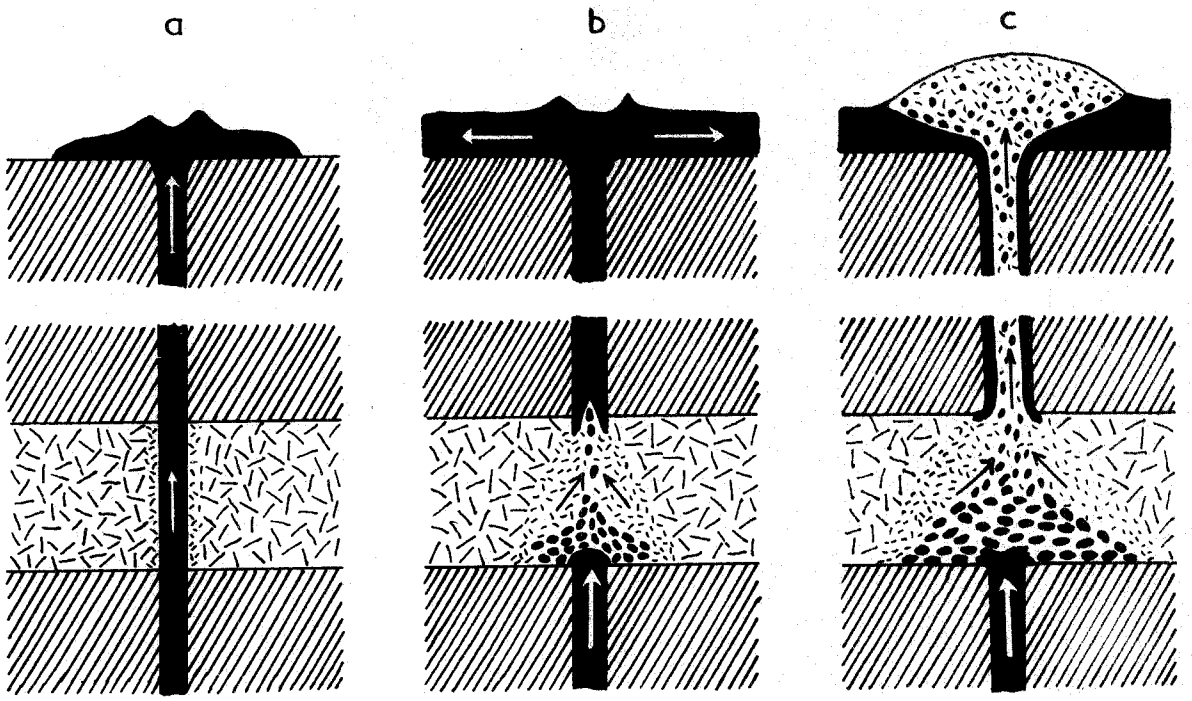

Basic magma

Basic pillows

Mobile acid magma

Viscous acid magma

place at this stage (Plates 23 and 27).

The development of basified (hybrid) granophyre has effectively separated the two magmas and has inhibited thorough mixing. Tomkeieff and Marshall (1935, p.274) have demonstrated a similar picture by suggesting the acid magma intruded into a central zone of weakness in the basaltic column and eviscerated the basic rock, as well as detached fragments of it. In this way the first intruded portion of the acid magma has become hybridized by assimilation. Continuation of the pressure forced the lower, uncontaminated acid magma into the still hot, liquid hybrid granophyre, which owing to its viscosity, did not mix with the later magma.

As to the origin of these two different co-existing magmas, the present writer favours the process of differentiation.

Harker (1904, p.230) suggested that the two co-existing magmas in Skye composite intrusions were complementary products of differentiation from the same magma chamber, a suggestion that has been adopted by Kennedy (1931, p.174) in the composite intrusions of Renfrewshire, Scotland. He argued that the two magmas giving rise to the porphyritic and non-porphyritic rock types must have undergone differentiation prior to intrusion and have existed as separate bodies within the same magma chamber. He then concluded that the two types of magma must have become available at the same time.

The relationship between acid and basic magma outlined above suggests that two sub-crustal magmas of widely different composition existed at the same time not far from each other, or perhaps co-existed in the same magma basin in the Mourne area.

Holmes (1931, p.244) suggested that acid and basic magmas could exist in the same chamber, maintaining their identities as a result of

gravity stratification. Such a dual magma, he postulated was the parent of the composite intrusions and hybrids of the Scottish districts.

As an alternative suggestion, the possibility of simultaneous tapping of two magma chambers in the Mourne area does not seem remote. There is abundant evidence that many of the basaltic eruptions of the world originate from fissures tapping deep-seated magma reservoirs, whereas most rhyolitic eruptions originate from chambers relatively shallow in the crust (Wilcox, 1944, p.1072). This would indicate that felsic magma might even lie in a separate chamber more or less directly above the chamber of basaltic magma, and that both might be tapped by the same or simultaneously formed fissures with a resultant mixture of the two magmas during eruption.

Bailey and co-workers (1924, p.33), in the Mull Memoir, favour the mechanism described by Holmes (1931), in the Mull composite intrusions and suggest that a fissure communicating with a reservoir in which the liquid contents are stratified, may often cut the wall of the reservoir obliquely, and thus offer itself as a channel of intrusion for both acid and basic magma. They further state that it may be expected in such a case that hot basic magma would proceed much more readily along a cold fissure than relatively cool acid magma. Once basic magma has prepared the way, acid magma can easily follow; field relations show that acid magma under hot subterranean conditions is extremely mobile, whereas under the conditions which generally attend the progress of lava-flow it is highly viscous.

Whether the two different magmas existed together or separately in the Mourne area, one thing is certain that they have been intruded into the fissures almost simultaneously and were hot and in fluid state

at the time of intrusion.

e.4) Chemical evidence for the incorporation of acid material into the basic magma

Basic rocks which contain xenocrysts of alkali feldspar and quartz may be assumed to have incorporated at least a small amount of acid material. The extent of this incorporation in the Glasdrumman marginal dolerite is demonstrated in Table 40 which includes 5 natural samples and 3 theoretical mixtures of dolerite and granophyre calculated on the basis of silica percentage. The theoretical mixture of 9% granophyre and 91% dolerite corresponds approximately the chemical composition of slightly contaminated marginal dolerite, No.GPCS-4. Similarly, the theoretical mixture of 30% acid and 70% basic material closely approaches the chemical composition of highly contaminated marginal dolerite, No.GPCS-12. The chemical analysis of the basified (hybrid) granophyre (No.GPCS-14) is fairly similar to the mixture of 76% granophyre with 24% dolerite.

The trace element concentrations in the natural examples are slightly different than those in the recalculated theoretical equivalents.

e.5) Summary and conclusions

Under the light of above evidence, some general comments on the relationships between acid and basic magmas giving rise to the composite minor intrusions in the Mourne area can be made.

There is evidence in such composite intrusions that the presence of basic magma increases the mobility of the acid magma (cf. Bailey et al., 1924, p.33; Blake et al., 1965, p.41). The evidence is furnished by differences in the normal crystallizing (liquidus) temperatures of

Table 40A: Chemical analyses and recalculated compositions of the Glasdrumman composite cone-sheet rocks

Wt. %	B Natural 13328	Natural GPCS-4	Theoretical GPCS-4	Natural GPCS-12	Theoretical GPCS12	Natural GPCS14	Theoretical GPCS-14	A Natural GPCS-20
SiO_2	47.44	50.05	49.99	56.02	55.92	69.00	68.93	75.72
Al_2O_3	16.93	15.13	16.64	15.28	15.97	14.24	14.50	13.73
Fe_2O_3	2.56	4.19	2.37	2.14	1.93	1.44	0.96	0.46
FeO	9.50	8.84	8.73	7.75	6.93	2.96	2.98	0.93
MgO	8.32	7.33	7.60	5.24	5.90	1.74	2.20	0.27
CaO	9.30	7.79	8.50	6.16	6.63	2.71	2.54	0.40
Na_2O	2.26	3.00	2.39	3.06	2.68	4.77	3.33	3.67
K_2O	1.15	1.35	1.46	2.28	2.20	2.42	3.80	4.64
TiO_2	1.79	1.86	1.64	1.56	1.29	0.48	0.51	0.11
P_2O_5	0.46	0.23	0.42	0.27	0.32	0.12	0.12	0.02
MnO	0.24	0.20	0.22	0.19	0.17	0.07	0.07	0.02
S	-	0.07	-	-	-	-	-	-
Total	99.95	100.04	99.96	99.95	99.94	99.95	99.94	99.97
Ba ppm	423	494	413	516	390	1300	339	312
Sr "	227	218	209	196	168	149	77	30
Rb "	38	43	56	173	99	179	192	241
Zr "	139	126	173	210	252	442	425	515
Ni "	66	55	60	51	48	12	20	5
Cu "	100	96	92	76	72	8	30	8
Zn "	96	82	90	116	77	60	47	32
	A_o-B_{100}		A_9-B_{91}		A_{30}-B_{70}		A_{76}-B_{24}	A_{100}-B_o
			Degree of mixing		Degree of mixing		Degree of mixing	

Key to the analyses:

13328: Uncontaminated marginal dolerite (B).

GPCS-4: Dolerite, slightly contaminated with acid material.

GPCS-12: Dolerite, highly contaminated with acid material.

GPCS-14: Basified (hybrid) granophyre.

GPCS-20: Uncontaminated central granophyre (A).

Table 40-B: C.I.P.W. norms of the Glasdrumman composite cone-sheet rocks

Wt. %	Natural 13328	Natural GPCS-4	Theoretical GPCS-4	Natural GPCS-12	Theoretical GPCS-12	Natural GPCS-14	Theoretical GPCS-14	Natural GPCS-20
Qz	-	-	-	6.15	6.90	22.71	24.72	34.80
Cor	-	-	-	-	-	-	0.51	1.97
Or	6.81	7.98	8.90	13.48	12.79	14.35	22.24	27.46
Ab	19.18	25.36	20.44	25.97	22.53	40.43	28.30	31.10
An	32.61	23.81	30.02	21.19	25.30	10.24	11.95	1.85
Di	8.54	10.76	7.69	6.26	4.76	1.98	-	-
Hy	11.85	18.66	21.35	20.19	21.72	6.96	9.72	1.86
Ol	12.76	3.14	4.01	-	-	-	-	-
Mt	3.71	6.07	3.48	3.11	2.78	2.09	1.39	0.67
Ilm	3.40	3.53	3.19	2.97	2.45	0.91	0.91	0.20
Ap	1.10	0.56	1.00	0.64	0.76	0.28	0.28	0.04
Py	-	0.13	-	-	-	-	-	-
DI	26.00	33.34	29.34	45.61	42.22	77.50	75.26	93.36
SI	34.97	29.66	33.70	25.60	30.04	13.05	16.58	2.71
Or	11.6	14.0	15.0	22.2	21.1	22.0	35.6	45.5
Ab	32.7	44.3	34.4	42.8	37.2	62.2	45.3	51.5
An	55.6	41.7	50.6	35.0	41.7	15.8	19.1	3.0

the two types of magmas.

Larsen (1929, p.94) in evaluating accumulated data on the temperatures of magmas, has concluded that the temperatures of most crystallizing felsic magmas are probably not far from 600°-700°C, while those of most crystallizing basaltic magmas are probably close to 800°-900°C.

At the time of the 1921 eruptive episode of Kilauea several temperature measurements were made of the liquid lava in Hawaii. Jagger (1947) reported that 1200°C, 1100°C and 1190°C were read. Yoder and Tilley (1962, p.385) showed that two of these were exceptionally close to the liquidus temperature observed experimentally for the 1921 lava.

MacDonald, in a personal communication to Buddington (Buddington, Fahey, and Vlisidis, 1955, p.502) gave evidence that the extrusion temperatures of Hawaiian basaltic flows were between 1000° and 1100°C and (aa) flows became immobile between 700° and 780°C.

Finally Ault, Eaton and Richter (1961, p.792) reported that the highest temperature in the lava during the 1959 eruption of Kilauea was between 1060° and 1190°C.

Sigurdsson (1970, p.106) considers the rise in temperature likely to occur within the acid magma as a result of intimate mixing with a much hotter basaltic magma. He then concludes that the temperature difference between the two magmas may be as much as 200°C.

Blake and co-workers (1965, p.41) suggest that acid magma normally experiences great difficulty in attaining high crustal levels but this difficulty is eased when it comes in contact with basic magma (cf. Bailey et al., 1924, p.33 or p. 94 of the present study). The presence of basic magma, according to them, may, indeed, be essential to

the uprise and even to the generation of acid magma in geological environments where the composite minor intrusions are common.

It would appear that acid magma has reached high crustal levels more frequently as a component of composite intrusions than as purely acid minor intrusions, which is, indeed, so in the Mourne area where composite sheets and dykes are more common than single acid sheets or dykes.

The intrusive nature of the Glasdrumman cone-sheet granophyre in contact with the marginal dolerite would also be expected with the mingling of simultaneously intruded basic and acid magmas. With each at its liquidus temperature, the acid magma could exert a cooling and solidifying effect on the basic magma, resulting in the production of basaltic xenoliths (Plates 24, 25 and 26). These xenoliths have chilled against the granophyre because of the sudden decrease in temperature caused by relatively cooler acid magma (cf. Plate 28).

The consistent production of basaltic xenoliths rather than felsic ones would be a natural result of the mutual effects of the two intermingling magmas. Since the magmas would be in motion, the contact between the two moving liquids could not be stable, and small masses of one liquid would be dragged into the main body of the other liquid by the turbulent movement. A small mass of basaltic liquid, isolated in acid magma, would immediately give off some of its heat to the

---

Plate 28: Photomicrograph of the contact between a xenolith of marginal dolerite and central granophyre of the Glasdrumman Port composite cone-sheet. The contact is chilled against granophyre and no xenocrysts of granophyric material can be seen in the fine-grained xenolith, x9.

cooler surrounding material. As the basaltic liquid was already crystallizing, any sudden lowering of temperature should accelerate the speed of crystallization so that it would almost immediately become a fine-grained mush (Plates 28 and 29). In the initial stages of mushiness, the basaltic mass would have been drawn out into elongated and rounded xenoliths or pillow-like, lobate bodies while involved in movement with the surrounding viscous acid liquid (Figure 32-b). Many of the pillow-like bodies of basaltic xenoliths in the Glasdrumman cone-sheet granophyre may be explained in this way (cf. Plate 26).

Considering now the small blebs of acid material dragged into the main mass of the basaltic liquid, no similar tendency towards the formation of felsic xenoliths is observed. Instead, a felsic bleb, quickly heated to the temperature of the surrounding basaltic material, would cease crystallizing and dissolve in the basaltic liquid. The resorption of the already formed quartz and alkali feldspar phenocrysts would proceed more slowly than the groundmass material, and these crystals might persist as xenocrysts in the basaltic rock. However, with more and more acid material dragged into the basaltic liquid, incomplete absorption of the acid mass before final consolidation would lead to the production of hybrid xenoliths (Plate 27). The relative scarcity of acid xenoliths over the basic ones in the Glasdrumman composite sheet has already been pointed out (p.90).

Wager and Bailey (1953, p.69) were the first to suggest that certain basic pillow-like masses in the granophyres from St. Kilda and Slieve Gullion could have been formed by the injection of basic magma into acid magma, in a manner analogous to the formation of pillow-lavas in sea-water. They considered the basic pillows to have been chilled against the acid magma which is in full agreement with the

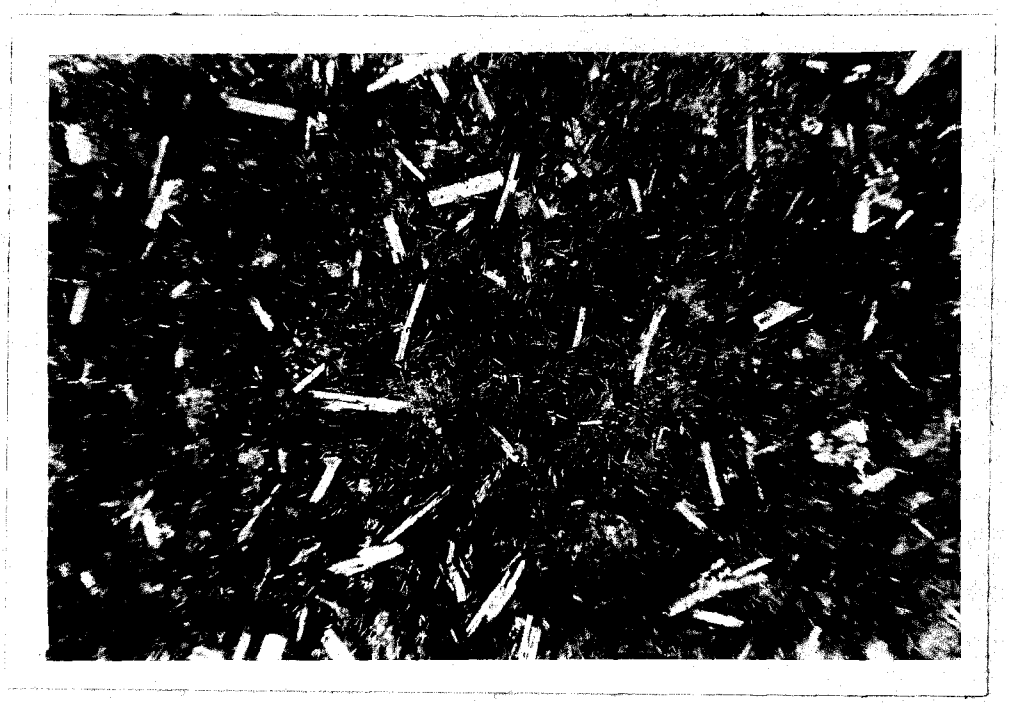

Plate 29: Fine-grained ophitic texture in the xenolith of marginal dolerite from the Glasdrumman composite cone-sheet, x45.

Plate 30: Coarse-grained ophitic texture in the marginal dolerite from the Glasdrumman composite cone-sheet, x45.

above mentioned temperature differences between the two types of magmas (p.96). Since then this hypothesis has been supported by a number of authors (e.g. Gibson and Walker, 1963, p.316; Bailey and McCallien, 1956, p.466; Elwell, 1958, p.57; Elwell et al., 1960, p.104; Blake et al., 1965, p.37).

Bailey and McCallien (1956, p.468) think it almost certain that many of the quartz and alkali feldspar xenocrysts in the basaltic component of the composite minor intrusions were picked up by the basic magma while passing through acid material which at a later stage, supplied the porphyritic interior of the composite sheet concerned. The present writer, however, favours the idea of selective absorption of the acid material by the basaltic liquid as outlined above (p. 98).

Bailey and McCallien further state that as the basic magma must have come from a greater depth than that of the exposed composite, and as it passed through acid material on its way; they interpret it as having risen through this acid material. This is, in keeping with the commonly held view that composites have been fed from gravity-stratified reservoirs (cf. Bailey et al., 1924, p.33; Holmes, 1931, p.244), a hypothesis fully supported by the present author.

The other ideas suggested by Bailey and McCallien (op.cit. p.468), concerning the composite minor intrusions in NE Ireland and supported by the present writer can be summarized as follows:

1. For the relatively heavy basic magma to rise through acid material, the latter must have been substantially solid, although quite possibly hot.

2. To yield xenocrysts such as quartz and alkali feldspar, the acid material must have been porphyritic with marked distinction between its phenocrysts and groundmass.

3. To convert phenocrysts to xenocrysts the uprising basic magma must have melted acid material along the containing walls of the fissure, and mixed with the product.

4. Progressive incorporation of xenocrysts with time can be observed with the first basic magma, free of xenocrysts when intruded to give marginal member of uncontaminated basaltic rock.

5. When acid magma instead of basic one began to appear in the upper region, it is inferred that deep-seated melting of acid material had become too widespread to allow further upward passage of basic magma (cf. Figure 32-b). Therefore the basic material could no longer pass through it in the form of a dyke but instead formed pillow-like, lobate bodies (Plate 26).

CHAPTER VI

PETROGENESIS OF THE MOURNE DYKE-SWARM

A. BASALT PETROGENESIS

A.1) Introduction

The majority of geologists recognize two principal lines of descent from a primitive source from which all magmas might have been derived (cf. Yoder and Tilley, 1962, p.346; MacDonald and Katsura, 1964, p.82):

1) Alkali basalt → hawaiite → mugearite → trachyte ⟨ phonolite / pantellerite ⟩ series.

2) Tholeiite → tholeiitic andesite → dacite → rhyolite series.

Some investigators (e.g. Bailey et al., 1924, p.31; Bowen, 1928, p.78) believed that both principal lines of descent might have stemmed from an alkali basalt magma by means of fractional crystallization or by assimilation. Others (e.g. Tilley, 1950, p.44; MacDonald, 1949b, p.88) present arguments indicating that tholeiite is the source magma of both lines of descent also by crystal fractionation. Still others (e.g. Kennedy and Anderson, 1938, p.78; Kuno, 1959, p.73) prefer the notion that two or more separate primary magmas of unspecified origin are derived from different levels in the crust or upper mantle, each producing its products independently of the other.

A number of authors have suggested source material essentially equivalent to basalt in composition, for example, eclogite (Holmes, 1926, p.321) and others (Holmes, 1932, p.552; Buddington, 1943, p.137) have proposed a more basic magma, of a composition such as peridotite,

from which all magma series are derived.

The great majority of geologists, however, accept basalt as the primary magma type even though it may have come initially from the partial melting of a peridotite layer (Bowen, 1928, pp.315-320).

Subsidiary geophysical observations, in addition, support the general view that basalt is the source of almost all other derivative magmas, excepting only those arising from contamination or from the partial melting of sediments (Yoder and Tilley, 1962, p.347).

Laboratory studies on synthetic systems, and studies of natural examples of fractional crystallization have shown that, at low pressure, the tholeiitic and alkalic basalt series are separated by a "thermal divide" (Yoder and Tilley, 1962, p.342).

The superposition of low pressure fractionation effect on magmas of the alkali olivine basalt type and on those of the olivine-tholeiite type causes a marked divergence of derivative liquids.

A.2) Magma generation in the mantle

A number of specific hypotheses of partial melting in the mantle to produce diverse basalt magma types have been proposed by various authors.

Bowen (1928, pp.315-318) favoured the selective fusion of peridotite as the source of basaltic magma and suggested (op.cit. p.318) that, although the basaltic fraction of the parental peridotite may exist in eclogite facies mineralogy, this would still constitute the low-melting portion of the peridotite.

The concept that garnet-peridotite is the parental rock to basaltic magmas has been followed by numerous other authors, e.g., Ringwood (1958, p.210), Yoder and Tilley (1962, p.342), and Green

(1968, p.839).

Kuno and co-workers (1957, p.179), in considering the evidence from Hawaii, concluded that tholeiitic and alkali basalt magmas must have originated within the mantle but at different levels. Kuno (1959, p.37) also suggested that alkali olivine basalts were derived from greater depths than the tholeiites and correlated the depth of origin of the magmas with the depth to deep-focus earthquake epicentres beneath Japan.

The relationship between depth of magma generation and the diverse magma types originated within the mantle has been extensively studied by a number of authors.

Clark (1959, p.498) considered, on purely theoretical grounds, that if basalts were originated by partial fusion of the upper mantle material, the first liquid to appear, presumably eclogitic, would be different from that in equilibrium with a gabbro of identical bulk composition. Pressure would affect the melting relations of the constituent minerals differently, and as new phases become stable the phase relations would change. He then concluded that the composition of basalts would, therefore, be a function of their depth of origin.

Kushiro (1961, p.31) considered, on the basis of experimental evidence, that tholeiites must have been generated at depths less than about 35 km. and suggested that they might have been developed by complete melting of a basaltic layer in continental regions but in oceanic areas must have been derived from peridotite by partial melting.

Kushiro and Kuno (1963, p.75) reported similar depth relations and argued that basalt magmas could be produced by partial melting of 2-9% of the peridotite at depths where incongruent melting of orthopyroxene was operative.

Finally, Green and Ringwood (1967) and Kushiro (1968) have inferred from high pressure experimental studies that silica undersaturated liquids are produced at deeper levels than silica saturated ones. These observations tend to support the suggestion of Kennedy (1966) that partial melting is strongly limited by pressure.

A.3) Origin of tholeiitic and alkali basalt magma types on the basis of trace element fractionation

Tholeiitic basalts having less than 0.3% K_2O by weight appear to be the primary and predominant magma type erupted on the oceanic floor (Engel and Engel, 1964a,p.1330; 1964b, p.485). Inspection of the chemical analyses in Table 19 shows that the majority of the Mourne olivine-tholeiites are very poor in K_2O. Correlation was made between the potassium and rubidium contents of these rocks and it was found that the low concentrations of K and Rb observed in the Mourne olivine-tholeiites (cf. Tables 19 and 31) could be of fundamental significance.

K/Rb ratios in the Mourne olivine-tholeiites and alkali basalts

The ratio of potassium to rubidium is very variable in basaltic rocks. Even in tholeiites alone the value ranges from near 200 in the Tasmanian quartz-dolerites (Heier et al., 1965, p.653) to around 500 for the Hawaiian tholeiites (Lessing et al., 1963, p.5853) and to over 1000 for very low K-tholeiites from the Mid-Atlantic Ridge (Gast, 1960, p.1290; 1965, p.859; 1968, p.1067; Kay et al., 1970, p.1602).

Gast (1965) has shown a correlation between high K/Rb ratios with low K contents, and low K/Rb ratios with high K contents through a spectrum of oceanic basalts comprising the submarine tholeiites of the Mid-Atlantic Ridge, the Hawaiian tholeiites and alkali basalts, and

alkali basalt suites of Gough and Ascension Islands. He concluded that the K/Rb ratio of the upper mantle was much higher than that observed in chondrites. Such a correlation between abundance of an element and variation in an element ratio could possibly be interpreted in terms of partial melting at the source of the magmas involving phases with low K content and high K/Rb ratio (e.g. pyroxene), and a minor, variable phase with high K content and low K/Rb ratio (e.g. phlogopite).

In a recent paper, Gast (1968, p.1057) postulates that the high K/Rb ratios in abyssal basalts (oceanic tholeiite flows) are characteristics of the upper mantle region that produced these basalts. He suggested (op.cit., p.1083) that abyssal basalts were derived by extensive (20-30%) partial melting of upper mantle material. This hypothesis is supported by Pb-isotopic evidence (cf. Tatsumoto, 1966a, 1966b; Gast, 1967; Bence and Hurley, 1967).

Viewing basalt petrogenesis in the Mourne area by applying this concept to the Mourne olivine-tholeiites, the high K/Rb ratios usually found in these rocks (cf. Table 41) would, therefore, be attributed to their primitive character. The K/Rb values of the Mourne olivine-tholeiites and alkali basalts are plotted in Figure 33.

A.4) Genetic relation of two magma types

The effect of pressure on the evolution of basaltic liquids is known from the work of numerous authors, e.g., studies on the system Fo-Di-SiO_2 at 20 kb. by Kushiro (1969), and the demonstration of

---

Fig. 33: A plot relating K/Rb ratios and K contents of the Mourne tholeiitic and alkalic basalts. Ellipsoidal fields are from Gast (1968, p.1067, fig.4).

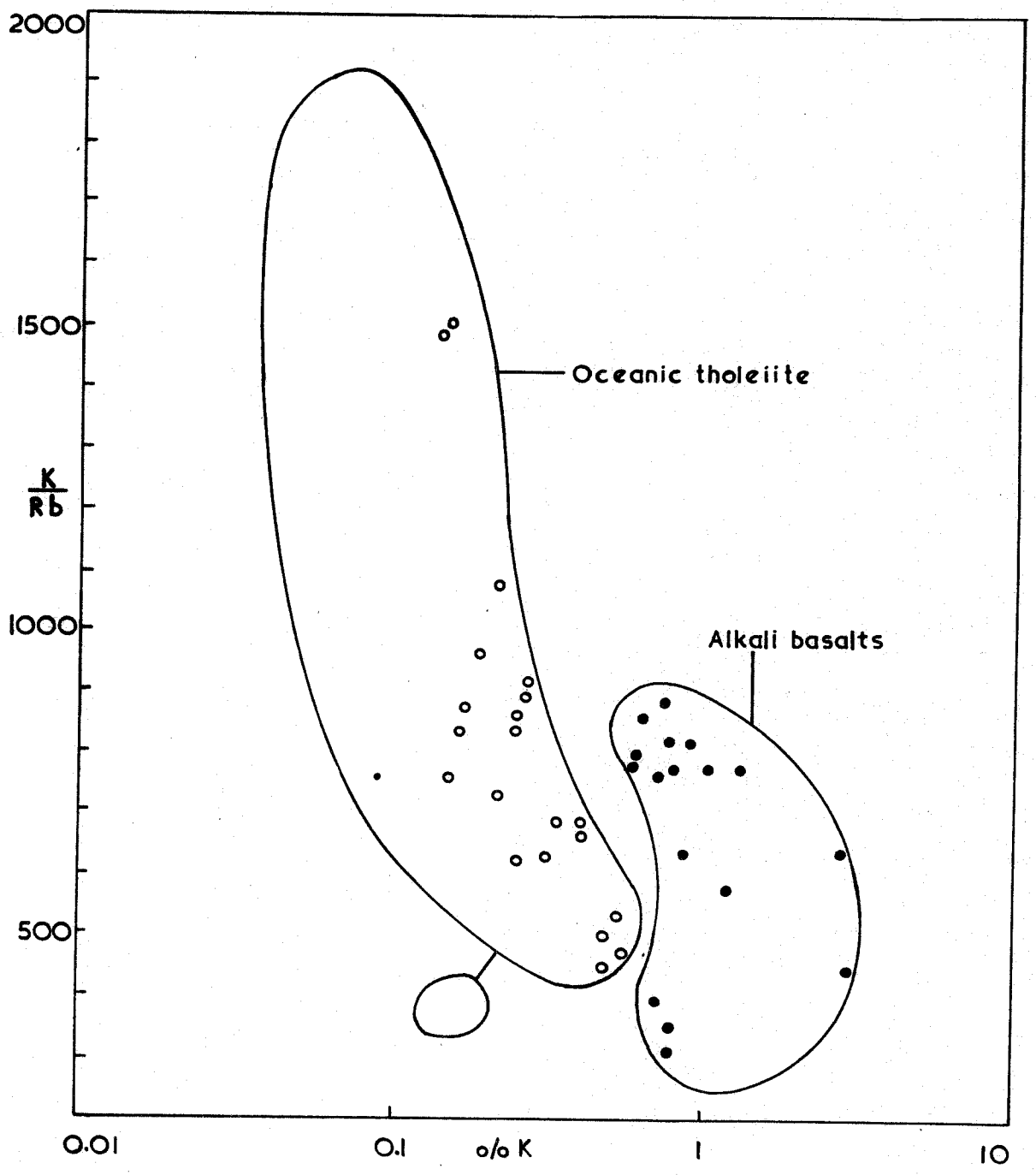
2000
1500
K/Rb
1000
500
Oceanic tholeiite
Alkali basalts
0.01
0.1
o/o K
1
10

Table 41: K/Rb ratios of the Mourne tholeiitic and alkalic basalts

Olivine-tholeiites				Alkali basalts	
No.	K/Rb	No.	K/Rb	No.	K/Rb
127-a	632	93	1027	129-a	315
127-c	625	76-b	531	129-b	355
127-d	490	62	1090	124-d	629
126-a	720	55-a	678	110-a'	465
126-b	950	47	1204	87	883
125	445	6	856	87-a	946
124-c	870	4	996	54-b	711
124-e''	1080	514	976	46-a	632
124-e'''	1500	Average:	896	45-a	499
121-c	1080			33	395
119-a'''	1060			28	441
119-b	663			27	638
118	830			26-a	794
117	913			26-b	332
116	1080			23	327
115	1176			22	783
112-a	830			21	772
112-b	745			19	811
110-a''	1103			18	415
109-a''	490			11	307
109-a'''	456			10	577
107-a	856			502	812
107-c	490			503	474
105	1490			504	778
104	1490			505	397
102	887			506	777
101	680			507	776
100-a	1079			509	857
100-b	1091			512	766
97	1195			513	1062
96	678			516	304
95	680			13340	367
94-b	1033			XB-1	304
				Average:	597

Table 42: K/Rb ratios of the Mourne and Killough rocks

Tholeiites		Quartz tholeiites		Killough alkalic basalts	
No.	K/Rb	No.	K/Rb	No.	K/Rb
127-b	276	401	183	KD 48	695
127-e	185	405	150	KS 49	1200
124-a	257	406	138	KD 51	370
124-e'	162	408	152	KD 52	740
123	193	409	179	KD 54	444
122	218	410	145	KD 57	438
121-a	219	411	121	KD 58	700
121-b	218	412	128	KD 59	593
114	300	414	241	Average:	648
111-a	199	Average:	160		
109-a'	199			Killough intermediate rocks	
108	208			KD 47	319
99	285			KD 53A	250
91	215			KD 53B	330
76	329			KD 56	256
68	260			KD 61B	239
67	230			KD 62	264
57-a	297			KD 63	252
57-b	221			KD 64	300
54-a	251			Average:	276
37-a	259				
30-a	249				
30-c	209				
29	200				
25-a	292				
25-c	318				
16	318				
508	182				
510	323				
Average:	244				

congruent melting of orthopyroxene above 5 kb. (Boyd and England, 1961; Green and Ringwood, 1964).

The replacement of olivine by orthopyroxene as the liquidus phase in an olivine-tholeiite liquid at approximately 15 km. depth, and subsequent fractionation by orthopyroxene crystallization will have the effect of sending the residual liquid towards more undersaturated compositions (Green and Ringwood, 1967, p.166).

Green (1969, p.415) suggests that the effect of fractional crystallization by separation of aluminous orthopyroxene is to deplete the residual liquid in silica, while enriching it in CaO and alkalies, thus shows olivine-tholeiites capable of producing a fractionation trend through olivine basalt to alkali olivine basalt.

It has been shown (Green and Ringwood, 1964, p.1276; 1967, p.167) that the degree of partial melting at 15-20 kb. and the depth of magma segregation from residual crystals are the two prime factors determining the composition and magma type of basalts derived directly by partial melting of the upper mantle material.

Green and Ringwood, in a recent paper (1969, p.492) suggest that it is possible for a single primary magma of olivine-rich and Hy-normative type to produce:

1) A continuous magma series from olivine-tholeiite to alkali olivine basalt to olivine basanite by fractionation at a depth of 35 to 70 km.

2) A continuous magma series from olivine-tholeiite to high-alumina olivine-tholeiite by fractionation at a depth of 15 to 35 km.

3) A continuous magma series from olivine-tholeiite to quartz tholeiite by fractionation at a depth less than 15 km.

A.5) Differentiation of the Mourne dyke rocks

i) Origin of the basaltic magmas

Yoder and Tilley (1962, p.506, 509) showed, on the basis of experimental work, that the probable source rock for basaltic magma was garnet peridotite. They suggested that this source would yield nepheline trending magmas at high pressure and silica trending magmas at low pressure and that alkali basalt magmas were generated at greater depths than tholeiitic magmas.

Yoder and Tilley's hypothesis on the origin of basaltic magmas has gained support later by Green (1968, p.839) who states that in considering the origin of basalt magmas within the mantle, the dominant rock type is peridotite. Basalt magmas must derive from this either by partial melting of the peridotite yielding a basalt liquid and residual refractory dunite or peridotite, or by complete melting of possible eclogite lenses or patches. The occurrence of such eclogite lenses within the peridotite would presumably result from fractional melting of the peridotite so that both processes require the fractional melting of peridotite to produce basaltic liquids.

ii) Parental magma

The Mourne tholeiitic series is believed to be derived by a process of fractionation from a basaltic parent, similar to that of the tholeiitic suite of Thingmuli (Carmichael, 1964), the composition of which is discussed as follows:

The rock equivalent of a parental magma is usually considered to be non-porphyritic and thus capable of existing as a true liquid, to be widespread and voluminous in the area concerned, and predominantly to

give a chemical indication that its liquidus temperature was higher than all its possible derivatives. In the chemical terms, this may approximate to a low content of the low-melting components of the feldspar and ferromagnesian solid-solution series. Those basalts which are essentially non-porphyritic, and are rich in magnesia and lime relative to iron and combined alkalis, may be taken to represent a possible parent.

iii) Role of oxygen pressure during differentiation

Recent experiments have indicated that variations in the oxygen pressure may have considerable influence on the formation of derivative magmas. A significant contribution was made by Osborn (1959) in amplifying the effects of oxygen pressure on the course of crystallization. On the basis of studies in the system $MgO-FeO-Fe_2O_3$ (Muan and Osborn, 1956), he concluded that an olivine-tholeiite magma may differentiate with iron-enrichment if the bulk composition (oxygen content) remains constant, or differentiate with silica-enrichment if the oxygen pressure remains constant (oxygen content variable). The iron-enrichment trend, with little change in silica content,he labelled "tholeiitic trend" of which well-known examples are given by the Skaergaard intrusion (Wager and Deer, 1939) and the Thingmuli volcano (Carmichael, 1964), and the silica-enrichment trend, labelled as " calc-alkali trend" of Cascades.

The close similarity between the Mourne and Thingmuli trends has already been pointed out earlier (Chapter IV, p.52).

iv) Mechanism of differentiation

The ratios of various chemically determined oxides provide possible

measures of parent-daughter relationships of rocks believed to represent magmas in the Mourne area. The values of the major oxides found in the basic, intermediate and acid rocks from the Mourne dyke-swarm lie on smooth curves in several variation diagrams. The smooth character of the curves in these diagrams is, indeed, the strongest evidence from natural rocks that their magmas are related to a parental magma mainly by a continuous process of fractional cyrstallization.

Another geochemical evidence for the process of differentiation in the Mourne dyke-swarm is given by potassium-rubidium ratios. There is increasing evidence that the K/Rb ratio decreases with differentiation of basaltic magma (cf. Tables 41 and 42). This is shown by Nockolds and Allen (1953, p.136), Heier and Taylor (1964, p.201), Taubeneck (1965, p.476) and Gast (1965, p.859).

It is believed that fractional crystallization was of major importance in the differentiation of the Mourne dyke rocks. The initial emplacement of a plug or pipe-like tholeiitic magma body, of crustal dimensions, similar to those indicated under some of the Scottish and Irish Tertiary igneous centres (Cook and Murphy, 1952; Tuson, 1959; McQuillin and Tuson, 1963), was followed by the establishment of a high-level subsidiary magma chamber under the Eastern Mournes. Magnesian olivine, pyroxene and calcic plagioclase crystallized early, causing the remaining liquid to become enriched in Fe relative to Mg and moderately enriched absolutely in Fe, as well as enriched in alkalis and in silica. Consequently pyroxene became more Fe-rich and plagioclase more sodic, but during the main stages of crystallization the liquid continued to become enriched in the less refractory components. Ultimately the residual liquid became impoverished in MgO, CaO and

Al_2O_3, and enriched in silica and combined alkalis, and was concentrated in the near-surface subsidiary magma chamber giving rise to the cone-sheet granophyres.

In the late stages Fe decreased because of the early separation of magnetite in increasing amount in the intermediate members of the Mourne tholeiitic series.

In the granophyres K_2O generally exceeds Na_2O and has increased more rapidly than Na_2O during fractionation. This relationship is in agreement with the experimental and observed evidence available for the system An-Ab-Or (Yoder et al., 1957, pp.206-214; Tuttle and Bowen, 1958, pp.130-135). The initial magma lies close to the An-Ab join of the diagram (cf. Figure 17-B), hence calcic plagioclase, which became progressively more sodic with fractionation, crystallized for an extended period until the liquid reached the cotectic between plagioclase and potassic feldspar. During this time the liquid became enriched in normative orthoclase.

A similar mechanism of differentiation is demonstrated by a number of authors (e.g. McDougall, 1962, p.310; MacDonald and Katsura, 1964, p.105; and Carmichael, 1964, p.449; 1967a, p.1839).

A mechanism of differentiation of the tholeiitic series by the movement and separation of the early crystallizing phases of the primitive olivine-tholeiite magma was favoured by MacDonald and Katsura (1964, p.105) and by Carmichael (1964, p.458).

Earlier workers (MacDonald, 1944, 1949a; Powers, 1955) have pointed out that the differentiation of a tholeiitic suite may be accounted for by the movement of olivine phenocrysts in the magma. Muir and Tilley (1957) concur in the general statement, but point out that the derivation of the tholeiitic Kilauean basalt involves

subtraction of subordinate pyroxene and plagioclase, as well as olivine, from the more "primitive" parental magma.

A re-study of the Hawaiian tholeiitic suite by Katsura (cf. MacDonald and Katsura, 1964, p.105), again confirms the general thesis that the main mechanism of differentiation of the tholeiitic series is the movement of olivine. Olivine would normally be considered to sink rapidly (or fractionate) in a tholeiitic liquid to yield olivine-tholeiites which contain olivine as the first ferromagnesian phase.

The other examples are given by Boyd and co-workers (1964, p.2108) who showed that the oversaturated Qz-normative tholeiites were produced by separation of olivine at very shallow levels from parental olivine-tholeiite.

Yoder and Tilley (1962, p.410) considered that removal of olivine would perpetuate an initial state of critical undersaturation and oversaturation. Magmas in a state of undersaturation may become saturated by separation of olivine. They concluded for these reasons that it was more likely that olivine-tholeiite was the parent of tholeiite.

It is apparent from above discussions that the basic, olivine free tholeiites of the Mourne dyke-swarm could have been derived from a primitive olivine-tholeiite parent by the sole subtraction of its early crystallizing phases.

B. ORIGIN OF THE ACID ROCKS IN THE MOURNE DYKE-SWARM

The existence of a magma chamber at a high-level in the tholeiitic basalt succession beneath the Eastern Mournes is indicated by the concentrations of dykes into a narrow swarm of great intensity, and the presence of basic and intermediate dykes and a composite cone-sheet.

It is clear that the origin of the acid rocks in the Mourne dyke-swarm is in some way related with the upward intrusion of basic magma into the fissures, and although the nature of this relationship is known vaguely, two possibilities in general exist; either the acid magma is produced by some process of fractional crystallization of a basaltic parent, or it exists in its own right, probably as a result of the fusion of sialic material.

While the process of partial fusion in the upper mantle or lower crust remains an attractive mechanism, conclusive evidence has yet to be presented to make it anything more than a tentative hypothesis.

The chemical affinities between basaltic and acid rocks observed in the Mourne dyke-swarm, the association of olivine-tholeiites, tholeiites, quartz-tholeiites, tholeiitic andesites (icelandites) and granophyres speak against an independent origin for the acid rocks by partial melting, as the chemistry of such magmas would be governed by the source rock chemistry alone and not necessarily related to field-associated basalts.

One of the factors limiting the hypothetical derivation of an acid liquid from a basaltic parent is the volume relationship of the product to the parent.

The process of near-surface basaltic fractionation has been shown to be capable of producing 5% of acid residuum from the Skaergaard initial magma (Wager and Brown, 1968), and from 7% to 12% in the case of Thingmuli tholeiitic series (Carmichael, 1964, p.455).

The amount of acid material related to the pre-granitic intrusion of the Mourne dyke-swarm appears to be approximately the same volume of an acid differentiate produced by extreme fractionation as calculated by Carmichael (op.cit., p.439, Table 2, Nos. 1, 4, 5 and 6).

However, the volume of acid magma, which is likely to be concentrated at the top of a magma column and therefore preferentially erupted (Kennedy, 1955), should be related to the volume of the magma body which may have given rise to it. Thus, in the case of the Mourne tholeiitic series, it would seem just possible that by virtue of the volume relationship, the presence of small volume of acid rocks can be accounted for by a high-level basaltic fractionation, keeping in mind the effect that re-cycling of the acid (low-melting) rocks will have on the volume relations between the acid and basic material.

A geochemical difference between the Mourne cone-sheet granophyres and the Eastern Mourne granites has already been pointed out earlier (Chapter III, section d.3). This indicates that the origin of the acid rocks in the Mourne dyke-swarm may well be different from that of the Eastern Mourne granites.

In summary, the present writer supports the idea that the origin of the acid rocks in the Mourne dyke-swarm can be closely related to the end-products of fractional crystallization of a tholeiitic magma, although some strontium and lead isotope studies have yet to be done in order to give more positive evidence on the petrogenesis of these rocks.

REFERENCES

Ahrens, L.H., 1953. The use of ionization potentials; Part 2. Anion affinity and geochemistry: Geochim. et Cosmochim. Acta, 3, 1-29.

_____, 1954. Quantitative Spectrochemical Analysis of Silicates: Pergamon Press, London, 122p.

_____, Pinson, W.H., and Kearns, M.M., 1952. Association of rubidium and potassium and their abundance in common igneous rocks and meteorites: Geochim. et Cosmochim. Acta, 2, 229-242.

Anderson, C.A., 1941. Volcanoes of the Medicine Lake Highland, California: Univ. Calif. Bull. Dept. Geol. Sci., 25, 347-422.

Anderson, E.M., and Radley, E.G., 1915. The pitchstones of Mull and their genesis: Quart. J. Geol. Soc. Lond., 71, 205-217.

Bailey, E.B., 1959. Mobilization of granophyre in Eire and sinking of olivine in Greenland: Liverpool and Manchester Geol. J., 2, 143-154.

_____, Clough, C.T., Wright, W.B., Richey, J.E., and Wilson, G.V., 1924. Tertiary and post-Tertiary geology of Mull, Loch Aline, and Oban: Mem. Geol. Surv. Scot., 445p.

_____, and McCallien, W.J., 1956. Composite minor intrusions, and the Slieve Gullion complex, Ireland: Liverpool and Manchester Geol. J., 1, 466-501.

Baker, I., 1969. Petrology of the volcanic rocks of Saint Helena Island, South Atlantic: Bull. Geol. Soc. Amer. 80, 1283-1310.

Baker, P.E., Gass, I.G., Harris, P.G., and Le Maitre, R.W., 1964. The volcanological report of the Royal Society expedition to Tristan da Cunha, 1962: Phil. Trans. Roy. Soc. Lond., Ser. A, 256, 439-578.

Barth, T.F.W., 1962. Theoretical Petrology: Wiley and Sons, New York, 416p.

Bell, J.D., 1965. Granites and associated rocks of the eastern part of the Western Red Hills complex, Isle of Skye: Phil. Trans. Roy. Soc. Edin., 66, 307-343.

Bence, A.E., and Hurley, P.M., 1967. Rubidium-strontium isotopic relationships in oceanic basalts: Trans. Amer. Geophys. Union, 48, 251-252.

Berger, J.F., 1816. On the dykes of the north of Ireland: Trans. Geol. Soc., 3, 223.

Berlin, R., and Henderson, C.M.B., 1968. A re-interpretation of Sr and Ca fractionation trends in plagioclases from basic rocks: Earth Planet. Sci. Letters, 4, 79-83.

_____, and Henderson, C.M.B., 1969a. Trace element fractionation trends in minerals: Earth Planet. Sci. Letters, 5, 423-424.

_____, and Henderson, C.M.B., 1969b. The distribution of Sr and Ba between alkali feldspar, plagioclase and groundmass phases of porphyritic trachytes and phonolites: Geochim. et Cosmochim. Acta, 33, 247-255.

Blake, D.H., Elwell, R.W.D., Gibson, I., Skelhorn, R.R., and Walker, G.P.L., 1965. Some relationships resulting from the intimate association of acid and basic magmas: Quart. J. Geol. Soc. Lond., 121, 31-50.

Bowen, N.L., 1928. The Evolution of the Igneous Rocks: Princeton Univ. Press, Princeton, 332p.

Boyd, F.R., 1961. Welded tuffs and flows in the rhyolite plateau of Yellowstone Park, Wyoming: Bull. Geol. Soc. Amer. 72, 387-426.

_____, and England, J.L., 1961. Melting of silicates at high pressures: Carnegie Inst. Wash. Year Book, 60, 116-125.

_____, England, J.L., and Davis, B.T.C., 1964: Effects of pressure on the melting and polymorphism of enstatite, $MgSiO_3$: J. Geophys. Res., 69, 2101-2110.

Brooks, C.K., 1968. On the interpretation of trends in element ratios in differentiated igneous rocks, with particular reference to strontium and calcium: Chem. Geol., 3, 15-20.

Brown, G.M., 1956. The layered ultrabasic rocks of Rhum, Inner Hebrides: Phil. Trans. Roy. Soc. Lond., Ser. B, 240, 1-53.

_____, 1957. Pyroxenes from the early and middle stages of fractionation of the Skaergaard intrusion, east Greenland: Mineral. Mag., 31, 511-543.

_____, 1967. Mineralogy of basaltic rocks, in Hess, H.H., and Poldervaart, A., ed., Basalts, The Poldervaart Treatise on Rocks of Basaltic Composition: Wiley and Sons, New York, Volume 1, 103-162.

_____, and Vincent, E.A., 1963, Pyroxenes from the late stages of fractionation of the Skaergaard intrusion, east Greenland: J. Petrol., 4, 175-197.

Brown, P.E., 1956. The Mourne Mountain granites - a further study: Geol. Mag., 93, 72-84.

_____, and Miller, J.A., 1963. An absolute age determination on the Mourne Mountain granite: Geol. Mag., 100, 93.

_____, and Rushton, B.J., 1960. Some chemical data on the Mourne Mountain granite, G-2: Geochim. et Cosmochim. Acta, 18, 193-199.

Buddington, A.F., 1943. Some petrological concepts and the interior of the Earth: Am. Mineral., 28, 119-140.

_____, Fahey, J., and Vlisidis, A., 1955. Thermometric and petrogenetic significance of titaniferous magnetite: Amer. J. Sci., 253, 497-532.

_____, and Lindsley, D.H., 1964. Iron-titanium oxide minerals and synthetic equivalents: J. Petrol., 5, 310-357.

Carmichael, I.S.E., 1963. The crystallization of feldspar in volcanic acid liquids: Quart. J. Geol. Soc. Lond., 119, 95-131.

_____, 1964. The petrology of Thingmuli, a Tertiary volcano in Eastern Iceland: J. Petrol., 5, 435-460.

_____, 1967a. The mineralogy of Thingmuli, a Tertiary volcano in Eastern Iceland: Am. Mineral., 52, 1815-1841.

_____, 1967b. The iron-titanium oxides of salic volcanic rocks and their associated ferromagnesian silicates: Contr. Mineral. Petrol., 14, 36-64.

Chapman, C.A., 1962. Diabase-granite composite dykes, with pillow-like structure, Mount Desert Island, Maine: J. Geol., 70, 539-564.

Charlesworth, J.K., 1963. Historical Geology of Ireland: Oliver and Boyd, Edinburgh, 565p.

Clark, S.P. Jr., 1959. Equations of state and polymorphism at high pressures, in Abelson, P.H., ed., Researches in Geochemistry: Wiley and Sons, New York, Volume 1, 495-511.

Cole, G.A.J., 1888. On some additional occurrences of tachylyte: Quart. J. Geol. Soc. Lond., 44, 300-308.

_____, 1892. The variolite of Annalong, Co. Down: Sci. Proc. Roy. Dublin Soc., (new series), 7, 511-519.

_____, 1894a. On variolites and other tachylytes at Dunmore Head, Co. Down: Geol. Mag., (new decade), 1, 220-222.

_____, 1894b. On derived crystals in the basaltic andesite of Glasdrumman Port, Co. Down: Trans. Roy. Soc. Dublin, Ser.2, 5, 239-248.

Cook, A.H., and Murphy, T., 1952. Measurements of gravity in Ireland; Gravity Survey of Ireland north of a line Sligo-Dundalk: Dublin Inst. Adv. Studies, Geophys. Mem., 2, part 4.

Cox, K.G., MacDonald, R., and Hornung, G., 1967. Geochemical and petrographic provinces in the Karroo basalts of Southern Africa: Am. Mineral., 52, 1451-1474.

Daly, R.A., 1933. Igneous Rocks and the Depths of the Earth: McGraw-Hill, New York.

Deer, W.A., Howie, R.A., and Zussman, J., 1962-1963. Rock Forming Minerals, Volumes 1-5: Longmans, London.

Egan, F.W., 1901. Geological Survey 1 inch to 1 mile map of Ireland, Sheet 60.

Elwell, R.W.D., 1958. Granophyre and hybrid pipes in a dolerite layer of Slieve Gullion: J. Geol., 66, 57-71.

_____, Skelhorn, R.R., and Drysdall, A.R., 1960. Inclined granitic pipes in the diorites of Guernsey: Geol. Mag., 97, 89-105.

_____, Skelhorn, R.R., and Drysdall, A.R., 1962. Net-veining in the diorite of north-east Guernsey, Channel Islands: J. Geol., 70, 215-226.

Emeleus, C.H., 1955. The granites of the Western Mourne Mountains: Sci. Proc. Roy. Dublin Soc., 27, 35-50.

_____, 1956. Studies of the granophyres and related rocks of the Slieve Gullion Tertiary Igneous Complex, Ireland. Unpub. Ph. D. Thesis, Oxford Univ.

Engel, A.E.J., and Engel, C.G., 1964a. Composition of basalts from the Mid-Atlantic Ridge: Science, 144, 1330-1333.

_____, and Engel, C.G., 1964b. Igneous rocks of the East Pacific Rise: Science, 146, 477-485.

_____, Engel, C.G., and Havens, R.G., 1965. Chemical characteristics of oceanic basalts and the Upper Mantle: Bull. Geol. Soc. Amer., 76, 719-734.

Eugster, H.P., and Wones, D.R., 1962. Stability relations of the ferruginous biotite; annite: J. Petrol., 3, 82-125.

Fenner, C.N., 1938. Contact relationships between rhyolite and basalt on Gardiner River, Yellowstone Park: Bull. Geol. Soc. Amer., 49, 1441-1484.

_____, 1944. Rhyolite-basalt complex on Gardiner River, Yellowstone Park, Wyoming - a discussion: Bull. Geol. Soc. Amer., 55, 1081-1096.

Fitton, J.G., and Gill, R.C.O., 1970. The oxidation of ferrous iron in rocks during mechanical grinding: Geochim. et Cosmochim. Acta, 34, 518-524.

Gast, P.W., 1960. Limitations on the composition of the Upper Mantle: J. Geophys. Res., 65, 1287-1298.

_____, 1965. Terrestrial ratio of potassium to rubidium and the composition of the Earth's Mantle: Science, 147, 858-860.

_____, 1967. Isotope geochemistry and volcanic rocks, in Hess, H.H., and Poldervaart, A., ed., Basalts, The Poldervaart Treatise on Rocks of Basaltic Composition: Wiley and Sons, New York, Volume 1, 325-358.

_____, 1968. Trace element fractionation and the origin of tholeiitic and alkaline magma types: Geochim. et Cosmochim. Acta, 32, 1057-1086.

Gibson, I., and Walker, G.P.L., 1963. Some composite rhyolite-basalt lavas and related composite dykes in eastern Iceland: Proc. Geol. Ass. Lond., 74, 301-318.

Goldschmidt, W.M., 1937. The principles of distribution of chemical elements in minerals and rocks: J. Chem. Soc., 1, 655-673.

_____, 1954. Geochemistry. (Ed. Alex Muir). Oxford Univ. Press, Oxford, 730p.

Green, D.H., 1968. Origin of basaltic magmas, in Hess, H.H., and Poldervaart, A., ed., Basalts, The Poldervaart Treatise on Rocks of Basaltic Composition: Wiley and Sons, New York, Volume 2, 835-862.

_____, 1969. The origin of basaltic and nephelinitic magmas in the Earth's Mantle: Tectonophys., 7, 409-422.

_____, 1970. A review of experimental evidence on the origin of basaltic and nephelinitic magmas: Phys. Earth Planet. Interiors, 3, 221-235.

_____, and Ringwood, A.E., 1964. Fractionation of basalt magmas at high pressures: Nature, 201, 1276-1279.

_____, and Ringwood, A.E., 1967. The genesis of basaltic magmas: Contr. Mineral. Petrol., 15, 103-190.

_____, and Ringwood, A.E., 1969. The origin of basalt magmas, in Hart, P.J., ed., The Earth's Crust and Upper Mantle: Amer. Geophys. Union, Wash., Geophys. Monograph, No.13, 489-495.

Green, T.H., and Ringwood, A.E., 1968. Genesis of the calc-alkaline igneous rock suite: Contr. Mineral. Petrol., 18, 105-162.

Griffin, W.L., and Murthy, V.R., 1969. Distribution of K, Rb, Sr and Ba in some minerals relevant to basalt genesis: Geochim. et Cosmochim. Acta, 33, 1389-1414.

Guppy, E.M., and Hawkes, L., 1925. A composite dyke from eastern Iceland: Quart. J. Geol. Soc. Lond., 81, 325-343.

Hamilton, D.L., and Anderson, G.M., 1967. Effects of water and oxygen pressures on the crystallization of basaltic magmas, in Hess, H.H., and Poldervaart, A., ed., Basalts, The Poldervaart Treatise on Rocks of Basaltic Composition: Wiley and Sons, New York, Volume 1, 445-482.

Harker, A., 1904. The Tertiary Igneous Rocks of Skye: Mem. Geol. Surv. U.K., 481p.

Harrison, J.W., 1925. The geology of a composite intrusion at Bennan, south Arran: Trans. Geol. Soc. Glas., 17, 173.

Haughton, S., 1877. On the trap dykes that penetrate the granites, metamorphic slates, and the Carboniferous limestones of the district of Mourne, in the north-east of Ireland: J. Roy. Geol. Soc. Ireland, (new series), 4, 91.

Hawkes, L., 1929. On a partially fused quartz-feldspar rock and on glomero-granular texture: Mineral. Mag., 22, 163-173.

_____, 1945. The Gardiner River rhyolite-basalt complex: Geol. Mag., 82, 182-184.

Heier, K.S., Compston, W., and McDougall, I., 1965. Thorium and uranium concentrations and the isotopic composition of strontium in the differentiated Tasmanian dolerites: Geochim. et Cosmochim. Acta, 29, 643-659.

_____, and Taylor, S.R., 1964. A note on the geochemistry of alkaline rocks: Norsk Geol. Tiddsk., 44, 197-203.

Holland, J.G., and Brindle, D.W., 1966. A self-consistent mass absorption correction for silicate analysis by X-ray fluorescence: Spectrochim. Acta, 22, 2083-2093.

Holmes, A., 1926. Contributions to the theory of magmatic cycles: Geol. Mag., 63, 306-329.

_____, 1931. The problem of the association of acid and basic rocks in central complexes: Geol. Mag., 68, 241-255.

_____, 1932. The origin of igneous rocks: Geol. Mag., 69, 543-558.

_____, and Harwood, H.F., 1929. The tholeiite dykes of the north of England: Mineral. Mag., 22, 1-52.

Hubbard, N.J., 1969. A chemical comparison of oceanic ridge, Hawaiian tholeiitic and Hawaiian alkalic basalts: Earth Planet. Sci. Letters, 5, 346-352.

Hull, E., 1881. Explanatory Memoir to 1 inch to 1 mile sheets 60, 61 and part of 71: Mem. Geol. Surv. Ireland.

Hyland, J.S., 1890. On some spherulitic rocks from Co. Down: Sci. Proc. Roy. Dublin Soc., (new series), 6, 420-437.

Iddings, J.P., 1896. Extrusive and intrusive igneous rocks as products of magmatic differentiation: Quart. J., Geol. Soc. Lond., 52, 606-617.

Jagger, T.A., 1947. Origin and development of craters: Mem. Geol. Soc. Amer., 21, 508p.

Johanssen, A., 1932-1938. A Descriptive Petrography of the Igneous Rocks, Volumes 1-4: Chicago Univ. Press, Chicago.

Judd, J.W., 1893. On composite dykes in Arran: Quart. J. Geol. Soc. Lond., 49, 536-565.

Kay, R., Hubbard, N.J., and Gast, P.W., 1970. Chemical characteristics and origin of Oceanic Ridge volcanic rocks: J. Geophys. Res., 75, 1585-1613.

Kennedy, G.C., 1955. Some aspects of the role of water in rock melts: Geol. Soc. Amer., Special Paper, 62, 489-504.

_____, 1966. The effect of pressure on melting: Trans. Amer. Geophys. Union, 47, 173-174.

Kennedy, W.Q., 1931. On composite lava flows: Geol. Mag., 68, 166-181.

_____, and Anderson, E.M., 1938. Crustal layers and the origin of magmas: Bull. Volcan., Ser. 2, 3, 23-82.

Kinahan, G.H., 1875. On the nomenclature of rocks: Geol. Mag., (new series), 2, 425-426.

Kracek, F.C., and Neuvonen, K.J., 1952. Thermochemistry of the plagioclase and alkali feldspars: Amer. J. Sci., Bowen Volume, 293.

Kulp, J.L., 1960. The geological time scale: 21st Int. Geol. Congr., 3, 18-27.

Kuno, H., 1959. Origin of Cenozoic petrographic provinces of Japan and surrounding areas: Bull. Volcan., Ser.2,,20, 37-76.

_____, 1960. High-alumina basalt: J. Petrol., 1, 121-145.

_____, 1968. Differentiation of basalt magmas, in Hess, H.H., and Poldervaart, A., ed., Basalts, The Poldervaart Treatise on Rocks of Basaltic Composition: Wiley and Sons, New York, Volume 2, 623-688.

_____, Yamasaki, K., Iida, C., and Nagashima, K., 1957. Differentiation of Hawaiian magmas: Japan. J. Geol. Geog., 28, 179-218.

Kushiro, I., 1960. Si-Al relation in clinopyroxenes from igneous rocks: Amer. J. Sci., 258, 548-554.

_____, 1961. A possible origin of tholeiitic magma: Japan. J. Geol. Geog., 32, 31-37.

_____, 1968. Compositions of magmas formed by partial zone melting of the Earth's Upper Mantle: J. Geophys. Res., 73, 619-634.

_____, 1969. The system forsterite-diopside-silica with and without water at high pressures: Amer. J. Sci., 267-A, 269-294.

_____, and Kuno, H., 1963. Origin of primary basalt magmas and classification of basaltic rocks: J. Petrol., 4, 75-89.

_____, and Schairer, J.F., 1963. New data on the system diopside-forsterite-silica: Carnegie Inst. Wash. Year Book, 62, 95-103.

Larsen, E.S., 1929. The temperatures of magmas: Am. Mineral., 14, 81-94.

_____, and Cross, W., 1956. Geology and petrology of the San Juan region, south-western Colorado: U.S. Geol. Surv. Prof. Pap., No.258.

Le Bas, M.J., 1962. The role of aluminium in igneous clinopyroxenes with relation to their parentage: Amer. J. Sci., 260, 267-288.

Lessing, P., Decker, R.W., and Reynolds, R.C., 1963. Potassium and rubidium distribution in Hawaiian lavas: J. Geophys. Res., 68, 5851-5856.

Lipman, P.W., 1969. Alkalic and tholeiitic basaltic volcanism related to the Rio Grande depression, southern Colorado and northern New Mexico: Bull. Geol. Soc. Amer., 80, 1343-1354.

MacDonald, G.A., 1944. Petrography of the Samoan Islands: Bull. Geol. Soc. Amer., 56, 1333-1362.

_____, 1949a. Hawaiian petrographic province: Bull. Geol. Soc. Amer., 60, 1541-1596.

_____, 1949b. Petrography of the Island of Hawaii. U.S. Geol. Surv. Prof. Pap., 214-D, 51-96.

_____, and Katsura, T., 1964. Chemical composition of Hawaiian lavas: J. Petrol., 5, 82-133.

McDougall, I., 1962. Differentiation of the Tasmanian dolerites; Red Hill dolerite-granophyre association: Bull. Geol. Soc. Amer., 73, 279-315.

McQuillin, R., and Tuson, J., 1963. Gravity measurements over the Rhum Tertiary Plutonic Complex: Nature, 199, 1276-1277.

Muan, A., and Osborn, E.F., 1956. Phase equilibria at liquidus temperatures in the system MgO-FeO-Fe_2O_3-SiO_2: J. Amer. Ceram. Soc., 39, 121-140.

Muir, I.D., and Tilley, C.E., 1957. Contributions to the petrology of Hawaiian basalts, 1) The picrite-basalts of Kilauea: Amer. J. Sci., 255, 241-253.

_____, and Tilley, C.E., 1963. Contributions to the petrology of Hawaiian basalts, 2) The tholeiitic basalts of Mauna Loa and Kilauea: Amer. J. Sci., 261, 111-128.

_____, and Tilley, C.E., 1964. Basalts from the northern part of the rift zone of the Mid-Atlantic Ridge: J. Petrol., 5, 409-434.

Nockolds, S.R., 1954. Average chemical compositions of some igneous rocks: Bull. Geol. Soc. Amer., 65, 1007-1032.

_____, and Allen, R., 1953. Geochemistry of some igneous rock series; Part I: Geochim. et Cosmochim. Acta, 4, 105-142.

_____, and Allen, R., 1954. Geochemistry of some igneous rock series; Part II: Geochim. et Cosmochim. Acta, 5, 245-285.

_____, and Allen, R., 1956. Geochemistry of some igneous rock series; Part III: Geochim. et Cosmochim. Acta, 9, 34-77.

_____, and Richey, J.E., 1939. Replacement veins in the Mourne Mountains granite, Northern Ireland: Amer. J. Sci., 237, 27-47.

Osborn, E.F., 1959. Role of oxygen pressure in the crystallization and differentiation of basaltic magma: Amer. J. Sci., 257, 609-647.

_____, 1962. Reaction series for sub-alkaline igneous rocks based on different oxygen pressure relationships: Am. Mineral., 47, 211-226.

Patrickson, S., 1833. A descriptive list of the dykes appearing on the shore which skirts the Mourne Mountains, and numbered from Thomas' Mountain near Warren Point: J. Geol. Soc. Dublin, 1, 182.

Patterson, E.M., 1946a. Late-stage veins in the cone-sheet of Bloody Bridge, Mourne Mountains: J. Irish Natural., 8, 72-76.

_____, 1946b. Age relationships in a Mourne granite quarry - a geological note: J. Irish Natural., 8, 123-124.

_____, 1952. A petrochemical study of the Tertiary lavas of north-east Ireland: Geochim. et Cosmochim. Acta, 2, 283-299.

_____, 1953. Petrochemical data for some acid intrusive rocks from the Mourne Mountains and Slieve Gullion: Proc. Roy. Irish Acad., 55, 171-188.

Poldervaart, A., 1964. Chemical definition of alkali basalt and tholeiite: Bull. Geol. Soc. Amer., 75, 229-232.

Powers, H.A., 1955. Composition and origin of basaltic magma of the Hawaiian Islands: Geochim. et Cosmochim. Acta, 7, 77-107.

Rankama, K., and Sahama, Th. G., 1950. Geochemistry: Chicago Univ. Press, Chicago, 912p.

Ramdohr, P., 1953. Ulvospinel and its significance in titaniferous iron ores: Econ. Geol. 48, 677-688.

Richey, J.E., 1927. The structural relations of the Mourne granites: Quart.J. Geol. Soc. Lond., 83, 653-688.

_____, and Thomas, H.H., 1930. The geology of Ardnamurchan, North-West Mull and Coll: Mem. Geol. Surv. U.K., 393p.

Ringwood, A.E., 1955. The principles governing trace element distribution during magmatic crystallization; Part I. The influence of electro-negativity: Geochim. et Cosmochim. Acta, 7, 189-202.

_____, 1958. The constitution of the mantle - III: Geochim. et Cosmochim. Acta, 15, 195-212.

Robbie, J.A., 1955. The Slieve Bingian Tunnel, an aqueduct in the Mourne Mountains, Co. Down: Bull. Geol. Surv. U.K., No. 8, 1-19.

Rutley, F., 1877. On microscopic structures in tachylyte from Slievenalargg, Co. Down, Ireland: J. Roy. Geol. Soc. Ireland, (new series), 4, 227.

Sigurdsson, H., 1968. Petrology of acid xenoliths from Surtsey: Geol. Mag., 105, 440-453.

_____, 1970. Petrology of the Setberg volcanic region and acid rocks of Iceland: Unpub. Ph.D. Thesis, Univ. Durham, 321p.

Simkin, T., and Smith, J.V., 1966. Minor element distribution in olivine: Ann. Meet. Geol. Soc. Amer., 1966, 203.

_____, and Smith, J.V., 1970. Minor element distribution in olivine: J. Geol., 78, 304-325.

Smellie, W.R., 1915. The Tertiary composite sill of South Bute: Trans. Geol. Soc. Glas., 15, 121.

Smith, J.V., and Gay, P., 1958. The powder patterns and lattice parameters of plagioclase feldspars, II: Mineral. Mag., 31, 744-762.

_____, and MacKenzie, W.S., 1958. The alkali feldspars; IV. The cooling history of high-temperature sodium-rich feldspars: Am. Mineral., 43, 872-889.

Sollas, W.J., 1893. On pitchstone and andesite from Tertiary dykes in Donegal: Sci. Proc. Roy. Soc. Dublin, (new series), 8, 87.

Streckeisen, A.L., 1967. Classification and nomenclature of igneous rocks: N.Jb. Miner. Abh., 107, 144-240.

Tatsumoto, M., 1966a. Isotopic composition of lead in volcanic rocks from Hawaii, Iwo Jima and Japan: J. Geophys. Res., 71, 1712-1733.

_____, 1966b. Genetic relations of oceanic basalts as indicated by lead isotopes: Science, 153, 1094-1101.

Taubeneck, W.H., 1965. An appraisal of some potassium-rubidium ratios in igneous rocks: J. Geophys. Res., 70, 475-478.

Taylor, J.H., 1940. The composite dyke at Brockhill, Worcestershire: Mineral. Mag., 25, 538-549.

Taylor, S.R., Emeleus, C.H., and Exley, C.S., 1956. Some anomalous K/Rb ratios in igneous rocks and their petrological significance: Geochim. et Cosmochim. Acta, 10, 224-229.

Thomas, H.H., and Bailey, E.B., 1915. Leidleite and Inninmorite, in Anderson, E.M., and Radley, E.G., The pitchstones of Mull and their genesis: Quart. J. Geol. Soc. London, 71, 207-209.

Thornton, C.P., and Tuttle, O.F., 1960. Chemistry of igneous rocks, I-Differentiation Index: Amer. J. Sci., 258, 664-684.

Tilley, C.E., 1950. Some aspects of magmatic evolution: Quart. J. Geol. Soc. Lond., 106, 37-61.

_____, 1960. Differentiation of Hawaiian basalts; some variants in lava suites of dated Kilauean eruptions: J. Petrol., 1, 47-55.

Tomkeieff, S.I., and Marshall, C.E., 1935. The Mourne dyke swarm: Quart. J. Geol. Soc. Lond., 91, 251-292.

_____, and Marshall, C.E., 1940. The Killough-Ardglass dyke swarm: Quart. J. Geol. Soc. Lond., 96, 321-338.

Traill, W.A., 1871. Sheets 60, 61 and part of 71 of the maps of the Geological Survey of Ireland: Dublin, H.M.S.O.

———, 1876. Sheet 71, 1 inch to 1 mile map of the Geological Survey of Ireland: Dublin, H.M.S.O.

Turner, F.J., and Verhoogen, J., 1960. Igneous and Metamorphic Petrology: McGraw-Hill, New York, 694p.

Tuson, J., 1959. A geophysical investigation of the Tertiary volcanic districts of Western Scotland: Unpub. Ph.D. Thesis, Univ. Durham.

Tuttle, O.F., 1952. Optical studies on alkali feldspars: Amer. J. Sci., Bowen Volume, 553-567.

_____, and Bowen, N.L., 1958. Origin of granite in the light of experimental studies in the system $NaAlSi_3O_8$-$KAlSi_3O_8$: Mem. Geol. Soc. Amer., 74, 153p.

Tyrrell, G.W., 1928. The Geology of Arran: Mem. Geol. Surv. Scot.

Vincent, E.A., and Phillips, R., 1954. Iron-titanium oxide minerals in layered gabbros of the Skaergaard intrusion, east Greenland: Geochim. et Cosmochim. Acta, 6, 1-26.

Vogt, J.H.L., 1923. On the content of nickel in igneous rocks: Econ. Geol., 18, 307-352.

Wager, L.R., 1960. The major element variation of the layered series of the Skaergaard intrusion and a re-estimation of the average composition of the hidden layered series and of the successive residual magmas: J. Petrol. 1, 364-398.

_____, and Bailey, E.B., 1953. Basic magma chilled against acid magma: Nature, 172, 68-70.

_____, and Brown, G.M., 1967. Layered igneous rocks: Oliver and Boyd, Edinburgh, 588p.

_____, Brown, G.M., and Wadsworth, W.J., 1960. Types of igneous cumulates: J. Petrol., 1, 73-85.

_____, and Deer, W.A., 1939. The petrology of the Skaergaard intrusion, Kangerdlugssuaq, east Greenland: Medd. om Grøn., 105, 352p.

_____, and Mitchell, R.L., 1951. The distribution of trace elements during strong fractionation of basic magma - a further study of the Skaergaard intrusion, east Greenland: Geochim. et Cosmochim. Acta, 1, 129-208.

_____, Vincent, E.A., Brown, G.M., and Bell, J.D., 1965. Marscoite and related rocks of the Western Red Hills Complex, Isle of Skye: Phil. Trans. Roy. Soc. Lond., Ser.A, 257, 273-307.

Walker, F., 1953. The pegmatitic differentiates of basic sheets: Amer. J. Sci., 251, 41-60.

_____, and Poldervaart, A., 1949. Karroo dolerites of the Union of South Africa: Bull. Geol. Soc. Amer., 60, 591-706.

_____, Vincent, H.C.G., and Mitchell, R.L., 1952. The chemistry and mineralogy of Kinkell tholeiite, Stirlingshire: Mineral. Mag., 29, 895-908.

Wedepohl, K.H., 1953. Untersuchungen zur Geochemie des Zinks: Geochim. et Cosmochim. Acta, 3, 93-142.

Wilcox, R.E., 1944. Rhyolite-basalt complex on Gardiner River, Yellowstone Park, Wyoming: Bull. Geol. Soc. Amer., 55, 1047-1080.

_____, 1954. Petrology of Paricutin Volcano, Mexico: Bull. U.S. Geol. Surv., No. 965-C.

Wilkinson, J.F.G., 1956. Clinopyroxenes of alkali olivine-basalt-magma: Am. Mineral., 41, 724-743.

Williams, H., 1932. Geology of the Lassen Volcanic National Park, Califormia: Univ. Calif. Bull. Dept. Geol. Sci., 21, 195-385.

_____, 1935. Newberry volcano of central Oregon: Bull. Geol. Soc. Amer., 46, 253-304.

_____, 1942. The Geology of Crater Lake National Park: Carnegie Inst. Wash. Publ., No. 540.

Wise, W.S., 1969. Origin of basaltic magmas in the Mojave desert area, California: Contr. Mineral. Petrol., 23, 53-64.

Wright, T.L., 1968. X-ray and optical study of alkali feldspar, II - An X-ray method for determining the composition and structural state from measurements of 2θ values for three reflections: Am. Mineral., 53, 88-104.

Yoder, H.S. Jr., Stewart, D.B., and Smith, J.R., 1957. Ternary feldspars, in Abelson, P.H., ed., Annual Report of the Director, Geophysical Laboratory: Carnegie Inst. Wash. Year Book, 56, 151-252.

_____, and Tilley, C.E., 1962. Origin of basalt magmas; an experimental study of natural and synthetic rock systems: J. Petrol., 3, 342-532.

APPENDIX

ANALYTICAL METHODS

A-1) X-ray diffraction technique

The composition and structural state of alkali feldspars, and the structural state of plagioclase feldspars have been determined by using a Philips (PW 1051) high-angle X-ray diffractometer.

The alkali feldspar crystals were drilled out from rock samples and separated under a binocular microscope. They were finely ground in an agate mortar and the powder was glued on the end of a pyrex glass hair using collodian as adhesive. The glass hair was mounted in a large camera (114.59 mm. in diameter) and centred. An exposure time of 12 to 18 hours for X-ray powder films has been found satisfactory. For the powder camera method, Ilford Industrial G-fast X-ray films were used and developed using standard processes. The films were measured on a standard Hilger and Watts film measuring scale, with a vernier capable of reading to $\pm$ 50 microns. The shrinkage corrections were applied to the films measured.

The structural state of plagioclase feldspars was determined from the relative separations of the peaks 220, $1\bar{3}1$, and 131 on X-ray diffractometer patterns from the powders of the whole-rock samples. The operating conditions are given in Table A-1.

A-2) Method of X-ray fluorescence spectrographic analysis of rock samples

Rock samples were split by a hydraulic jack reducing the size to a few cm. They were then crushed in a jaw rock crusher, quartered and

ground to approximately - 300 mesh (about 50 microns) in a Tema swing mill (type T-100) for about 5 min. per sample.

Pelletizing was carried out under 5-6 tons ram pressure, using 4-5 drops of Mowiol as a binder material for rock powder and borax backing disos of a high polish on either side of the pellet.

In this study, a Philips (PW 1212) automatic X-ray fluorescence spectrograph was used and Table A-2 gives the operating conditions for various elements.

In the major element analysis, three samples were run simultaneously, along with a monitoring pellet. The instrument was programmed for the accumulation of a fixed number of counts for each element on the monitoring pellet and corresponding elements in the unknown samples allocated equal counting time. The advantage of a standard monitor sample and the ratio method is the exclusion of instrumental drift.

The absolute method was used in the trace element analysis and each element was measured for a fixed counting period. Background measurements were made on both sides of the spectral peak when a significantly sloping background was present, and a geometric mean was derived for the background correction. The interference of Sr $K\beta$ in the analysis of Zr was corrected for by subtracting 10% of Sr peak height from the Zr K_α peak. All the trace element analyses were carried out on loose rock powders.

The major element analysis was performed following the method of Holland and Brindle (1966), using a bank of comparable igneous rock standards. Mass absorption corrections were then made by an iterative process, giving a chemical composition which subsequently is compared further to a set of standards by regression analysis.

A-3) The determination of FeO by the permanganate method

The finely ground rock powder was weighed (approximately 0.5 gm) into a platinum crucible and was moistened with about 1 ml. of distilled water. 5 ml. of distilled water, 5 ml. of concentrated sulphuric acid and 10 ml. of hydrofluoric acid were then added into the crucible and covered. The crucible was gently heated over a bunsen burner for 8-10 minutes. When rock powder had fully dissolved, the crucible was transferred into a 400 ml. glass beaker which was filled with 200 ml. of distilled water, 10 ml. of 50% H_2SO_4 and 10 ml. of saturated boric acid solution.

The solution in the beaker was then titrated with a standardized potassium permanganate solution by stirring vigorously until a stage was reached where a faint pink tinge remained even after a lot of stirring. The amount of permanganate solution needed to reach this point was noted and was used in calculating the FeO content.

A-4) Method of electron microprobe analysis of constituent minerals

An electron probe X-ray microanalyser (Cambridge Scientific Instrument Company-Mk.II Geoscan), equipped with two spectrometers, was used for quantitative analysis of a number of elements in feldspars, pyroxenes and olivines, as well as some Fe-Ti oxide minerals. The electron beam was focussed to about 1 micron diameter, giving a spot, or volume of analysis of 3 microns diameter. The specimen current was near 0.04 micro-amps in all runs. Analyses for two elements were always done simultaneously, using W K_α radiation. Operating conditions of the microprobe for the analysis of various elements are given in Table A-3.

Although corrections for background are small in the analysis of

major elements, background readings were always carried out on comparable mineral standards and one of the unknown minerals at the beginning and end of each run. Drift corrections were also derived from these data. Initial corrections for instrument drift, dead-time (4 microsec.) and background were obtained by use of an Olivetti "Programa 101" desk computer, which provided crude element concentrations by straight ratioing against standards. Further computerized corrections for fluorescence effects, mass absorption, atomic number (electron back-scattering and electron retardation), developed and written by Dr. J.W. Aucott in "KDF 9 Algol", followed by iterations with reference to standards.

Detection is satisfactory for Fe, Ca, Mg and Mn, but somewhat poorer for Ti, Na and Al. The Ti Kβ interferes with the V K$_\alpha$ line, and the values of V_2O_3 need to be treated with caution.

Table A-1: Operating conditions of the Philips (PW 1051) X-ray diffractometer for the study of plagioclase feldspars

Radiation:	Cu K , Ni filter, 40 kV, 20 mA.
Slits:	1^{o}, 0.1^{o}, 1^{o}.
Goniometer:	$1/8^{o}$/min.
Counter:	Scintillation, 1730 V.
Chart-speed:	400 mm/hr.
Counter:	Rate-meter 4, Time-constant: 8, Mult. 1.
Operation:	R.M.
Range scanned:	2θ : 28^{o} - 32^{o}.
Analysis peaks:	2θ : 30.15, 30.48, 31.23; no int.std.
Mount type:	Cavity.

Table A-2: Operating conditions for the Philips (PW 1212) automatic X-ray fluorescence spectrograph in the analysis of major and trace elements

Element	2θ	Tube	Gen.	kV	mA	Cryst.	Path	Coll.	Counter	Counts	Time (sec)
Si	109.15	Cr	1575	60	32	PE	V+G	Coarse	Flow	10^6	FC
Al	145.13	Cr	1575	60	32	PE	V+G	Coarse	Flow	$3x10^5$	FC
Fe	85.72	Cr	1575	60	8	LiF(110)	V+G	Coarse	Flow	$3x10^5$	FC
Mg pk	81.30	Cr	1575	50	40	ADP	V+G	Coarse	Flow	$3x10^4$	FC
Mg bg	79.05	Cr	1575	50	40	ADP	V+G	Coarse	Flow	$3x10^4$	FC
Ca	45.07	Cr	1575	60	8	PE	V+G	Coarse	Flow	10^6	FC
Na pk	103.12	Cr	1575	50	40	ADP	V+G	Coarse	Flow	10^4	FC
Na bg	105.05	Cr	1575	50	40	ADP	V+G	Coarse	Flow	10^4	FC
K	50.58	Cr	1575	60	8	PE	V+G	Coarse	Flow	$3x10^5$	FC
Ti	36.58	Cr	1575	60	8	PE	V+G	Coarse	Flow	$3x10^5$	FC
P pk	89.45	Cr	1575	50	40	PE	V+G	Fine	Flow	10^4	FC
P bg	87.50	Cr	1575	50	40	PE	V+G	Fine	Flow	10^4	FC
Mn pk	95.35	W	1575	70	30	LiF(110)	Air	Fine	Flow	FT	20
Mn bg	97.00	W	1575	70	30	LiF(110)	Air	Fine	Flow	FT	20
S pk	75.65	Cr	1575	50	40	LiF(110)	V+G	Fine	Flow	10^4	FC
S bg	73.50	Cr	1575	50	40	LiF(110)	V+G	Fine	Flow	10^4	FC
Ba pk	15.61	W	1675	80	24	LiF(110)	V	Coarse	Scint.	FT	40
Ba bg	16.80	W	1675	80	24	LiF(110)	V	Coarse	Scint.	FT	40
Sr bg	35.00	W	1675	60	32	LiF(110)	V	Coarse	Scint.	FT	40
Sr pk	35.83	W	1675	60	32	LiF(110)	V	Coarse	Scint.	FT	40
Sr bg	36.90	W	1675	60	32	LiF(110)	V	Coarse	Scint.	FT	40
Zr bg	30.95	W	1675	60	32	LiF(110)	V	Coarse	Scint.	FT	40
Zr pk	32.12	W	1675	60	32	LiF(110)	V	Coarse	Scint.	FT	40
Zr bg	33.15	W	1675	60	32	LiF(110)	V	Coarse	Scint.	FT	40
Rb bg	36.90	W	1675	60	32	LiF(110)	V	Coarse	Scint.	FT	40
Rb pk	37.98	W	1675	60	32	LiF(110)	V	Coarse	Scint.	FT	40
Rb bg	39.35	W	1675	60	32	LiF(110)	V	Coarse	Scint.	FT	40
Cu bg	64.80	W	1675	40	32	LiF(110)	V	Coarse	Scint.	FT	100
Cu pk	65.62	W	1675	40	32	LiF(110)	V	Coarse	Scint.	FT	100
Cu bg	66.50	W	1675	40	32	LiF(110)	V	Coarse	Scint.	FT	100
Ni bg	70.00	W	1675	60	32	LiF(110)	V	Coarse	Scint.	FT	100
Ni pk	71.32	W	1675	60	32	LiF(110)	V	Coarse	Scint.	FT	100
Ni bg	73.20	W	1675	60	32	LiF(110)	V	Coarse	Scint.	FT	100
Zn bg	59.40	W	1675	60	32	LiF(110)	V	Coarse	Scint.	FT	100
Zn pk	60.63	W	1675	60	32	LiF(110)	V	Coarse	Scint.	FT	100
Zn bg	61.40	W	1675	60	32	LiF(110)	V	Coarse	Scint.	FT	100

Table A-3: Operating conditions for the electron microprobe analyser

Element	E t'hold	E gate	Crystal	2θ peak	backgr.	Counter	Slits	Time(sec)
Na	0.54	1.0	KAP	53.12	+1.30	FC	Out	20
Mg	0.75	1.0	KAP	43.40	-2.00	FC	Out	20
Al	0.74	1.5	KAP	36.32	±2.00	FC	Out	20
Si	0.74	2.0	KAP	31.06	±1.30	FC	Out	20
K	0.69	2.5	QTZ	68.03	-2.00	FC	Out	20
Ca	1.54	1.5	QTZ	60.18	-2.00	FC	Out	20
Ti	1.80	2.0	QTZ	48.33	+2.00	SC	Out	20
Mn	2.66	2.0	QTZ	36.39	+2.00	SC	Out	20
Fe	2.73	2.5	QTZ	33.40	+2.00	SC	Out	20
Ba	1.74	2.0	QTZ	49.04	-1.30	FC	Out	20
Sr	0.75	2.0	KAP	29.54	±1.30	FC	Out	20
V	2.60	2.0	QTZ	43.59	±1.30	SC	Out	20
Cr	2.60	2.0	QTZ	40.03	±1.30	SC	Out	20

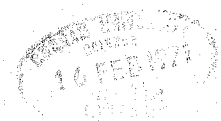

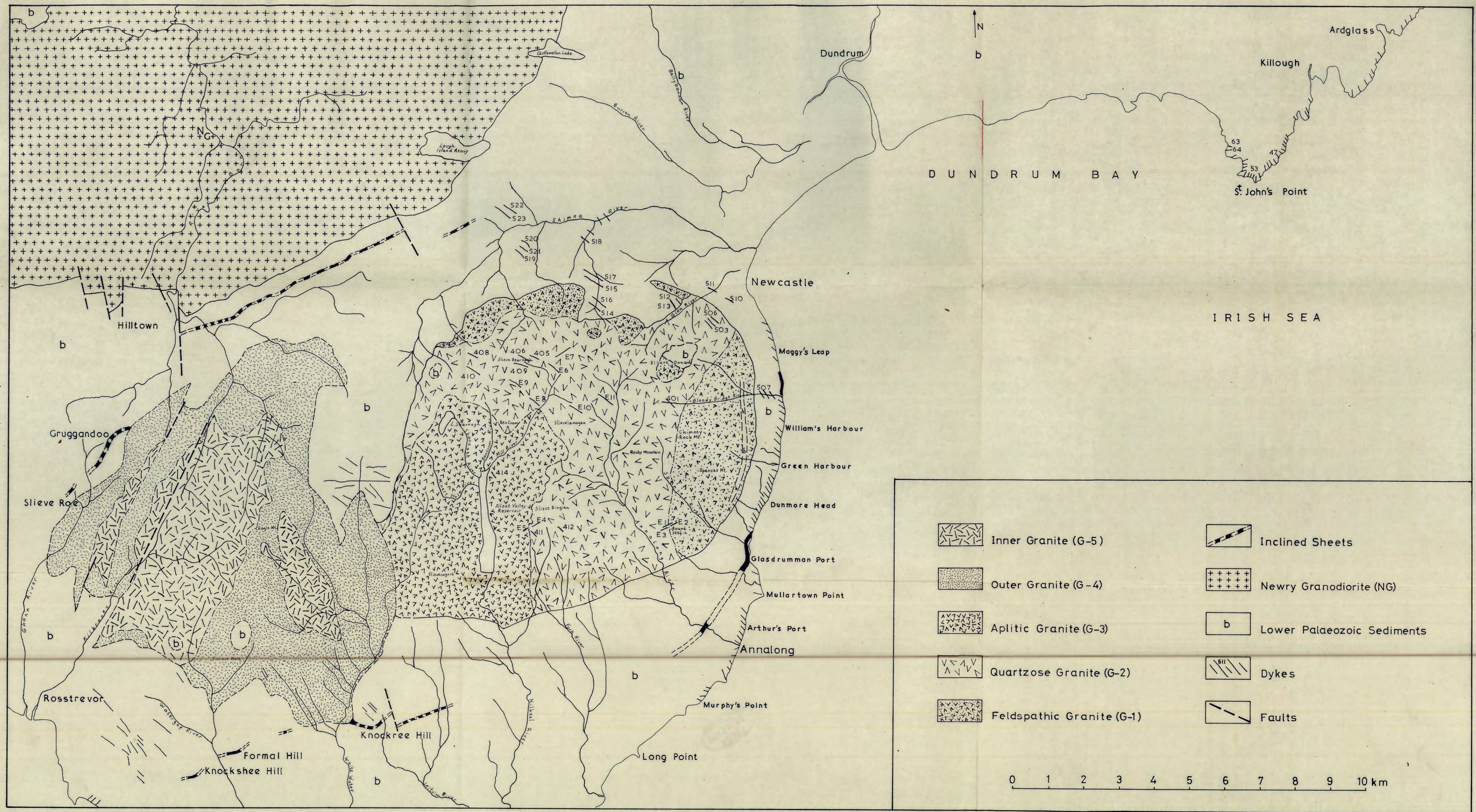

MAP 1: GEOLOGICAL MAP OF THE MOURNE AREA (After Geological Survey)

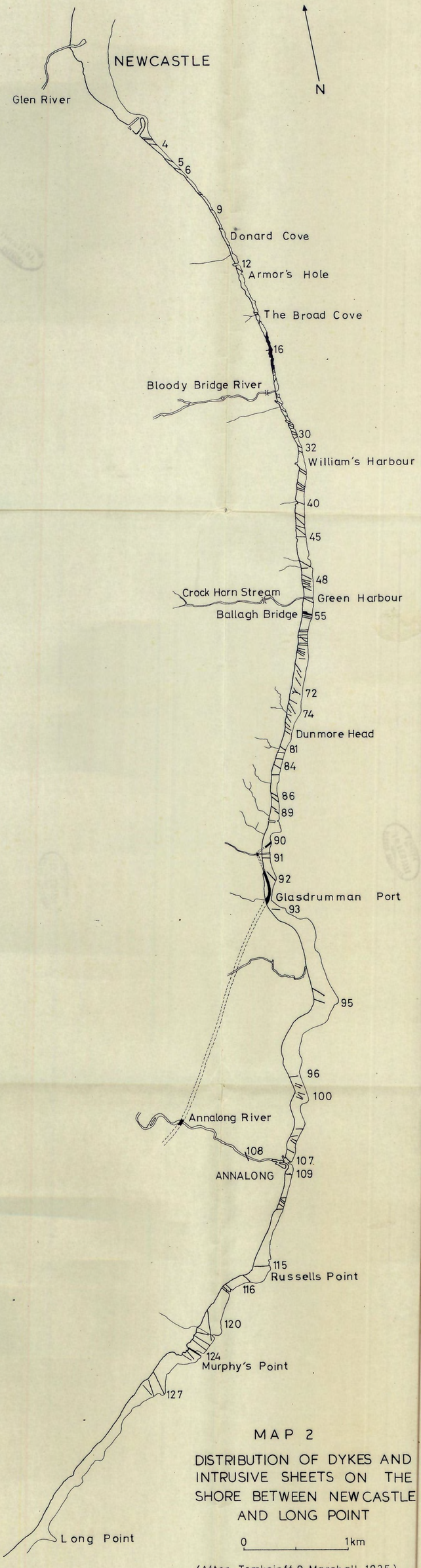

MAP 2

DISTRIBUTION OF DYKES AND INTRUSIVE SHEETS ON THE SHORE BETWEEN NEWCASTLE AND LONG POINT

(After Tomkeieff & Marshall, 1935)